PRESENILIN complexes in *Arabidopsis*:
Novel plant cell-signalling components?

J. Ross Walker

Supervisor: Dr Gwyneth Ingram

PhD
The University of Edinburgh
2009

Declaration

I declare that this is my own work and contributions by others are clearly cited

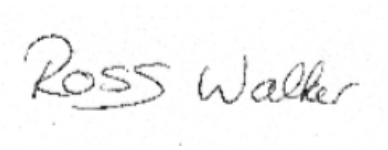

I. Abstract

Intercellular signalling is essential for multicellular organisms to coordinate growth and development, and is mediated by a huge variety of proteins. Some signalling pathways rely on the proteolytic cleavage of membrane proteins by a relatively newly discovered process of regulated intramembrane proteolysis (RIP), the cleavage of proteins within a transmembrane domain. There are four classes of intramembrane cleaving proteases (ICliPs) – Rhomboids, Site-2-proteases, Signal peptide peptidases and γ-secretase. Of all the ICliPs studied to date, γ-secretase is unique, as it is comprised of a four-protein complex, and is only found in multicellular organisms. A vast amount of research is carried out on the γ-secretase complex, not just because of its role in developmentally important pathways, such as NOTCH signalling, but also due to its role in Alzheimer's disease. The β-amyloid precursor protein (APP) is cleaved by γ-secretase, and defects in this process result in the release of abnormal peptides that form the senile plaques in the brains of Alzheimer's disease patients. Homologues of the four components of γ-secretase (PRESENILIN (PS), NICASTRIN (NCT), ANTERIOR PHARYNX DEFECTIVE-1 (APH-1) and PRESENILIN ENHANCER-2 (PEN-2)) are found in plants. The aim of this thesis was to characterise the potential γ-secretase components in *Arabidopsis thaliana*, to determine whether they form a complex, and to analyse what role, if any, they play in plant signalling. The members of the putative *Arabidopsis* γ-secretase complex (*AtPS1* and *2, AtNCT, AtAPH1* and *AtPEN2*) were identified through BLAST searches, and found to be uniformly expressed. Analysis of T-DNA insertion mutants in each of these genes, and combinations there of, revealed no gross morphological differences to wild type under normal growth conditions and when subjected to a range of stresses. Protein fusions to GFP under the control of the 35S promoter were constructed and stably transformed into plants. AtPEN2:GFP is expressed throughout the plant, and accumulates in BFA sensitive Golgi bodies in roots. AtPS1:GFP, only accumulates strongly in developing seeds. Native blue PAGE was used to look for high molecular weight complexes (HMW) containing AtPEN2:GFP and AtPS1:GFP. Both fusion proteins were found in similar sized HMW complexes. A variety of methods were used to look for substrates of the

putative γ-secretase complex in *Arabidopsis*, and although no specific substrates were identified, a potential role in seed development has been established.

II. Acknowledgements

Many people deserve thanks for helping me through this carry-on. First and foremost, I have to thank Gwyneth Ingram, not only for giving me the chance to make the step from technician to being a student once again, but also for all her help and guidance throughout the time I have worked in her lab, not to mention her understanding of my lack of time keeping. Simply put, Gwyneth is a far greater supervisor than I could ever have wished for. Kim Johnson, for teaching me the mystical ways of western blots, microscopes and many other protocols. Britta Kümpers, who carried out her honours project in the lab, and provided some beautiful confocal images. Also, anyone in the department that ever answered a question or lent me a piece of equipment, in particular the Hardwick lab for their protein gel rig. And the Leverhulme Trust for their generous funding.

Aside from work related business, thanks to all the people I've ever shared a pint or two (or more) with – especially Frazer, Manuel and Kim. Thanks for keeping me sane. My little sister Ruth, and George for being great flatmates and putting up with all by brewing kit. My brother Scott, for somewhere free to stay on holiday, and starting my golf obsession. Lastly, but certainly not least, to Mum and Dad for their constant support in everything I've ever done. I couldn't have done it without them.

Cheers,
Ross

III. Abbreviations and Nomenclature

Abbreviations used:

0.5xMS	half strength Murashige and Skoog
ABA	Abscisic acid
AD	Alzheimer's disease
APH1	ANTERIOR PHARYNX DEFECTIVE 1
APP	Amyloid beta precursor protein
APS	ammonium persulphate
BFA	Brefeldin A
bp	base pair
BSA	Bovine serum albumin
cDNA	complimentary DNA
CHAPS	3-[(3-Cholamidopropyl)dimethylammonio]-1-propanesulfonate
CTF	C-terminal fragment
dATP	2'-deoxyadenosine 5'-triphosphate
dCTP	2'-deoxycyidine 5'-triphosphate
DDM	n-dodecyl beta-D- maltoside
dGTP	2'-deoxyguanosine 5'-triphosphate
DMPC	dimethyl pyrocarbonate
DNA	deoxyribonucleic acid
dTTP	2'-deoxythymidine 5'-triphosphate
EDTA	Diaminoethanetetraacetic acid
EM	electron microscopy
EtOH	ethanol
FAD	familial Alzheimer's disease
GA	Gibberellic acid
GFP	GREEN FLUORESCENT PROTEIN
GFPc	C-terminal GFP fusion
GFPi	internal GFP fusion
HMW	high molecular weight
HRP	horse radish peroxidase
I-CliP	intramembrane cleaving protease
ICD	intracellular domain
JA	Jasmonic acid
kb	kilobase
L	litre
LB	Lauria broth
M	molar
MeOH	methanol
mg	milligram
mM	millimolar
MS	mass spectrometry
NCT	NICASTRIN
ng	nanogram
NTF	N-terminal fragment
o/n	overnight
PBST	phosphate buffered saline Tween

PCR	polymerase chain reaction
PEN2	PRESENILIN ENHANCER 2
pM	picomolar
PS	PRESENILIN
RIP	regulated intramembrane proteolysis
RNA	ribonucleic acid
RT-PCR	reverse transcriptase PCR
S2P	site 2 protease
SA	Salicylic acid
SDS	sodium dodecyl-sulphate
SP	signal peptidase
SPP	signal peptide peptidase
SSC	standard saline citrate
T-DNA	transfer DNA
TE	Tris, EDTA
TEMED	tetramethylethylenediamine
TMD	transmembrane domain
Tris	tris(hydroxymethyl)aminomethane
ug	microgram
uL	microlitre
uM	micromolar
UTR	untranslated region
UV	ultraviolet
V	volts
Y-SD	yeast synthetic media, dextrose
YEP	yeast extract, peptone
YPDA	yeast extract, peptone, dextrose, adenine

Nomenclature

Throughout this thesis, proteins, genes and mutants from a range of model biological systems are described. To avoid confusion between the different naming systems, I have applied the accepted *Arabidopsis* nomenclature for all eukaryotic species. This was laid down by Meinke and Koornneef (1997) as follows:

ALPHABETICAL	Full wild type gene name, capital italics
ABC	Shortened wild type gene name, capital italics
alphabetical	Mutant name, lowercase italics
ALPHABETICAL	Protein product, capitals

IV. Contents

1.0. Introduction

The γ-secretase complex is a multi-protein membrane spanning protease, essential to correct animal development due to its role in intracellular signalling through regulated intramembrane proteolysis (RIP). The four core components of the γ-secretase complex are PRESENILIN 1 or 2 (PS1/2), NICASTRIN (NCT), ANTERIOR PHARYNX DEFECTIVE 1 (APH1) and PRESENILIN ENHANCER 2 (PEN2). Studies have identified presenilins in every multi-cellular organism studied, including the model plant species *Arabidopsis thaliana*. This thesis aims to elucidate the role of the PRESENILINs in *Arabidopsis* and if they form a proteolytic complex as in animals.

This introduction will, firstly, outline some of the major roles for proteases in plants, from degradation to activation. Secondly, the 3 main classes of intramembrane cleaving proteases (I-Clips) responsible for RIP will be examined, including any information available from research in plants. Lastly, a more detailed explanation of the γ-secretase complex will be carried out, explaining the need for research into the *Arabidopsis* presenilins.

1.1. Proteolysis in plant cells

Proteolysis is an essential process in all cells. Almost 3% of the *Arabidopsis* proteome is made up of predicted proteases, however few have been shown to have proteolytic activity (Garcia-Lorenzo et al., 2006). There are five main classes of proteases, which are categorised based on having a serine, cysteine, aspartic acid, threonine or metal ions at the active site. Cleavage of certain peptide bonds can have a variety of effects on different proteins, from degradation of unwanted proteins to activation of zymogen precursors and processing of regulatory proteins. Protease substrate selectivity is tightly regulated, so as to protect the cell's contents from destruction. A number of methods are used to control proteases, such as restricted access to the active site, for example the 26S proteasome, restriction to certain compartments (e.g. the vacuole), and production of inactive precursors. Many proteases are essential in *Arabidopsis*, as mutations are lethal, and are involved in diverse pathways such as chloroplast development (Inoue et al., 2005), epidermal specification (Johnson et al., 2005), cuticle formation (Tanaka et al., 2001), programmed cell death during embryogenesis (Ge et al., 2005), and the proteasome machinery (26S protein subunits and Ubiquitin-specific proteases (Doelling et al., 2001; Brukhin et al., 2005)). A selection of proteases and their function in plants will be discussed and includes the more extensively characterised 26S proteasome and other developmentally important regulatory proteases.

1.1.1. The 26S proteasome – degradation in hormone signalling

The 26S proteasome is immensely important in a wide range of signalling cascades in eukaryotes, and in higher plants includes hormonal responses, environmental adaptation and flower development (Callis and Vierstra, 2000). The 26S proteasome is made up from 31 principal subunits forming two subcomplexes – the 20S core protease (CP) and the 19S regulatory particle (RP; Smalle and Vierstra, 2004). The CP is roughly barrel shaped with the active site threonine residues exposed to the internal chamber. The CP is capped on both ends by RPs that provides substrate specificity by recognition of poly-ubiquitinated proteins. The active site is contained

within the interior of the barrel, restricting access to unfolded proteins. Therefore, selected substrates are recognised, and unfolded, prior to entering the CP where proteolysis takes place.

The 26S proteasome specifically recognises poly-ubiquitinated proteins as substrates. The Ubiquitin (Ub) monomer is a small globular protein of 76 amino acids with a characteristic structure known as the Ubiquitin fold, consisting of five β-strands and an α-helix (Orengo et al., 1994). Many other proteins contain the Ub fold, such as SUMOs, HUBs, RUBs and MUBs (Downes et al., 2006), however they may not have much sequence or functional conservation with Ub. In addition to its role in signalling a protein's degradation, mono-ubiquitylation, or addition of other Ub-fold proteins, acts in regulation of activity and sorting of these proteins (Hicke, 2001). Ub is covalently attached to lysine residues of substrate proteins through a series of Ub transfers. First, an Ub monomer is attached to a cysteine residue of an Ub-activating enzyme (or E1) through a thioester bond by an ATP-dependent reaction. The activated Ub monomer is transferred from the E1 to an Ub-conjugating enzyme (E2) by transesterification of the thioester bond (Vierstra, 2003). Ub-protein ligases (E3s) mediate the addition of Ub to the substrate. The final result is an Ub-protein assembly, which can have additional Ubs attached to specific lysine residues in Ub. This poly-ubiquitinated protein is recognised as a substrate for the 26S proteasome and degraded, releasing the Ub moieties for reuse. In this fashion, unfolded/abnormal proteins are degraded, or functional proteins can be destroyed to stop their function (such as enzymes or transcription factors). E3s are vital to the whole process as they provide substrate specificity. E3s fall into 2 main classes - those that mediate transfer of Ub directly from E2-Ub (SCF, Ring/U-box, APC/C) and those that form an E3-Ub intermediate (HECT).

HECT domain containing E3s are named for their homology to the C-terminus of E6-AP (the first protein with this domain characterised (Huibregtse et al., 1991)), which contains the E2 binding pocket and cysteine for transfer of Ub (Verdecia et al., 2003). In addition to the HECT domain, various protein-protein interaction motifs are present, and this has been suggested as the reason for substrate specificity

(Downes et al., 2003). *Arabidopsis* contains seven HECT-domain E3s (UPL1-7), only one of which has an assigned function - UPL3 acts in trichome development (Downes et al., 2003). UPL3-mediated ubiquitination and subsequent degradation of certain, unidentified, factors acts to repress trichome branch growth and DNA replication.

The RING/U-box class of E3s has been greatly expanded in plants compared to humans and yeast (Yee and Goring, 2009). The U-box is a well-conserved motif with structural homology to the RING-finger domain, but lacking the zinc ion binding capacity (Aravind and Koonin, 2000). Like HECT domain E3s, U-box E3s act alone to bring the substrate and E2-Ub into close proximity (Hatakeyama et al., 2001), however U-box E3s do not form an E3-Ub intermediate. The U-box E3s identified in *Arabidopsis* are divided into classes depending on the domains contained in the rest of the protein, mainly involved in protein-protein interactions for substrate binding (Azevedo et al., 2001). Examples of U-box E3s include AtCHIP and the PUB (PLANT U-BOX) proteins. AtCHIP appears to cause the degradation of subunits of the thylakoid membrane bound FtsH protease complex, leading to an increased sensitivity to high light intensity (Shen et al., 2007). A group of PUBs have been implicated in responses to drought and pathogen attack. Knockouts of *pub22, 23,* and *24* lead to increased tolerance to high salt and drought (Cho et al., 2008), and increased responses to pathogen attack (greater ROS production and resistance; Trujillo et al., 2008). These proteins seem to cause degradation of subunits of the 19S regulatory particle of the 26S proteasome itself, resulting in a lowered tolerance to certain stresses that result in degradation of proteins via the Ub/proteasome pathway (Kurepa et al., 2008).

Plants grow via tightly controlled cell division and cell expansion and the proteasome has an important role in this process through regulation of the cell cycle. The anaphase promoting complex or cyclosome (APC/C) is a multi-subunit Ub-ligase controlling the cell cycle, which is present in *Arabidopsis* (Capron et al., 2003). Proteins containing a D-box motif, such as cyclins, are degraded at specific points to allow progression through the cell cycle (Glotzer et al., 1991). The D-box

is recognised by CDC20 and CDH1 (CCD52 in *Arabidopsis*), providing substrate specificity to the E3 complex (Fulop et al., 2005). Two components in the APC/C show some similarity to the Cullin and RBX1 proteins of the SCF complex, acting as scaffolds to bring substrates and E2-Ub conjugate into proximity. Other components of the APC/C may be involved with integrating cellular signals, such as differentiation of meristematic cells through the *Arabidopsis* HOBBIT protein, a homologue of yeast CDC27 (Blilou et al., 2002).

The final class of E3 Ub-ligases comprises the SCF complex (SKP/Cullin/F-box protein/RBX1). ASK1, AtCUL1 and AtRBX1 (the *Arabidopsis* versions of SKP, Cullin and RBX1) act as scaffolding, with an F-box protein providing substrate specificity. RBX1 is a small protein, containing a RING-finger domain that binds the E2-Ub conjugate, and another domain to bind the Cullin (Zheng et al., 2002). SKP provides a bridge between a F-box protein and the Cullin. The F-box family of proteins contains various protein-protein interaction motifs important for substrate recognition, in addition to the F-box motif (Gagne et al., 2002). Given that there are almost 700 predicted F-box proteins in *Arabidopsis*, and the possibility of forming heterodimers (Risseeuw et al., 2003), there is a huge potential for regulation of diverse substrates. Indeed, F-box proteins are involved in numerous hormone-signalling pathways, such as auxin, gibberellic acid and jasmonate signalling.

The plant hormone auxin plays a role in nearly all aspects of plant growth and development. TIR1, a F-box protein, acts as a receptor for auxin (Dharmasiri et al., 2005; Kepinski and Leyser, 2005), and specifically binds AUX/IAA proteins (Gray et al., 2001). AUX/IAA proteins block transcription by binding to auxin response factors (ARFs) and acting as negative regulators of auxin signalling (Guilfoyle et al., 1998). Upon binding of auxin, SCF^{TIR1} causes poly-ubiquitination and degradation of AUX/IAAs (Kepinski and Leyser, 2005) allowing transcription of auxin responsive genes.

Gibberellic acid (GA) signalling affects a wide range of plant growth including stem elongation, flowering, fruit development and seed germination. Like auxin, GA

causes the degradation of negative regulators of its own signalling. For GA, there are five negative regulators, the DELLA proteins, including RGA (REPRESSOR OF *ga1-3*) and GAI (GIBBERELLIC ACID-INSENSITIVE) in *Arabidopsis*, which are ubiquinated by the SCF^{SLY1} complex (SCF complex containing the F-box protein SLEEPY1) (Silverstone et al., 1997). Unlike auxin signalling, where the F-box protein itself is a receptor for the signalling molecule, GA is bound by GIBBERELLIN INSENSITIVE DWARF 1 (GID1; Murase et al., 2008). Binding of bioactive GA causes conformational changes in GID1 that allows binding of DELLA proteins and presentation of them as substrates to the SCF^{SLY1} complex.

Jasmonate (JA) signalling is mediated by the F-box protein COI1 (CORONATINE INSENSITIVE 1), again through degradation of repressor proteins, such as JAZ1 (Thines et al., 2007). JA derivatives promote the association of COI1 and JAZ1 in the absence of other proteins, and it has been suggested that COI1 is the receptor, much like TIR1/auxin. Degradation by the 26S proteasome is thus a key component of signalling by plant hormones and plays roles in many other key plant pathways. However, proteolysis is not necessarily the end of a protein's function, as cleavage of specific peptide bonds can either release a signalling peptide or activate by exposure of an active site. Examples of these forms of limited proteolysis will be discussed in the following sections.

1.1.2. Signalling through small secreted peptides

Insulin, a mammalian hormone, is produced from a larger inactive peptide by limited proteolysis (Csorba, 1991). It has also been shown in plants that active signalling peptides are produced from larger proproteins. The first example discovered was systemin, a small 18 amino acid peptide produced from the C-terminus of prosystemin (McGurl et al., 1992), which is mobile in tomato and activates defence genes through the JA pathway (Farmer and Ryan, 1992). The tomato SYSTEMIN RECEPTOR 160 (SR160) was identified, and subsequently discovered to also be the brasinolide receptor tBRI1 (BRASSINOSTEROID INSENSITIVE 1; Szekeres, 2003). As yet, no prosystemin protease has been identified.

In the same vein as prosystemin processing in tomato, CLAVATA3 and the CLAVATA3-related proteins (CLAVATA3/ESR-like; CLEs) are thought to be processed to release an active ligand in *Arabidopsis* (Ni and Clark, 2006). CLV3 is expressed in the outermost layers of the shoot meristem and acts as a negative regulator of the transcription factor WUSCHEL (WUS), expressed in the underlying layers (Schoof et al., 2000). Signalling takes place through the leucine-rich-repeat receptor-like kinase (LRR-RLK) CLAVATA1 (CLV1) and its dimerisation partner CLV2, a LRR receptor-like protein. CLAVATA signalling promotes differentiation of stem cells by repressing expression of WUS, which works to maintain stem cells in an undifferentiated state. The 14 amino acid CLE motif found at the C-terminus of CLV3 is sufficient to replace the CLV3 protein for CLAVATA signalling. *In vitro* experiments with cauliflower protein extracts showed a potential proteolytic activity specific for CLE proteins, however this protease has not been identified (Ni and Clark, 2006). Similarly, cleavage of the other 25 CLE proteins also have the potential to produce ligands for some of the 400 RLKs present in *Arabidopsis*. Although no proteases for CLV3 or CLE cleavage have been identified to date, other developmentally important proteases involved in regulatory cleavage of signalling components have been described.

Stomatal development requires a series of asymmetric divisions that lead to a non-random pattern of stomata with at least one epidermal pavement cell between each guard cell complex. Stomatal production is under the control of a signalling pathway that includes the extracellular subtilase-like serine protease SDD1 (STOMATAL DENSITY AND DISTRIBUTION 1), a receptor-like protein TMM (TOO MANY MOUTHS), the receptor kinases ERECTA (ER), ER-LIKE 1 (ERL1), ERL2, a mitogen-activated protein kinase kinase (MAPKK) kinase, YODA, and a number of basic helix-loop-helix transcription factors (bHLH TFs), SPEECHLESS, MUTE and FAMA (Shpak et al., 2005; Ohashi-Ito and Bergmann, 2006; Lampard et al., 2008; Pillitteri et al., 2008). SDD1 is produced in meristemoids and guard mother cells (GMCs), and exported to the apoplast. The *sdd1-1* knockout or overexpression of *SDD1* leads to an increased and decrease in stomatal density, respectively, showing

that SDD1 is a negative regulator of stomatal formation (Von Groll et al., 2002). In cotyledons, the *tmm* mutation is epistatic to overexpression of *SDD1*. It is thought that SDD1 processes a ligand for a TMM/receptor kinase (ER/ERL) complex, which signals downstream through a kinase cascade involving YODA to repress stomatal formation. SDD1 processing to release active signalling peptides is completely feasible, as in animal systems, subtilase proteases also process pro-hormones such as insulin (Bergeron et al., 2000). As yet, no substrates have been identified for SDD1.

There are about 40 subtilase-like proteins predicted to be secreted into the apoplast, and along with 25 papain-like cysteine proteases and 45 pepsin-like aspartic proteases (Beers et al., 2004; van der Hoorn and Jones, 2004), there is potential for a wide range of ligand and/or receptor processing.

1.1.3. Maturation by proteolysis

Unregulated proteolysis is a dangerous thing in any living cell, so the need for strict activation regimes or substrate specificity is essential. Many proteases are therefore produced as inactive precursors, or zymogens, that require removal of auto-inhibitory peptides. Other classes of proteins are produced as precursors and require limited proteolysis to assume their final conformation. The activation of vacuolar processing enzymes (VPEs) and their involvement in storage protein maturation and breakdown brings together an example of both proteolytic activation and maturation.

Four VPEs exist in *Arabidopsis* – two vegetative (α and γ) and two seed (β and δ) specific versions, however they are all expressed to some degree in developing seeds (Gruis et al., 2002). The vegetative VPEs are located in lytic vacuoles in leaves, whereas seed VPEs are found in protein storage vacuoles (Kinoshita et al., 1999). VPEs are produced as inactive zymogens that are activated in an acidic environment, such as that found in vacuoles (Hiraiwa et al., 1999; Kuroyanagi et al., 2002). Cleavage of a C-terminal auto-inhibitory peptide is carried out by the VPE protein itself, activating the protease. The VPE family of proteases have roles in programmed cell death following infection (Yamada et al., 2004; Kuroyanagi et al.,

2005), various stresses (Kinoshita et al., 1999) and during senescence (Hayashi et al., 2001). VPEγ has been shown to activate a carboxypeptidase and degrade an invertase (Rojo et al., 2003). In seeds, VPEδ is involved in seed coat formation (Nakaune et al., 2005), and VPEβ is responsible for maturation of storage proteins (Shimada et al., 2003b).

Specific proteins are stored in seeds as a nitrogen source for germinating seedlings (Muntz, 1998). CRA1, an 11S globulin storage protein, is the single most abundant protein in *Arabidopsis* seeds (Shewry et al., 1995). CRA1 is produced as an ~50 kDa protein that is transported to protein storage vacuoles (PSVs; Shimada et al., 2003a). The CRA1 precursor is cleaved by VPE into a ~30 kDa acidic α-peptide linked to a ~20 kDa basic β-peptide by a single disulphide bond (Dickinson et al., 1989; Gruis et al., 2004). Mature CRA1 monomers are assembled into stacks of hexamer units (Jung et al., 1998). Although both VPE and CRA1 proteins remain in the same PSVs in dry seed, susceptible protein bonds in CRA1 are hidden within the structure, granting protection from further degradation by VPE. Given the role of VPEβ in seed storage maturation, defects in seedling germination and development would be expected in *vpeβ* mutants. In fact, this is not observed. Apart form accumulation of differentially processed seed storage proteins, no gross morphological phenotypes were observed in a quadruple *vpeα/vpeβ/vpeγ/vpeδ* mutant (Gruis et al., 2004). However, there is an alternate, non-VPE pathway for processing seed storage proteins (Gruis et al., 2002). During germination, the seed storage proteins are degraded to provide amino acids for protein synthesis in the growing seedling. The highly ordered protein storage structures are attacked by proteases, manufactured *de novo* during germination, which causes destabilisation leading to open attack by a range of proteases present in the PSVs (Muntz et al., 2001).

Proteolysis plays essential roles in plant life from germination, through development to seed production and finally death. The importance of regulated proteolysis to produce signalling components in plants is becoming more apparent. This has led to the investigation of more unusual types of proteolysis.

1.2. Regulated intramembrane proteolysis

Proteolysis, until relatively recently, was thought to be carried out by proteases in hydrophilic environments, such as the cytoplasm of vacuole. This is due to the requirement for water during the hydrolysis reaction carried out when cleaving a peptide bond. However, a new class of proteases, the intramembrane cleaving proteases (I-CliPs), has changed this view. All I-CliPs are intrinsic membrane proteins, capable of carrying out proteolysis within the plane of the membrane. Indeed, the active site amino acids are contained within the transmembrane domains (TMDs) of these proteases. So far, four classes of I-CliPs have been identified – Rhomboids, Site-2-proteases, Signal peptide peptidases and γ-secretase. Members from each class have been identified within the *Arabidopsis* genome, and some have assigned functions. Here, I will describe prototypical members of each class, and include any information from plant versions that is available, with γ-secretase covered in greater detail in the following section.

1.2.1. Rhomboids

Drosophila melanogaster RHOMBOID 1 (DmRHO1) was discovered through its phenotypic similarities to a group of embryonic mutants (Mayer and Nusslein-Volhard, 1988), however it was not identified as an I-Clip for another 13 years (Lee et al., 2001). In *Drosophila*, the epidermal growth factor (EGF) SPITZ is synthesised and maintained as an inactive precursor resident in the endoplasmic reticulum (ER). SPITZ is structurally similar to human TGFα (TRANSFORMING GROWTH FACTOR ALPHA), and acts in a wide range of developmental processes from dorsal-ventral axis formation to muscle development through EGF receptors (Rutledge et al., 1992). The chaperone STAR is required for the relocation of SPITZ to the Golgi, where SPITZ cleavage is carried out by DmRHO1 to release the EGF-like portion of the protein to be secreted from the cell (Lee et al., 2001; Urban et al., 2001).

A protein with homology to DmRHO1 is present in the bacteria *Providencia stuartii* and is involved in cell-to-cell signalling to monitor colony size, known as quorum sensing. The *P. stuartii* Rhomboid protein, AarA, is responsible for cleavage, and subsequent export of a quorum sensing factor (Rather et al., 1999). Homology between AarA and DmRHO1 is still maintained, as AarA can rescue *rho1* mutants, and vice versa. Many Rhomboid-like proteases exist, with their structures being conserved throughout the prokaryotic and eukaryotic kingdoms. Proteolytic cleavage takes place through the active site GxSx motif in TMD 4 and a histidine in TMD 6 (Lemberg and Freeman, 2007a). Crystal structures of purified bacterial Rhomboids have been resolved, and show the active site serine residue within a water filled indentation in the membrane (Wang et al., 2006b; Lemberg and Freeman, 2007b). This is formed from a number of TMDs surrounding a shorter α-helix containing the GxSx motif, in close proximity to the histidine from TMD 6, proving that this is capable of activating the serine nucleophile. How substrates enter the active site is still unknown, but two hypothesises exist – from the "front" between TMDs 1 and 3, or from the "back" through TMDs 2 and 5 (Freeman, 2008). A number of gating mechanisms have also been described, but no structures of Rhomboid-substrate complexes exist to prove any of them. Rhomboids recognise specific TMD features of substrates – the first seven residues of the TMD in DmSPITZ are enough to convert a non-substrate protein to a substrate (Urban and Wolfe, 2005). The other classes of I-CliPs require cleavage of the substrate by another protease prior to intramembrane proteolysis. Rhomboids, however, are able to carry out proteolysis without the need for this cleavage.

Arabidopsis contains 15 genes predicted to encode RHOMBOID-LIKE proteins, AtRBL1 to 15 (Kmiec-Wisniewska et al., 2008). Of these, the Golgi localised AtRBL2 has been shown to be capable of intramembrane cleavage. This was performed by expression of AtRBL2 in a mammalian cell line, where it was able to cleave DmSPITZ, but not HsTGFα (Kanaoka et al., 2005). This shows that plant Rhomboids have some substrate specificity, however, since the epidermal growth factor system does not exist in plants identification of substrates will not be trivial. For example, like the yeast Rhomboid PCP1, AtRBL12 is located in the

mitochondria. Assays carried out with AtRBL12 showed that it was unable to cleave known substrates of PCP1 (Kmiec-Wisniewska et al., 2008). So far, no native substrates for the AtRBLs have been identified.

1.2.2. Site-2-proteases

Site-2-proteases (S2Ps) are metalloproteases and carry out the second cleavage of certain membrane bound transcription factors. A substrate for HsS2P is STEROL-REGULATORY ELEMENT BINDING PROTEIN (SREBP), a large precursor with a bHLH TF domain at the N-terminus of the protein. In animal cells, SREBP is bound in the ER in a hairpin conformation, with both N- and C-termini located in the cytoplasm, and hence unable to affect transcription (Bengoechea-Alonso and Ericsson, 2007). Under conditions of cholesterol starvation, the sterol sensing chaperone SCAP (SREBP-CLEAVAGE ACTIVATING PROTEIN) transports SREBP to the Golgi, where cleavage takes place (Edwards et al., 2000). SREBP is first cleaved by a site-1-protease (S1P) in its lumenal loop allowing it to be processed by S2P, which releases the bHLH TF to travel to the nucleus (Rawson et al., 1997). S2P exists in the ER with SREBP, however cleavage of the STRBP TMD does not take place without prior cleavage by S1P. Relocating S1P to the ER is sufficient to cause constitutive SREBP signalling, showing that S1P cleaved SREBP is sufficient for S2P mediated cleavage (DeBose-Boyd et al., 1999). This method of regulation is similar to DmRHO1 cleavage of SPITZ, in that protease and substrate are kept in separate compartments until a signal is perceived, which allows transport of substrate to protease. The major difference is that Rhomboids are able to cleave unmodified proteins, but S2Ps require processing of their substrates by another protease.

E. coli bacterial responses to envelope stress, such as heat-shock, are mediated by the TF SIGMA-E (σ^E (Ades, 2008). Under normal growth conditions, σ^E is maintained in an inactive complex with the N-terminal cytoplasmic domain of the type II transmembrane protein RseA. Following envelope stress, DegS recognition of unfolded proteins in the outer membrane leads to DegS activation and cleavage of the C-terminal domain of RseA (Campbell et al., 2003; Young and Hartl, 2003).

This cleaved RseA becomes a substrate for RseP (Akiyama et al., 2004), a metalloprotease with homology to animal S2P. Following release from the membrane, RseA is degraded by ClpXP to release σ^E to initiate transcription of factors to restore membrane integrity (Flynn et al., 2003).

Important motifs have been identified in three of the core TMDs of S2Ps (Kinch et al., 2006). The HExxH motif in TMD2 contains the catalytic glutamate (E) and two of the metal co-ordinating amino acid residues (both histidines (H)). TMD3 contains a GxxxN/S/G motif, and GxxxG has been shown to be important in helix packing (Russ and Engelman, 2000). The third zinc binding residue, an aspartate (D), is placed in TMD4 in the NxxPxxxxDG motif. Indeed, the resolved structure of a bacterial S2P homologue shows a single zinc ion co-ordinated by the two histidines and the aspartate, and presumably a water molecule, with the glutamate in a position to activate the water molecule for proteolysis (Feng et al., 2007). A potential gating mechanism was also suggested by the conformation of two S2P molecules in the crystal structure. In the "closed" state, TMDs 1 and 5/6 are adjacent to each other and restrict access to the active site. A pore leading to the active site, large enough to admit water molecules and lined with polar residues is formed on the cytoplasmic face in this conformation. To allow substrate access, TMD 1 is rotated away from TMD2 and TMDs 5/6 move slightly away, forming a channel the length of the protein that exposes the active site. These pore and channel conformations show a different way of granting access to water than the indentation formed in Rhomboids.

Under conditions of ER stress, such as caused by the drug Tunicamycin (TM) which inhibits N-glycosylation and leads to the unfolded protein response (UPR), there is a general upregulation of genes, including those that create a more optimal protein folding environment in the ER. The mammalian ER stress sensing protein ATF6 (ACTIVATING TRANSCRIPTION FACTOR 6) is proteolytically processed by S1P and S2P, the same proteases responsible for release of SREBP (Ye et al., 2000). Liu *et al*. (2007) identified an *Arabidopsis* transcription factor (bZIP28) resident in the ER, which is released and translocated to the nucleus following a stress response to Tunicamycin. The same group also reported that a related TF (bZIP17) is released

from the ER following salt stress (Liu et al., 2008). The release of bZIP17 is dependent on *Arabidopsis* S1P, leading to the assumption that it is an *Arabidopsis* S2P that causes cleavage of the transmembrane domain of bZIP17. However, another TF resident in the ER and released following stress caused by Tunicamycin, pZIP60, is not dependent on the action of the *Arabidopsis* homologues S1P or S2P (Iwata et al., 2008). Six proteins with homology to S2P metalloproteases are predicted in *Arabidopsis* (Kinch et al., 2006). EGY1 was isolated in a screen for ethylene dependent gravitropism mutants and identified as a homologue to the SREBP class of S2Ps located in chloroplasts (Chen et al., 2005). The mutant phenotype associated with *egy1-1* includes lower accumulation of chlorophyll and defects in hypocotyl bending. AraSP, a S2P in the same family as EGY1, is also located in the chloroplast but a knockout is lethal (Bolter et al., 2006). Neither of these two plastid localised S2Ps have any identified substrates.

1.2.3. The GxGD I-CliPs

Proteins have been identified with three common amino acid motifs (GxGD, YD and PAL) in transmembrane domains, from bacteria to higher eukaryotes. Out with the areas surrounding these motifs, little sequence homology is maintained. These proteins fall into the classes of type-IV prepilin peptidases (TFPPs), signal peptide peptidases (SPPs) and presenilins (PS). TFPPs are found only in prokaryotes, while all eukaryotes contain SPPs and only multicellular organisms contain PSs. Members of each group have been shown to carry out intramembrane cleavage, and in every case the aspartate residues in GxGD and YD are essential for proteolysis (Wolfe et al., 1999; LaPointe and Taylor, 2000; Weihofen et al., 2002). Eukaryotic presenilins and SPPs and bacterial TFPPs are not related to *E. coli* Signal peptide peptidase A (SppA), whose structure has recently been solved (Kim et al., 2008). SppA is multimeric membrane-tethered serine protease complex that degrades signal peptides, and has a homologue in the thylakoid membrane of chloroplasts (Lensch et al., 2001).

Type IV pili (TFPs) are hair-like appendages used for transfer of DNA and movement of bacterial cells. TFPs are assembled from pilin subunits, secreted from the cell and processed at their N-terminus to cleave the signal peptide. The *Vibrio cholerae* type IV prepilin TcpA is cleaved by TcpJ, a type IV prepilin peptidase (TFPP; LaPointe and Taylor, 2000). Numerous TFPPs have been identified in other bacteria species, and were the first GxGD I-Clips identified, however at the time their role in RIP was not known.

Many proteins being synthesised contain a leader sequence directing them to the ER. This signal peptide is cleaved by a signal peptidase (SP) to release the nascent protein from the membrane (Blobel and Dobberstein, 1975). Human SIGNAL PEPTIDE PEPTIDASE (HsSPP) is the founding member of a eukaryotic class of GxGD I-Clips and cleaves a subset of membrane embedded signal peptides (Weihofen et al., 2002). At first it was thought that HsSPP was simply acting to clear signal peptides to prevent their build up in the membrane. However, the released peptides have been shown to have various functions. The HIV-1 gp160 protein signal peptide has been found bound to calmodulin in a calcium dependent manner and inhibits its function (Martoglio and Dobberstein, 1998). Also, released signal peptides from viral proteins are bound by the major histocompatibility complex (MHC) class 1 receptors and transported to the cell surface to act as activation signals for T-cell, leading to destruction of the infected cell (Lemberg et al., 2001). Other HsSPP-like proteins (HsSPPL2a, b, c, and 3) have different functions, and locations. HsSPPL2a and b have been shown to cleave TUMOUR NECROSIS FACTOR ALPHA (TNFα; Fluhrer and Haass, 2007). Like other I-Clip substrates, the cytosolic portion of TNFα acts as a transcription regulator. HsSPP2a is located in endosomes, whereas HsSPP2b is sorted to the plasma membrane (Krawitz et al., 2005). Substrates of SPPs show a type II orientation in the membrane, i.e. N-terminus in the cytoplasm and C-terminus in the ER lumen (Wang et al., 2006a).

The final member of the GxGD class of I-Clips is the presenilin/γ-secretase complex. Unlike the other classes of I-Clips, γ-secretase is a heterotetrameric complex with

presenilin at its core. Presenilin and SPP show greater homology to each other in their amino acid sequence than either does towards the TFPPs. Indeed, besides the YD, GxGD and PAL motifs, TFPPs have virtually no homology to the other members of the GxGD class. The γ-secretase complex, as will be described in detail later, cleaves NOTCH, a regulator of animal development (Lai, 2004), and APP, a protein that gives rise to the senile plaques in the brains of Alzheimer's disease patients (Blennow et al., 2006). γ-secretase substrates are almost exclusively type I transmembrane proteins (N-terminus in lumen and C-terminus cytosolic). This it is not surprising, given that presenilin and SPP occupy opposite orientations in the membrane with respect to each other (Friedmann et al., 2004). No high-resolution crystal structures for any of the GxGD I-Clips have been produced, so the conformation of the active site and access to water is not known. However, as γ-secretase exists as a high molecular weight complex, its conformation may be significantly different. Also, SPP appears to form a homodimer (Nyborg et al., 2006), and although the γ-secretase complex was once thought to contain a presenilin homodimer (Schroeter et al., 2003), it has recently been shown to contain only one member of each component (Osenkowski et al., 2009).

Arabidopsis contains six predicted SPP homologues (AtSPP, AtSPPL 1-5; Tamura et al., 2008) and two presenilins (including a single copy of NCT, PEN2 and APH1). AtSPP has the highest similarity to HsSPP and is resident the ER, whereas AtSPPL1 and 2 are located in endosomes. A T-DNA insertion mutant *spp-2* has revealed an essential role for AtSPP in pollen maturation and development (Han et al., 2009), however no substrates have been identified. As yet, no research has been carried out on the predicted *Arabidopsis* PRESENILINs, or the other conserved members of the γ-secretase complex. The next section will comprise a detailed discussion of γ-secretase, including its more noteworthy substrates, mode of action and regulation.

1.3. The γ-secretase complex

γ-secretase is unique among the I-Clips as it is a complex comprised of four proteins – PRESENILIN 1 or 2 (PS1/2), NICASTRIN (NCT), ANTERIOR PHARYNX DEFECTIVE 1 (APH1) and PRESENILIN ENHANCER 2 (PEN2). To date, every multicellular organism studied contains predicted γ-secretase complex members, however single celled eukaryotes, such as yeast, do not. These four core proteins are necessary and sufficient to reconstitute γ-secretase activity in yeast (Edbauer et al., 2003). Like most of the other classes of I-Clips, γ-secretase substrates must be proteolytically processed by another protease prior to intramembrane cleavage by γ-secretase. This section will start with an explanation of each of the four core components, detailing roles for any known motifs, and their function in the γ-secretase complex, followed by complex formation and important animal substrates.

1.3.1. Presenilin

Human *PRESNILIN 1* (*HsPS1*, also known as *HsPSEN1*) was first identified and subsequently cloned due to its involvement as a causative agent in early-onset familial Alzheimer's disease (FAD; Sherrington et al., 1995). A second gene, *HsPS2*, also implicated in FAD, was identified shortly thereafter through homology searches (Levy-Lahad et al., 1995). Knockout mutations of mouse *ps1* (*Mmps1*) causes severe developmental phenotypes, including deformation of the skeleton and loss of neuronal tissue, and animals die shortly after birth (Shen et al., 1997). *Mmps2* mutants, on the other hand, are fertile and survive into adulthood (Steiner et al., 1999). Double mutants, *ps1/ps2*, show an additive effect similar to loss of NOTCH signalling, which is lethal during embryo development (Conlon et al., 1995; Herreman et al., 1999). Most studies into PRESENILN/γ-secretase focus on PS1, due to the more severe phenotypes associated with mutations in PS1, and hence more information is available on γ-secretase complexes containing PS1.

PS1 and 2 are intrinsic membrane proteins, the current model showing them to pass through the membrane nine times, with the N-terminus in the cytoplasm (Fig 1.1;

Laudon et al., 2005; Spasic et al., 2006). Like the other members of the GxGD I-Clips, the PRESENILINs contain the active site aspartic acids, buried within the plane of the membrane. However, for a number of years following the discovery of HsPS1, the make-up of the active site was in question. Labelling of the aspartate residues with γ-secretase specific inhibitors, and functional chimeric protein fusions has proven that these aspartates are responsible for proteolysis (Li et al., 2000b; Yamasaki et al., 2006). TMD 6 contains the first aspartate, in the YD motif, with the GxGD motif residing in TMD 7. Mutation of either of these aspartates leads to loss of function of the γ-secretase complex (Wolfe et al., 1999). In addition, the first proline (P) within the highly conserved PAL(P) motif in TMD 9 is essential to active site conformation and activity (Tomita et al., 2001; Wang et al., 2006a; Sato et al., 2008).

PRESENILIN undergoes endoproteolysis to a dimer of N- and C-terminal fragments (PS-NTF/CTF), prior to activation of γ-secretase. This cleavage takes place within the large cytoplasmic loop, at the amino side of a conserved valine residue (between M292 and V293 with respect to HsPS1; Brunkan et al., 2005). It is thought that this endoproteolysis is autoproteolytic and carried out by an immature version of γ-secretase prior to a conformational change into the active complex (Brunkan et al., 2005). Cleavage is blocked by some γ-secretase specific inhibitors (Campbell et al., 2002) and requires both active site aspartates (Wolfe et al., 1999). Although some lines of evidence point toward dimerisation of PS, such as co-immunoprecipitation of PS1-NTF with PS1-NTF (Schroeter et al., 2003), yeast two-hybrid studies showing interaction between NTF:NTF and CTF:CTF (Cervantes et al., 2001), and the fact that active SPP exists as a dimer (Nyborg et al., 2006), PS does not form a dimer within γ-secretase (Osenkowski et al., 2009) and nor does it require interaction between two γ-secretase complexes for endoproteolysis (Brunkan et al., 2005). Mutation of M292 and V293 lowers, but does not completely abolish, HsPS1 endoproteolysis, and physiological levels of substrate processing remain (Brunkan et al., 2005). However, cleavage of PS is not necessarily essential for γ-secretase

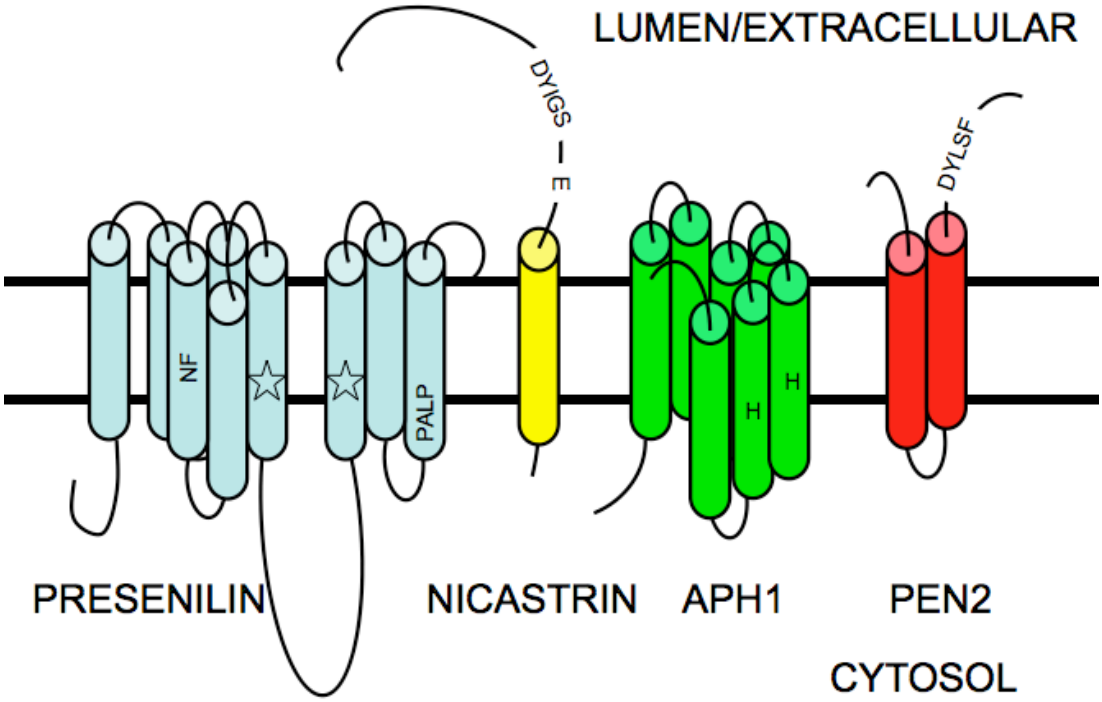

Fig 1.1 Members of the γ-secretase complex. Cartoon representations of the four core components required for γ-secretase activity. PS (blue) contains nine TMDs, with the active site aspartate residues in TMDs 6 and 7, represented by stars. The PALP motif in TMD 9 is also part of the active site. TMD 4 harbours the NF motif required for PEN2 incorporation. The large cytoplasmic loop is cleaved prior to activation of the complex. NCT (yellow) is a large type I membrane protein, with the DAP region, containing the DYIGS motif and E333, located N-terminally of the single TMD. APH1 (green) has functions in stabilisation of the complex and potentially in active site conformation through the histidine (H) residues in TMDs 5 and 6. PEN2 (red) occupies a hairpin conformation in the membrane, with both N- and C-termini lumenal. The DYLSF in HsPEN2 has functions in stabilisation of PS-NTF/CTF fragmants following endoproteolysis.

function. A natural FAD mutation in HsPS1, which removes exon 9 (HsPS1ΔE9) and is missing 30 amino acids around the area of the cleavage site, does not form NTF/CTF fragments but is still active (Lee et al., 1997). Mutations in HsPS1 that stop endoproteolysis (changing the active site aspartates or proline) also lead to inactivation of HsPS1ΔE9 containing γ-secretase complexes (Wolfe et al., 1999; Wang et al., 2004). Therefore, endoproteolysis of wild type (non-mutant) PS is a hallmark of γ-secretase activity.

1.3.2. Nicastrin

NICSTRIN (NCT) was the second member of the γ-secretase complex discovered. It is a large type I transmembrane glycoprotein, with a short cytoplasmic C-terminal tail (Fig 1.1). NCT is thought to act in substrate recognition, amongst other activities. A portion of the protein within the lumenal/extracellular N-terminus (residues 306-360 of HsNCT) that contains the well conserved DYIGS motif (Yu et al., 2000) and shows some homology to a peptidase, has been named the DAP domain (for DYIGS and peptidase homology; Shah et al., 2005). Deletion mutants spanning parts of the DAP domain lead to a decrease in γ-secretase activity, however specific mutations within the DYIGS motif (DY to AA) resulted in an increase in substrate processing (Murphy et al., 2003). The loss of γ-secretase activity caused by deletions in the DAP domain may be the result of a decrease in association between NCT and PS (Yu et al., 2000), or the loss of a highly conserved glutamate residue (E333 in HsNCT). The carboxylate side chain of E333 is thought to interact with the free amino terminus of the substrate (Shah et al., 2005). The reason for this is that mutation of E333 to any amino acid, other than aspartate, leads to inactivation of γ-secretase. Other evidence also supports NCT acting in substrate recognition. The γ-secretase substrates APP and NOTCH can both be found physically associated with the NCT ectodomain (Chen et al., 2001; Shah et al., 2005).

The assembly of γ-secretase will be covered in more detail later, however some important facts must be covered prior to that. Maturation of PS through

endoproteolytic cleavage is one of the hallmarks for active γ-secretase. Another indicator of activity is the accumulation of a mature, glycosylated form of NCT (mNCT; Arawaka et al., 2002). During trafficking through the secretory pathway, NCT undergoes glycosylation in the Golgi apparatus. In cells lacking PS, immature NCT (iNCT) accumulates in the ER in a minor sub-complex with APH1 (Herreman et al., 2003). Different evidence raises the question over the necessity of glycosylation in γ-secretase activity. One group showed that the level of overexpression of iNCT did not affect ammount of γ-secretase activity, and that it was only heightened mNCT levels that increases γ-secretase activity (Arawaka et al., 2002). However, following inhibition of the glycosylation machinery in the ER/Golgi, active γ-secretase is still found at the plasma membrane (Herreman et al., 2003).

1.3.3. APH1 and PEN2

ANTERIOR PHARYNX DEFECTIVE 1 (APH1) and PRESENILIN ENHANCER 2 (PEN2) were both first discovered in genetic screens in *C. elegans* (Francis et al., 2002; Goutte et al., 2002). Various model animal systems contain different numbers of APH1 homologues – *C. elegans* contains just one (*CeAPH1*), whereas two *APH1* genes exist in humans (*HsAPH1a* and *b*) and mice encode three (*MmAPH1a, b* and *c*), which form discreet γ-secretase complexes (Shirotani et al., 2004b). The mice genes show regulated tissue expression and discreet roles in development. A mouse *aph1a* knockout mutation is embryo lethal, however the double *aph1b/aph1c* double mutants do not show a phenotype (Serneels et al., 2005). APH1 contains seven TMDs (Fig 1.1), and until recently was thought to act solely in complex stabilisation (Niimura et al., 2005). In particular, a known α-helix structural motif, GxxxG, is present in TMD 4 of APH1 and is important for interactions with NCT and PS. Mutation of the first glycine (G) residue in this motif causes destabilisation of the early sub-complex between APH1 and NCT, leading to proteasomal degradation of APH1 (Niimura et al., 2005). This destabilisation may be due to a loss of stability within the APH1 protein itself. Recently, (Pardossi-Piquard et al., 2009) attributed further functions to APH1. A pair of highly conserved histidine residues, one in

TMD 5 and the other in TMD 6, have a potential role in active site conformation. Mutation of either histidine to an amino acid with an uncharged or acidic side chain disrupts binding of other γ-secretase complex members. Conservative mutations to lysine allowed maturation of NCT and PS (glycosylation and endoproteolysis respectively) and formation of what appears to be active γ-secretase, however substrates cannot be processed.

The final member of the complex is PEN2. This small protein occupies a hairpin conformation in the membrane with both N- and C-termini located in the lumen of the ER/extracellularly (Fig 1.1). PEN2 is required for endoproteolysis of PS, however PEN2 is not thought to have any native proteolytic activity itself. The N-terminal two thirds of HsPEN2 TMD 1 is essential for association with a well-conserved NF motif in PRESENILIN TMD 4, and subsequent endoproteolysis (Kim and Sisodia, 2005a, b). This was shown through production of chimeric proteins, where portions of PEN2 TMD 1 were replaced with the corresponding parts of the membrane spanning helix of an unrelated protein, and functionality measured by their ability to co-immunoprecipitate PS1-CTF. Aside from its role in PS endoproteolysis, PEN2 is required for stabilisation of the PS-NTF/CTF dimer (Prokop et al., 2004). A motif in the C-terminal tail, conserved between human and mouse PEN2 as DYLSF, is necessary for interactions between PEN2 and other members of the γ-secretase complex following endoproteolysis of PS (Hasegawa et al., 2004). Therefore, although other species do not contain a perfectly conserved DYLSF motif, this may be due to evolutionarily sequence variation in the other proteins at the point of interaction.

In summary, PRESENILIN contains the active site aspartate residues, NICASTRIN functions in substrate recognition, APH1 acts in stabilisation and active site conformation, and PEN2 is necessary for endoproteolysis of PS and stability of the mature complex. The various homologues of PS and APH1 form distinct complexes, i.e. there are two possible in *C. elegans*, four in humans and six in mice. This gives rise to the possibility of each complex having different roles in substrate specificity and therefore function.

1.3.4. Complex formation

Despite vast amounts of research, the precise order of γ-secretase complex formation is still not clear. Immature NCT and APH1 form a stable sub-complex in the ER (Hu and Fortini, 2003), and in *presenilin* knockout lines NCT is retained in the ER and does not become glycosylated (Niimura et al., 2005). Certain pieces of information point towards a sequential addition of the final two complex members, whereas other evidence indicates another sub-complex between PS1 and PEN2. A short-lived pool of PS1 is present, however it is rapidly degraded, with a half-life of only 1-2 hrs (Ratovitski et al., 1997). It is thought that some of this PS1 holoprotein pool is stabilised through interactions with other proteins. In the absence of PEN2 protein (*pen2* knockout lines), PS1 holoprotein is stably accumulated in a complex with iNCT and APH1, found in the ER and Golgi (Capell et al., 2005; Niimura et al., 2005), suggesting stabilisation of PS1 precedes PEN2-dependent endoproteolysis and activation. However, PS1 holoprotein has been shown to associate with PEN2 in the absence of NCT or APH1, suggesting that addition of PS1 to the NCT/APH1 sub-complex is in the form of a heterodimer with PEN2 (Fraering et al., 2004). Which of these scenarios is correct is not clear at the present time, but greater evidence is available for the stepwise addition of PS1 and PEN2. Therefore, a working model of complex formation is shown in Figure 1.2. PS1 holoprotein alone is unstable and degraded, but is stabilised when incorporated into a sub-complex with iNCT and APH1. PEN2 association with the complex likely takes place in the ER, as PEN2 is retained in the ER in the absence of PS1 (Bergman et al., 2004). Endoproteolysis of PS1 potentially takes place in the ER (Capell et al., 2005; Kim et al., 2007), where NCT becomes glycosylated (Morais et al., 2006). The active γ-secretase is transported through the secretory pathway where it cleaves substrates in the plasma membrane or endosomes (Kaether et al., 2006).

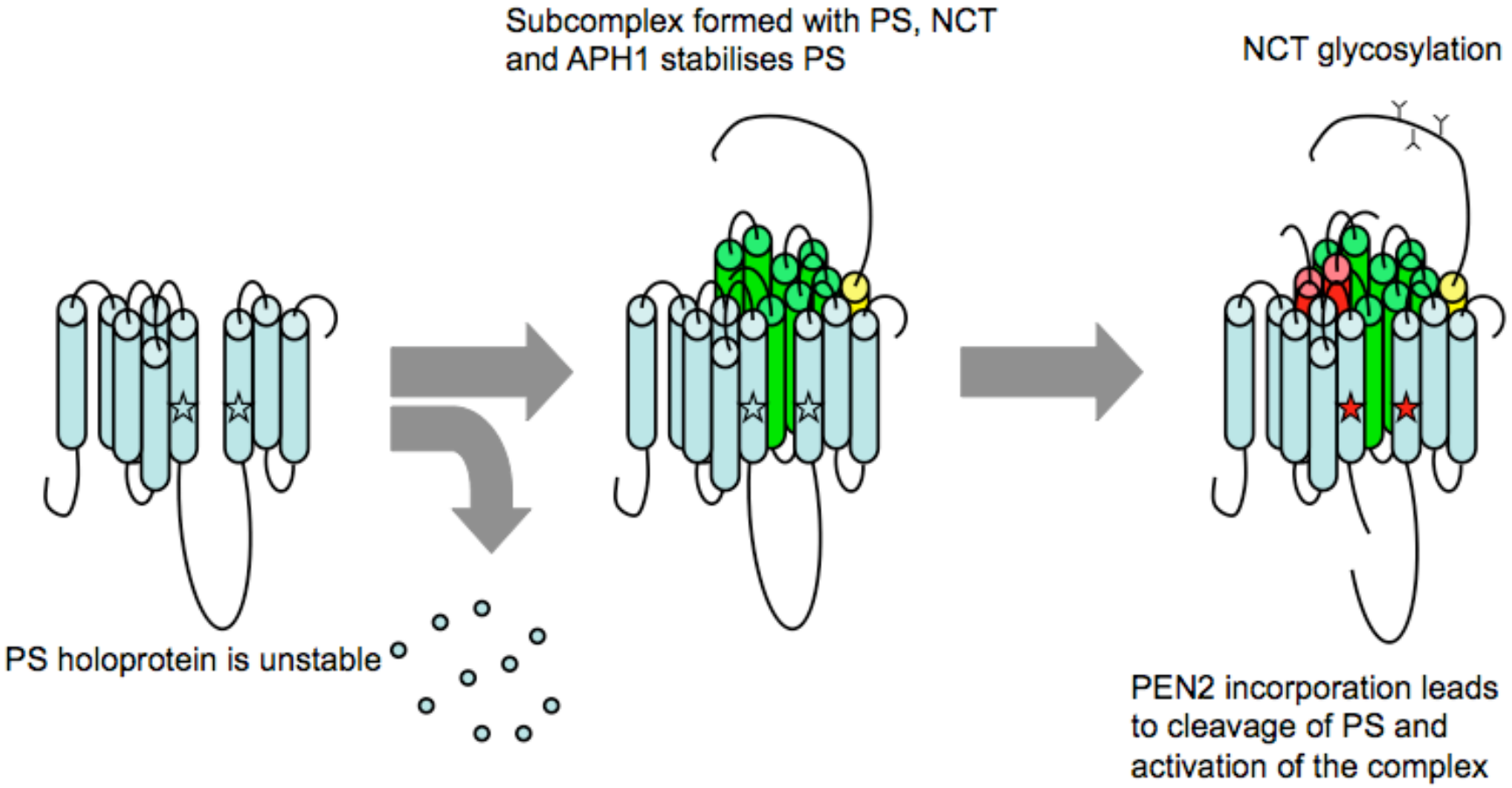

Fig 1.2 γ-secretase complex formation. The PS holoprotein has a short half-life and is degraded by the proteasome. However, when in a complex with APH1 and iNCT, PS becomes stabilised. It is not clear at which point PEN2 enters the complex, however its presence is necessary for endoproteolytic cleavage and activation of PS. Passage through the secretory pathway leads to glycosylation of the lumenal domain of NCT.

Intermolecular interactions within the γ-secretase complex are thought to mainly take place within the transmembrane domains of each protein. The transmembrane domain and a small portion of the lumenal juxtamembrane domain of NCT are essential for interactions with APH1 (Morais et al., 2003). Also, mutation of the GxxxG motif in APH1 TMD 4 results in destabilisation of interactions between NCT and PS (Niimura et al., 2005). Various detergents are used in research into membrane bound proteins, such as Triton-X100, Digitonin, DDM and CHAPS. TritonX-100 is not used in research into γ-secretase as it causes dissociation of the complex members (Li et al., 2000a). DDM, at a concentration of 0.5% is routinely used to solubilise membranes containing animal γ-secretase complexes, however raising the concentration to 1% causes destabilisation, and results in smaller inactive complexes. This higher concentration of detergent has been used as a research tool to identify which proteins in the γ-secretase complex interact with each other (Fraering et al., 2004). The inactive complexes discovered include NCT/APH1, NCT/APH1/PS1-CTF, PEN1/PS1-NTF and PS1-NTF/CTF. These dissociation complexes are supported by other investigations – APH1 and NCT forming an early sub-complex (Hu and Fortini, 2003) and the NF motif in PS1 TMD 4 and TMD 1 of PEN2 interaction (Kim and Sisodia, 2005a, b). A recent chemical cross-linking study revealed direct interactions between PS1-NTF/CTF, PEN2-PS1-NTF, NCT/APH1, APH1/PS1-CTF and NCT/PS1-CTF (Steiner et al., 2008), very similar to the subcomplexes seen following DDM mediated dissociation.

The Li group have made advances in elucidating the structure of γ-secretase through electron microscopy (EM) of purified active complexes. At first, a low-resolution structure revealed a large barrel shaped complex with pore-like structures facing the cytoplasm and extracellular space (Lazarov et al., 2006). The active site aspartate residues were believed to reside within the complex, within a hydrophilic interior chamber. Thus, it was postulated that proteolysis would take place in the interior chamber and the cleaved substrate pieces could exit through the holes at the "top" and "bottom" of the complex. Following production of a new cell line that could produce five times more γ-secretase complex than the original line they used, other methods of EM were possible. Cryo-EM was used to produce a 12Å resolution

structure, revealing more features of active γ-secretase (Fig 1.3; Osenkowski et al., 2009). The cytoplasmic region was found to be relatively small and smooth compared to the large, irregular extracellular region. Also, the extracellular region was divided into four distinct domains (differently coloured sections in Fig 1.3a). The main difference seen between the low- and high-resolution structures is the existence of multiple interior chambers and a membrane-facing groove (red dotted lines in Fig 1.3b and solid red line in Fig 1.3a respectively). Other classes of I-Clips that have determined crystal structures (the bacterial Rhomboid GlpG and mjS2P) have shown similar features. The membrane-spanning groove is thought to act in substrate docking, whereas the interior chambers presumably give access for water molecules to the active site. Due to the presence of four different proteins, containing numerous transmembrane domains, no crystal structure for γ-secretase has yet been produced to show the location of important structural motifs.

Although γ-secretase is a unique protease with a complex assembly mechanism, research into the γ-secretase complex is largely due to its substrates, and the roles they play in animal development and disease. The following sections will describe the role of γ-secretase in a typical signalling cascade (NOTCH signalling) and the role of γ-secretase as a causative agent in Alzheimer's disease (through APP processing).

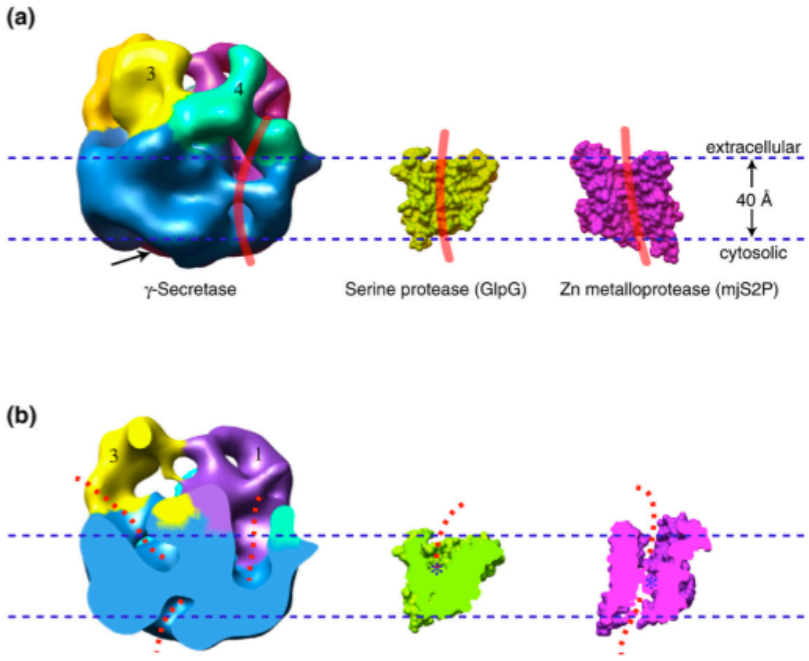

Fig 1.3 12Å resolution cryo-EM structure of active γ-secretase. The γ-secretase complex is a lot larger than the monomeric I-Clips of the Rhomboid (GlpG) and S2P (mjS2P) classes. The extracellular region of γ-secretase can be divided into four sub-domains, represented here by various colours. Although they do not share any sequence homology, the three I-Clips depicted here all share some structural similarities. Each has a membrane-facing grove potentially for substrate docking, depicted by red lines in (a), and water access routes to the active sites, shown by dotted red lines in (b). Taken from Osenkowski et al. (2009).

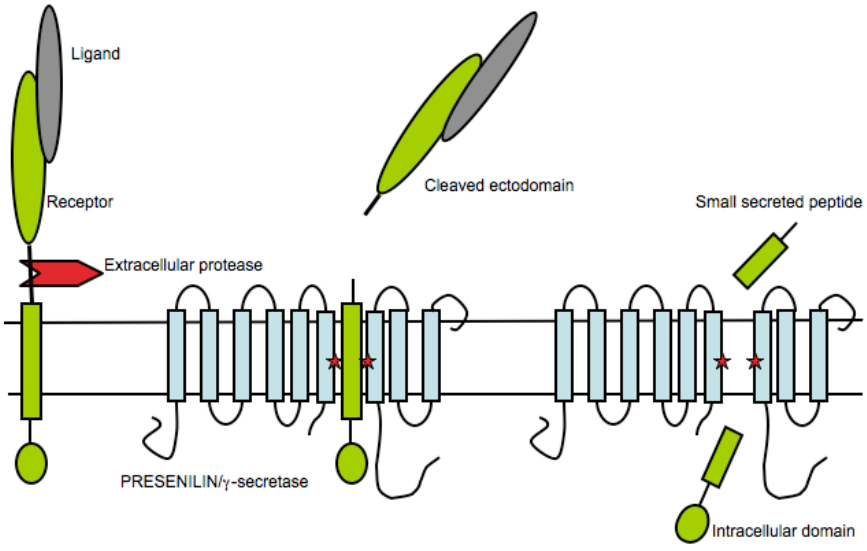

Fig 1.4 Proteolytic cascade of γ-secretase signalling. Following receptor-ligand (green-grey) interaction, the membrane bound receptor is cleaved close to its transmembrane domain by an extracellular protease (red). γ-secretase (depicted by PRESENILIN only; blue) recognises the extracellular stump of its substrates, and carries out the second step in the proteolytic cascade. In many cases, the intracellular domain translocates to the nucleus to act as a transcriptional regulator, and the small secreted peptide is degraded.

1.3.5. NOTCH

Animal body plans, unlike those of plants, are laid down during embryogenesis and relatively few signalling cascades are responsible for the developmental switches between cell types. The NOTCH signalling pathway is responsible for a range of diverse cell-fate choices, such as that between neuronal and epidermal cells in *Drosophila* (reviewed in Lai (2004)). Disruption of NOTCH signalling in humans leads to a range of diseases, mainly associated with abnormal tissue differentiation (Gridley, 2003). The NOTCH protein is a large type I transmembrane protein that is well conserved throughout the animal kingdom, and is a prime example of a signalling cascade involving the γ-secretase complex.

During trafficking from the ER, NOTCH is first cleaved by a furin-like convertase in the *trans* Golgi, at the so-called S1 site, to arrive at the plasma membrane as a non-covalently bound NTF/CTF heterodimer (Logeat et al., 1998; Kidd and Lieber, 2002). NOTCH ligands of the DSL class (for DELTA, SERRATE/JAGGED of *Drosophila* and humans and LAG2 of *C. elegans*) are expressed in and displayed at the cell surface of adjacent cells. DSL ligands are also mainly type I transmembrane proteins. Receptor-ligand binding causes a conformational change in the NOTCH ectodomain, resulting in exposure of a previously hidden proteolytic cleavage site (Gordon et al., 2007). This site, termed S2, is recognised by a member of the metalloprotease ADAM family, which cleaves the extracellular domain of NOTCH-CTF approximately 12 amino acids from the membrane (Brou et al., 2000). This membrane bound NOTCH extracellular truncation (NEXT) is now a substrate for γ-secretase. Cleavage of NEXT takes place within the transmembrane domain, at site S3 towards the membrane-cytoplasm interface, to release NOTCH intracellular domain (NICD; De Strooper et al., 1999). The NICD is transported to the nucleus where it, in conjunction with other factors, regulates transcription of a range of factors (Struhl and Adachi, 1998). Intriguingly, the DSL ligands are also processed in a similar way by an ADAM protease and γ-secretase to release an active signalling intracellular domain (ICD; Ikeuchi and Sisodia, 2003; LaVoie and Selkoe, 2003). As

these protein ligands are membrane bound, NOTCH/DSL mediated signalling takes place between adjacent cells, setting up defined boundaries between cell types. See Figure 1.4 for a simplified version of this proteolytic cascade.

During animal development, the NOTCH signalling pathway can trigger identical cells to differentiate into unrelated tissues. Numerous in-depth reviews are available, detailing the specific roles of the NOTCH signalling pathway in various aspects of metazoan development (for example Campos-Ortega, 1993; Portin, 2002; Iso et al., 2003; Callahan and Egan, 2004; Katsube and Sakamoto, 2005). The model of NOTCH "lateral inhibition" relies on the positive and negative feedback loops set up through NOTCH and DSL ligand transcriptional regulation. Initially, the two adjacent cells both express similar amounts of NOTCH and ligand, however small differences in protein levels occur over time. If one cell starts to produce slightly more NOTCH protein than the other, NICD levels are elevated and NICD mediated transcription leads to an increase in *NOTCH* transcription and downregulation of ligand. Therefore, the adjacent cell will stop receiving signal, so becoming the "signal sending" cell. The definition of signal sending and signal receiving cells seems fairly arbitrary, an assignment made due to the discovery of NOTCH prior to its ligands. Ligand ICD signalling leads to *NOTCH* downregulation and ligand upregulation within the signal sending cell. Thus, small differences in the NOTCH or ligand level in a cell leads to a great imbalance between two adjacent cells, and subsequently a different choice in differentiation. However, the factors responsible for this initial imbalance are not understood as yet.

NOTCH signalling is a typical example of γ-secretase mediated transcriptional regulation – perception of ligand leads to ectodomain shedding to produce a membrane anchored protein with a short extracellular stump that is recognised by γ-secretase and processed to release the intracellular domain. However, the ICD is not the reason for interest in APP, as it is the small secreted peptide that causes the plaques found in brains of Alzheimer's disease patients.

1.3.6. AMYLOID-β PRECURSOR PROTEIN

Alzheimer's disease (AD) is a neurodegenerative disorder affecting millions of people worldwide (Blennow et al., 2006). Over 90% of AD cases are sporadic and affect people over the age of 65, whereas the remainder of AD suffers show early-onset symptoms due to heritable mutations in a few select genes known as familial Alzheimer's disease (FAD). These mutations are mainly associated with PS1 and 2 and the AMYLOID-β PRECURSOR PROTEIN (APP). AD is becoming a greater problem as more of the world's population is surviving into later age. The hallmarks of AD are amyloid plaques and neurofibrilary tangles in patient's brain tissue. These amyloid plaques are formed of Aβ peptides, a small piece of the APP produced by sequential processing by β- and γ-secretases.

APP is expressed throughout the human body, and processing is a regular cellular event. Non-amyloidgenic processing takes place through primary cleavage by α-secretase (an ADAM metalloprotease) releasing the α-APP ectodomain, followed by γ-secretase cleavage to release the APP intracellular domain (AICD) and a small secreted peptide, p3 (Fig 1.5; Haass and Selkoe, 1993). α-secretase cleavage takes place within the Aβ peptide sequence, hence the lack of formation of an amyloidgenic peptide in this case. However, APP can also be processed by β-secretase, also known as β-site APP CLEAVING ENZYME (BACE), at the N-terminus of the Aβ peptide, resulting in a 99 amino acid membrane anchored C-terminal fragment (CTF_{99}). Subsequent cleavage by γ-secretase releases AICD from the membrane, but also produces a variety of small secreted peptides of 39-43 amino acids in length. Of these peptides, Aβ-40 and Aβ-42 (referring to the size of the peptide) are the most abundant (Kirkitadze and Kowalska, 2005). While both Aβ-40 and Aβ42 are cytotoxic, Aβ-42 is insoluble and acts as a "seed" for amyloid plaque formation, and only mature plaques contain Aβ-40 (Iwatsubo et al., 1994). Many of the mutations that lead to FAD are found in PRESENILIN1 and APP, and lead to the generation of the longer, amylogenic form of Aβ. Due to this amylogenic processing mechanism, β- and γ-secretases are important targets for AD drugs.

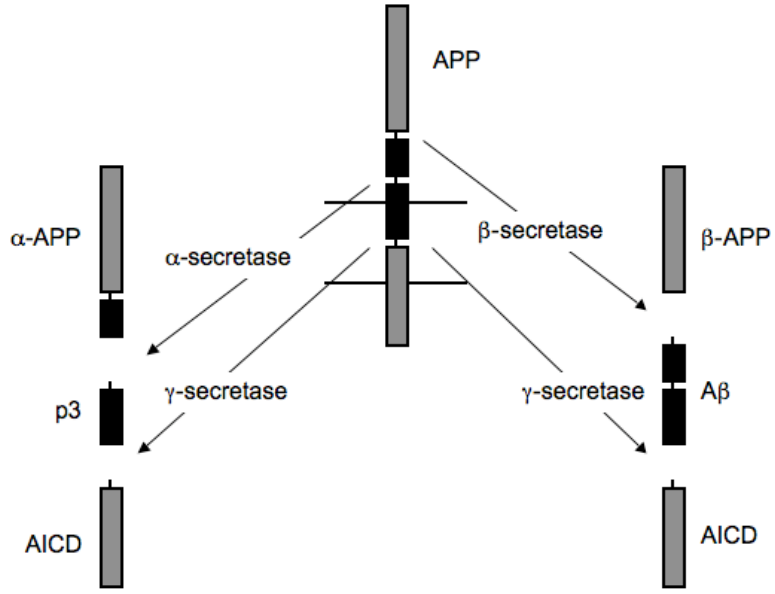

Fig 1.5 APP processing via α- and β-secretases. APP is a type I transmembrane domain protein, cleaved by extracellular proteases to release its soluble ectodomain. α-secretase cleaves within the Aβ peptide (black rectangles within APP) and hence acts in the non-amyloidgenic APP signalling pathway. β-secretase, however, cleaves APP at the N-terminus of the Aβ peptide, allowing the release of amyloidgenic Aβ-40/42 fragments following cleavage by γ-secretase.

However, the γ-site cleavage that gives rise to Aβ-40/42 is not the only activity associated with γ-secretase. The intracellular domain of APP found in cells is comprised of amino acids 50-99 ($AICD_{50-99}$ produced from the CTF_{99} fragment), but no Aβ-49 moiety has ever been detected. It is believed that γ-secretase cleaves CTF_{99} at three sites, termed γ-, ε-, and ζ-sites. ε-site cleavage releases $AICD_{50-99}$ from the membrane, with a cut in a similar place to the S3 cleavage that releases NICD (Zhao et al., 2005). A second cleavage takes place at the ζ-site, between amino acids 46 and 47, to produce an intermediary Aβ-46 moiety that is further processed to release Aβ-40/42 (Weidemann et al., 2002). NOTCH also undergoes further cleavage by γ-secretase, at a S4 site towards the middle of its TMD, releasing an Aβ-like peptide, called Nβ (Okochi et al., 2002). More similarities exist between NOTCH and APP, as the AICD has recently been shown to translocate to the nucleus

to act in transcriptional regulation (Muller et al., 2008; Slomnicki and Lesniak, 2008).

Nearly all γ-secretase substrates identified to date (over 60 in total) are type I transmembrane proteins, and many of these regulate transcription through their intracellular domain. Further descriptions of γ-secretase substrates, including substrate specificity, will be provided in the introduction to Chapter 6.

This introduction has described some proteolytic processes in plants, from degradation of inhibitory transcription factors in hormone signalling to maturation of proteins through limited proteolysis. The novel form of intramembrane proteolysis carried out by I-Clips has been described for Rhomboids, S2Ps and SPPs, including any *Arabidopsis* specific experimental evidence for these groups of proteases. Finally, a more detailed description of γ-secretase was carried out to include the complex members, formation and activity. No research into the putative γ-secretase complex in *Arabidopsis* has been carried out before now.

1.4. Aims and objectives

PRESENILIN homologues have been identified in every multicellular organism studied to date. Due to the wide-ranging and essential activity of γ-secretase in animal systems, a study of the *Arabidopsis* PRESENILINs and the potential γ-secretase complex is needed. The aims of this project were four-fold:

1) Functional characterisation of the putative *Arabidopsis* γ-secretase complex

2) Expression analysis of the putative *Arabidopsis* γ-secretase complex members

3) Analysis of the physical association between potential components of the *Arabidopsis* γ-secretase complex

4) Initiation of target identification for the *Arabidopsis* γ-secretase complex

2.0. Materials and methods

Unless otherwise stated chemicals were obtained from Sigma-Aldrich Inc., and restriction endouncleases from New England Biolabs (NEB).

2.1. Plant genotyping

2.1.1. Arabidopsis growth conditions and selection on antibiotics

Fully mature and dried Arabidopsis seeds were surface sterilised in 70% EtOH with 0.05% Triton X-100 for 15 mins, followed by a 5 min wash in 96% EtOH. Seeds were resuspended in 96% EtOH and transferred for drying on sterile 3MM filter papers in a sterile tissue culture hood. Seed was sprinkled on 0.5xMS plates (0.5x Murashige and Skoog salt and vitamin mix (Gibco/BRL, Gaithersberg, MD, USA), 0.6% sucrose, 1% microagar (Detroit, MI, USA); pH 5.7 with KOH) containing any appropriate antibiotics (Kanamycin 50 μg/mL, Hygromycin 15 μg/mL). Plates were stratified for at least 2 days at 4°C before being transferred to growth conditions (16 hrs light/ 8 hrs dark, 22°C) for 10-14 days.

Seedlings were transferred to a soil mixture (3 parts soil: 1 part sand: 1 part perlite, with 'Intercept' fungicide (Clydeside Trading Society Ltd, Strathclyde, UK)) and grown under long day conditions (16 hrs light/8 hrs dark, 22°C, 50% humidity). Seedlings were protected from desiccation by covering with clear plastic covers for the first 3-4 days on soil.

Crosses were carried out on 6-7 week old plants by first emasculating 3-5 flowers that had not yet dehisced on a lateral shoot of the acceptor plant. Carpels were hand pollinated the following day with pollen from two flowers from the donor plant. Tweezers used for crosses were rinsed in 70% EtOH between flowers to avoid contamination. Mature seed was collected and stored in air permeable envelopes.

2.1.2. Germination experiments

Modified 0.5xMS was made without ammonium nitrate (2 mM MES, 3 mM $CaCl_2$, 1mM $MgSO_4$, 1 mM K_2HPO_4, 6.2 mg/L H_3BO_4, 0.025 mg/L $CoCl_2.6H_2O$ 0.025 mg/L $CuSO_4.5H_2O$, 37.2 mg/L $Na_2EDTA.2H_2O$, 27.8 mg/L $FeSO_4.7H_2O$, 370 mg/L $MnSO4_4.7H_2O$, 0.25 mg/L $NaMoO_4.2H_2O$, 0.83 mg/L NaI, 8.6 mg/L $ZnSO_4.7H_2O$; pH 5.7 with KOH), and supplemented with 1000x NH_4NO_3 (1M) for control media containing nitrogen.

2.1.3. Genomic DNA extractions

3-4 leaves were removed from 3-5 week old plants grown on soil and frozen in liquid nitrogen. Leaves were ground to a fine powder in 1.5 mL eppendorfs using pre-chilled mini-pestles before mixing with 500 μL extraction buffer (100 mM Tris pH 8.0, 50 mM EDTA, 100 mM NaCl, 1% w/v SDS) and re-freezing until required. Samples were defrosted at 65°C prior to addition of 500 μL phenol/chloroform (1:1 ratio Tris-saturated phenol (pH 7.9): chloroform), vortexed vigorously and incubated at room temp for 5 mins. Phases were separated by spinning at 14,000 rpm for 5 mins and upper aqueous phase recovered to a fresh tube. DNA was precipitated with 50 μL 3 M NaAc (pH5.3) and 350 μL 2-pronanol with gentle mixing, and collected by spinning at 14,000 rpm for 5 mins. DNA pellets were washed in 70% EtOH and air-dried before resuspension in 50 μL R40. 1 μL of a 1/10 dilution was routinely used as template in PCR genotyping reactions.

2.1.4. PCR Reactions

Polymerase chain reaction (PCR) amplification was used exclusively for determination of presence of T-DNA insertions in genes of interest. A master mix was made up for each reaction with: 2 μL 10x PCR buffer (50 mM Tris pH 8.3, 500 μg/mL BSA, 0.5% Ficoll, 1% w/v sucrose, 30 mM KCl, 3 mM $MgCl_2$, 1 mM Tartrazine), 1 μL 10 mM forward primer, 1 μL 10 mM reverse primer, 0.4 μL 10

mM dNTPs (10 mM of each dATP, dTTP, dGTP, dCTP; Roche), 1 μL Taq DNA polymerase and 1 μL genomic DNA dilution in a final volume of 20 μL.

Reactions were carried out in a T3 Thermocycler (Biometra, Gottingen, Germany) with the following program: 94°C for 3 mins, followed by 30 cycles of [94°C for 30 secs, 55-60°C (depending on primers) for 30 sec, 72°C for 1 min per kb amplified]. Reactions were completed at 72°C for 5 mins and stored at 4°C until required.

2.1.5. Agarose gels

1% w/v agarose (Melford, Ipswich, UK) was dissolved in TAE (40 mM Tris-acetate pH 8.0, 1 mM EDTA) by boiling. After cooling to 60-70°C, 0.0005 μg/mL ethidium bromide was added to visualise DNA under UV illumination, and gel allowed to set in Owl moulds (Autogen Bioclear, Santa Cruz, CA, USA) at a thickness of 8-12 mm. PCR samples could be loaded directly onto the gels due to the inclusion of dye and sucrose/Ficoll in the PCR buffer. 1 kb or 100 bp DNA ladders (NEB) were used as size and concentration markers according to manufacturer's instructions. Gels were run at 100 V for 30-40 mins at room temp and visualised on a transilluminator.

2.1.6. Mutant lines

Line	Seed stock	Position from ATG		WT primers		Size of product	Mutant primers		Size of product
ps1-1	SALK 016037	484	exon	5' Sal	3' Xho	1204	Salk LB	3' Xho	975
ps1-2	SALK 016085	554	exon	5' Sal	3' Xho	1204	Salk LB	3' Xho	647
ps1-3	SALK 013158	459	exon	5' Sal	3' Xho	1204	Salk LB	3' Xho	717
ps2-1	SALK 038487	-60	5' UTR	5'	3' Xho	1886	Salk LB	3' Xho	1568
ps2-2	SALK 069469	-85	5' UTR	5'	3' Xho	1886	Salk LB	3' Xho	1583
ps2-3	SALK 145544	942	exon	5' Sal	3' Xho	1681	Salk LB	3' Xho	981
nct1	SALK 106245	3144	exon	3-5'	3-3'	1208	Salk LB	3-3'	381
nct2	WISC DS LOX 502 C 06	1140	exon	2-5'	2-3'	916	WISC LB	2-3'	508
nct3	SAIL 1209 B12	2734	intron	3-5'	3-3'	1208	3-5'	SAIL LB	600
pen2-1	SALK 128110	622	intron	1	2	531	Salk LB	2	370
pen2-2	SALK 140461	875	intron	1	2	531	1	Salk LB	414
pen2-3	SALK 128111	650	intron	3	4	530	3	Salk LB	407
pen2-4	SAIL 103 B 03	1211	3' UTR	5	6	506	SAIL LB	6	502
aph1-1	SALK 118799	1547	exon	1	2	389	1	Salk LB	328
aph1-2	WISC DS LOX 413-416 L 12	1586	exon	1	2	389	1	WISC LB	361
aph1-3	SAIL 1057 G 07	375	intron	3	4	616	SAIL LB	4	551
aph1-4	SAIL 1057 B 03	217	intron	3	4	616	SAIL LB	4	546
aph1-5	SAIL 159 E 06	1335	intron	5	6	369	5	SAIL LB	457

Table 2.1 Mutant lines, including seed stock number, genomic position of insertion from ATG, primers used to amplify both wild type and mutant bands, and expected sizes of products. All mutant lines were obtained from the National *Arabidpsis* Stock Center (NASC).

2.1.7. Primer sequences

Gene	Name	Sequence 5'-3'
PS1	5' Sal	GTCGACACATGGATCGAAATCAAAGACCCAG
PS1	3' Xho	TCAGGCTCGAGCGAACATCACAAGGTTAGAAGAACATTGC
PS1	Bam F	AGGATCCGAACATGTTGGTTCAAGTGAAAGAG
PS1	Bam R	AGGATCCTTCTTCTACTTCTGCTGATTCAACC
PS2	5' Sal	GTCGACACATGGAGTCTAGTATCCTCGATTCCC
PS2	3' Xho	TCAGGCTCGAGGAGACCCGAACATCATCAAGTTTGTTGTCACCCC
PS2	5'	GCCTAATGGGCTGTTATTGTTGT
PS2	Bam F	AGGATCCCCTCTAGTTGGAAGTCCCAGTG
PS2	Bam R	AGGATCCTGACCTCCAAGTCCACCTCTG
NCT	5' Sal	GTCGACACATGGCAATGGGACTTATTCG
NCT	3' Xho	TCAGGCTCGAGGAGACGCCCTGGTTGTGGAGACAACACATGT
NCT	Bam R	AGGTACCTTACGTCTCGGATCTGTCCTGCTTCAAGGCTTTTGTG
NCT	2-5'	TCACTTGGTTGTTGGTGCAT
NCT	2-3'	GCAATGGTCAATGGCTAGAGA
NCT	3-5'	TCAAATGCATGTTGCTTTCC
NCT	3-3'	CACAGGCAACTTTTTCCACA
PEN2	5' Sal	GTCGACACATGGAGGCTACACGGAGCGACG
PEN2	3' Xho	TCAGGCTCGAGCAGCCAAACCAGACAAGCCGAGACG
PEN2	Bam R	AGGTACCTTAGGATCCAGCCAAACCAGACAAGCCGAG
PEN2	1	TGGCTTGTGGATTGCAAGTA
PEN2	2	ACGCGGAGAGAAGAGCTGTA
PEN2	3	GCCTGTTCTCCGTCACTCTC
PEN2	4	ACACATCAAAGCCAGTCGTG
PEN2	5	TCTCGGCTTGTCTGGTTTG
PEN2	6	TTAAGGAATCGCGAACAAGG
PEN2	MUT1	CGAATCCAAACCCATTGTCTACGATCATCTCTTCAGC
PEN2	MUT2	GCTGAAGAGATGATCGTAGACAATGGGTTTGGATTCG
APH1	5' Sal	GTCGACACATGACGGTCGCGGCGGGTATC
APH1	3' Xho	TCAGGCTCGAGCCCGTGAGGCGCTGCTTTGGTTC
APH1	Bam R	AGGTACCTTAGGATCCCCGTGAGGCGCTGCTTTGGTTC
APH1	1	CGCTAGTGGTTTGATTTTTG
APH1	2	TTTCCACAATGCACAAGAGT
APH1	3	CTCCGTCATCTCCAGAAAGC
APH1	4	CGGAAAGCGTACCTAGAGCA

APH1	5	GCTGGTGGTTTAGGTCATGG
APH1	6	GATCTTACCAACATTCCAGCAG
PS1	PROM 5'	CTCGAGTGATCCCGAAACCGAATTTTAT
PS1	PROM 3'	GTCGACGAGACCCGTTATCGATTTCGGTGGATTTTTTGGC
PS2	PROM 5'	CTCGAGATAAGTTTGAGGCTAGCCTGTTAC
PS2	PROM 3'	GTCGACGGGTACTCAAAGATTTCAGCTTTGGC
NCT	PROM 5'	CTCGAGAATCATTGGAACAAAAATGAGAG
NCT	PROM 3'	GTCGACAGCATCCGTCAGAGAGTTGCG
PEN2	PROM 5'	CTCGAGATAAAGTTCAGTCACCTTAAAC
PEN2	PROM 3'	GTCGACTTTTGCTCAGCCACTAACGAAAAG
APH1	PROM 5'	CTCGAGTCTTAAGTTTTTCAATGAAGGATGTG
APH1	PROM 3'	GTCGACGCCACACCGGTCTCAGAGACTT

Table 2.2 Sequences of primers used to amplify DNA. All primers were obtained from Operon.

2.2 RT-PCR

2.2.1. RNA extraction

For amplification of coding sequences, total RNA was isolated from plants. All solutions were made up in DMPC treated water and samples kept on ice unless stated otherwise for incubations. 50-60 mg leaf tissue was collected form 5-6 week old plants grown on soil under long day conditions, and frozen in liquid nitrogen. Leaves were ground to a fine powder in liquid nitrogen using a pre-chilled mini-pestle and re-frozen. Samples were placed on ice and suspended in 600 μL ice-cold Trizol (38 % water-saturated phenol, 0.8 M guanidine thiocyanate, 0.4 M ammonium thiocyanate, 0.1 M NaAc pH 5.0, 5% (v/v) glycerol) with vigorous vortexing. Phase separation was carried out by addition of 120 μL chloroform, vortexed again, incubated at room temp for 2-3 mins and spun at 14,000 rpm for 10 mins at 4°C. 400 μL of the aqueous (upper) phase was recovered to a fresh tube and RNA precipitated by addition of 200 μL 0.8 M sodium citrate/1.2 M NaCl, 200 μL propan-2-ol, with mixing by inversion. Samples were incubated at room temperature for 10 minutes and RNA pelleted at 14,000 rpm for 10 min at 4°C, followed by a wash in 75% EtOH. RNA pellets were briefly air dried and resuspended in 30 μL water at 50°C for 5 mins. To further clean the RNA prep, insoluble carbohydrates were

pelleted at 14,000 rpm for 5 mins at 4°C, and the supernatant recovered to another fresh tube. A lithium chloride precipitation step was carried out by adding 9 μL 10 M LiCl and 90 μL 96% EtOH and RNA precipitated at -20°C overnight. The RNA was collected by spinning at 14,000 rpm for 15 mins at 4°C, followed by a 75% EtOH wash and fully air dried. RNA was resuspended in 30 μL DMPC water on ice for 10 mins, and concentration determined using a NanoDrop (Fisher Scientific, DE, USA) photospectromoter.

2.2.2. cDNA synthesis

Full-length cDNA was synthesised from total RNA extracted from leaves of plants using the *Reverse*-iT 1st Strand Synthesis Kit (ABgene, Surrey, UK), with slight modifications. 1 mg RNA was diluted to 6 μL in a thin walled PCR tube with DMPC water and 0.5 μL anchored oligo-dT (500 ng/μL) added. RNA was denatured at 70^0C for 5 mins and placed on ice. 3.5 μL of premixed synthesis reaction mix was added (2 μL 5x First Strand Synthesis buffer, 1 μL dNTP mix (5 mM each), 0.5 μL *Reverse*-iT™ RTase blend, 0.05 μL 1 M DTT) to each sample and incubated at 47°C for 50 mins. Heating to 75°C for 10 mins inactivated the RTase blend. The 10 μL reactions were diluted to 40 μL and 4 μL used to test the cDNA with TUB primers.

2.3. Fusion protein construction

2.3.1. PCR amplification for cloning

High fidelity *PfuTurbo* DNA polymerase (Stratagene, La Jolla, CA, USA) was used any time a PCR product was to be cloned for manufacturing constructs to be expressed in plants. PCR reactions were set up using kit components (0.4 μL *PfuTurbo* polymerase, 2 μL 10x reaction buffer, 0.4 μL 10 mM dNTPs) with 1 μL each of forward and reverse primers (0.5 mM final concentration), 1-4 μL DNA template (depending on source) made up to 20 μL final volume with water.

Extension temperature required for *PfuTurbo* is 68°C and the extension time was set at 1 min/kb. Following the PCR amplification, 0.4 μL *Taq* polymerase was added to the reaction and incubated at 37°C for 30 mins to allow addition of a poly-A track to the PCR products. This is to facilitate ligation into the cloning vector pGEM-T easy.

2.3.2. Ligation onto pGEM-T easy

The vector pGEM-T easy (Promega, Madison, WI, USA) is a versatile cloning tool with many unique restriction enzyme sites in its MCS. It is commercially available as a cleaved linear DNA fragment with protruding 3' terminal thymidines on both ends, suitable for ligating PCR products with poly-A tails. Ligation into pGEM-T easy was carried out according to the manufacturers' guidelines. In general, 1 μL PCR product (insert) was mixed with 0.5 μL pGEM-T easy vector, 0.5 μL DNA ligase, 5 μL 2x reaction buffer, and 3 μL water, and the reaction carried out at room temperature for 1 hr before transformation into *E. coli*.

2.3.3. PCR based site directed mutagenesis

Due to the cloning strategy for GFP fusion proteins using a *Sal*I site at the 5' end of each gene, the *Sal*I site within the PEN2 coding sequence had to be destroyed. Complimentary primers were designed with 17-19 bp either side of the intended mutation point (GTCGAC to GTAGAC), and PCR was carried out from purified plasmid DNA containing the PEN2 coding sequence in the vector pGEM-T easy. The following were mixed in a thin walled PCR tube: 10 ng DNA, 5 μL 5x buffer, 125 ng top primer, 125 ng bottom primer, 1 μL 10 mM dNTP mix, 1 μL Pfu turbo DNA polymerase, made up to 50 μL with water. The reaction was run with the following conditions: 95°C for 30 secs, then 12 cycles of [95°C for 30 secs, 55°C for 60 secs, 68°C for 3.5 mins]. The template DNA was digested with *Dpn*I for 1 hr and 1 μL of the PCR reaction transformed into *E. coli*. Negative control (no polymerase in PCR reaction) did not produce colonies. Resulting clones were sequenced to ensure mutation.

2.3.4. Sequencing

Boiling mini-preps produce a large amount of plasmid DNA, although it contains other contaminants. The QIAEX II Gel Extraction Kit (Qiagen, Cologne, Germany) was used to clean the DNA samples prior to the sequencing reaction. Following the manufactures' guidelines, DNA samples were made up to 100 μL and treated as a 100 mg gel slice. Cleaned DNA was quantified on an agarose gel. Sequencing reactions were set up in PCR tubes as follows: 100 ng DNA, 2 μL BigDye Version 3.1 sequencing mix (Applied Biosystems, Foster City, CA, USA), 1 μL 0.8 pM oligo, made up to 10 μL with water. PCR reaction conditions: 96°C for 2 mins, followed by 30 cycles of [96°C for 30 secs, 50°C for 15 secs, 60°C for 4 mins]. Samples were analysed in house at the Gene Pool (School of Biological Sciences, University of Edinburgh) using an ABI 3730 DNA Analyzer (Applied Biosystems).

2.3.5. Restriction digestions of plasmid DNA

Restriction digests were carries out according to the manufacturers' (New England Biolabs, Ipswich, MA, USA) guidelines, at the recommended temperature with appropriate buffer and bovine serum albumin (BSA). Diagnostic digests using 1 μL boiling mini-prep DNA were preformed in a reaction volume of 10 μL for 1 hr. 5 μL alkaline lysis prep DNA was digested in a final volume of 15 μL. Digested products were separated on agarose gels (as above, loaded with 1/10 vols 10x loading dye (40% w/v sucrose, 0.25% w/v bromophenol blue)).

For preparatory digests, 5-15 μL DNA (~200 ng) was digested in a volume of 50 μL for 3 hrs. Where DNA was to be cut by two different enzymes, they were both added at the same time, if the buffer permitted. Otherwise, the digest requiring a lower salt concentration was performed first, and the buffer adjusted for the second enzyme. To prevent religation of vectors cut with a single enzyme or those leaving complimentary overhangs, calf intestinal alkaline phosphatase (CIP; Promega) was

used to remove the 3' phosphate group of the cleaved DNA ends. DNA fragments were separated by agarose gel electrophoresis (as described above, at 70 V for 1-2 hrs), bands excised with a clean scalpel and cleaned using the QIAEX II Gel Extraction Kit (Qiagen).

Large vectors (>10 kb) were cleaned from the reaction without gel separation using a phenol/chloroform method. Reactions were diluted to 100 μL, mixed with an equal volume 50:50 (v/v) phenol:chloroform and separated by spinning at 14,000 rpm for 15-20 secs. The aqueous (upper) phase was recovered to a fresh tube and washed in the same way with 100% chloroform to remove traces of phenol. DNA was precipitated with 1/10 vols of 3 M NaAc (pH 5.3) and 2 vols ice cold EtOH and incubated on ice for at least 15 mins, followed by centrifugation at 14,000 rpm for 5 mins at 4 °C. The pellet was washed with 70% EtOH, air dried and suspended in 10 μL 10 mM Tris-HCl (pH 8.0). All cleaned DNA was quantified by agarose gel electrophoresis.

Ligations were carried out with T4 DNA ligase (NEB) following the manufactures' guidelines. Typically 10-20 ng linearised plasmid DNA and 50-60 ng insert DNA was included in a 10 μL reaction (including 2μL 10x buffer, 0.5 μL T4 DNA ligase) and incubated at 16°C overnight or at room temp for 1 hr. 5 μL was transformed into competent E. coli.

2.4. Bacterial manipulations

2.4.1. Heat shock transformation *E. coli*

Heat shock competent *E. coli* DH5α were prepared by the method of Inoue *et al*. (1990). Cells were thawed on ice for 10 mins. 100 μL aliquots were incubated on ice with DNA to be transformed (5 μL ligation or >10 ng circularised plasmid prep) for at least 20 mins. Cells were heat shocked for 60 sec at 42°C, and immediately chilled on ice. 1 mL LB (1% tryptone, 0.5% yeast extract, 0.5% NaCl; pH 7.0) was added to the tubes and cells were allowed to recover at 37°C for 30 mins. Cells were pelleted

at 7,000 rpm for 3 mins, resuspended in 100 μl LB and plated on LB agar (LB containing 1% bactoagar (Difco, Haarlem, The Netherlands)) containing appropriate antibiotics to select for transformed bacteria. Antibiotics used for *E. coli* were ampicilin (100 μg/mL final concentration) or kanamycin (50 μg/mL). For cloning vectors carrying the LacZ, where an insertion disrupts the coding sequence, blue/white selection could also be used (e.g. pGEM-T easy, pBluescript). Plates were spread with 100 μL X-gal solution (20 mg/mL 5-bromo-4-chloro-3-iodyl-β-D-galactodidase in dimethylformamide (DMF)) and only white colonies picked. Plates were incubated overnight (16hrs) at 37°C. Individual colonies were selected using a sterile toothpick and grown in 3 mL LB with antibiotics at 37°C with shaking for 16 hrs. Plasmid DNA was recovered from E. coli by either boiling or alkaline lysis methods.

2.4.2. Boiling minipreps

1.5 mL of overnight *E. coli* culture was spun down at 7,000 rpm for 3 mins and supernatant removed. Pellet was resuspended using a pipette in 350 μl boiling buffer (8% (w/v) sucrose, 50 mM EDTA, 0.5% TRITON X-100, 10 mM Tris-HCl pH 8.0, 0.01% lysozyme (Sigma)), heated in a boiling water bath for 60 sec, and immediately chilled on ice. Bacterial proteins and genomic DNA were pelleted at 14,000 rpm for 20 mins and removed using a sterile toothpick. Plasmid DNA was precipitated with 35 μL sodium acetate (pH 5.3) and 350 μL 2-propanol, and mixed by gentle inversion. The DNA was pelleted at 14,000 rpm for 5 mins, washed in 1 mL 70% EtOH and allowed to fully air dry. Pellets were resuspended in 50 μL R40 (10 mM Tris-HCl pH 8.0, 1 mM EDTA, 40 mg/mL RNase A (Sigma)).

2.4.3. Alkaline lysis

A more gentle miniprep method was used for large plasmids (>10 kb binary vectors). 1.5 mL of *E. coli* culture was spun down at 7,000 rpm for 3 mins and supernatant removed. Pellet was resuspended using a pipette in 200 μL ice cold buffer P1 (50

mM Tris-HCl pH 8.0, 10 mM EDTA). 200 μL freshly prepared buffer P2 (0.2 M NaOH, 1% SDS) was added, mixed gently by inversion and incubated in ice for 2 mins. Proteins and genomic DNA was precipitated by addition of 200 μL buffer P3 (3 M potassium acetate, pH 4.3 with acetic acid) and incubation on ice for 5 mins. Precipitate was pelleted at 14,000 rpm for 10 mins at 4°C and supernatant recovered to a fresh tube. Plasmid DNA was precipitated with 420 μL 2-propanol and pelleted at 14,000 rpm for 20 mins. Pellets were washed in 1 mL 70% EtOH, air dried and resuspended in 20 μL R40.

2.4.4. Cold shock transformation of *Agrobacteria*

Cold shock competent *Agrobacterium tumefaciens* GV3101 were prepared according to Cui *et al*. (1995) and available in the lab, stored at -80°C. 100 μL aliquots were thawed on ice for 2 hrs, prior to 30 min incubation with 1 μg plasmid DNA. Cells were cold shocked in liquid nitrogen for 1 min and thawed in a 37°C water bath for 2 mins. 1 mL YEP (1% bactopeptone, 1% yeast extract, 0.5% NaCl; pH 7.5) was added and cells allowed to recover at 28^0C for 2-3 hrs with shaking. Cells were pelleted at 7,000 rpm for 5 mins, resuspended in 100 μL YEP and plated on solid YEP plates (YEP with 1% bactoagar) containing appropriate antibiotics. Colonies transformed with a binary vector were selected by 50 μg/mL kanamycin and 80 μg/mL gentamycin (Sigma) for general *Agrobacteria* GV3101 selection. Plates were incubated at 28°C for 2-3 days, and resultant colonies grown in 3 mL YEP (with kanamycin and gentamycin) overnight at 28°C with shaking.

2.4.5. Alkaline lysis of *Agrobacteria*

A modified version of the *E. coli* alkaline lysis was used to recover plasmid DNA from *Agrobacteria*. 1.5 mL of fresh culture was spun down at 14,000 rpm for 3 mins and supernatant removed. Pellet was resuspended using a pipette in 100 μL ice cold buffer P1 (50 mM Tris-HCl pH 8.0, 10 mM EDTA) containing 1/3 volume lysozyme. 200 μL freshly prepared buffer P2 (0.2 M NaOH, 1% SDS) was added,

mixed gently by inversion and incubated in ice for 5 mins. Protein and genomic DNA was precipitated by addition of 150 μL buffer P3 (3 M potassium acetate, pH 4.3 with acetic acid), vortexed upside down for 10 secs and incubated on ice for 5 mins. Precipitate was pelleted at 14,000 rpm for 10 mins at 4°C and supernatant recovered to a fresh tube. Plasmid DNA was precipitated with 315 μL 2-propanol and pelleted at 14,000 rpm for 20 mins. Pellets were washed in 1 mL 70% EtOH, air dried and resuspended in 10 μL R40. 2 μL was transformed into *E. coli* and prepped to check the vector was correct. Glycerol stocks of strains were made with equal volumes bacterial culture: 80% glycerol and stored at -80°C.

2.5. Plant expression systems

2.5.1. *Arabidopsis* transformation by floral dipping

Agrobacteria mediated plant transformation was carried out by the floral dip method according to Clough and Bent (1998). *Arabidopsis* plants for transformation were grown under short day conditions (8 hrs light/16 hrs dark, 22°C) for 6 weeks, before transfer to long days (16 hrs light/8 hrs dark, 22°C) and allowed to bolt. Inflorescences were cut off to stimulate auxiliary inflorescence formation, and allowed to grow for a further 2 weeks. *Agrobacteria* harbouring the appropriate plasmid were propagated from glycerol stocks (stored at -80^{0}C) over a number of steps. First, 5 mL cultures were inoculated and grown overnight in YEP (kanamycin/gentamycin) at 28°C with shaking. These 5 mL cultures were inoculated into 50 mL cultures, and then into 500 mL cultures. Cells were pelleted at 7,000x g for 20 mins and resuspended in 5% (w/v) sucrose with 400 μL/L 'Silwet' detergent (Lehle Seeds, Round Rock, USA). *Arabidopsis* plants were dipped in bacterial solution for 1-2 mins.

Seed from transformed plants were surface sterilised and plated on 0.5xMS plates containing 200 mg/L Timentin (Galaxo-Smith-Kline, Brentford, UK) for selection against Agrobacterium, with 15 mg/mL Hygromycin B (Calbiochem, Darmstadt, Germany) or 50 μg/mL kanamycin, depending on binary vector. Transformed

seedlings were visible within 2 weeks as plants able to develop true leaves (resistant to the antibiotic). Resultant T_1 lines were selected again on antibiotic-containing plates to identify lines carrying one insertion (segregating 3 resistant: 1 susceptible plant). Homozygous T_2 lines were identified as segregating 100% resistant to antibiotics.

2.5.2. *Agrobacterium* infiltration

Agrobacterium carrying the appropriate plasmid were grown from glycerol stocks in 3 mL YEP containing antibiotics at 28 ^{O}C overnight. 0.2 OD_{600} units of strain carrying plasmid of interest were mixed with 0.07 OD_{600} units of strain carrying pK19 and pelleted. Cell pellet was resuspended in infiltration buffer (10 mM MES, pH 6.8) and incubated at room temp for 2 hrs in the dark. A small hole was made in a tobacco leaf and *Agrobacterium* solution forced into the leaf, using a 1 mL syringe. Plants were allowed to recover for 2-4 days, and portions of infected leaves tested for expression under the confocal microscope.

2.5.3. Particle bombardment

A full rosette of plants expressing *p35S:AtPEN2:GFP* were bombarded with gold particles carrying a vector to express HDEL-tdT (gift from J. Tilsner), using a PDS-1000 Helium Biolistic particle delivery system, at 1100 psi. Leaves were allowed to recover overnight in a humid environment and tested for expression under the confocal microscope.

2.5.3. Microscopy and image processing

GFP-tagged proteins were imaged with a Bio-Rad Radiance 2100 confocal microscope (Hemel Hematead, UK), using 500 nm long pass and 530 nm short pass filters. Images of co-localisation of GFP-tagged proteins with FM4-64 were captured on a Leica SP2 confocal laser scanning microscope (Leica Microsystems),

using standard TRITC filter settings. Images were subsequently processed using ImageJ (http://rsb.info.nih.gov/ij/).

2.6. Protein work

2.6.1. Protein extraction for SDS-PAGE

Separation of proteins on a polyacrylamide gel containing SDS allows visualisation of the proteins through various staining methods, or transfer to nitrocellulose membrane for immunodetection. Plant material was harvested and ground in 10 fold excess ice cold extraction buffer (50 mM Tris-HCl pH 7.5, 150 mM NaCl) containing Complete-Mini protease inhibitor cocktail (1 tablet per 10 mL solution; Roche, Basel, Switzerland) on ice using prechilled mortar and pestles (for large scale preps) or in 1.5 mL tubes using a mini-pestle. Cell debris and intact organelles was pelleted at 14,000 rpm for 10 mins at 4°C. The supernatant was recovered to a fresh tube, membranes solubilised with 0.05-0.1% TritonX-100 (final concentration) and 1/5 vols of 6x protein loading dye (350 mM Tris-HCl pH 6.8, 10.28% w/v SDS, 36% w/v glycerol, 0.6 M dithiothreitol (DTT), 0.012% w/v bromophenol blue) added and the proteins denatured at 80°C for 5 mins. Samples were stored at -80°C until needed.

2.6.2. Running SDS-PAGE gels

SDS-PAGE gels were prepared in the lab using the BIORAD mini-protean II system (Hercules, CA, USA) using 0.75 mm casts as follows: separation gel (12% w/v acryl/bis-acrylamide 37.5:1 (Severn Biotech Ltd., Kiddiminster, UK), 375 mM Tris pH 8.8, 0.1% w/v SDS, 0.1 % w/v ammonium persulphate (APS), 0.01% v/v N,N,N',N'-tetraethylenediamine (TEMED)) overlaid with 1/5 depth of stacking gel (6% w/v acryl/bis-acrylamide 37.5:1, 125 mM Tris pH 6.8, 0.1% w/v SDS, 0.1 % w/v APS, 0.01% TEMED). Protein samples (including a standard protein size marker (Sigma)) denatured in loading dye were applied to the gels and ran at 100-

110 V at room temp in running buffer (0.6% w/v Tris, 2.28% w/v glycine, 1.0% w/v SDS; pH8.3) until the dye front reached the bottom of the gel.

For Coomassie staining, gels were soaked in stain (45% MeOH, 10% acetic acid, 0.25% Coomassie Brilliant Blue R-250) for 30 mins followed by destaining in 30% MeOH/10% acetic acid washes until desired stain had been attained. Stained gels were air dried between sheets of cellophane (Sigma).

2.6.3. Western blotting

Following separation of proteins on PAGE gels, proteins can be immobilised on nitrocellulose membrane for detection with antibodies. Gels were soaked in ice-cold soak buffer (0.3% w/v Tris, 1.44% w/v glycine, 20% v/v MeOH) for 3-5 minutes before transfer to Hybond-N nitrocellulose membrane (GE Healthcare Bio-sciences AB, Uppsala, Sweden) in transfer buffer (0.3% w/v Tris, 1.44% w/v glycine, 20% v/v MeOH, 0.1% w/v SDS) using a BIORAD mini-protean II transfer cassette and tank. Transfer was carried out at 4°C for 2 hrs at a constant 70 V. Proteins were fixed and visualised on the membrane following transfer by staining with Ponceau S (5% v/v acetic acid, 0.1% Ponceau S) and protein ladder marked, before removal by rinsing in phosphate buffered saline with Tween (PBST: 1.5 mM KH_2PO_4, 150 mM NaCl, 5 mM Na_2HPO_4, 11 mM KCl, 0.02% Tween-20; pH7.2). The membrane was blocked for 30 mins in PBST milk (5% Sainsbury's milk powder in PBST) before incubation with 1/1000 dilution of primary antibody of choice in PBST milk overnight at 4°C on a rolling incubator.

The membrane was washed in 15 mL PBST for 45 mins with three changes of buffer before incubation with secondary antibody. A 1/5000 dilution of HRP linked antibody in PBST milk was added to the membrane and incubated at room temp for 1 hr on a rolling incubator. The membrane was then washed in PBST for 45 mins with 3 changes of buffer. Sites of antibody attachment were detected by an electrochemiluminescence (ECL) reaction by soaking the membrane in ECL Western Blotting Substrate (Pierce) (1:1 mix of Western detection reagents 1 and 2) for 1-2

mins and exposed to X-ray film (CL-Xposure; Thermo Scientific) for 5 mins to 2 hrs. Film was developed using a Konica developing machine (Konica, Langenhagen, Germany).

2.6.4. Immunoprecipitations

GFP fusion proteins stably expressed in Arabidopsis were subjected to immunoprecipitation studies to identify binding partners. Extractions were carried out as for SDS-PAGE samples. Following membrane solubilisation with 0.05% Triton X-100 or 2% CHAPS, 1 mL extract was incubated with 10 μL GFP binding protein (GBP)-Sepharose (Rothbauer et al., 2008) for 60 mins at 4°C with mixing. Beads were recovered by spinning at 14,000 rpm for 60 secs and washed in 1 mL extraction buffer. The wash step was repeated a total of 3 times. Bound proteins were eluted from the beads by resuspending in 50 μL 1x loading buffer (6x stock diluted to 1x in extraction buffer) and heated to 80°C for 5 mins. 5 μL tested on a Western blot using anti-GFP antibody.

2.6.5. Silver staining

For high sensitivity staining of SDS-PAGE gels, the Silver Snap II kit (Pierce, Rockford, IL, USA) was used according to the manufacturer's instructions. Gels were washed in water to remove excess SDS and proteins fixed in a 30% EtOH/10% acetic acid solution, followed by removal of acetic acid in a 10% EtOH wash. Gels were incubated in 'Sensitizer' and 'Enhancer' before 'Developer' wash for 3-5 mins. Colour development was stopped with 8% acetic acid. Bands were cut from the gel and stored at -20°C until needed for mass-spectrometry analysis.

2.6.6. Extractions for 2D DIGE

Two-dimensional differential in gel electrophoresis (2D DIGE) was carried out in conjunction with the Thomas group at the University of York. Pools of differentially

fluorescent-labelled proteins are run on two-dimensional gels, allowing accurate analysis of protein abundance between samples. Total protein was extracted from all above ground tissues of 3 plants of wild type Col-0 and plants homozygous for the *ps1-1/ps2-3* mutations. Plants were grown on soil under long day conditions for 5 weeks, harvested, weighed and immediately frozen in liquid nitrogen. Tissue was ground to a fine powder using chilled mortar and pestles, and suspended in precipitation solution (10% trichloroacetic acid (TCA) in acetone, supplemented with 0.07% 2-mercaptoethanol). 1 mL aliquots were stored at -20°C for at least 45 mins before precipitate collected by spinning at 14,000 rpm for 10 mins at 4°C. Pellets were washed in 1mL 100% ice-cold acetone (with complete resuspension between spins) a total of 3 times and air dried for 1 hr. Pellets from 1 mL aliquots were resuspended in 50 μL solubilisation buffer (8 M urea, 2% CHAPS, 30 mM Tris-HCl pH 8.5) and incubated at room temp for 5 mins. Insoluble material was pelleted at 14,000 rpm for 10 mins and supernatant containing proteins recovered to a fresh tube. To remove any last traces of insoluble material, preps were passed through a 0.22 μm filter.

2.6.7. Native PAGE

Proteins can be separated on denaturating/reducing gels, as in the SDS-PAGE system describe above, to identify individual proteins by size alone. Blue native PAGE allows protein complexes to be separated under non-denaturating conditions by inclusion of the dye Coomassie Brilliant Blue G-250 in the loading and running buffer. G-250 acts by binding to proteins and rendering them with a net negative charge, allowing movement through polyacrylamide gels while maintaining the proteins and protein complexes in their native conformations. Extractions were carried out according to the recommendations supplied with the Invitrogen Native PAGE Novex 4-16% Bis-Tris gradient gels.

20 mg tissue was ground in 200 μL BN-PAGE extraction buffer (50 mM Bis-Tris pH 7.2, 50 mM NaCl, 10% w/v glycerol, 0.001% w/v Ponceau S, 1% w/v Digitonin) with protease inhibitor cocktail, and insoluble material removed by spinning at

20,000xg for 20 min at 4°C. Samples were mixed with 10x loading dye (750 mM ε-aminocaproic acid, 5% Coomassie G-250) and loaded on precast gradient gels. Running conditions started at 150 V at 4°C using a XCell SureLock Mini-cell (Invitrogen) with blue cathode buffer (50 mM Bis-Tris pH 7.2, 50 mM tricine, 0.02% w/v Coomassie G-250) in the upper chamber of the tank. After approximately 1 hr, the gel front had reached one-third the way down the gel and the blue cathode buffer was replaced with colourless cathode buffer (50 mM Bis-Tris pH 7.2, 50 mM tricine) and voltage increased to 250 V for the remainder of the run (~1.5 hrs). Following separation, gels were either subjected to Coomassie staining or transferred to membrane for immunodetection.

Western transfer of proteins from blue native PAGE gels was carried out using a XCell II blot module in 1x NuPAGE transfer buffer (Invitrogen) at 52 V for 2 hrs at 4°C onto PVDF (polyvinyldifluoride) membrane. Following transfer, the membrane was washed in 8% acetic acid to fix proteins, and air dried. Coomassie G-250 was washed from the dry membrane with 100% MeOH, followed by a water rinse and used for immunodetection as described above.

2.6.8. 2D electrophoresis

Second dimension electrophoresis was carried out using 12% polyacrylamide gels prepared in 1.5 mm casts as above, with the stacking gel poured to 8-10 mm from the top of the cast. Lanes from a BN-PAGE gel were excised using a clean scalpel, and incubated in solubilisation buffer (66 mM Na_2CO_3, 2% w/v SDS, 0.67% v/v 2-mercaptoethanol) for 20 mins. The lane was placed onto the stacking gel and layered over with 0.5% agarose (w/v) in 1x SDS running buffer. 5 μL protein marker was applied to a narrow strip of filter paper and placed in the agarose before setting. Running conditions and western transfer for 2D gels were as for 1D SDS electrophoresis.

2.7. *RNA* in situ *hybridisations*

All RNA work was carried out using RNse free equipment and DMPC water. Floral meristems were harvested from plants grown under short day conditions for 8-9 weeks and fixed in 4% paraformaldehyde (1x PBS pH 10.5 with NaOH, 4% w/v paraformaldehyde, after heating to dissolve paraformaldehyde, solution was cooled and pH adjusted to 7.0 with sulphuric acid) by vacuum infiltration, and stored in paraformaldehyde solution at 4°C until required. Samples were washed twice in 1x PBS prior to going through an EtOH dehydration series (30-50-70%) and embedded in paraffin wax. Wax blocks were cut into 7-8 μm sections and affixed to Probe On Plus glass slides (Fisher) at 42°C overnight and stored at 4°C until required.

Probes were prepared from 10 μg plasmid DNA (cloned cDNA for *PS1*, *PS2*, *NCT*, *APH1* and *PEN2*) cleaved with *Nco*I (to leave a 5' overhang) and EtOH precipitated overnight at -20°C. Transcription reaction was set up with reagents from Roche as follows: 1 μg DNA, 5 μL 5x transcription buffer, 1 μL RNase inhibitor, 2.5 μL each of ATP, CTP and GTP (all 5 mM), 2.5 μL DigUTP (1 mM), 1 μL SP6 RNA polymerase, final volume 25 μL. Reaction was allowed to proceed at 37°C for 60 mins before being stopped by addition of 75 μL water and 1 μL 100 mg/mL tRNA. Template DNA was digested with RNase free DNase at 37°C for 10 mins. RNA was cleaned as follows: precipitation by addition of 100 μL 4 M ammonium acetate and 200 μL EtOH, incubated o/n at -20°C; pelleted at 14,000 rpm for 30 mins at 4°C; washed in 70% EtOH, 0.5 M NaCl; air dried and resuspended in 20 μL water. Probes were stored at -80°C until required.

Slides of sectioned material were washed twice in Histoclene clearing agent (Cell Path, Newtown, Powys, UK) for 10 mins to remove paraffin and hydrated through a EtOH series (30-60 sec washes in 100, 100, 95, 85, 70, 50 and 30% EtOH) followed by a 5 min water wash and a 15 min 2xSSC (0.3 M NaCl, 30 mM sodium citrate) wash. Proteins were digested for 30 mins with proteinase K (50 mM Tris-HCl pH 7.5, 5 mM EDTA, 20 μg/mL protease) at 37°C and the reaction quenched with a 2 min wash in 0.2% glycine in 1x PBS. Samples were washed in 1x PBS and fixed in

4% paraformaldehyde for 5 mins, rinsed twice with 1xPBS and treated with acetic anhydride (0.25% w/v in 100 mM triethanolamine, pH 8.0 with HCl) for 10 mins to reduce non-specific background. Following brief washes in 1x PBS and water, sections were dehydrated through an EtOH series (30-60 sec washes: 30, 50, 70, 85, 95, 100 and 100% EtOH) and stored to dry in an EtOH rich environment at 4°C.

Hybridisation of probes was carried out with pairs of slides at 52°C overnight. 250 μL hybridisation solution was prepared per slide pair as follows: 100 μL deionised formamide, 25 μL 10x in situ salts (3 M NaCl, 100 mM Tris-HCl pH 8.0, 100 mM sodium phosphate buffer pH 6.8, 50 mM EDTA), 50 μL 50% (w/v) dextran sulphate, 1.25 μL 100x Denhardt's solution, 2.5 μL tRNA (100 mg/mL), 2 μL denatured probe. Following over night incubation, slides were washed in three changes of 0.2x SSC for 3 hrs at 52°C, followed by a 45 min wash in 1% Boehringer block (Roche) at room temp. Prior to anti-DIG antibody incubation, slides were blocked in BSA solution (1% BSA, 0.3% Triton X-100, 100 mM Tris-HCl pH 7.5, 150 mM NaCl) for 45 mins, and antibody diluted 1/1000 in BSA solution and incubated for 2 hrs. Unbound antibody was removed with four washes in BSA solution for 20 mins each.

Slides were washed in buffer V (100 mM Tris-HCl pH 9.5, 100 mM NaCl, 50 mM $MgCl_2$) twice for 5 mins before proceeding to Western blue staining. Staining was carried out overnight with NBT/BCIP (4.5 μL NBT (30 mg/mL in 70% DMF), 3.5 μL BCIP (15 mg/mL in DMF) in 1 mL buffer V). When staining had progressed to desired amount, reaction was stopped by washing in 1x TE, rinsed in water and air-dried. Stained samples were preserved by covering with Entellan (Sigma) and affixing a glass cover slip.

2.8. Yeast manipulations

2.8.1. Small scale transformation of NMY51

Untransformed yeast strain NMY51 (DualSystems Biothch, Schlieren, Switzerland) was maintained on YPDA agar (1% w/v bacto yeast extract, 2% w/v bacto peptone,

2% w/v glucose monohydrate, 40 mg/L adenine hemisulphate, 2% bacto agar) plates. Several colonies were inoculated into 50 mL YPDA and grown overnight at 28^0C to an OD_{546} of 0.6-0.8. Yeast was pelleted at 700x g for 5 mins and resuspended in 2.5 mL sterile water. A master mix of PEG/LiOAc was prepared as follows: 1.2 mL 50% polyethylene glycol 4000 (PEG), 180 μL 1M lithium acetate (LiOAc), 125 μL 5 mg/mL boiled single-stranded carrier DNA (ssDNA)). In a sterile 1.5 mL tube the following reagents were mixed: ~1.5 μg bait construct, 300 μL PEG/LiOAc mix, 100 μL resuspended yeast cells. Heat shock transformation was carried out at 42^0C for 45 mins. Yeast cells were pelleted at 700x g for 5 mins, resuspended in 0.9% NaCl and plated on 90 mm selective media plates (6.7 g/L yeast nitrogen base without amino acids, 610 mg/L complete supplement mixture –Leu-Trp-His-Ade (Formedium), 2% glucose monohydrate, 2% agar; supplemented with amino acids Ade (200 mg/L), His (200 mg/L), Trp (200 mg/L) and Leu (1000 mg/L), depending on selection needed). Plates were incubated at 28^0C for 2-3 days until colonies appeared. Colonies were picked and restreaked on selective media to obtain single colonies.

For transformation of a second test construct, the lines were grown overnight in SD-Leu and the transformation procedure repeated, with selection on SD-Leu-Trp plates. cDNA constructs were tested for expression and auto-activation on SD-Leu-Trp-His and SD-Leu-Trp-His-Ade by spotting out serial dilutions of the double transformed lines.

2.8.2. Large scale (library) transformation of NMY51

Several colonies of the bait strain were inoculated into 10 mL SD-Leu and grown at 28^0C for 8 hrs. The culture was inoculated into 100 mL SD-Leu and grown overnight. 30 OD_{546} units were collected at 700x g for 5 mins and resuspended in 200 mL YPDA (final OD_{546} 0.15), and grown to OD_{546} 0.6 (3-5 hrs, 2 cell divisions). The culture was split into 50 mL Falcon tubes and pelleted, washed once in 30 mL water, and resuspended in 1 mL LiOAc/TE mix (110 mM LiOAc, 110 mM Tris-HCl pH 7.5, 1.1 mM EDTA). PEG/LiOAc mastermix was prepared with the following:

1.5 mL 1 M LiOAc, 1.5 mL 10x TE (1 M Tris-HCl pH 7.5, 0.1 M EDTA), 12 mL 50% PEG). The transformation reaction was set up in four 50 mL Falcon tubes prepared with the following: 7 μg library plasmid, 100 μL ssDNA (boiled twice), 2.5 mL PEG/LiOAc mix, 600 μL yeast cells. Cells were incubated at 30^0C for 45 mins, 160 μL DMSO (dimehtyl sulphoxide) added and heatshocked at 42^0C for 20 mins. Yeast cells were pelleted, resuspended in 3 mL YPDA per tube and pooled. After allowing the yeast to recover at 30^0C for 90 mins, cells were pelleted and resuspended in 4.8 mL 0.9% NaCl. 300 μL aliquots were spread on 150 mm SD-Leu-Trp-His-Ade plates, sealed with Parafilm and incubated at 28^0C for 3-4 days until colonies appeared.

2.8.3. Plasmid recovery from yeast

Individual colonies were inoculated into 5 mL YPDA and grown overnight at 28^0C. 3 mL culture was pelleted at 4000x g for 5 mins and pellet resuspended in 200 μL yeast lysis buffer (10 mM Tris-HCl pH 8.0, 1 mM EDTA, 100 mM NaCl, 1% SDS, 2% Triton X-100). 0.3 g glass beads were added and mixture vortexed vigorously to disrupt the cells. 200 μL phenol/chloroform (50:50 v/v) was added and tubes vortexed again. Aqueous phase (containing DNA) was separated by spinning at 14,000 rpm for 5 mins, and recovered to a fresh tube. DNA was precipitated by addition of 20 μL 3 M NaOAc (pH 5.3) and 500 μL EtOH, and pelleted at 14,000 rpm for 20 mins. The pellet was washed with 1 mL 70% EtOH, fully air dried and resuspended in 10 μL water. 1 μL was used for transformation into electrocompetent *E. coli*.

2.8.4. Electroporation of *E. coli*

Electrocompetent *E. coli* HB101 were prepared ahead of time and stored frozen at -80^0C. 80 μL cells were defrosted on ice per transformation, and placed in 1 mm electroporation cuvette with 1 μL DNA recovered form yeast. Electroporation was carried out at 25 μFD, 200 Ω, and 1.7 kV in a Gene Pulser XCell (BioRad).

Immediately following transformation, 1 mL ice cold LB was added to cuvette and cells transferred to a 1.5 mL tube. Cells were allowed to recover at 37^0C for 1-1.5 hrs, and plated on LB agar containing appropriate antibiotics. Individual colonies were grown overnight and plasmid DNA recovered by the alkaline lysis method (see above). Due to the HB101 strain used, plasmids were retransformed into *E. coli* DH5α and prepped by the boiling miniprep method to obtain sufficient plasmid for sequencing and transformation into yeast.

3.0. Members of the potential γ-secretase complex in *Arabidopsis*

3.1. Introduction

Proteolysis is an essential component in many cellular processes. Versions of the basic proteolytic machinery are conserved throughout the various kingdoms, for example the multimeric 20S proteasome core (Maupin-Furlow et al., 2000). Regulated intramembrane proteolysis (RIP) is a relatively newly discovered form of protein cleavage that, as the name suggests, takes place within the lipid bilayer of a membrane. There have been four main classes of I-Clips (intramembrane cleaving proteases) characterised to date – the serine proteases of the Rhomboid class, the metallo-proteases in the S2P class and the GxGD aspartyl proteases, SPP and γ-secretase. Evolutionarily, many I-Clips have been maintained from prokaryotes through to multicellular eukaryotes. Homologues of Rhomboids, S2Ps, SPPs and PRESENILINs have all been identified in *Arabidopsis*, although very few (if any) substrates have been identified for these proteases (see Chapter 1 – Introduction for more detailed information).

In animal systems, the γ-secretase complex is involved in all stages of development through its processing of Notch (Lai, 2004), and in numerous other cell-to-cell signalling processes. Here, I have identified homologues of the γ-secretase complex members PRESENILIN, NICASTRIN, APH1 and PEN2 in *Arabidopsis* and attempted to ascertain a function for the potential complex they may form. Although the members of the complex are conserved, the substrates identified in animals do not seem to be present in plants.

3.2. Identification of potential Arabidopsis *γ-secretase complex members*

BLAST searches against the predicted *Arabidopsis* proteome (Rhee et al., 2003) using human PRESENILIN 1 (HsPS1; AAH11729) identified two proteins with a high degree of similarity, which were named *Arabidopsis* PRESENILIN 1 (AtPS1;

At2g29900) and AtPS2 (At1g08700). ClustalW 2.0 multiple sequence alignments showed AtPS1 has 54% similarity to HsPS1 (AAH11729) and 53% with respect to HsPS2 (AAH06365). AtPS2 has slightly less similarity to HsPS1, at 50%, but a marginally greater degree to HsPS2 with 55%.

Arabidopsis NICASTRIN (AtNCT; At3g52640) was identified with 44% similarity to human nicastrin precursor (AAH47621). Three splice variants of *AtNCT* have been recovered from various *Arabidopsis* tissues (At3g52640.1, At3g52640.2 and At3g52640.3; Fig 3.1). At3g52640.1 has an extra intron in the penultimate exon, compared to At3g52640.2, resulting in predicted proteins of approximately 73 kDa and 76.3 kDa respectively. At3g52640.3 does not code for the final exon, resulting in a smaller protein of 66.7 kDa, which lacks the transmembrane domain predicted at the C-terminus of the other splice variants. Primers were designed to amplify the three predicted splice variants of *AtNCT* from the 5' ATG to the 3' STOP codon (incorporating restriction enzyme sites for later cloning). Total RNA was extracted from leaves of wild type Col-0 plants and a reverse transcription kit (ReverseIt, Invitrogen) was used to produce cDNA. Following high fidelity PCR amplification (*Pfu* Turbo, Fermentas) with gene specific primers, the products were cloned into pGEMT-easy and sequenced (BigDye v3.1, Applied Biosystems) using universal and reverse primers present in the cloning vector. At3g52640.1 has an extra intron in the 15th exon compared to At3g52640.2 and At3g52640.3, which removes 87 nucleotides from the cDNA. None of the clones sequenced contained the predicted exon sequence excised in At3g52640.1, suggesting that At3g52640.1 is the only predicted splice variant expressed in leaves. A full-length cDNA clone for At3g52640.2 is listed on the GenBank database (GSLTPGH28ZG08), recovered from hormone treated callus tissue. In this study, I have limited my research to At3g52640.1 (hereafter referred to as AtNCT).

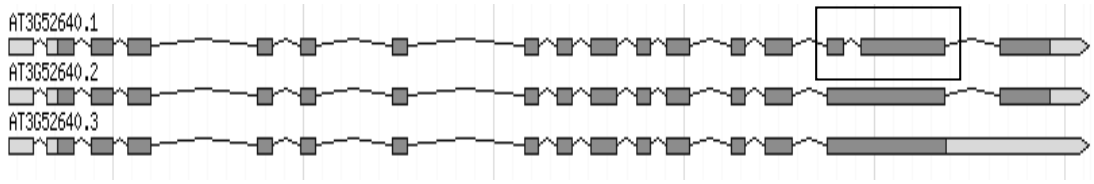

Fig 3.1 Gene model for At3g52640, *AtNICASTRIN* showing three splice variants. Light grey boxes represent 5' and 3' UTRs, dark grey boxes exons and joining lines are introns. Version At3g52640.1 varies from At3g52640.2 with an extra intron removed towards the 3' end of the transcript (boxed region). No sequences amplified contained this intron. Gene model taken from the TAIR database (Swarbreck et al., 2008).

A single *Arabidopsis* ANTERIOR PHARYNX DEFECTIVE 1 (AtAPH1; At2g31440) homologue was identified through BLAST searches with HsAPH1 isoform a (NP_057106), however it actually has a greater similarity with HsAPH1b (NP_112591) at 50%.

The final member of the putative γ-secretase complex, *Arabidopsis* PRESENILIN ENHANCER 2 (AtPEN2; At5g09310) has 56% similarity to HsPEN2 (AAH09575, also known as PSENEN).

The high degree of similarity between human and putative *Arabidopsis* γ-secretase proteins is quite striking, given the lack of any conserved substrates.

3.3. Conservation of protein motifs important to γ-secretase complex formation and function

Multiple sequence alignments were carried out between the predicted *Arabidopsis* proteins identified above and those from a number of model animal systems, along with predicted proteins from rice (*Oryza sativa*; see alignments in Fig 3.2) and serve to highlight the many conserved protein motifs.

PRESENILIN harbours the active site aspartic acids (D in the single letter amino acid code), and a mutation in either of these in HsPS1 or 2 renders the complex inactive (Wolfe et al., 1999). The sequence similarity between the presenilins is

(a) PRESENILINs

```
AtPS1           ------------------------------------------------------------
AtPS2           ------------------------------------------------------------
OsPS1           ------------------------------------------------------------
OsPS2           ------------------------------------------------------------
HsPS1           -------------------------------------MTELPAPLSYFQNAQMSEDNHL 22
HsPS2           MLAGTVRFARHCLKFFPAQKPACVDFGASRGRAMLTFMASDSEEEVCDERTSLMSAESPT 60
MmPS1           -------------------------------------MTEIPAPLTYFQNAQMSEDSHS 22
MmPS2           ---------------------------------MLAFMASDSEEEVCDERTSLMSAESPT 27
DmPS            ------------------------MAAVNLQASCSSGLASEDDANVGSQIGAAERLERPP 36
CeSel-12        ------------------------------------------------------MPS 3
CeHOP-1         ------------------------------------------------------------


AtPS1           ---------------------------------------------------MDRNQRPRSI 10
AtPS2           -------------------------------------------------------MESSI 5
OsPS1           ------------------------------------------------------------
OsPS2           ------------------------------------MADAAAATVPGEASSSSSAAATTTV 25
HsPS1           SNTVRSQNDNRERQEHNDRRSLGHP----EPLSNGRPQGNSRQVVEQD----EEEDEELT 74
HsPS2           PRSCQEGRQGPEDGENTAQWRSQEN----EEDGEEDPDRYVCSGVPGRP---PGLEEELT 113
MmPS1           SSAIRSQNDSQERQQQHERQRLDNP----EPISNGRPQSNSRQVVEQDC---MEEDEELT 75
MmPS2           SRSCQEGRPGPEDGESTAQWRTQES----EEDCEEDPDRYACSGAPGRP---SGLEEELT 80
DmPS            RRQQQRNNYGSSNQDQPDAAILAVPNVVMREPCGSRPSRLTGGGGGSGGPPTNEMEEEQG 96
CeSel-12        TRRQQEGGGADAETHTVYGTNLITN-------RNSQED--------------ENVVEEAE 42
CeHOP-1         ------------------------------------------------------MPRTK 5


AtPS1           LDSLGEELIAILTPVSICMFTVVLLVCILNSDPSSSSASFSSIATAAYSESDSDSSWDKF 70
AtPS2           LDSLGVEIIGVMAPVSICMFLVVLLTYSLS---VTSDPQIRSAANLIYIENPSDSTTVKL 62
OsPS1           ----------------------------AA---AAQPPPPVTAATLVYLESPTDTPGQKL 29
OsPS2           LDSLGEDITRIVTPVSTCMLLVVLLVSLLS---SPSSPSPFTAAFSAAAG--PGGGGDDI 80
HsPS1           LKYGAKHVIMLFVPVTLCMVVVVATIKSVS----FYTRKDG-QLIYTPFTEDTETVGQRA 129
HsPS2           LKYGAKHVIMLFVPVTLCMIVVVATIKSVR----FYTEKNG-QLIYTPFTEDTPSVGQRL 168
MmPS1           LKYGAKHVIMLFVPVTLCMVVVVATIKSVS----FYTRKDG-QLIYTPFTEDTETVGQRA 130
MmPS2           LKYGAKHVIMLFVPVTLCMIVVVATIKSVR----FYTEKNG-QLIYTPFTEDTPSVGQRL 135
DmPS            LKYGAQHVIKLFVPVSLCMLVVVATINSIS----FYNSTDV-YLLYTPFHEQSPEPSVKF 151
CeSel-12        LKYGASHVIHLFVPVSLCMALVVFTMNTIT----FYSQNNGRHLLSHPFVRETDSIVEKG 98
CeHOP-1         RVYSGKTITGVLYPVAICMLFVAINVKLSQ----PEQQEQS-KVVYGLFHSYDTADSG-- 58


AtPS1           VGALLNSVVFVAAITVATFVLVLLFYLRCVKFLKFYMGFSAFIVLGNLGGEILVLLIDRF 130
AtPS2           EGSLANAIVFVVLIAAVTFILVLLFYYNFTNFLKHYMRFSAFFVLGTMGGAIFLSIIQHF 122
OsPS1           VGALLDAAVFVALVAVVTFVLVALYYYRCTGFLKNYMRFSAFFVLFSMGGAIAAAVLRRL 89
OsPS2           TTALITAVTFVVAVTAATFLLAFLFYLRCTPCLRAYLGFSSLSVLLLLGGHVALLLLSRL 140
HsPS1           LHSILNAAIMISVIVVMTILLVVLYKYRCYKVIHAWLIISSLLLLFFFSFIYLGEVFKTY 189
HsPS2           LNSVLNTLIMISVIVVMTIFLVVLYKYRCYKFIHGWLIMSSLMLLFLFTYIYLGEVLKTY 228
MmPS1           LHSILNAAIMISVIVIMTILLVVLYKYRCYKVIHAWLIISSLLLLFFFSFIYLGEVFKTY 190
MmPS2           LNSVLNTLIMISVIVVMTIFLVVLYKYRCYKFIHGWLIMSSLMLLFLFTYIYLGEVLKTY 195
DmPS            WSALANSLILMSVVVVMTFLLIVLYKKRCYRIIHGWLILSSFMLLFIFTYLYLEELLRAY 211
CeSel-12        LMSLGNALVMLCVVVLMTVLLIVFYKYKFYKLIHGWLIVSSFLLLFLFTTIYVQEVLKSF 158
CeHOP-1         ----TITLYLIGFLILTTSLGVFCYQMKFYKAIKVYVLANSIGILLVYSVFHFQRIAEAQ 114
                      :  ::  :   * .    :  .    :: ::  .:: :*          :


AtPS1           RFPIDSITFLILLFNFSVVGVFAVFMSK-FSILITQGYLVWIGVLVAYFFT-LLPEWTTW 188
AtPS2           SIPVDSITCFILLFNFTILGTLSVFAGG-IPIVLRQCYMVVMGIVVAAWFT-KLPEWTTW 180
OsPS1           GAPLDAATALVLLFNASAVGVLSVFASA-VPIVVRQGYMVALAVIVAAWLS-RLPEWTTW 147
OsPS2           RLPLDAASFALLLPNAAAALALAALSPASVPIALHQAALVAIAVLTAFWFT-LLPEWTTW 199
HsPS1           NVAVDYITVALLIWNFGVVGMISIHWKG--PLRLQQAYLIMISALMALVFIKYLPEWTAW 247
HsPS2           NVAMDYPTLLLTVWNFGAVGMVCIHWKG--PLVLQQAYLIMISALMALVFIKYLPEWSAW 286
MmPS1           NVAVDYLTVALLIWNFGVVGMIAIHWKG--PLRLQQAYLIMISALMALVFIKYLPEWTAW 248
MmPS2           NVAMDYPTLFLAVWNFGAVGMVCIHWKG--PLVLQQAYLIVISALMALVFIKYLPEWSAW 253
DmPS            NIPMDYPTALLIMWNFGVVGMMSIHWQG--PLRLQQGYLIFVAALMALVFIKYLPEWTAW 269
CeSel-12        DVSPSALLVLFGLGNYGVLGMMCIHWKG--PLRLQQFYLITMSALMALVFIKYLPEWTVW 216
CeHOP-1         SIPVSVPTFFFLILQFGGLGITCLHWKS--HRRLHQFYLIMLAGLTAIFILNILPDWTVW 172
                  . .     . : :       .          : *  :: :. : *  :   **:*:.*
```

```
AtPS1           VLLVALALYDIAAVLLPVGPLRLLVEMAISRDED-IPALVYEARPVIRNDS--------- 238
AtPS2           FILVALALYDLVAVLAPGGPLKLLVELASSRDEE-LPAMVYEARPTVSSGNQRRNRGSSL 239
OsPS1           VMLIALALYDLVAVLAPRGPLRMLVELASSRDDE-LPALVYESRPTVGPAS-----GSSS 201
OsPS2           ALLVAMAVYDLAAVLLPGGPLRLLLELAIERNEE-IPALVYEARPVDPRHGHNWRLWRER 258
HsPS1           LILAVISVYDLVAVLCPKGPLRMLVETAQERNETLFPALIYSSTMVW-LVNMA------- 299
HsPS2           VILGAISVYDLVAVLCPKGPLRMLVETAQERNEPIFPALIYSSAMVW-TVGMA------- 338
MmPS1           LILAVISVYDLVAVLCPKGPLRMLVETAQERNETLFPALIYSSTMVW-LVNMA------- 300
MmPS2           VILGAISVYDLVAVLCPKGPLRMLVETAQERNEPIFPALIYSSAMVW-TVGMA------- 305
DmPS            AVLAAISIWDLIAVLSPRGPLRILVETAQERNEQIFPALIYSSTVVY-ALVNT------- 321
CeSel-12        FVLFVISVWDLVAVLTPKGPLRYLVETAQERNEPIFPALIYSSGVIYPYVLVT------- 269
CeHOP-1         MALTAISFWDIVAVLTPCGPLKMLVETANRRGDDKFPAILYNSSSYVNEVDSP------- 225
                  * .::.:*: *** * ***: *:* *  *.:  :**::*.:

AtPS1           ------------RSVQRRVWRE---------QRSSQNNANRNEVRVVESAEVE-EEHVGS 276
AtPS2           RALVGGGGVSDSGSVELQAVRN---HDVNQLGRENSHNMDYNAIAVRDIDNVD-DGIGNG 295
OsPS1           -------YASAMGSVEMQPVADPGRSGGNQYDRVEQE--DDSSRAVVEMRDVG-GSRSSI 251
OsPS2           ----------TQSGAELDANST-----VEVLGEVLGTNLGASSAGNLGVSAIRSDERVGL 303
HsPS1           ---------EGDPEAQRRVSKN------SKYNAESTER-ESQDTVAE------------- 330
HsPS2           ---------KLDPSSQGALQLP------YDPEME-------EDSYDS------------- 363
MmPS1           ---------EGDPEAQRRVPKN------PKYNTQRARRDETQDSGSG------------- 332
MmPS2           ---------KLDPSSQGALQLP------YDPEM--------EDSYDS------------- 329
DmPS            ---------VTPQQSQATASSS------PSSSNSTTTTRATQNSLASPEAAAASGQRTGN 366
CeSel-12        ---------AVENTTDPREPTS------SDSNTSTAFPGEASCSSETPK------------ 303
CeHOP-1         ---------DTTRSNSTPLTEF------NNSSSSRLLE---SDSLLR------------- 254
                                .                         .

AtPS1           SER--------AEISVP-------------LIDRRPEQAENSETFLEGIGLGSSG----- 310
AtPS2           SRGGLERSPLVGSPSASEHSTSVG--TRGNMEDRESVMDEEMSPLVELMGWGDNR--EEA 351
OsPS1           RERNLEREAPMA-VSVSGHSSNQGGSSQHAVIQIEQHEEGETVPLVSAASANNAAPNEEH 310
OsPS2           AGDARNLRLGTSMPNLSSDSASAQVEVLPASPEISVSVPEMRVPLIQPRPERTRDEEDDE 363
HsPS1           -------------------------------NDDGGFSEEWEAQRDSHLGPHRSTPESRA 359
HsPS2           -------------------------------FGEPSYPEVFEPPLTGYPG---------- 382
MmPS1           -------------------------------NDDGGFSEEWEAQRDSHLGPHRSTPESRA 361
MmPS2           -------------------------------FGEPSYPEAFEAPLPGYPG---------- 348
DmPS            SHPRQNQRDDGSVLATEGMPLVTFKSNLRGNAEAAGFTQEWSANLSERVARRQIEVQSTQ 426
CeSel-12        ------------------------RPKVKRIPQKVQIESNTTASTTQNSGVRVERELAAE 339
CeHOP-1         ---------------------------------PPVIPRQIREVR--------------- 266


AtPS1           ---------------------------AIKLGLGDFIFYSVLVGRAAMY---DLMTVYAC 340
AtPS2           RGLEESDN------------VVDISNRGIKLGLGDFIFYSVLVGRAAMY---DLMTVYAC 396
OsPS1           RENSSSDSGME--------FEMFESTRGIKLGLGDFIFYSVLVGRAAMY---DLMTVYAC 359
OsPS2           DGIGLSSS-----------------GAIKLGLGDFIFYSVLVGRAAMY---DYMTVYAC 402
HsPS1           AVQELSSSIL---------AGEDPEERGVKLGLGDFIFYSVLVGKASATASGDWNTTIAC 410
HsPS2           --EEL---------------EEEEERGVKLGLGDFIFYSVLVGKAAATGSGDWNTTLAC 424
MmPS1           AVQELSGSIL---------TSEDPEERGVKLGLGDFIFYSVLVGKASATASGDWNTTIAC 412
MmPS2           --EEL---------------EEEEERGVKLGLGDFIFYSVLVGKAAATGNGDWNTTLAC 390
DmPS            SGNAQRSNEYRTVTAPDQNHPDGQEERGIKLGLGDFIFYSVLVGKASS--YGDWTTTIAC 484
CeSel-12        RPTVQDANFHR----------HEEEERGVKLGLGDFIFYSVLLGKASS--YFDWNTTIAC 387
CeHOP-1         ----------------------EVEGTIRLGMGDFVFYSLMLGNTVQT--CPLPTVVAC 301
                                       ::**:***:***:::*.:        *. **

AtPS1           YLAIIAGLGITLMLLSVYQKALPALPVSIMLGVVFYFLARLLLEVFVVQCSSNLVMF--- 397
AtPS2           YLAIISGLGCTLILLSVYNRALPALPISIMLGVVFYFLTRLLMEPFVVGVTTNLMMF--- 453
OsPS1           YLAIIAGLGCTLILLSICKHALPALPISILLGVTFYFLTRLLMEPFVVGSSTNLVMF--- 416
OsPS2           YLAIIAGLGITLLLLAFYPCGPKGIKAYEVDGPR-------------------------- 436
HsPS1           FVAILIGLCLTLLLLAIFKKALPALPISITFGLVFYFATDYLVQPFMDQLAFHQFYI--- 467
HsPS2           FVAILIGLCLTLLLLAVFKKALPALPISITFGLIFYFSTDNLVRPFMDTLASHQLYI--- 481
MmPS1           FVAILIGLCLTLLLLAIFKKALPALPISITFGLVFYFATDYLVQPFMDQLAFHQFYI--- 469
MmPS2           FIAILIGLCLTLLLLAVFKKALPALPISITFGLIFYFSTDNLVRPFMDTLASHQLYI--- 447
DmPS            FVAILIGLCLTLLLLAIWRKALPALPISITFGLIFCFATSAVVKPFMEDLSAKQVFI--- 541
CeSel-12        YVAILIGLCFTLVLLAVFKRALPALQFPFSPDSFFTFVPAGSSPHLLHKSLKSVYYINSL 447
CeHOP-1         FVSNLVGLTITLPIVTLSQTALPALPFPLAIAAIFYFSSHIALTPFTDLCTSQLILI--- 358
                ::: : **  ** :::.   .  .:
```

(b) NICASTRIN

```
AtNCT           --MAMGLIRLLSIAFTLVLLSILPLHLSLADEITSIESVPDLQKLMYVAVDG-FPCVRLL 57
OsNICASTRIN     --MGGGSTAPLLAAFACVFLAVFPPVAS--GDAATLESVPDLVKAMYINVES-FPCVRLL 55
HsNicastrin     -------------------MDFNLILES-------LCRGNSVERKIYIPLNKTAPCVRLL 34
MmNicastrin     MATTRGGSGPDPGSRGLLLLSFSVVLAG-------LCGGNSVERKIYIPLNKTAPCVRLL 53
DsNicastrin     -----MEMRLNAASIWLLILSYGATIAQ----------GERTRDKMYEPIGG-ASCFRRL 44
CeAPH-2         -----------MKKWLVIVLIIAGIRCDG--------FSDQVFRTLFIGEGN--ACYRTF 39
                                     :                        ::       .* * :

AtNCT           NLSGEIGCSN--PGINKVVAPIIKLKDVKD-------LVQPHTILVTADEMEDFFTR--V 106
OsNICASTRIN     NHSGQVGCSN--PGHDKVIAPIVRFGNRNDQ------LVQPSAVLLPLNQMTDFFLR--V 105
HsNicastrin     NATHQIGCQSSISGDTGVIHVVEKEEDLQWV------LTDGPNPPYMVLLESKHFTRDLM 88
MmNicastrin     NATHQIGCQSSISGDTGVIHVVEKEEDLKWV------LTDGPNPPYMVLLEGKLFTRDVM 107
DsNicastrin     NGTHQTGCSSTYSGSVGVLHLINVEADLEFL------LSSPPSPPYAPMIPPHLFTRNNL 98
CeAPH-2         NKTHEFGCQANRENENGLIVRIDKQEDFKNLDSCWNSFYPKYSGKYWALLPVNLIRRDTI 99
                * : : **.    .   ::  :    : :        :              . : *  :

AtNCT           STDLSFASKIGGVLVESGSNF--QQKLKGFSPDKRFPQAQFSPYEN---------VEYKW 155
OsNICASTRIN     SNDPELYRKIAGVLVEANG----VDNMLEFSPDRKFPQQAFAPYSN---------LSHHW 152
HsNicastrin     EKLKGRTSRIAGLAVSLTK----PSPASGFSPSVQCPNDGFGVYSNSYGPEFAHCREIQW 144
MmNicastrin     EKLKGTTSRIAGLAVTLAK----PNSTSSFSPSVQCPNDGFGIYSNSYGPEFAHCKKTLW 163
DsNicastrin     MRLKEAGPKNISVVLLINR----TNQMKQFSHELNCPNQYSGLNSTSETCDASN-PAKNW 153
CeAPH-2         SQLKSSKCLSGIVLYNSGESIHPGDESTAASHDAECPNAASDYYLQDKNEEYCERKINSR 159
                           :           .     * . . *:

AtNCT           NSAA-SSIMWRNYNFPVYLLSESG-ISAVHEILSKKKMKHGTYTSDVAEFNMVMETTKAG 213
OsNICASTRIN     NPTG-SGIMWNKYDFPVFLLSEES-TQTLQNLADKNEKSANGYLANVAEFDLVMQTTKAG 210
HsNicastrin     NSLG-NGLAYEDFSFPIFLLEDENETKVIKQCYQDHNLSQNGSAPTFPLCAMQLFSHMHA 203
MmNicastrin     NELG-NGLAYEDFSFPIFLLEDENETKVIKQCYQDHNLGQNGSAPSFPLCAMQLFSHMHA 222
DsNicastrin     NPWG-TGLLHEDFPFPIYYIADLDQVTKLEKCFQDFNNHNYETHALRSLCAVEVKSFMSA 212
CeAPH-2         GAITRDGLMKIDWRIQMVFIDNSTDLEIIEKCYSMFNKPKEDGSSGYPYCGMSFRLANMA 219
                .     .:   .: : :  : :      :.:  .  :       .  .   : .     .

AtNCT           THNSEACLQ------------------EGTCLPLGGYSVWSSLPPISVSS-----SNNRK 250
OsNICASTRIN     THDSESCLR------------------EQSCLPLGGQSVWTSLPPISNSS-----TKHQK 247
HsNicastrin     VISTATCMRRS------SIQSTFSINPEIVCDPLSDYNVWSMLKPINTTG-----TLKPD 252
MmNicastrin     VISTATCMRRS------FIQSTFSINPEIVCDPLSDYNVWSMLKPINTSV-----GLEPD 271
DsNicastrin     AVNTEVCMRRT------NFIN--NLGGSKYCDPLEGRNVSPPCTPESQQSETTLETVHTN 264
CeAPH-2         AGNSEICYRRGKNDAKLFQMNIDSGDAPQLCGAMHSDNIFAFPTPIPTSPTN---ETIIT 276
                . .:  * :                     * .: . .: .   *

AtNCT           PVVLTVAS-MDTASFFRDKSFGADSPISGLVALLGAVDALSRVD-----GISNLKKQLVF 304
OsNICASTRIN     PIIMVTAS-QDSASFFRDRSLGADSPISGLIALLTAVDALSHLH-----DISNLKKQLVF 301
HsNicastrin     DRVVVAATRLDSRSFFWNVAPGAESAVASFVTQLAAAEALQKAP-----DVTTLPRNVMF 307
MmNicastrin     VRVVVAATRLDSRSFFWNVAPGAESAVASFVTQLAAAEALHKAP-----DVTTLSRNVMF 326
DsNicastrin     EKFILVTCRLDTTTMFDGVGLGAMDSLMGFAVFTHVAYLLKQLLP----PQSKDLHNVLF 320
CeAPH-2         SKYMMVTARMDSFGMIPEISVGEVSVLTSIISVLAAARSMGTQIEKWQKASNTSNRNVFF 336
                   : .:   *:  ::   . *  . : .:     ..  :           ..  :::.*

AtNCT           LVLTGETW GYLGS RRFLHEL DLHSDAVAGLSN---------TSIETVLEIGSVGKGLSGG 355
OsNICASTRIN     AVFNGEAW GYLGS RKFLQEL DQGADSVNGISS---------LLIDQVLEIGSVGKAISQG 352
HsNicastrin     VFFQGETF DYIGS SRMVYDM EKGKFPVQLEN------------VDSFVELGQVALRTSLE 355
MmNicastrin     VFFQGETF DYIGS SRMVYDM ENGKFPVRLEN------------IDSFVELGQVALRTSLD 374
DsNicastrin     VTFNGESY DYIGS QRFVYDM EKLQFPTESTG-------------TPPIAFDNIDFMLDIG 367
CeAPH-2         AFFNGESL DYIGS GAAAYQM ENGKFPQMIRSDRTHIHPIRPNELDYILEVQQIGVAKGRK 396
                  : **: .*:**     :::    .    .                : . .:    .

AtNCT           INTFFAHKTR-VSSVTNMTLDALKIAQDSLASK--NIKILSADTANPGIPPSSLMAFMRK 412
OsNICASTRIN     YPLFYAHAAG-NSSISMKMVDALQSASESLGSD--NVKVKPAASSNPGVPPSSLMSFLGK 409
HsNicastrin     LWMHTDPVSQKNESVRNQVEDLLATLEKSGAGV--PAVILRRPNQSQPLPPSSLQRFLRA 413
MmNicastrin     LWMHTDPMSQKNESVKNQVEDLLATLEKSGAGV--PEVVLRRLAQSQALPPSSLQRFLRA 432
DsNicastrin     TLDDISNIKLHALNGTTLAQQILERLNNYAKSPRYGFNLNIQSEMSAHLPPTSAQSFLRR 427
CeAPH-2         YYVHVD--GERYQQNKTQTDRVIDRIERGLRSH--AFDLEKPSGSGDRVPPASWHSFAKA 452
                             .       :   .    .      :      .  :**:*   *

AtNCT           NPQTSAVVLEDFDTNFVNKFYHSHLDDLSNINS---SSVVAAASVVARTLYILASDN--- 466
OsNICASTRIN     NSSTPGLVLEDFDSQFSNRFYHSTLDGPANVNS---SSIAAAAALIARSLYILASAD--- 463
HsNicastrin     RN-ISGVVLADHSGAFHNKYYQSIYDTAENIN----VSYPEWLSPEEDLNFVTDTAK--- 465
MmNicastrin     RN-ISGVVLADHSGSFHNRYYQSIYDTAENIN----VTYPEWQSPEEDLNFVTDTAK--- 484
DsNicastrin     DPNFNALILNARP---TNKYYHSTYDDADNVDFTYANTSKDFTQLTEVNDFKSLNPDSLQ 484
CeAPH-2         DAHVQSVLLAPYGKEYEYQRVNSILDKNEWTED---EREKAIQEIEAVSTAILAAAAD-- 507
                     .::*         :  :*  *     :
```

```
AtNCT            -KDTSNSALGSIHVNASFVEELLTCLLACEPGLSCNLVKDYISPTNT--CPGNYAGVILG 523
OsNICASTRIN      -LPIDLITLNTIKVNVSLVEELIGCLLKCDPGLSCGIVKSFISPSNS--CPSHYVGVFQD 520
HsNicastrin      -ALADVATVLGRALYELAGGTNFSDTVQADPQTVTRLLYGFLIKANNSWFQSILRQDLRS 524
MmNicastrin      -ALANVATVLARALYELAGGTNFSSSIQADPQTVTRLLYGFLVKANNSWFQSILKHDLRS 543
DsNicastrin      MKVRNVSSIVAMALYQTITGKEYTGTKVANPLMADEFLYCFLQSADCPLFKAASYPGSQ- 543
CeAPH-2          -YVGVETDEVVAKVDKKLITTIFDCLITSNFWFDCDFMQKLDGGRYHKLFNSYGFNQKST 566
                              :             .:      ::            .

AtNCT            EPSSKPYLGYVGDVSRFLWNFLADKTSVQKGNTTSVCSKGVCSKTDEVCIKAESNKEGTC 583
OsNICASTRIN      LPAGTQFPSYADDISRFIWNFLADRTSSLAGNSSSCT--GQCHDEGEICVGAEVEGGGRC 578
HsNicastrin      YLGDGPLQHYIAVSSPTNTTYVVQYALANLTGTVVNLTREQCQDPSKVPSENKDLYEYSW 584
MmNicastrin      YLDDRPLQHYIAVSSPTNTTYVVQYALANLTGKATNLTREQCQDPSKVPNESKDLYEYSW 603
DsNicastrin      ----------LTNLPPMRYISVLGGSQESSGYTYRLLGYLLSQLQPDIHRDNCTDLPLHY 593
CeAPH-2          YISMES-----HTAFPTVLHWLTIFALGSDKETLNVKSEKSCSHLG--QFQAFQMYTYTW 619
                               :   :     .       .

AtNCT            VVS------TTRYVPAYSTRLKYNDGAWTILP-QNSSDSMGMVDPVWTESNWDTLRVHVY 636
OsNICASTRIN      VVS------TTRYVPAYSTRLKFEDNVWHVLP-VNSSDPFSAADPVWTESFWNTIGLRVY 631
HsNicastrin      VQGPLHSNETDRLPRCVRSTARLARALSPAFE-LSQWS--STEYSTWTESRWKDIRARIF 641
MmNicastrin      VQGPWNSNRTERLPQCVRSTVRLARALSPAFE-LSQWS--STEYSTWAESRWKDIQARIF 660
DsNicastrin      FAG------FNNIGECRLTTQNYSHALSPAFL-IDGYDWSSGMYSTWTESTWSQFSARIF 646
CeAPH-2          QPNP-----YTGNFSCLKSAIVKKVMVSPAVDSQTPEEEMNTRYSTWMESVYIIESVNLY 674
                   .           .  :          .      .  .   ..* ** :     .::

AtNCT            TVQHSAYDNAVLVAGITVTTLAYIGILAAKSIITKALKQD--------- 676
OsNICASTRIN      AVQATSYDWLVLLIGIIITVASYFAVIVGRSYISKIIKRD--------- 671
HsNicastrin      LIASKELELITLTVGFGILIFSLIVTYCINAKADVLFIAPREPGAVSY- 689
MmNicastrin      LIASKKLEFITLIVGFSILIFSLIVTYCINAKADVLFVAPREPGAVSY- 708
DsNicastrin      LRPSNVHQVTTLSVGIVVLIISFCLVYIISSRSEVLFEDLPASNAALFG 695
CeAPH-2          LMEDASFEYTMILIAVISALLSIFAVGRCSETTFIVDEGEPAAEGGEPL 723
                       :   :  ..     :
```

(c) APH1

```
AtAPH1           MTVAAGIGYALVALGPSLSLFVSVISRKPFLILTVLSSTLLWLVSLIILSGLWRPFLPLK 60
OsAPH1           MTVAAGLGYALVALGPAFSLFAGVVARKPFLVLTLLTSTLFWLISLIILSGIWRVFLPIR 60
HsAph1B          MTAAVFFGCAFIAFGPALALYVFTIATEPLRIIFLIAGAFFWLVSLLISSLVWFMARVII 60
MmAph1B          MTAAVFFGCAFIAFGPALALYVFTIATDPLRVIFLIAGAFFWLVSLLLSSVFWFLVRVIT 60
DmAph1           MTLPEFFGCTFIAFGPPFALFVFTIANDPVRIIILIAAAFFWLLSLLISSLWYALIP--- 57
CeAph1           MGYLLTIACYIASFSPSIALFCSFIAHDPVRIILFFLGSFFWLVSLLFSSLAWLGLSTVL 60
                 *     :.  : ::.*.::*:   :: .*. :: .: .:::**:**:: *  :

AtAPH1           AN-----VWWPYALLVITSVCFQEGLRFLFWKVYKRLEDVLDSFADRISRPRL-----FL 110
OsAPH1           SG-----AWWPYAILILTSVAFQEGIRLVFWRLYKKMEEMLDSFADRISKPRL-----CL 110
HsAph1B          DNKDGPTQKYLLIFGAFVSVYIQEMFRFAYYKLLKKASEGLKSINPGE----------TA 110
MmAph1B          DNRDGPVQNYLLIFGVLLSVCIQELFRLAYYKLLKKASEGLKSINPEE----------TA 110
DmAph1           -------LKEFLAFGVVFSVCFQEAFRYIIYRILRSTEQGLHAVAEDTR---------VT 101
CeAph1           PD--------TFLLSLTVCIIAQELSRVAYFMLLKKAQRGLNKITRQGQISVAPGVSDLH 112
                            :    .:  **  *   : : :  .  *. .

AtAPH1           TDKLQIALAG GLGHG VAHAVFFCLSLLTPAFGPATFYVE----------RCSKVPFFLIS 160
OsAPH1           TDKMLISLAG GLGHG VAHAVFFCLSLLTPAFGRATFYVE----------KCSRMPFFLVS 160
HsAph1B          PSMRLLAYVS GLGFG IMSGVFSFVNTLSDSLGPGTVGIH----------GDSPQ-FFLYS 159
MmAph1B          PSMRLLAYVS GLGFG IMSGVFSFVNTLSNSLGPGTVGIH----------GDSPQ-FFLNS 159
DmAph1           DNKHILAYVS GLGFG IISGMFALVNVLADMSGPGTMGLK----------GGTEL-FFVTS 150
CeAph1           NARHMLALVC GLGMG VISALFYTMNAFAIFSGPGTIGLPNALKTGEIDTNRAGKYLPLCY 172
                      :: . *** *:  .:*  :. ::   * .*. :             :   : :

AtAPH1           AIIALAFVTI HTFSMVIAFEGYAKGNKVDQIIVP-----VI HLTAGMLTLVNF---ASEG 212
OsAPH1           AIISLGFLVI HTFSMIIAFNGYDERKRSDQVFVP-----VV HLIASVMTLINL---APGG 212
HsAph1B          AFMTLVIILL HVFWGIVFFDGCEKKKWGILLIVL-----LT HLLVSAQTFISS--YYGIN 212
MmAph1B          AFMTLVVIML HVFWGVVFFDGCEKNKWYTLLTVL-----LT HLVVSTQTFLSP--YYEVN 212
DmAph1           AAQALSIILL HTFWSVIFFNAFDTNNYIHIGYVV-----FS HLFVSLITLLNANELYTTT 205
CeAph1           TLSAILLTLF HVTWTIMVWDSCHKIGRIPSAFVPGAAAVVS HLLVTFLSSLNSRGFHVLV 232
                 :  :: .  :*.   :: ::.           *      . ** .   : :.
```

```
AtAPH1          CVIGVPLLYLVASLTLVHCGKMVWQRLLESRNQSSASR---------------------- 250
OsAPH1          CVIGTPLLCVMGAVTLQYCWQMVWRRLSEQQHRQFSS---------------------- 249
HsAph1B         LASAFIILVLMGTWAFLAAGGSCRSLKLCLLCQDKNFLLYNQRSR--------------- 257
MmAph1B         LVTAYIIMVLMGIWAFYVAGGSCRSLKLCLLCQDKDFLLYNQRSR--------------- 257
DmAph1          LLINYLVTILTGVLAFRVAGGTSRSFRKFITCQ---------------------------- 238
CeAph1          FAVQFLILLICIAYCNVIMGGTISSFVNGIGQSITDAVTLKQVRTLIEERKLRTQRQSVP 292
                      :  :

AtAPH1          ----------------
OsAPH1          ----------------
HsAph1B         ----------------
MmAph1B         ----------------
DmAph1          ----------------
CeAph1          DEPMTERAGTSNTVNA 308
```

(d) PEN2

```
AtPEN2          MEATRSDDPS--LNPIRNRNPNPNPNPNPLSTIISS-AQVWPTIDGPLGLTEEASVDYAR 57
OsPEN2          MEARVAGVPEDEESGLLPRPSAAGRRPSVAAARRAPPPPVWATVDGPLGLPLEEAEGHAR 60
HsPen2          ---------------------------------------------MNLERVSNEEKLNLCR 16
MmPen2          ---------------------------------------------MNLERVSNEEKLNLCR 16
DsPen2          ---------------------------------------------MNISKAPNPRKLELCR 16
CePen2          ---------------------------------------------MDISKLTDVKKVDLCK 16
                                                                .    .       .:

AtPEN2          RFYKFGFALLPWLWFVNCFYFWPVLR------HSRAFPQIRNYVVRSAIGFSVFTALLSA 111
OsPEN2          RFFLWGFACLPFLWAINCCYFWPVLRSPATFPSSAAFSRIRPYVVRSAIGFTIFSVVLLT 120
HsPen2          KYYLGGFAFLPFLWLVNIFWFFREAFLVP---AYTEQSQIKGYVWRSAVGFLFWVIVLTS 73
MmPen2          KYYLGGFAFLPFLWLVNIFWFFREAFLAP---AYTEQSQIKGYVWRSAVGFLFWVIILAT 73
DsPen2          KYFFAGFAFLPFVWAINVCWFFTEAFHKP---PFSEQSQIKRYVIYSAVGTLFWLIVLTA 73
CePen2          KYFLIGACFLPLVWIVNTFWFFSDAFCKP---INAHRRQIRKYVIASIVGSIFWIIVLSA 73
                :::  * . ** :* :*  :*:               :*: **  * :*  .:  :* :

AtPEN2          WALTFSIGGEQLFGPLY**DKLVM**YNVADRLGLSGLA- 146
OsPEN2          WATTFIIGGERLFGPGWN**DLVMY**NVADKLGISGFMG 156
HsPen2          WITIFQIYRPRWG--ALG**DYLSF**TIPLGTP------ 101
MmPen2          WITIFQIYRPRWG--ALG**DYLSF**TIPLGTP------ 101
DsPen2          WIIIFQTNRTAWG--ATA**DYMSF**IIPLGSA------ 101
CePen2          WEIFFQHYRAQGL--VWT**DFLTF**VFPTGRV------ 101
                *   *             . : : ..
```

Fig 3.2 *Arabidopsis* γ-secretase component homologues contain many domains conserved with animal versions. ClustalW 2.0 multiple sequence alignments of γ-secretase components from model organisms. Plants *Arabidopsis thaliana* (At) and rice (*Oryza sativa,* Os) have not been shown to contain γ-secretase activity, however homologues of each of the components exist. Human (*Homo sapiens*, Hs), mouse (*Mus musculus*, Mm), fruit fly (*Drosophila melanogaster*, Dm) and nematode (*Caenorhabditis elegans*, Ce) are all model animal systems used to study γ-secretase. Underlined sequences represent TMDs identified for human proteins. (a) PRESENILIN 1 and 2 alignments. The active site YD and GxGD motifs in TMD 6 and 7, and the PAL(P) domain in TMD 9 are highlighted in bold. Also highlighted is the MV motif in the cytosolic loop between TMDs 6 and 7, where endoproteolysis of HsPS takes place, and the NF motif in TMD 4 that is involved in PEN2 incorporation into the complex. *C. elegans* PS homologues are called HOP1 and Sel-12. (b) NICASTRIN alignments. The DYIGS motif, with a possible role in substrate recognition, is highlighted. *C. elegans* NCT is called APH-2. (c) APH1 alignments. The only motif with specific function in APH1 is GxxxG in TMD 4. Two conserved histidine (H) residues in TMDs 5 and 6 have been shown to be important in γ-secretase complex formation and activity. (d) PEN2 alignments. The human DYLSF motif is essential for interaction of HsPEN2 with HsPS1-NTF.

most evident around the GxGD motif (containing the second active site aspartic acid) in transmembrane domain (TMD) 7. There is also a good degree of similarity throughout TMD 6, which incorporates the first active site aspartic acid in the YD motif. Another well conserved area, shown to have an important role in active site conformation, is the PAL(P) motif in TMD 9. TMD 4 contains the NF motif shown to have a function in PEN2 incorporation into the complex and is perfectly conserved in many of the proteins aligned, including both predicted *Arabidopsis* PRESENILINs. The sequence similarity is lower in the N-terminal tails, which are almost non-existent in the *Arabidopsis* and rice PRESENILINs, and the cytosolic loops. The cleavage site in the cytosolic loop, characterised by a MV motif in humans, is not fully conserved in the *Arabidopsis* PRESENILINs, similar to the situation in *C. elegans* (SEL-12 and HOP1). However there is a valine present in a suitable position for cleavage in all the proteins aligned. Mutation analysis of the MV motif has shown no effect on endoproteolysis of PS1, showing that the cleavage site is more context-specific rather than sequence specific (Brunkan et al., 2005).

Hydropathy plots of HsPS1 and AtPS1 and 2 show 8 predicted TMDs (Fig 3.3; Tusnady and Simon, 2001), with the characteristic cytoplasmic loop (approximately between amino acids 260 and 400 of HsPS1). However, the current experimentally determined model for HsPS1 is that of 9 TMDs (Laudon et al., 2005; Spasic et al., 2006). The ten hydrophobic domain (HD) conformation predicted for HsPS1 is believed to be correct, with HD 7 being membrane associated and HD 8 forming TMD 7 (containing the GxGD motif). This evidence leaves some amount of doubt about the reliability of such prediction programs, including others that produce different hydropathy plots with too few HDs (Hirokawa et al., 1998) or too many HDs (Cserzo et al., 1997). The plot in Figure 3.3(c) for HsPS1 marginally predicts the intracellular loop to be extracellular, as in the plot for AtPS2, again shedding some doubt on the reliability of these prediction programs.

AtNCT is predicted to have one transmembrane domain at the C-terminus and a signal peptide at the N-terminus, directing it through the secretory pathway (Fig 3.3d; Tusnady and Simon, 2001). The highly conserved DYIGS motif from animal

a) AtPS1

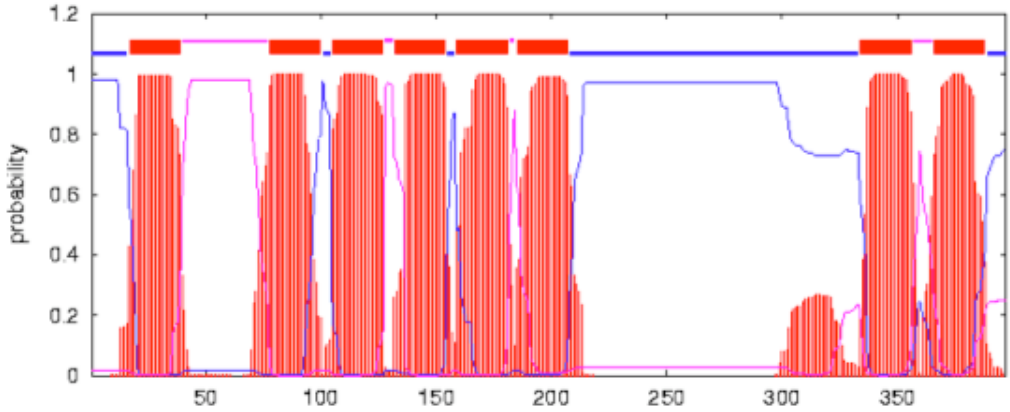

b) AtPS2

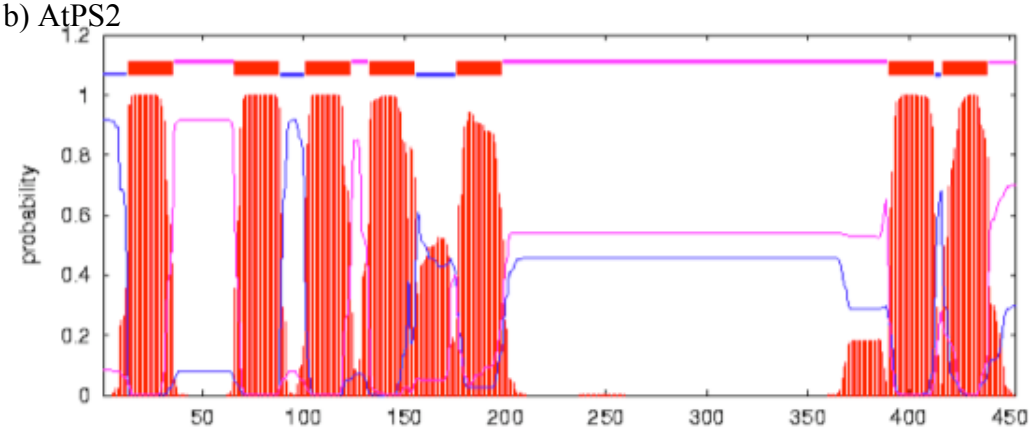

c) HsPS1

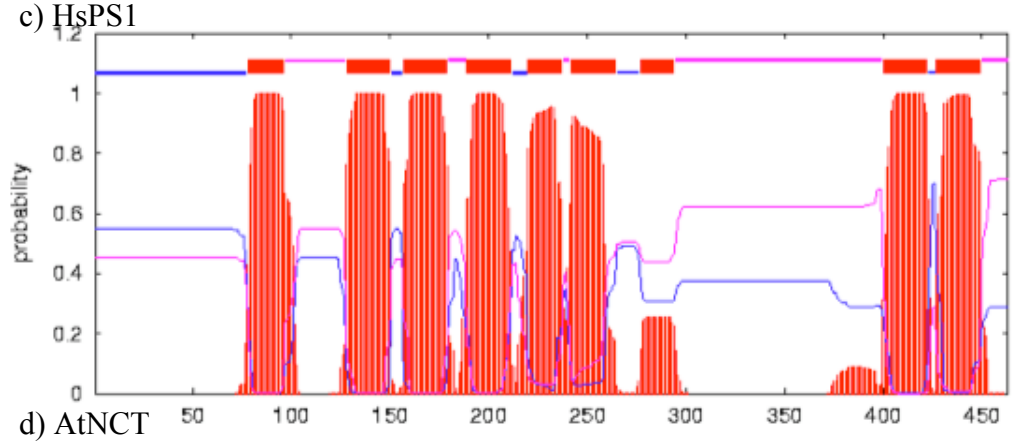

d) AtNCT

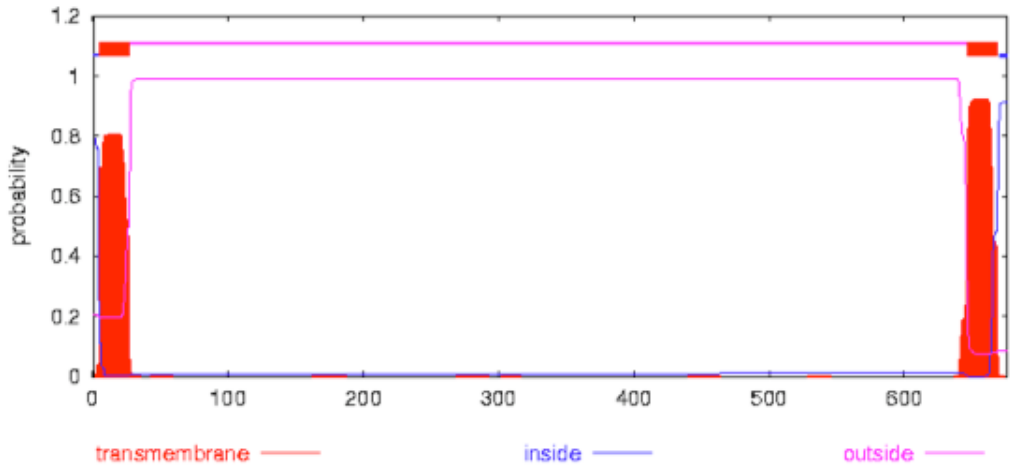

Fig 3.3 Transmembrane prediction plots for AtPS1 (a), AtPS2 (b) HsPS1 (c) and AtNCT (d) as performed by TMHMM2.0 (Tusnady and Simon, 2001). Numbers along the x-axis refer to the amino acids of the protein, with probability of internal (blue line), external (pink line) and transmembrane helix (red blocks) sequences on the y-axis. Ten hydrophobic domains are predicted for HsPS1, with HDs 1-6 and 8-10 being TMDs. HD 7 is thought to be membrane associated. The HD at the N-terminus of AtNCT is predicted to be a signal peptide. Experimental evidence shows HDs 1-6 and 8-10 are transmembrane domains.

NICASTRIN, which is thought to act in substrate recognition and binding due to its effects on APP processing (Shah et al., 2005), is replaced in *Arabidopsis* by GYLGS (this is also the case in rice; Fig 3.2b). However, there is evidence that the DYIGS motif may not be involved with substrate presentation, but in NICASTRINs interaction with PRESENILIN. A mutated version (DYIGS to AAIGS) is able to rescue an egg laying phenotype in *C. elegans* caused by a transposon insertion mutation in *Ceaph2* (the nematode *NCT* gene; Yu et al., 2000). However, deletion of this region results in a decrease in the association of CeAPH2 (NCT) with CeSEL-12 (PS). If this is the case, the difference in sequence of this motif may be due to a divergent sequence in the *Arabidopsis* PRESENILINs. The carboxylate side chain of a glutamate residue (E333 in HsNCT) is thought to interact with the free amino terminus of the substrate (Shah et al., 2005). Indeed, mutation of this residue to a variety of other amino acids abolished γ-secretase dependent cleavage of APP, and only substitution with aspartate able to restore function. All animal NCTs aligned here have a glutamate in this position, however the plant NCTs have an aspartate (Fig 3.2b).

There are 7 transmembrane domains predicted for AtAPH1, the same as for HsAPH1a and b (data not shown), with TMD 4 containing the three glycines of the GxxxG motif. This motif is essential for interactions of APH1 with other members of the complex, in particular PRESENILIN (Niimura et al., 2005). This GxxxG motif is among a number of well-conserved sites in this group of homologues (Fig 3.2c), although the only other functional significance has been seen for two conserved histidines (H) in TMDs 5 and 6. Mutation of either of these histidines to uncharged residues results in a destabilization of the γ-secretase complex and lowered activity, suggesting they are important for structural cohesion or even active site conformation (Pardossi-Piquard et al., 2009).

Little is known about the function of PEN2, apart from its importance in maturation of the γ-secretase complex. A single domain at the extreme C-terminus (conserved in humans and mice as DYLSF; Fig 3.2d) is thought to be critical for binding PEN2 to the other members of the complex (Hasegawa et al., 2004). In *Arabidopsis*, this

motif has not been conserved perfectly and is replaced by DKLVM and in rice as NDLVM. Again, given the divergence of the other proteins, and its proposed function, perfect conservation may not be necessary. The N-terminal portion of HsPEN2 is required for association with the conserved NF motif in HsPS1 TMD 4, and subsequent endoproteolysis (Kim and Sisodia, 2005a, b).

In conclusion, a number of protein motifs have been shown to be important in γ-secretase complex formation and activity. Some of these motifs are well conserved between *Arabidopsis* and animal proteins, such as the active site YD, GxGD and PAL(P) motifs in PS and the histidines in APH1. Others, with functions in protein-protein interactions within the complex, show some sequence divergence (DYIGS to GYLGS in NCT and DYLSF to DKLVM in PEN2).

3.4. Putative members of the Arabidopsis *γ-secretase complex are expressed and cDNA predictions are correct*

The five genes of interest in *Arabidopsis* are predicted to encode proteins with similarity to each of the members of the animal γ-secretase complex. Gene specific primers were designed to amplify the coding sequence of each of the genes from the ATG to the STOP codons and to incorporate restriction enzyme sites for further cloning. Total RNA was extracted from leaves of wild type Col-0 plants and a reverse transcription kit (Invitrogen) was used to produce cDNA. Following high fidelity PCR amplification (*Pfu* Turbo) with gene specific primers, the products were cloned into pGEMT-easy and sequenced using universal and reverse primers present in the cloning vector. A number of sequenced clones perfectly matched the annotated coding sequences from TAIR (Swarbreck et al., 2008) for each gene. The predictions for *AtPS2*, *AtAPH1* and *AtPEN2* all contained at least one intron, absent from the amplified sequence, showing that the mRNAs are processed as annotated. *AtPS1* does not contain any introns, and the whole open reading frame was amplified. As detailed above, *AtNCT* is predicted to have three splice variants (Fig 3.1). Only variant At3g52540.1 was amplified from leaf RNA, suggesting that this is the only variant expressed in leaves.

3.5. Expression analysis of the putative Arabidopsis *γ-secretase complex members*

In order to form a complex, each member of the complex must be expressed in a similar developmental/organ specific and temporal fashion. A vast amount of digital microarray data in now available online, such as GeneVestigator (genevestigator.ethz.ch), AtGenExpress (weigelworld.org) and e-FP browser (bar.utoronto.ca). This data has been supplemented over time as more microarray experiments have become publicly available. At the start of my PhD, GeneVestigator results showed a universal expression profile for each gene under investigation, with an increased expression in inflorescences for *AtPS2* and *AtAPH1*.

RNA *in situ* hybridisations were carried out with wild-type Columbia-0 plants. Floral meristems were chosen due to data (available at the time) showing relatively higher expression of the genes under investigation in this particular area. The staining pattern, as shown by a dark brown colouration, is confined to the inflorescence meristem area and young developing floral organs. This pattern is relatively similar for all five genes (Fig 3.4), which supports the possibility of the gene products forming a complex in *Arabidopsis*. Expression of *AtPS1, AtPS2, AtNCT, AtAPH1* and *AtPEN2* is seen by staining in the meristems regions, and young developing floral organs. Little, if any, expression is seen in the tissues of the stem.

Since performing these *in situs*, a greater amount of data has become available (such as that in Fig 3.5) showing that each member of the putative *Arabidopsis* γ-secretase complex is expressed to some degree in all organs of the plant at all points of development. This data also shows no significant change in expression following a range of stresses, both hormonal/chemical and biotic (Fig 3.6).

To experimentally validate the *in silico* expression profiles, RT-PCR analysis of each gene in various organs/tissues of the plant was also carried out. The tissues chosen were 10 day old seedlings grown on 0.5x MS agar, rosette leaves from 6-week-old plants grown on soil, inflorescences including young (unopened) floral buds and open flowers including young developing siliques. Figure 3.7 shows the results from

these RT-PCR reactions, carried out in duplicate for each tissue. Full-length transcript can be amplified from all tissues examined, with *TUBULIN* included as a loading control. It is thus likely that *in silico* data showing that the expression of these genes is not notably changed in response to either biotic or abiotic stresses, is accurate. Amplification of *AtNCT* produces a single band, suggesting that only one of the splice variants is produced.

In conjunction with RT-PCR, reporter lines were made by fusing upstream regions from each of the five genes to a HISTONE-2B:YELLOW FLUORESCENT PROTEIN (H2B:YFP) construct (Gifford et al., 2003). Promoter regions (including any 5' UTR) were amplified from Col-0 genomic DNA using primers to introduce an *Xho*I site at the extreme 5' end and a *Sal*I site immediately prior to the ATG start codon of the genes. These sites were chosen to be compatible with GFP fusion constructs designed to be used for subcellular localisation (see Chapter 4). Surprisingly, for four of the five genes the available promoter sequence was very short, less than 300 bp between the ATG and the upstream gene. The promoter sequence amplified for *AtPS1* was 263 bp, *AtPS2* was 282 bp, *AtPEN2* was 172 bp and *AtAPH1* was 160 bp. There was more sequence upstream of *AtNCT*, so a 1700 bp region was chosen to use as promoter.

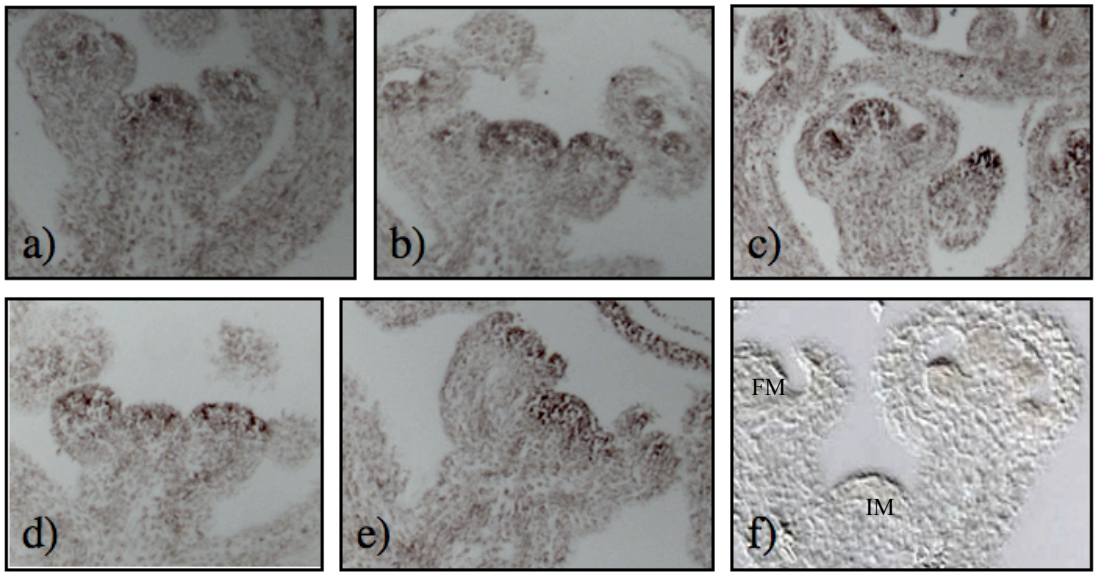

Fig 3.4 RNA *in situ* hybridisations carried out on wild type Col-0 inflorescence meristems with probes against *AtPS1* (a), *AtPS2* (b), *AtNCT* (c), *AtPEN2* (d), *AtAPH1* (e) and a sense control (f). Signal is present in (a) through (e) as dark brown staining in the inflorescence meristems (IM in (f)), and young developing floral organs. All images were acquired at the same magnification.

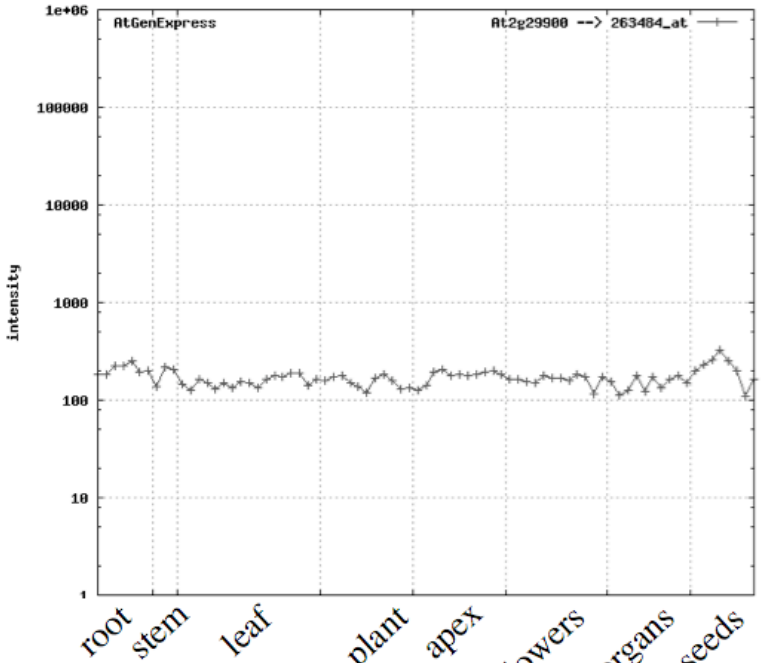

a) *AtPS1*

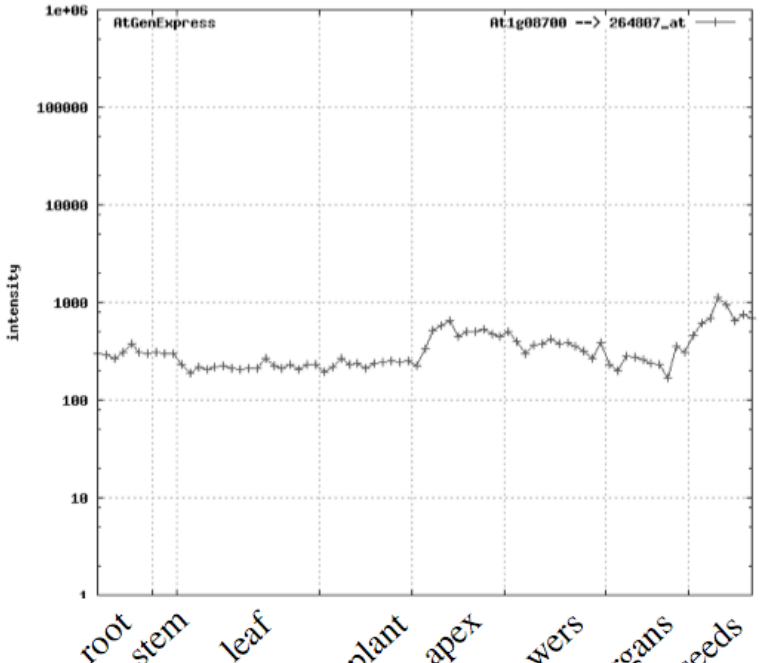

b) *AtSP2*

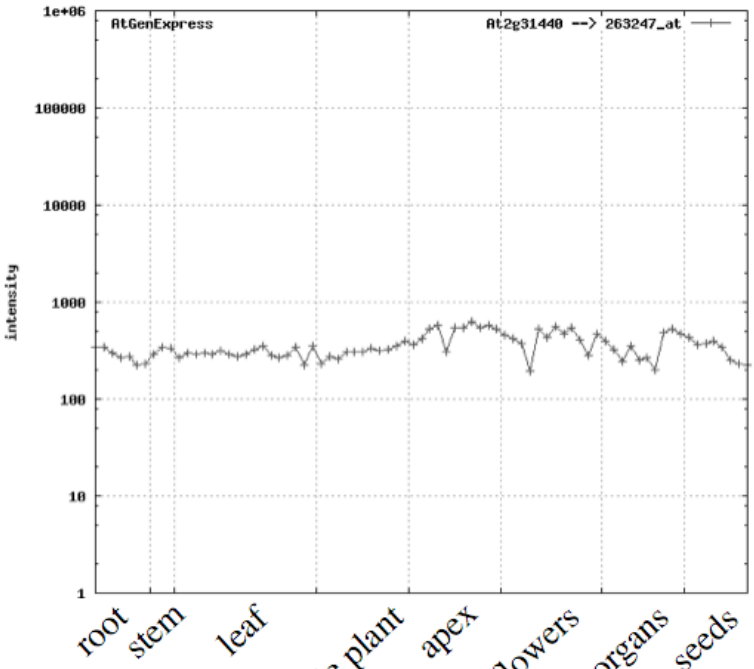

c) *AtAPH1*

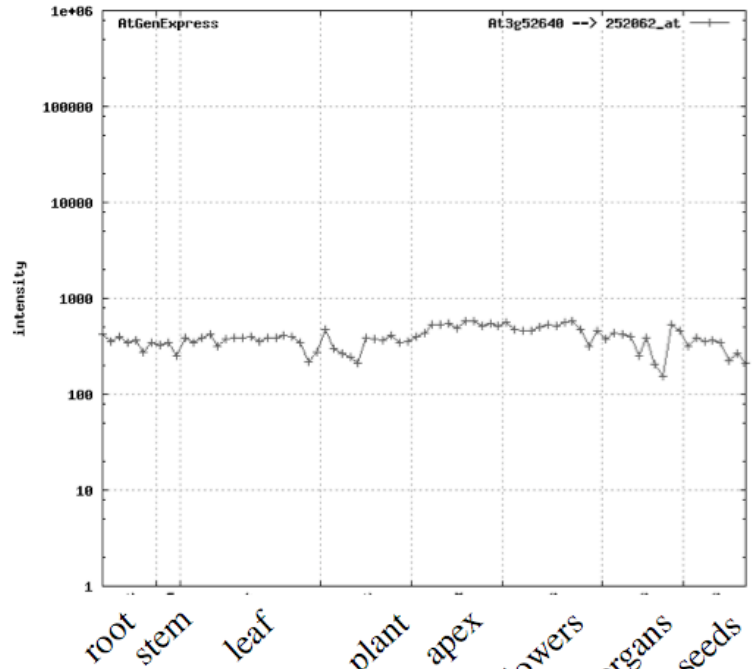

d) *AtNCT*

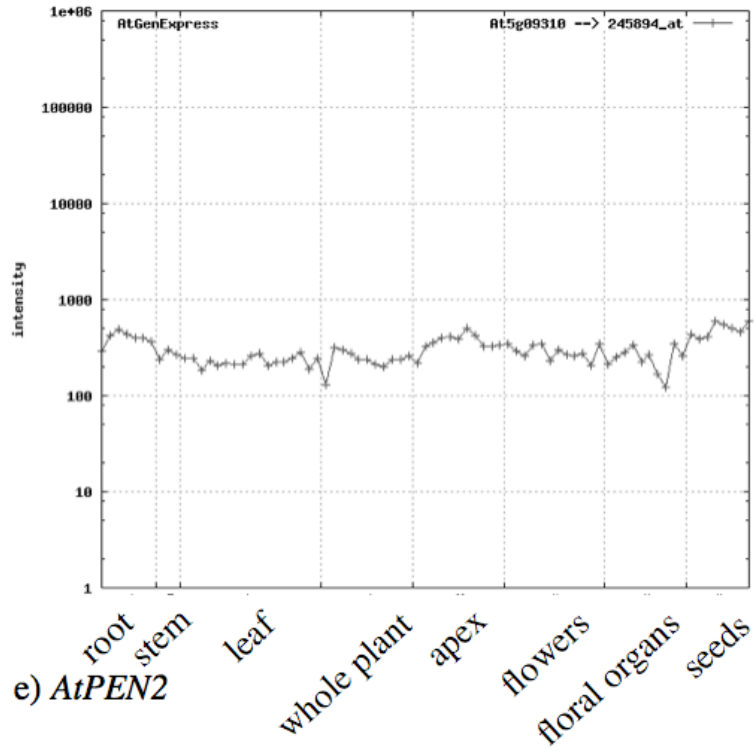

e) *AtPEN2*

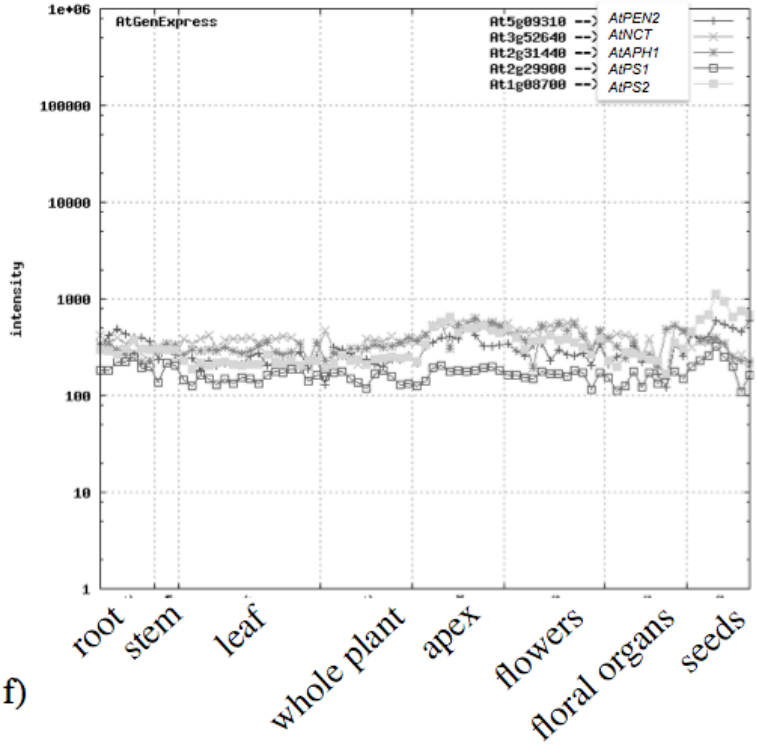

f)

Fig 3.5 Expression profiles of the members of the potential γ-secretase complex in *Arabidopsis*, produced from Weigelworld's microarray database web-browser (Schmid et al., 2005). Data points in each tissue cluster correspond to various sample time points, specific parts of the tissue studied, or responses in different genetic backgrounds (for a list of samples, see appendix). (a) *AtPS1*, (b) *AtPS2*, (c) *AtAPH1*, (d) *AtNCT*, (e) *AtPEN2*, (f) combination of all five genes.

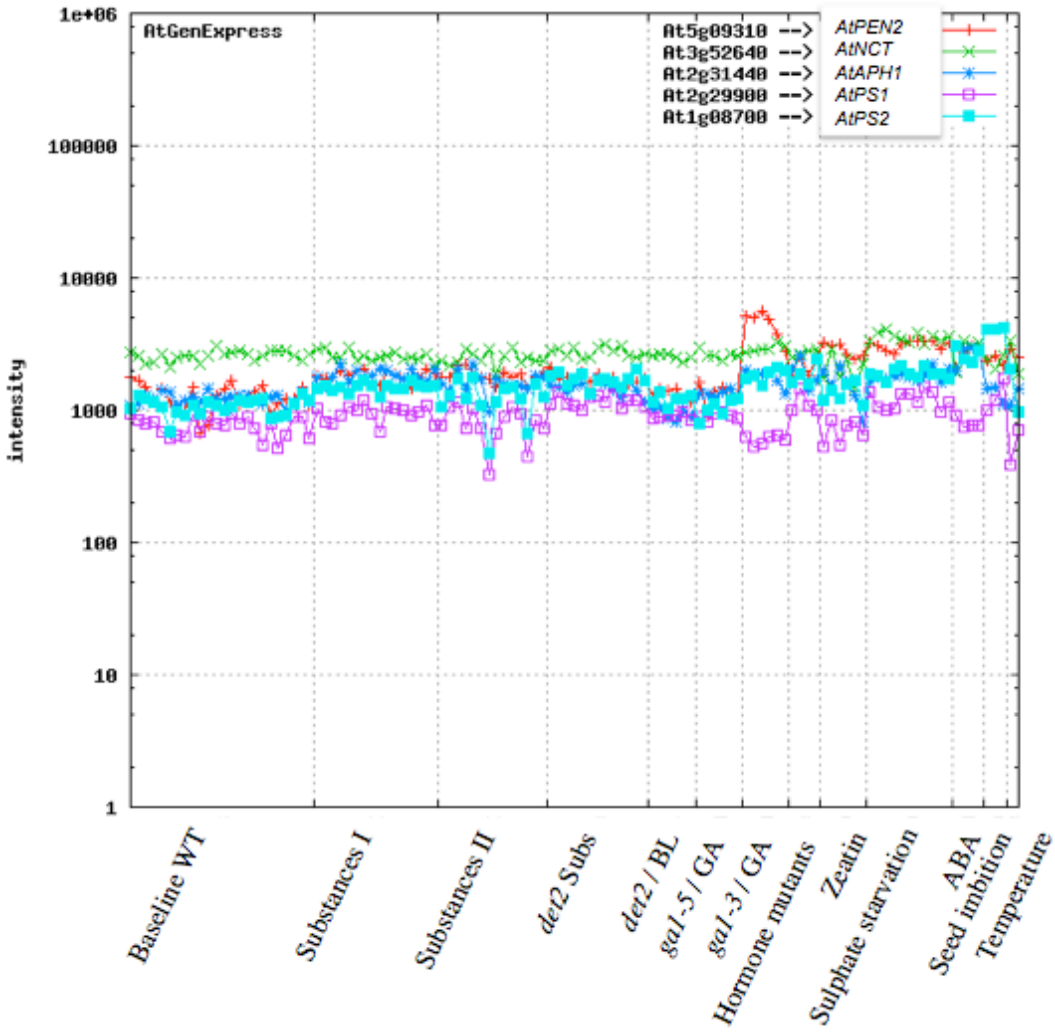

Fig 3.6 Expression profiles for the members of the potential γ-secretase complex in *Arabidopsis* following treatment with a range of stresses. Normalised expression for each gene, in arbituary units. See Appendix for stress conditions.

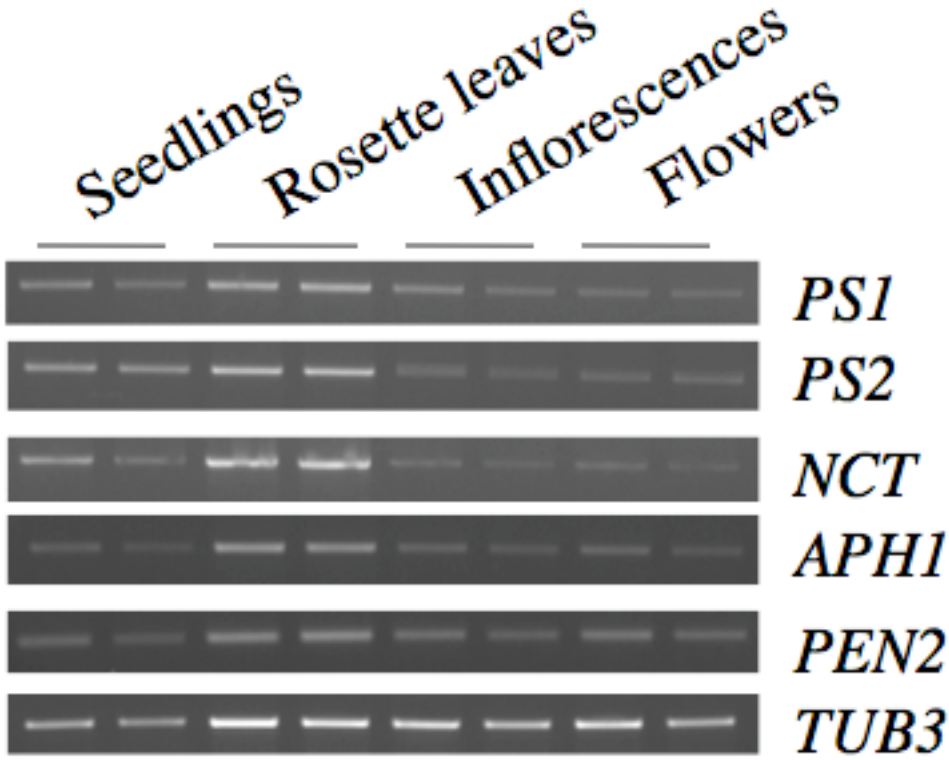

Fig 3.7 RT-PCR analysis of gene expression in various tissues. Gene specific primers were used to amplify the five genes of interest, along with *TUBULIN* as a loading control for each tissue. Tissues chosen were seedlings, rosette leaves, inflorescences/young flower buds, and open flowers/developing siliques. As a control, cDNA was also amplified with primers for a ubiquitously expressed *TUBULIN3* gene (*TUB3*, At5g62700*)*.

When stably transformed into *Arabidopsis*, homozygous lines were identified, but unfortunately no signal was observed, suggesting that either the promoter sequence chosen was not sufficient or there are other sequence elements (such as introns) required for expression of these genes. This latter supposition was supported by subsequent production of an *AtPEN2* construct consisting of the putative promoter, 5' UTR and coding sequence (including intron) fused in frame to GFP at the 3' end. Stably transformed *Arabidopsis* plants expressing the construct produced AtPEN2:GFP protein (Fig 3.12) in all tissues studied.

3.6. Protein distribution of AtPS1 and AtAPH1 is not uniform throughout Arabidopsis *plants*

Recently, Baerenfaller *et al*. (2008) composed an *Arabidopsis* proteome map comprising 13,029 proteins (with 86,456 unique peptides) through a tandem mass spectrometry approach. The proteins identified account for nearly 50% of the *Arabidopsis* gene models, and the information is publicly available at AtProteome.ethz.ch. Samples were taken from roots, cotyledons, juvenile leaves, flower buds, open flowers, carpels, siliques, seeds and undifferentiated cell culture.

Queries to this database revealed that it contains three of the five proteins under investigation here – AtPS1, AtNCT and AtAPH1. AtPS1 and AtAPH1 were identified through a single peptide each, both of which were found in the silique sample pool (Fig 3.8). Twelve peptides from AtNCT were identified in this study (a total of 45 times), 5 of which identified in the silique sample pool, some numerous times. A single peptide relating to one of the other splice variants of AtNCT was found in a cell culture sample, suggesting that the splice variants are tissue specific. From this data, it is possible to forward the hypothesis that any potential γ-secretase complex is restricted to the siliques. However, given the small number of peptides identified from AtPS1 and AtAPH1, and the expression profiles of the genes, this may artificially limit the search for a plant γ-secretase complex. This information only became available towards the end of my PhD, after many of the experiments had been carried out. However, as much time and resources as possible were devoted to this new information since then.

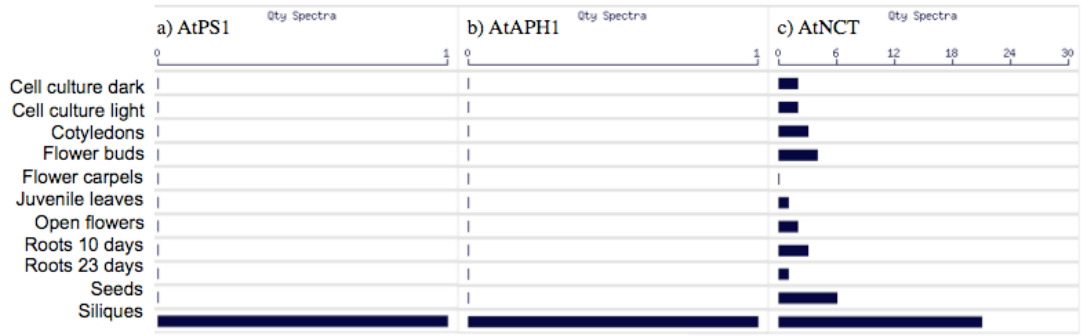

Fig3.8 Spectrum summary from AtProteome showing tissues where individual peptides from AtPS1 (a), AtAPH1 (b) and AtNCT (c) were found. Black bars represent proportion of peptides identified in each sample. AtPS1 and AtAPH1 were only identified in silique samples, whereas AtNCT was found throughout the plant. AtPEN2 and AtPS2 were not identified in this study.

3.7. Insertion mutant identification and analysis

A number of insertion mutants were available for each gene of interest, and all possible mutant lines were obtained from the stock centre (Table 3.1). A PCR based approach for genotyping each line was developed to identify homozygous mutants (Table 3.2 and Fig 3.9). For each gene, at least two homozygous mutants were identified (Table 3.1), but a number of lines obtained apparently contained no T-DNA insertion. Total RNA was extracted from each of the mutants and further analysis by RT-PCR identified alleles which show a down-regulation of full length transcript, to the point where it is undetectable by this method (Fig 3.10). Homozygous insertion mutants that still produced transcript (generally having the insertion in the 3' or 5' UTR) were discarded and only certain alleles were subjected to further investigation. Mutants chosen were *ps1-1*, *ps2-3*, *nct2*, *aph1-1* and *pen2-2* (see section 3.8 for discussion of *pen2-1*).

Arabidopsis gene number	Allele	Stock center code number	Position from ATG	Position in gene	Insertions identified?	Transcript detected?
At2g29900	*ps1-1*	SALK 016037	+575	exon	Y	N
	ps1-2	SALK 016085	+645	exon	N	N/A
	ps1-3	SALK 013158	+550	exon	Y	N
At1g08700	*ps2-1*	SALK 038487	-60	5' UTR	Y	Y
	ps2-2	SALK 069469	-85	5' UTR	Y	Y
	ps2-3	SALK 145544	+1072	exon	Y	N
At3g52640	*nct1*	SALK 106245	+3144	exon	Y	N
	nct2	WISC DS LOX502C06	+1140	intron	Y	N
	nct3	SAIL 1209 B12	+2734	intron	N	N/A
	nct4	FLAG 152 A08	+3100	intron	N	N/A
At5g09310	*pen2-1*	SALK 128110	+622	intron	Y	N
	pen2-2	SALK 140461	+875	intron	Y	N
	pen2-3	SALK 128111	+650	intron	N	N/A
	pen2-4	SAIL 103 B 03	+1211	3' UTR	Y	Y
	pen2-5	FLAG 501 D03	+1304	3' UTR	N	N/A
At2g31440	*aph1-1*	SALK 118799	+1547	exon	Y	N
	aph1-2	WISC DS LOX413-416L 12	+1586	intron	Y	N
	aph1-3	SAIL 1057 G 07	+375	intron	N	N/A
	aph1-4	SAIL 1057 B 03	+217	intron	N	N/A
	aph1-5	SAIL 159 E 06	+1335	intron	Y	N

Table 3.1 Insertion mutant alleles obtained from stock centre. Position from ATG refers to the insertion site of the T-DNA with respect to the ATG start codon for each gene.

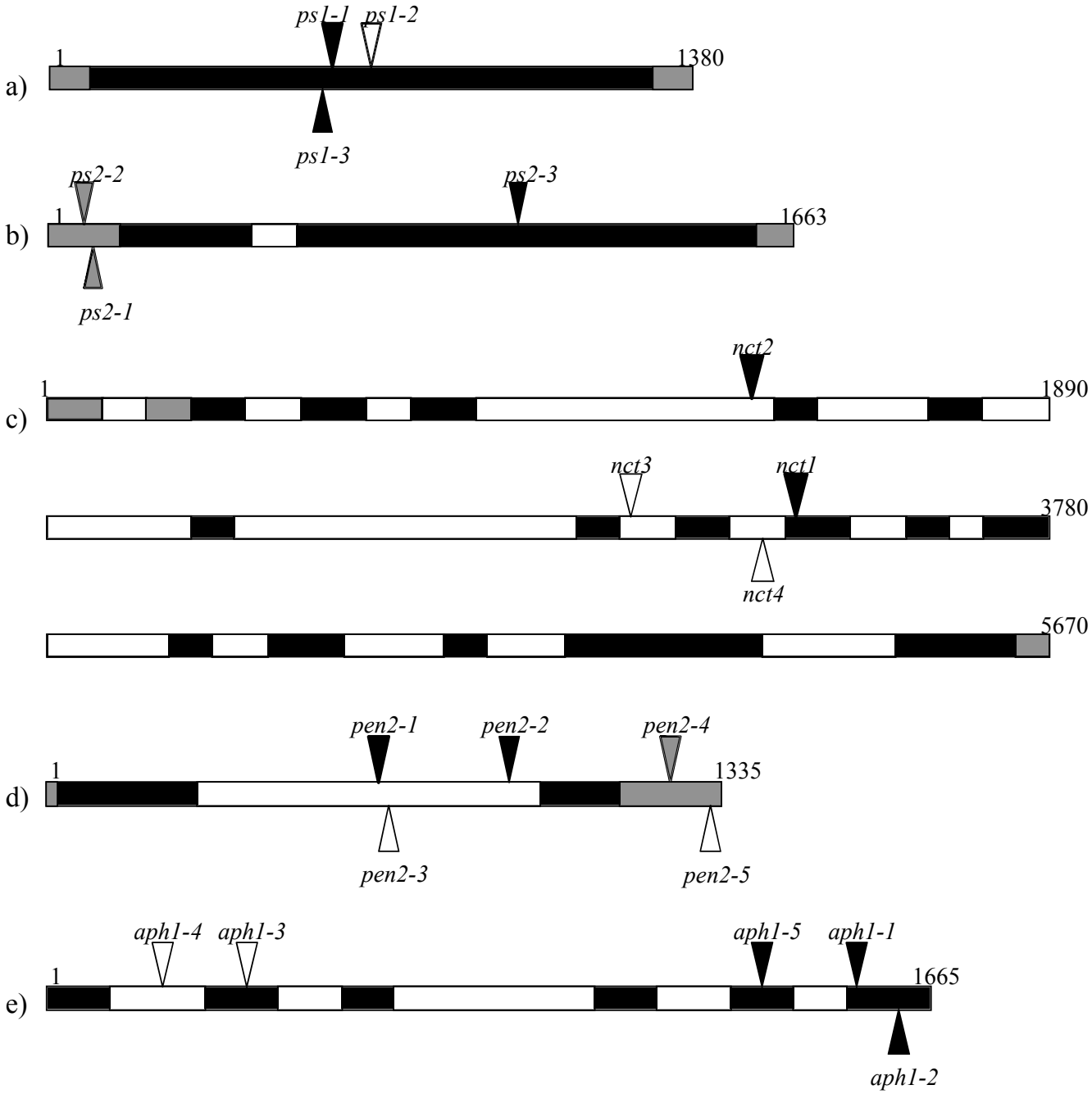

Fig 3.9 Gene structure showing exons (black rectangles), introns (open rectangles) and untranslated regions (grey rectangles where present), approximately to scale for each gene. a) *AtPS1* (At2g29900), b) *AtPS2* (At1g08700), c) *AtNCT* (At3g52640), d) *AtPEN2* (At5g09310), e) *AtAPH1* (At2g31440). Positions of insertions are indicated by triangles. Black triangles represent downregulated homozygous mutants identified, grey triangles homozygous insertion mutants still producing transcript and open triangles represent lines lacking a T-DNA insertion.

Allele	Wild type			Mutant			
	5’	3’	Size	5’	3’	Predicted	Insertion
ps1-1	-4	+1200	1204	Salk LB	+1200	975	Exon
ps1-2	-4	+1200	1204	Salk LB	+1200	647	Exon
ps1-3	-4	+1200	1204	Salk LB	+1200	717	Exon
ps2-1	-184	+1497	1681	Salk LB	+1497	1568	5’UTR
ps2-2	-184	+1497	1681	Salk LB	+1497	1583	5’UTR
ps2-3	-184	+1497	1681	Salk LB	+1497	981	Exon
nct1	+2194	+3402	1208	Salk LB	+3402	381	Exon
nct2	+822	+1738	916	WISC LB	+1738	508	Intron
nct3	+2194	+3402	1208	+2194	Sail LB	600	Intron
nct4	+2194	+3402	1208	+2194	FLAG LB	762	Intron
pen2-1	+461	+992	531	Salk LB	+992	370	Intron
pen2-2	+461	+992	531	+461	Salk LB	414	Intron
pen2-3	+237	+767	530	+237	Salk LB	407	Intron
pen2-4	+1075	+1581	506	Sail LB	+1581	502	3’UTR
pen2-5	+1075	+1581	506	FLAG LB	+1581	311	3’UTR
aph1-1	+1219	+1608	389	+1219	Salk LB	328	Exon
aph1-2	+1219	+1608	389	+1219	WISC LB	361	Exon
aph1-3	+66	+628	616	Sail LB	+628	551	Exon
aph1-4	+66	+628	616	Sail LB	+628	546	Intron
aph1-5	+1027	+1422	369	+1027	Sail LB	457	Exon

Table 3.2 Position of primers used in PCR genotyping of insertion mutants. Numbers indicate position of primer with respect to ATG start codon, and size of PCR product expected in base pairs. SALK, WISC, Sail and FLAG refer to the T-DNA specific left border primer. A list of primer sequences is provided in Chapter 2 (Materials and Methods).

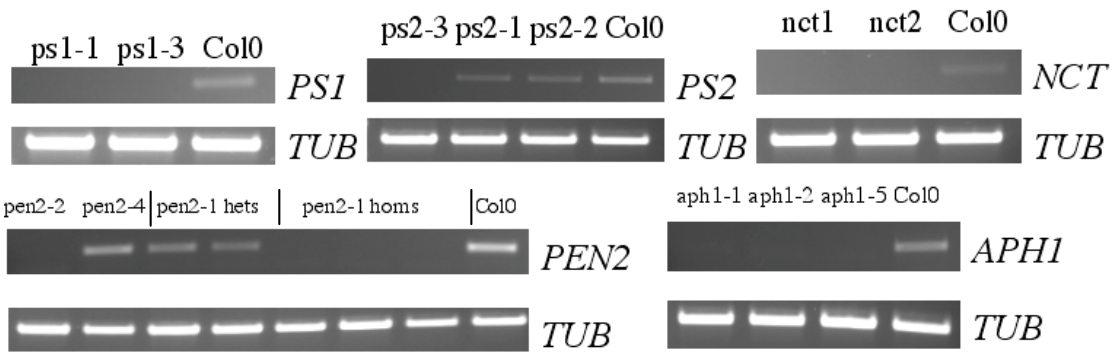

Fig 3.10 RT-PCR analysis of mutant lines. RNA was extracted from mutant and wild-type (Col-O) plants. cDNA was synthesized from each sample, and analysed with gene-specific and control (*TUBULIN (TUB))* primers. Several mutant alleles, *ps2-1* and *ps2-2,* and *pen2-4* show wild-type gene expression despite the presence of mutagenic T-DNAs in the corresponding gene. These alleles were discarded.

3.8. pen2-1 *mutant analysis*

A single mutant allele of *AtPEN2* showed a very distinctive phenotype. Segregating from heterozygous parents in a 3:1 ratio, slow growing seedlings (Fig 3.11 a), b), e) and f)), which produce small leaves with necrotic-like lesions (Fig 3.11g)) and fail to produce a functional inflorescence, have been genotyped as homozygous for the *pen2-1* insertion. Altering the growth conditions to cold short days (8hrs light, 16hrs dark, 16^{o}C) relieves the phenotype slightly but the plants still show retarded growth and cannot bolt (Fig 3.11 c) and d)). All plants showing this phenotype which were genotyped were homozygous for the *pen2-1* insertion (n = 8). Any wild type-looking plants segregating from the same parents have been either heterozygous for *pen2-1* or wild type. Three individual homozygous plants were analysed by RT-PCR (Fig 3.10), which revealed they do not produce full-length transcript. However, it is possible to amplify *AtPEN2* transcript from heterozygous mutant plants.

The phenotype observed for *pen2-1* suggests the mutants may constitutively express defence genes, a response to increased levels of the plant hormone salicylic acid (SA), such as that seen in the *len3* and *acd11* mutants (Brodersen et al., 2002; Ishikawa et al., 2006). To investigate this possibility, crosses to *sid2* and *nahG* plants were carried out. *sid2* and *nahG* are both deficient in salicylic acid accumulation due to a mutation in a SA biosynthesis protein coding gene, and a

transgene encoding a bacterial SA hydroxylase respectively. The *nahG* transgene is able to rescue the lesion mimic phenotypes in *len3* and *acd11*, however similar mutants are not SA dependent, such as *lsd2* and *lsd4* (Hunt et al., 1996). The *pen2-1* homozygous phenotype is not relieved by SA deficiency, suggesting the mutant phenotype is not due to an over accumulation of SA.

Due to the severity of the *pen2-1* phenotype compared to the *pen2-2* homozygous insertion mutants, I felt it best to try to complement the phenotype with an *AtPEN2* cDNA construct to check that it is not caused by a very tightly linked insertion in another gene. A construct consisting of the 35S promoter from cauliflower mosaic virus (CMV) driving the *AtPEN2* cDNA fused in frame with the green fluorescent protein (*p35S:AtPEN2:GFP*; see Chapter 4) was crossed into a heterozygous *pen2-1* plant. Progeny were selected on antibiotic for the transgene, and lines homozygous for the transgene carrying the *pen2-1* mutation were identified. From these plants, uncomplemented mutants still segregated in the offspring at a frequency of 25%, suggesting that this construct does not complement the mutation giving rise to the phenotype.

To further investigate this mutant, a genomic fragment consisting of the supposed *AtPEN2* promoter (from 172 bp upstream of the ATG start codon) through to the stop codon, including the intron, was cloned and fused to GFP. This was used to transform wild-type looking plants segregating from a heterozygous *pen2-1* parent. Primary transformants were selected for and genotyped for the *pen2-1* insertion. Again, homozygous T-DNA lines carrying the *pen2-1* mutation were identified but still produced mutant offspring. Western blot analysis of these lines shows that in a wild type background, AtPEN2:GFP is accumulated at relatively high levels (Fig 3.12). Both *p35S:AtPEN2:GFP* and *pAtPEN2:AtPEN2g:GFP* give rise to ~45 kDa proteins, the predicted size for AtPEN2:GFP. However, heterozygous *pen2-1* plants show a lower accumulation/expression, and in mutant homozygotes it is completely eradicated, possibly due to the presence of multiple T-DNA insertions carrying the 35S promoter. Therefore, it is not possible to say whether the transgene is able to complement the mutation, due to this apparent down regulation.

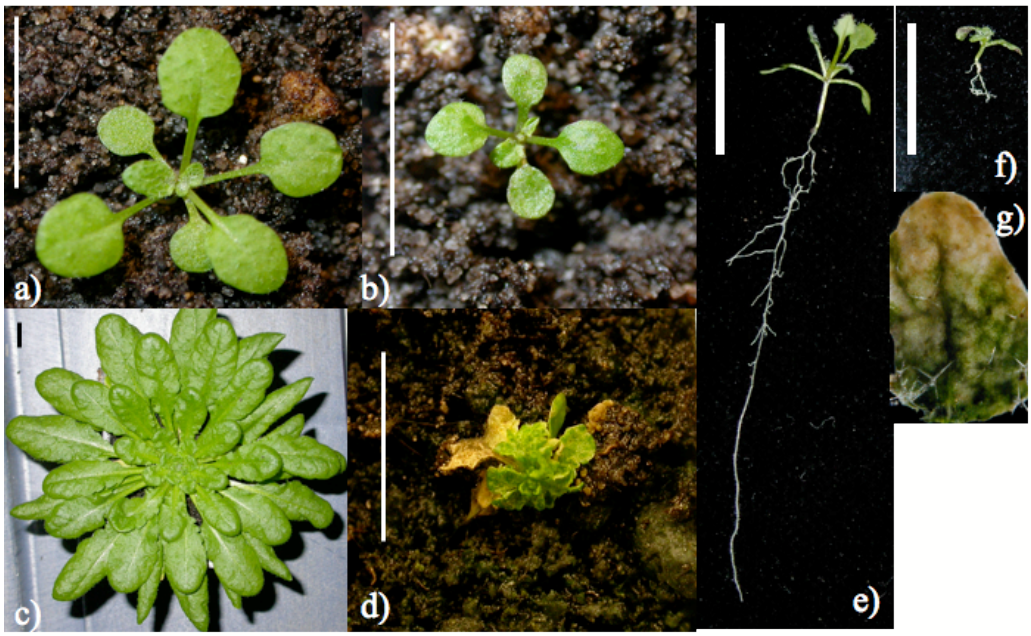

Fig 3.11 Phenotype of *pen2-1* homozygous insertion plants. *pen2-1* heterozygous parents segregate 3:1 for wild type to mutant phenotypes. 4-week-old seedlings grown in short days show a wild type (a) or slow growing mutant phenotype (b). (c) and (d) 3 month old plants grown in cold short days (16^{o}C). The mutant in d) was genotyped as a *pen2-1* homozygote and the plant in c) is wild type. Wild type (e) and mutant (f) seedlings grown for 14 days on vertical 0.5x MS plates. (g) Lesions on a mutant leaf. Scale bars a) and b) 0.5cm, c) to f) 1cm.

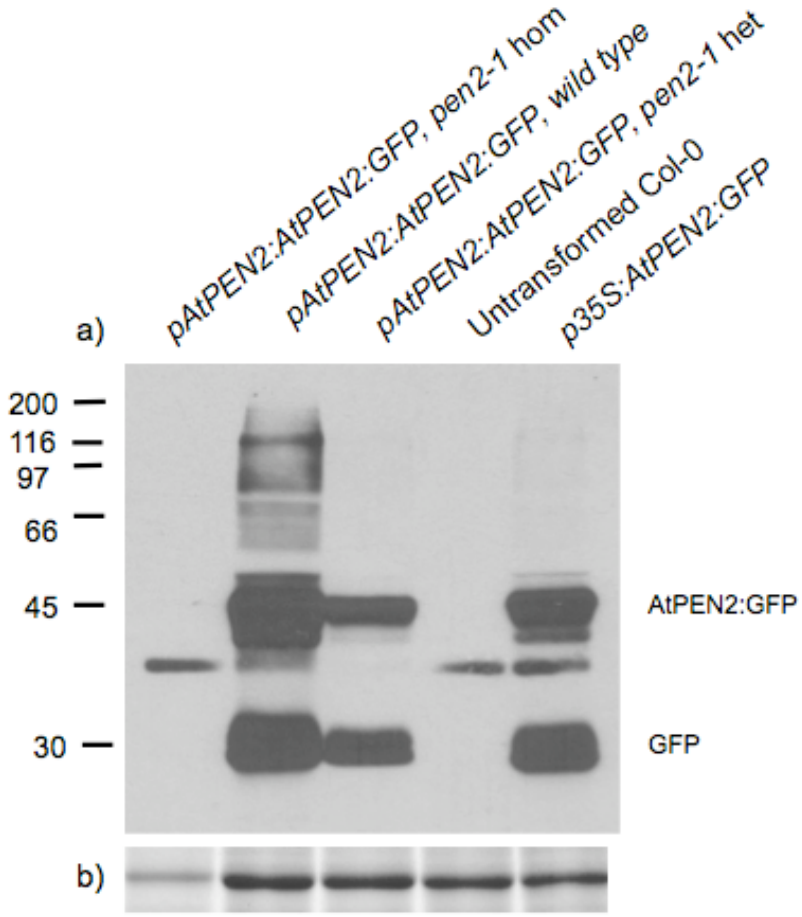

Fig 3.12 Presence of the *pen2-1* mutation causes downregulation of *pAtPEN2:AtPEN2g:GFP*. Heterozygous *pen2-1* mutants were transformed with pRW492 (*pAtPEN2:AtPEN2g:GFP*), and selected for transformants carrying the *pen2-1* mutation and segregating 3:1 for *pAtPEN2:AtPEN2g:GFP* in the T_1 generation.
(a) Western blot carried out on protein extracted from 10-day-old seedlings with α-GFP primary antibody. AtPEN2:GFP fusion protein ~45 kDa, GFP ~30 kDa. Homozygous and heterozygous *pen2-1* insertional mutants show lower GFP fusion protein accumulation compared to the wild type background. Size markers in kDa are indicated on left.
(b) Coomassie stained gel showing large RUBISCO subunit as loading controls for (a).

3.9. Phenotypic analysis of insertion mutants

When grown under long day conditions (16 hrs light, 8 hrs dark, 22^{o}C), none of the other transcript null mutants (*ps1-1*, *ps2-3*, *nct2*, *aph1-1* and *pen2-2*) displayed a gross morphological difference to the Col-0 wild type control. Crosses were preformed to produce *ps1-1/ps2-3* and *nct2/aph1-1* double homozygous mutants. Again these lines did not differ from wild-type controls. In order to uncover a phenotype, mutant plants were exposed to a number of hormone treatments and stresses and compared to wild type under the same conditions.

Digital Northern data indicated an increase in *AtPEN2* transcript in *ga1-3* mutant seed, which was reduced by application of gibberellic acid (GA; Fig 3.6). GA is a plant hormone with roles in seed germination, cell elongation, flowering time and floral development (Richards et al., 2001), and Paclobutrazol is an inhibitor of GA biosynthesis. The *ga1-3* mutant shows a non-germinating, male-sterile dwarf phenotype that can be relieved by application of GA (Sun et al., 1992). To test for potential γ-secretase involvement in GA signalling, seed was surface sterilised and imbibed in water for 3 days prior to germination on 0.5x MS plates supplemented with a range of concentrations of GA or Paclobutrazol (see Table 3.3 for specific concentrations), and allowed to grow for 14 days. Lines chosen were wild type Col-0, each of the homozygous insertion mutants (*ps1-1*, *ps2-3*, *nct2*, *aph1-1*, *pen2-2* and the *ps1-1/ps2-3* and *nct2/aph1-1* double mutants), as well as *p35S:AtPEN2:GFP*. No gross morpholigical changes were seen between wild-type and mutant, or the *p35S:AtPEN2:GFP* seedlings.

Numerous substrates have been identified for the animal γ-secretase complex, such as Notch, APP and ErbB-4, all of which are type 1 transmembrane proteins. The *Arabidopsis* genome is predicted to encode over 400 receptor-like kinases (RLKs; Shiu and Bleecker, 2003) type 1 transmembrane proteins, of which very few have assigned functions. Examples of those RLKs that have been studied in detail include FLS2 which acts as a receptor for the bacterial elicitator flg22 (Chinchilla et al., 2006) and EFR which recognises EF-Tu (Zipfel et al., 2006). Although these RLKs

are thought to signal through a kinase cascade through interaction with BAK1, there remains the possibility that others may signal through dissociation of the kinase domain from the extracellular N-terminus, through the action of an *Arabidopsis* γ-secretase complex. To test this, plants were grown on soil for 4 weeks prior to leaf infusion with *Pseudomonas syringae* variants *avrB*, *avrRps4* and *vir*. None of the lines tested showed a difference compared to wild type.

Many biotic and abiotic stresses lead to an accumulation of reactive oxygen species (ROS) in plants. An 'oxidative burst' occurs prior to the hypersensitive response following attack by pathogens, potentially leading to systemic acquired resistance (Kotchoni and Gachomo, 2006). An artificial method of simulating this stress response is to grow plants in the presence of Paraquat (which catalyses the production of ROS), hydrogen peroxide (one of the most stable ROS) or GSNO (a nitric oxide (NO) donor). Again, no difference was seen between the wild type and mutant seedlings when grown in the presence of these chemicals.

Proteins destined for the secretory pathway are produced in the endoplasmic reticulum (ER), where they are provided a suitable environment to undergo correct folding. "ER stress" caused by the unfolded protein response (UPR) leads to an upregulation of ER resident chaperones, such as BiP (Kozutsumi et al., 1988; Martinez and Chrispeels, 2003). The mammalian transcription factor p90ATF6 is resident in the ER under unstressed cellular conditions (Haze et al., 1999). Following ER stress, ATF6 is processed sequentially by S1P and S2P to release the p50ATF6 cytoplasmic N-terminal domain to translocate to the nucleus (Lee et al., 2002). Recently, Liu *et al*. (2007) has shown that an *Arabidopsis* transcription factor (bZIP17) involved in salt stress is located in the ER. bZIP17 release and translocation to the nucleus is S1P dependent. This group also identified pZIP28 as being involved in Tunicamycin (TM) stress signalling from the ER, and have presumed it is processed in the same fashion as bZIP17 (Liu et al., 2008). bZIP60 is also involved in the ER stress response to TM and DTT (Iwata et al., 2008). Much like bZIP17 and bZIP28, cleavage releases the N-terminal TF domain from the ER membrane, however this event is not S1P or S2P dependent.

To test for the putative *Arabidopsis* γ-secretase complex's involvement in ER stress signalling, seedlings were exposed to high salt (seed germinated and grown on 0.5x MS supplemented with 150 mM NaCl) and TM (seed germinated and grown on 0.5x MS containing 0.3 μg/mL tunicamycin for 6 days and transferred to 0.5x MS plates and allowed to recover for 10 days). All mutant lines tested responded identically to wild-type plants.

Potassium is the most abundant inorganic cation in plants. A recent study using quantifiable two-dimensional polyacrylamide gel electrophoresis reported a large number of proteins up- or down-regulated in response to potassium deprivation (Kang et al., 2004). One of the proteins upregulated following 7 days of potassium deprivation was AtPS2. To investigate the potential for the putative *Arabidopsis* γ-secretase complex in potassium starvation, seeds were germinated and grown on 0.5x MS modified with varying amounts of potassium (0-1000 mM). No differences were seen between wild type Col-0 and the mutant lines tested (data not shown).

The lack of visible phenotype likely suggests that we have not yet identified the signalling pathways in which these proteins may act. We are now relying on identification of binding partners to help us to identify these pathways (see Chapter 6 – Substrate Identification).

Stress	Conditions
Gibberellic acid (GA)	0 μM 50 μM 100 μM
Paclobutrazol	0 μM 1 μM 10 μM
Paraquat (MV)	0 μM 1 μM
Hydrogen peroxide	0 μM 1.94 μM
GNOS	0 μM 200 μM
Potassium starvation	0 mM 10 mM 100 mM 1000 mM
Biotic	Mock (10 mM $MgCl_2$) *Pst avrB* *Pst avrRps4* *Pst vir*
High salt (NaCl)	0 mM 150 mM
Tunicamycin	0 μg/mL 0.3 μg/mL

Table 3.3 Abiotic and biotic stresses tested to uncover a phenotype for insertional mutants identified. For abiotic stresses, seed was sterilised and germinated and grown on 0.5x MS supplemented with chemicals listed for 14 days, with exception of tunicamycin (seedlings grown for 6 days on TM containing plates then transplanted and allowed to recover on 0.5x MS for 10 days). For *Pst* trials, leaves from 4-week-old plants were infiltrated with bacteria and incubated for 3-4 days until symptoms appeared.

3.10. Summary and Conclusions

Homologues of the components of the γ-secretase complex exist in plants. Digital Northern data revealed that each member of the putative *Arabidopsis* γ-secretase complex is expressed in every tissue, at all stages of development. RT-PCR analysis with cDNA synthesised from various tissues of Col-0 wild type plants confirmed this ubiquitous expression pattern. Therefore, it was surprising that transcript-null insertion mutants in each of the genes did not have any gross morphological phenotypes. The mutants were tested with a series of stresses (exogenous hormones, inhibitors, salts and pathogen challenge) in an attempt to uncover any "hidden" phenotypes, however there was no difference seen compared to wild type plants. Searching for a role for these gene products could have continued without success for all the time I had available. It was therefore decided to concentrate on the potential of complex formation and a search for substrates of the putative complex (see Chapters 5 and 6).

In addition to RT-PCR analysis, native promoter driven reporter fusions were constructed for each of the five genes under investigation. These did not produce any signal. In the case of *AtPEN2*, a genomic fragment, comprising the promoter, 5' UTR and coding sequence including intron, was fused in frame with *GFP* at the 3' end (*pAtPEN2:AtPEN2g:GFP*). This construct, when transformed into plants, produced a protein that was the predicted size for AtPEN2:GFP. This shows that the intron sequence has an effect on transcription, and that this is possibly the reason that no signal was seen when just the promoter and 5' UTR were used for the other genes. Other such genomic fusions could be made for *AtPS1, AtPS2* and *AtAPH1*. *AtPS1* does not contain any introns, so the lack of signal from the promoter when fused to *H2B:YFP* may be due to a need for downstream sequences. *pAtNCT:AtNCTg:GFP* would be harder to produce due to the large number of introns present in genomic *AtNCT*.

Towards the end of this project, a resource was launched that has an *Arabidopsis* proteome map, compiled from MS data for different organs at various developmental

stages. AtNCT was identified in most of the tissues tested, not surprising given the expression profile, but the greatest abundance was in siliques. AtPS1 and AtAPH1 were also identified, but only in siliques. This was not expected, given the ubiquitous expression profile for each gene. Results obtained prior to this, from the search for substrates of the putative *Arabidopsis* γ-secretase complex (Chapter 6), had made little sense, as they identified silique (or developing seed) specific proteins that were decreased in the *ps1-1/ps2-3* double mutant. Taken with the protein localisation data, this points towards a role for the putative *Arabidopsis* γ-secretase complex in seed development, which was further investigated in Chapter 6.

4.0. Subcellular localisation

4.1. Introduction

γ-secretase is a membrane spanning protein complex comprised of four core components – a PRESENILIN, NICASTRIN, APH1 and PEN2 (Edbauer et al., 2003). The animal systems studied show a progression from ER through the Golgi network to the plasma membrane as the complex is assembled and matures (Kaether et al., 2002). Early in the research of γ-secretase/PRESENILIN, a "spatial paradox" questioning the subcellular localisation of the protein complex versus the activity was raised (Annaert and De Strooper, 1999). It was known that much of the stabilised PS, in a complex with NCT and APH1, resided mostly in the ER and *trans*-Golgi network (TGN; Kovacs et al., 1996). However, γ-secretase activity was seen not just in the ER/TGN, but also at the plasma membrane (Chyung et al., 2005) and endosomes (Vetrivel et al., 2004). A small proportion of the presenilin complex has been visualised at the PM using a PS1:GFP fusion protein (Kaether et al., 2002), estimated at $1/30^{th}$ of the total cellular population. This same group have visualised similar PS1:CFP fusions co-localising with NCT:YFP at the PM and in vesicles within the cell (Kaether et al., 2006).

Here, I have constructed *GFP* fusions to members of the putative γ-secretase complex in *Arabidopsis*, stably transformed them into plants and verified transcription and protein production. Subcellular localisation of AtPEN2:GFP was carried out through confocal microscopy techniques, and AtPS1:GFP expression was also detected.

4.2. Production of GFP tagged lines and transformation of Arabidopsis

Primers were designed to amplify each of the members of the putative γ-secretase complex in *Arabidopsis* to incorporate restriction nuclease sites to allow efficient cloning of fusion constructs. A previously cloned coding sequence for *mGFP6* was available in the lab, with a *Sal*I site (GTCGAC) immediately 5' of the ATG start

codon and an *Xho*I site (CTCGAG) at the 3' end upstream of the STOP codon. This was used as a basis of the GFP fusion protein constructs.

Open reading frames were amplified from cDNA synthesised from wild type Col-0 *Arabidopsis* total RNA, with primers carrying restriction sites at the 5' and 3' ends. Following high fidelity PCR amplification (*Pfu* Turbo, Stratagene) with gene specific primers, the products were cloned into pGEM-T easy (Invitrogen) and sequenced (BigDye v3.1) using universal and reverse primers present in the cloning vector. A number of sequenced clones perfectly matched the predicted coding sequences from TAIR for each gene, and contained the appropriate enzyme sites.

At the 5' end, a *Sal*I site was introduced upstream of the start (ATG) codon in all cases. At the 3' end, an *Xho*I site was introduced before the stop codon for *AtPS1* (PS1 5' Sal and PS1 3' Xho), *AtAPH1* (APH1 5' Sal and APH1 3' Xho) and *AtPEN2* (PEN2 5' Sal and PEN2 3' Xho). Type II restriction enzyme sites were incorporated to leave an *Xho*I type overhang for *AtPS2* (PS2 5' Sal and PS2 3' Xho, *Bsa*I site) and *AtNCT* (NCT 5' Sal and NCT 3' Xho, *Bsm*BI site) after digestion. The *AtPEN2* coding sequence contained a *Sal*I site, which was mutated through site directional mutagenesis using *Pfu* turbo high fidelity DNA polymerase (Stratagene) with primers PEN2 mut1 and PEN2 mut2, causing a conservative base change (TCG to TCT) 86 nt from the start codon. See Table 2.2 for primer sequences.

*Sal*I and *Xho*I leave complimentary overhangs (TCGA) following cleavage, and upon ligation destroy the recognition sites for both enzymes. Using this strategy, the GFP coding sequence can be easily cloned at both the 5' and 3' ends. For C-terminal fusion proteins, plasmids containing the cDNA from each gene of interest were digested with *Xho*I (or type II enzyme) and treated with calf intestinal phosphatase (CIP) to prevent re-ligation. The *mGFP* coding sequence was digested from its vector using *Sal*I/*Xho*I and inserted into the cut vector. Fusion constructs were cut out from pGEM-T easy using *Sal*I/*Pst*I and cloned into similarly digested pLitmus 38, with the exception of *AtAPH1* where *Sal*I/*Eco*RI was used.

From here, the constructs were cut out with *Sal*I/*Sac*I and inserted into a cut binary vector pBIB-Hyg-35S (pBIB-Hyg; Becker, 1990) containing the 35S promoter from cauliflower mosaic virus), to produce constructs pRW350 (*p35S:AtPEN2:GFP*), pRW440 (*p35S:AtNCT:GFP*), pRW349 (*p35S:AtPS1:GFPc*; 'c' for C-terminal fusion), pRW439 (*p35S:AtPS2:GFPc*) and pRW442 (*p35S:AtAPH1:GFP*) for transformation into plants. *mGFP6* coding sequence was inserted into pBIB-Hyg-35S, as a *Sal*I/*Sac*I fragment cut from pGEM-T easy, to produce pRW443 (*p35S:GFP*).

All N-terminal fusions (with the exception of *p35S:AtAPH1:GFP*) were constructed by first transferring cDNA sequences from the original cloning vector (pGEM-T easy) as *Sal*I/*Pst*I fragments and cloned into similarly cut vector pLitmus38. Resultant clones were cut with *Sal*I and treated with CIP to allow insertion of the *Sal*I/*Xho*I cut *mGFP* sequence. Fusion constructs were transferred to pBluescriptII (Stratagene) as *Sal*I/*Pst*I fragments. *Kpn*I/*Sac*I fragments were transferred from pBluescriptII to pBIB-Hyg-35S to produce constructs pRW332 (*p35S:GFP:AtPS1*), pRW331 (*p35S:GFP:AtPS2*), pRW333 (*p35S:GFP:AtPEN2*), and pRW334 (*p35S:GFP:AtNCT*). *AtAPH1* contains a *Pst*I site within the coding sequence. For this reason, the *AtAPH1* sequence was transferred to pBluescriptII as a *Sal*I/*Eco*RI fragment. *mGFP* was inserted as a *Sal*I/*Xho*I fragment into *Sal*I and CIP treated vector. The fusion construct was transferred to pBIB-Hyg-35S as a *Kpn*I/*Sac*I fragment to produce pRW368 (*p35S:GFP:AtAPH1*).

All C-terminal fusion constructs were transformed into *Agrobacterium tumefaciens* GV3101 for transformation of *Arabidopsis* by the floral dipping method. The *AtPS2* fusion constructs were found to be toxic to *Agrobacteria*, as transformations did not produce any colonies containing the appropriate vector. Due to this, no fusions containing *AtPS2* could be transformed into plants. It was also later discovered that the *p35S:AtAPH1:GFP* fusion (pRW442) contained two copies of the *AtAPH1* coding sequence, caused by a mistake during the cloning procedure, and not recognised due to the similar size and restriction sites in the *AtAPH1* and *mGFP* coding sequences. Therefore, there is no data for these fusion constructs. With the

exception of *p35S:GFP:AtPEN2*, none of the N-terminal fusions were transformed into plants. It was thought that the lack of signal sequence caused by preceding the native proteins with GFP would cause the fusion proteins to be mis-sorted and so not provide any useful data.

A genomic version of *AtPEN2:GFP* was produced under the control of the native *AtPEN2* promoter. Genomic DNA was amplified with sequence specific primers to introduce a *Xho*I site 172 bp upstream of the *AtPEN2* ATG start codon, and a *Bam*HI site immediately 5' to the STOP codon. A *Kpn*I site was introduced 3' of the STOP codon to facilitate cloning. Following amplification, the PCR product was cloned into pGEMT easy and sequenced. *mGFP* (amplified with *Bam*HI and *Bgl*II sites at the 5' and 3' ends respectively) was inserted into *Bam*HI cut vector to produce *pAtPEN2:AtPEN2g:GFP* ("g" representing the genomic version including the intron). The fusion construct was transferred to pBIB-Hyg as an *Xho*I/*Kpn*I fragment into *Sal*I/*Kpn*I cut vector.

4.3. AtPEN2:GFP fusion protein is stably accumulated throughout Arabidopsis

Both *p35S:GFP:AtPEN2* and *p35S:AtPEN2:GFP* (*pRW333* and *pRW350* respectively) were transformed into *Arabidopsis*. Immunoblots were carried out on total protein extracted from 10-day-old seedlings grown on plates, and a band at 45 kDa was seen for AtPEN2:GFP (Fig 4.1, lane 3), the predicted size for the fusion protein. In the case of GFP:AtPEN2, a lower band was seen, at approximately 42 kDa (Fig 4.1, lanes 4-6). The reason for this difference in size of the fusion proteins is unknown, but may be due to an inherent instability of the GFP fusions, as seen by the cleaved GFP band at ~30 kDa. However, only AtPEN2:GFP could be visualised through confocal microscopy. Figure 4.2 shows a confocal microscope image of a typical leaf from a plant stably transformed with pRW350 (*p35S:AtPEN2:GFP*), displaying a punctate distribution around the edge of the cell. This punctate distribution is not seen when the plants express free GFP (*p35S:GFP*; Fig 4.2d), suggesting that this distribution is caused by the subcellular localisation of AtPEN2:GFP. Fusions of GFP to animal PEN2 proteins have been successfully

carried out. In *C. elegans*, fusions of GFP N-terminally and within the loop of PEN2 (between the two TMDs) were both shown to rescue *pen2* mutants (Francis et al., 2002). This same study showed that a C-terminal PEN2:GFP fusion not only did not rescue the *pen2* phenotype, but had a dominant-negative effect similar to the knockout. However PEN2:FLAG and PEN2:HA C-terminal fusions are functional in *Drosophila* and human cell lines, respectively (Hu and Fortini, 2003; Kaether et al., 2007).

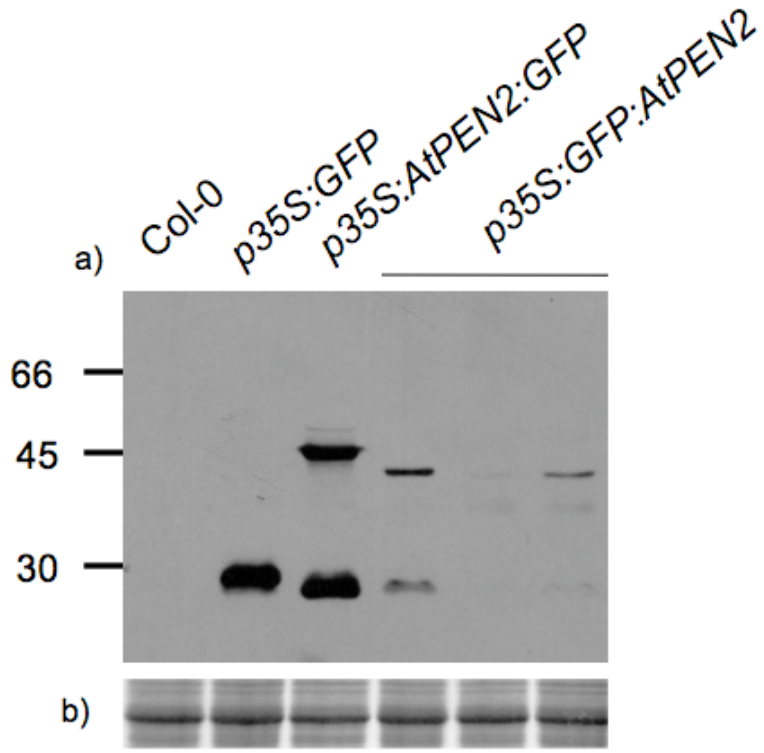

Fig 4.1 AtPEN2:GFP is stably accumulated in seedlings. Total protein extracted from 10-day-old seedlings was subjected to immunoblot analysis, using an α-GFP primary antibody (a). Full-length AtPEN2:GFP protein can be seen at 45 kDa and cleaved GFP at ~30 kDa. Three independent RW333 (GFP:AtPEN2) lines tested here show different protein accumulation levels. The predicted size for both AtPEN2:GFP and GFP:AtPEN2 is 45 kDa, and the reason for the difference in size seen unknown. Size markers in kDa are indicated on left.
(b) Coomassie stained gel showing large RUBISCO subunit as loading controls for (a).

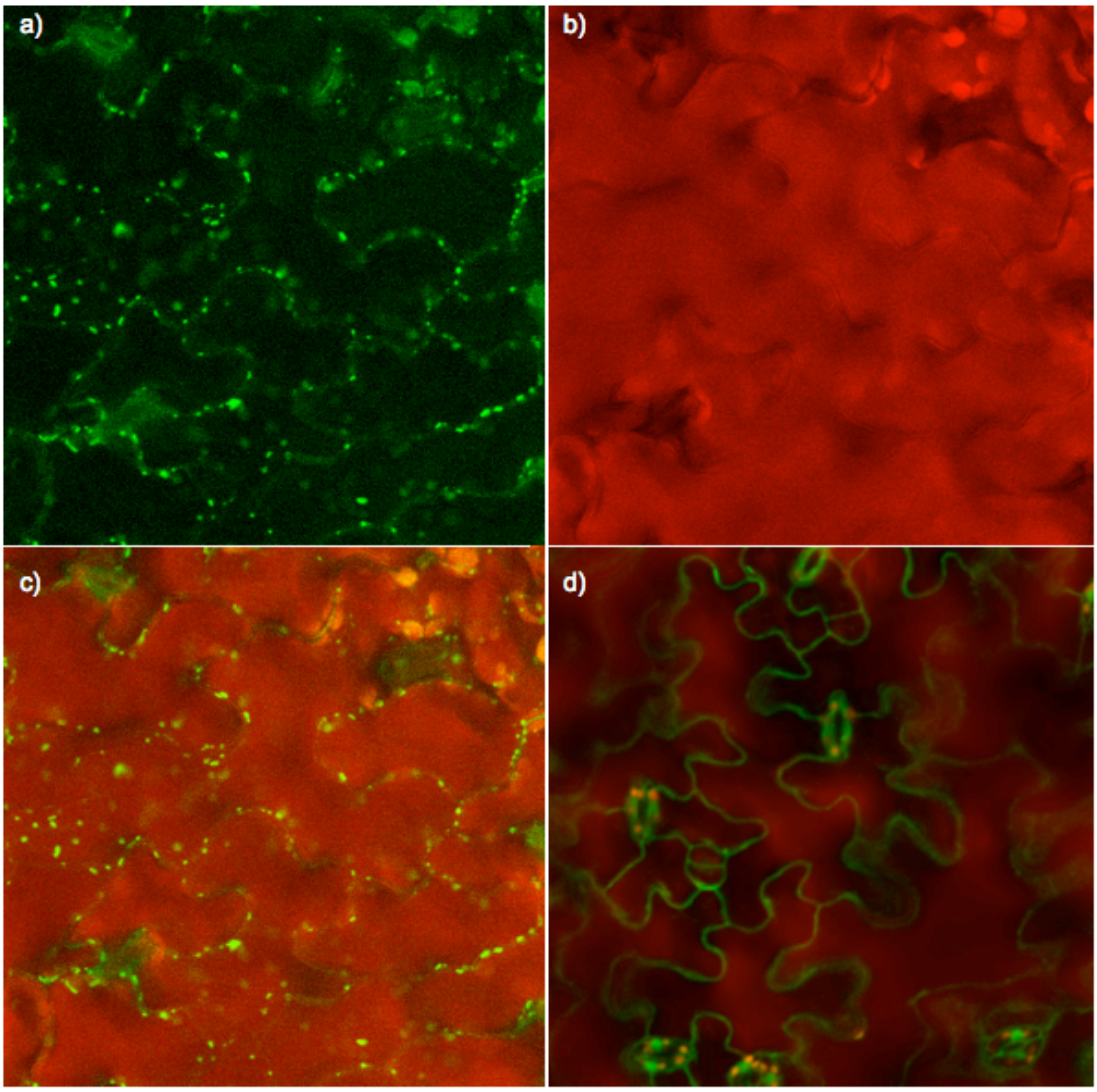

Fig 4.2 Subcellular distribution pattern of AtPEN2:GFP. AtPEN2:GFP is found in a punctate pattern around the periphery of leaf cells. Confocal microscopy was used to visualise plants stably transformed with pRW350 (AtPEN2:GFP; a-c) and pRW443 (free GFP; d).
(a) AtPEN2:GFP fluorescence showing a punctate distribution.
(b) Chlorophyll auto-fluorescence.
(c) Merged image of (a) and (b).
(d) Merged image of GFP and auto-fluorescence from a plant expressing free GFP, not showing the punctate distribution seen with AtPEN2:GFP.
Images were acquired at same magnification.

Various other proteins show a similar punctate distribution, for example the potassium channel protein KAT1 (Sutter et al., 2006) and plasmodesmata associated proteins (Escobar et al., 2003). The similarity to the distribution of KAT1 was intriguing, due to the publication of a paper showing an upregulation of *AtPS2* following 7 days of potassium starvation (Kang et al., 2004). To investigate the potential of AtPEN2 (and the putative γ-secretase complex) being involved in potassium sensing/homeostasis, seeds were germinated on 0.5x MS containing a range of potassium concentrations (0-1000 mM) and grown for 10 days. There was no difference observable between wild type Col-0, the homozygous *pen2-2* mutant and RW350 plants (*p35S:AtPEN2:GFP*). Confocal microscopy revealed that there was no change seen in AtPEN2:GFP localisation in roots due to the potassium starvation.

Plasmodesmata (Pds) are intercellular channels capable of transport of proteins and mRNAs between cells (Maule, 2008). They are formed of a membrane-lined pore, with a strand of ER, connecting adjacent cells, although the extent of their functions and protein complement is not fully determined. A common feature of most Pd associated proteins is their continued association with the cell wall following plasmolysis, as the plasma membrane retreats. A family of proteins with plasmodesmata localisation (called PDLP1) show continued association with the cell wall following plasmolysis (Thomas et al., 2008). Another example of this is seen in a GFP fusion to *Arabidopsis* REVERSIBLY GLYCOSYLATED POLYPEPTIDE 2 (AtRGP2:GFP), which also remains in the cell wall following plasmolysis (Sagi et al., 2005). Roots of seedlings stably expressing AtPEN2:GFP were subjected to plasmolysis by incubation in 0.8 M mannitol. Following plasmolysis, spots of AtPEN2:GFP could be seen within the shrunken protoplast (Fig 4.3), indicating that AtPEN2:GFP is not likely to be associated with plasmodesmata.

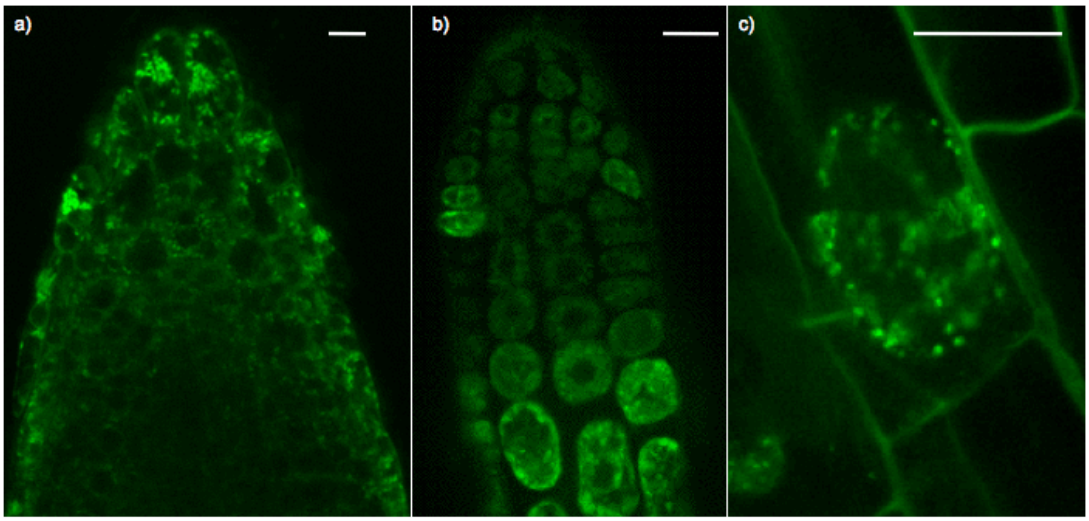

Fig 4.3 Effect of plasmolysis on AtPEN2:GFP expressing root cells. Seedlings expressing AtPEN2:GFP grown on plates were treated with (a) water or (b-c) 0.8 M mannitol and observed under the confocal microscope.
(a) Normal distribution of AtPEN2:GFP in seedling root tips, showing a punctate distribution around the periphery of the cells.
(b) Following treatment with mannitol, the cells become plasmolysed and the PM shrinks back away from the cell wall. AtPEN2:GFP is retained within the shrinking protoplast.
(c) Higher magnification of a typical plasmolysed cell, showing the punctate distribution of AtPEN2:GFP.
Scale bars 15 μm.

4.4. AtPEN2:GFP spots are not located in the ER

Rosette leaves of *Arabidopsis* plants stably expressing the AtPEN2:GFP fusion protein were bombarded with gold particles carrying an expression vector containing the ER marker ER-tdT (tdTomato carrying an HDEL ER retention signal; gift from J. Tilsner). Leaves were imaged through confocal microscopy, to look for potential co-localisation of AtPEN2:GFP with the ER. The punctate spots of AtPEN2:GFP are not in the ER, however a portion of the GFP signal does show co-localisation with the ER marker (Fig 4.4). The signal associated with the ER is weak, but increasing the laser intensity or gain settings of the microscope to obtain better images resulted in overexposure from the spots.

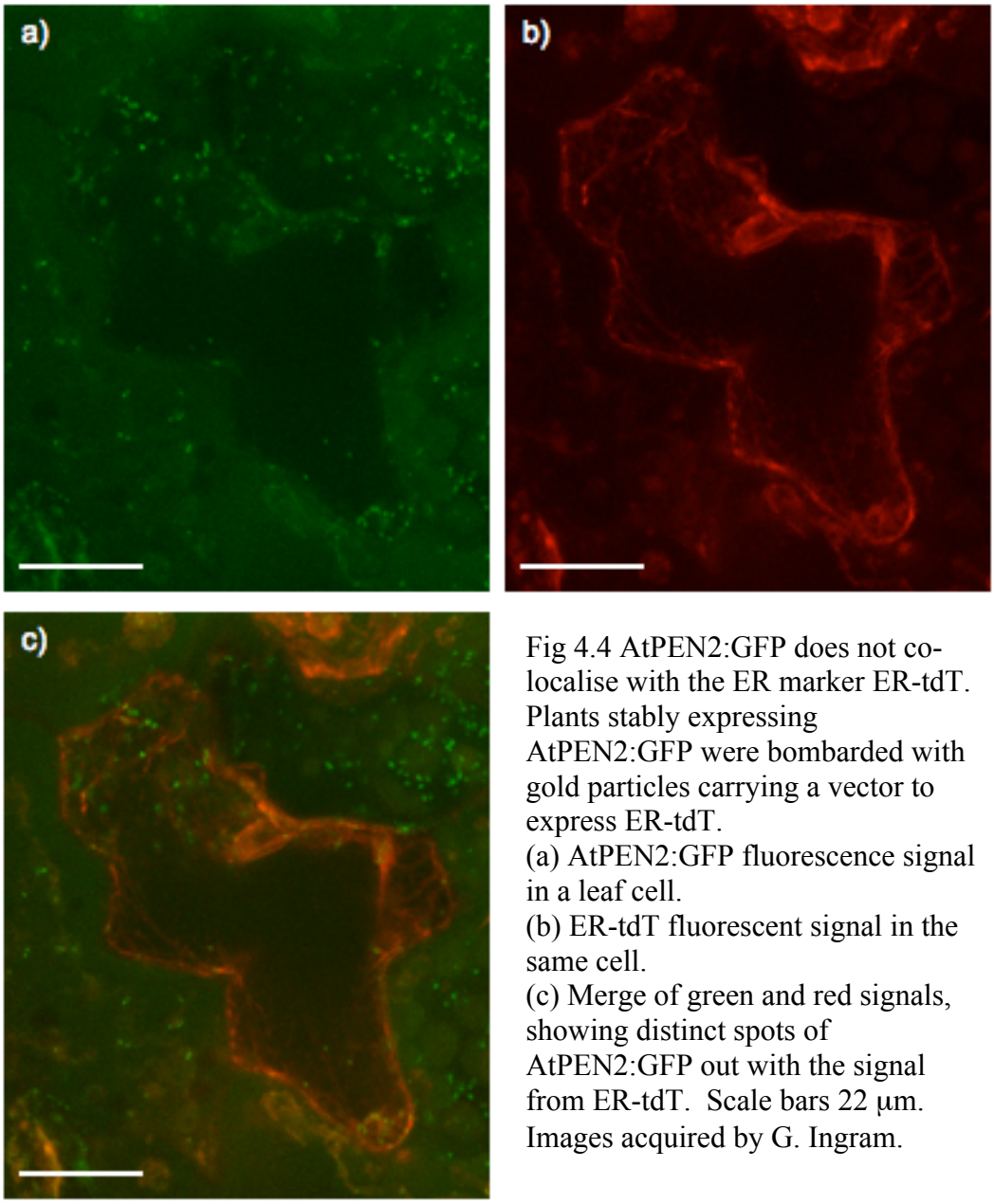

Fig 4.4 AtPEN2:GFP does not co-localise with the ER marker ER-tdT. Plants stably expressing AtPEN2:GFP were bombarded with gold particles carrying a vector to express ER-tdT.
(a) AtPEN2:GFP fluorescence signal in a leaf cell.
(b) ER-tdT fluorescent signal in the same cell.
(c) Merge of green and red signals, showing distinct spots of AtPEN2:GFP out with the signal from ER-tdT. Scale bars 22 μm. Images acquired by G. Ingram.

4.5. Effect of BFA on subcellular localisation of AtPEN2:GFP

In roots, AtPEN2:GFP seems to be present in vesicular compartments located around the periphery of the cell (Fig 4.5a, plants transformed with *p35S:AtPEN2:GFP*). Plants transformed with *pAtPEN2:AtPEN2g:GFP*, a GFP fusion to genomic *AtPEN2* under its own promoter, showed the same localisation, but there is a higher expression from the native promoter compared to the 35S promoter (see Fig 3.11). To investigate these vesicles, seedlings were treated with the drug Brefeldin A (BFA), a fungal macrocyclic lactone that inhibits ARF GTPases (Jackson and Casanova, 2000). Endocytic vesicles are formed at the PM and become part of the early endosome, thought to make up a subset of the TGN membranes (Robinson et al., 2008). BFA treatment of *Arabidopsis* roots causes accumulation of "BFA compartments" comprised from elements of the TGN at its core, surrounded by Golgi stacks (Satiat-Jeunemaitre and Hawes, 1994). Export from the Golgi network is not completely inhibited by BFA, as newly synthesised proteins are still transported to the PM (Grebe et al., 2003), however these BFA compartments do contain some secretory vesicles (Satiat-Jeunemaitre and Hawes, 1994). Figure 4.5 shows confocal images of *Arabidopsis* roots stably expressing the genomic AtPEN2:GFP (*pAtPEN2:AtPEN2g:GFP*) treated with BFA for 30 mins, where it is possible to see accumulation of GFP signal into BFA compartments (arrows in Fig 4.5b). However, there is still a proportion of AtPEN2:GFP that has not entered these BFA compartments, showing the punctate distribution around the cell periphery, which persists for over 2 hrs.

The styryl dye FM4-64 is only fluorescent when in a hydrophobic environment such as lipid membranes. When applied to plant tissues for short periods of time, staining first occurs at the PM. Following longer incubation, endocytosis causes intracellular membrane compartments to become stained, starting with the endosomes and spreading to the *trans*-Golgi network (TGN), pre-vacuolar compartments (PVC) and the vacuole (Bolte et al., 2004). AtPEN2:GFP does not show co-localisation with FM4-64 stained vesicles (Fig 4.6), showing that AtPEN2:GFP is not located in endocytic compartments or at the PM. The presence of AtPEN2:GFP in BFA bodies

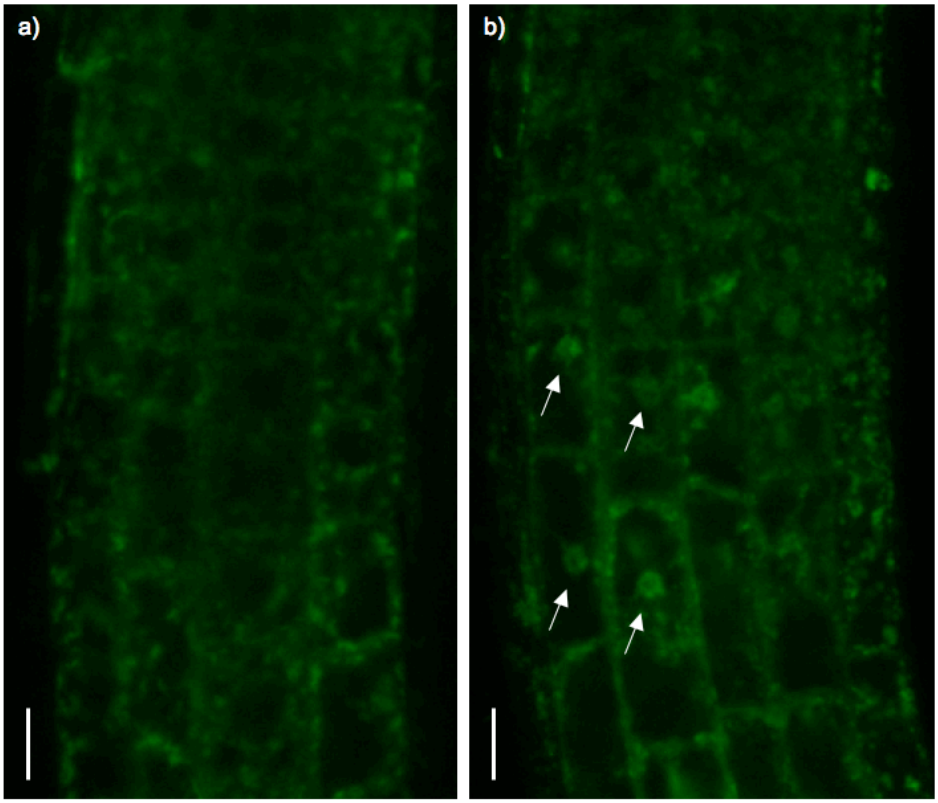

Fig 4.5 AtPEN2:GFP localises to BFA sensitive compartments in roots.
(a) Seedlings expressing AtPEN2:GFP were treated with control and
(b) BFA for 30 mins.
Following treatment with BFA, AtPEN2:GFP can be seen to accumulate in BFA bodies, indicated by arrows in (b). A proportion of AtPEN2:GFP can still be seen at the periphery of cells treated with BFA.
Scale bars 15 μm.

(which are composed of elements of the TGN surrounded by stacks of the Golgi apparatus (Satiat-Jeunemaitre and Hawes, 1994)), and the lack of co-localisation with FM4-64 (which stains the TGN) suggests that AtPEN2:GFP is located in the Golgi.

A combination of FM4-64 staining and BFA treatment resulted in formation of BFA bodies stained with FM4-64. The core of these BFA bodies was stained with the dye, however AtPEN2:GFP still does not co-localise with the FM4-64, but is located on the periphery of the bodies (Fig 4.7). This provides further evidence that AtPEN2:GFP is resident in the Golgi apparatus.

In plant cell biology, the rat enzyme 2,6-SIALYLTRANSFERASE (ST) can be used as a marker for Golgi bodies (Munro, 1995; Boevink et al., 1998). Tobacco plants (*Nicotiana clevelandii*) stably expressing the anchor signal of ST fused to the fluorescent protein DsRed (ST-DsRed) were infiltrated with *Agrobacteria* carrying pRW350 (*p35S:AtPEN2:GFP*), and imaged with a confocal microscope. The cytosolic punctate distribution of ST-DsRed in tobacco cells co-localises with AtPEN2:GFP (Fig 4.8a-c), proving that AtPEN2:GFP is located in the Golgi of living plant cells. Upon closer inspection, the co-localisation of the GFP and DsRed signals is not perfect (Fig 4.8d). In fact, there appears to be a central area of co-localisation with two "poles" being formed in the Golgi bodies, one containing ST-DsRed and the other AtPEN2:GFP. The reason for this association is not understood, but could be due to some form of compartmentalisation within the Golgi body.

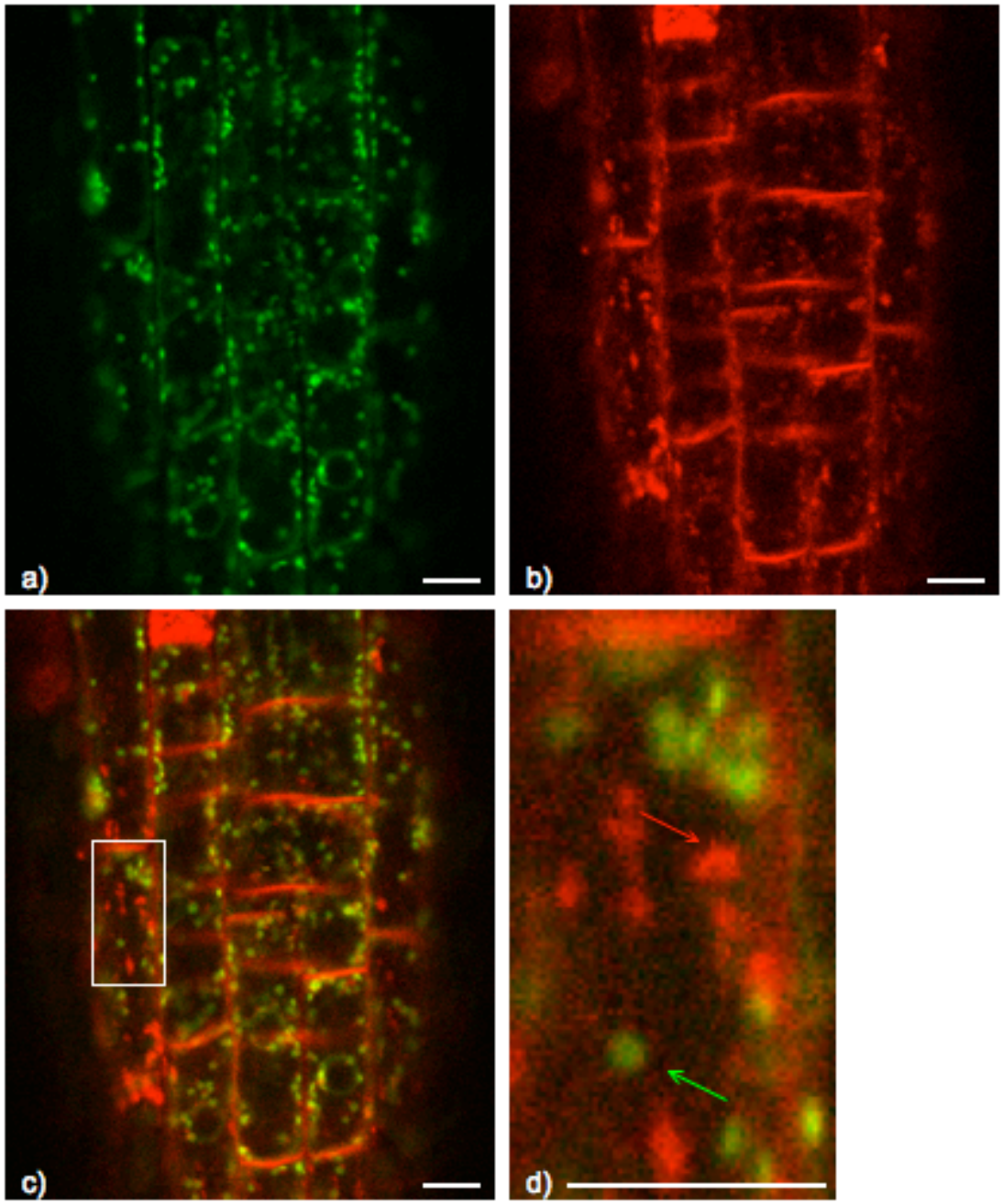

Fig 4.6 AtPEN2:GFP is not present in the early endocytic pathway. Seedlings expressing *pAtPEN2:AtPEN2g:GFP* were treated with FM4-64 and imaged by confocal microscopy.
(a) AtPEN2:GFP fluorescence showing characteristic punctate distribution.
(b) FM4-64 fluorescence, showing staining of the plasma membrane and endocytic vesicles.
(c) Merge of images showing AtPEN2:GFP and FM4-64 fluorescence does not overlap.
(d) Enlarged image of boxed region in (c), showing vesicles stained with FM4-64 (red arrow) and vesicles containing AtPEN2:GFP (green arrow). Scale bars 15 μm. Images acquired by B. Kümpers and G. Ingram.

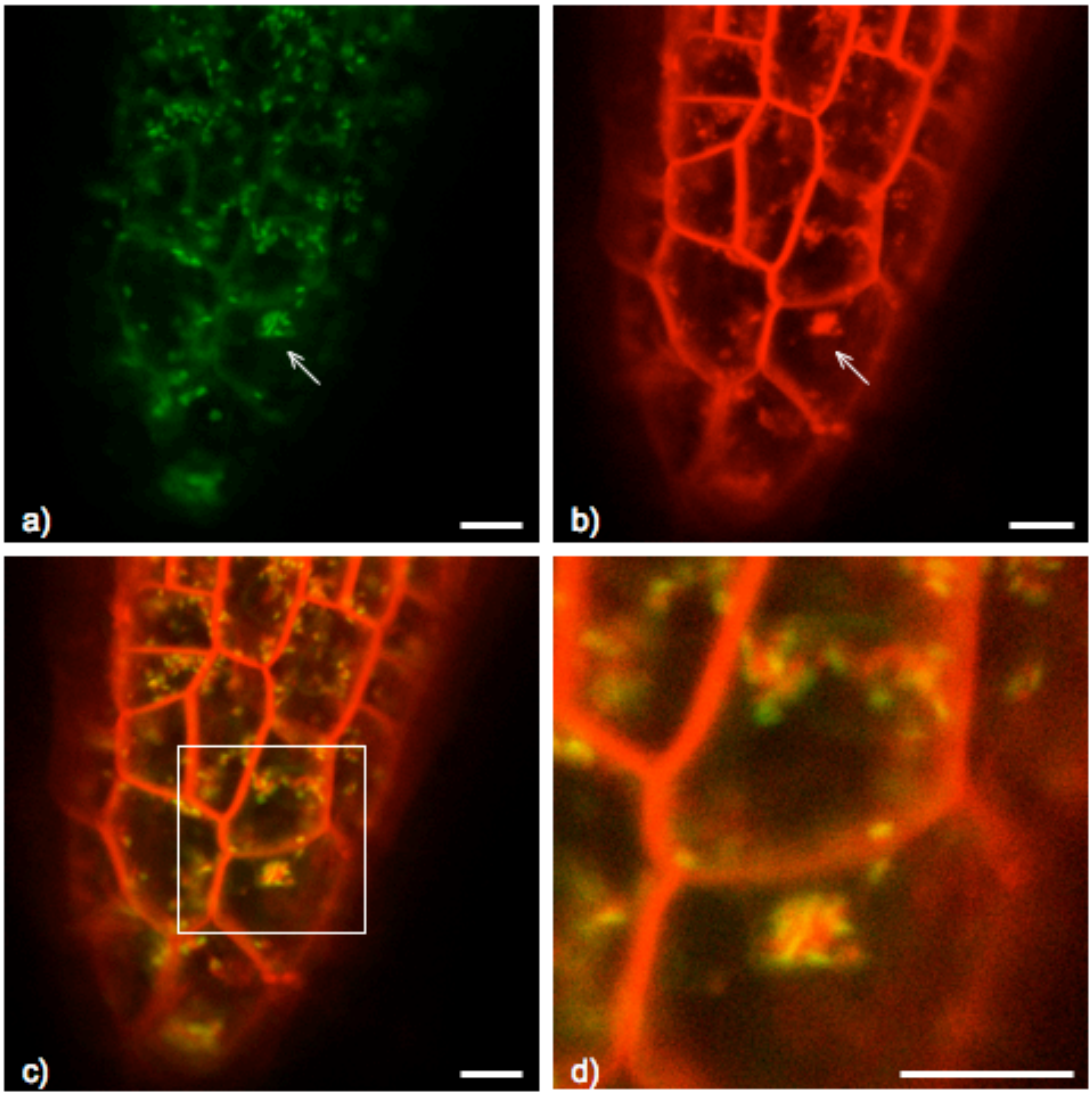

Fig 4.7 AtPEN2:GFP is present at the periphery of BFA bodies in roots. Seedlings expressing *pAtPEN2:AtPEN2g:GFP* were treated with FM4-64 and BFA and imaged by confocal microscopy.
(a) AtPEN2:GFP fluorescence, showing localisation to BFA bodies (arrow).
(b) FM4-64 fluorescence, showing staining of PM, endocytic vesicles and BFA bodies (arrow).
(c) Merge of images showing AtPEN2:GFP and FM4-64 fluorescence in the same BFA bodies, however co-localisation is not complete.
(d) Enlarged image of boxed region in (c), showing red fluorescence from FM4-64 at the core of the BFA body, with the green signal from AtPEN2:GFP at the edge. Scale bars 15 μm. Images acquired by B. Kümpers and G. Ingram.

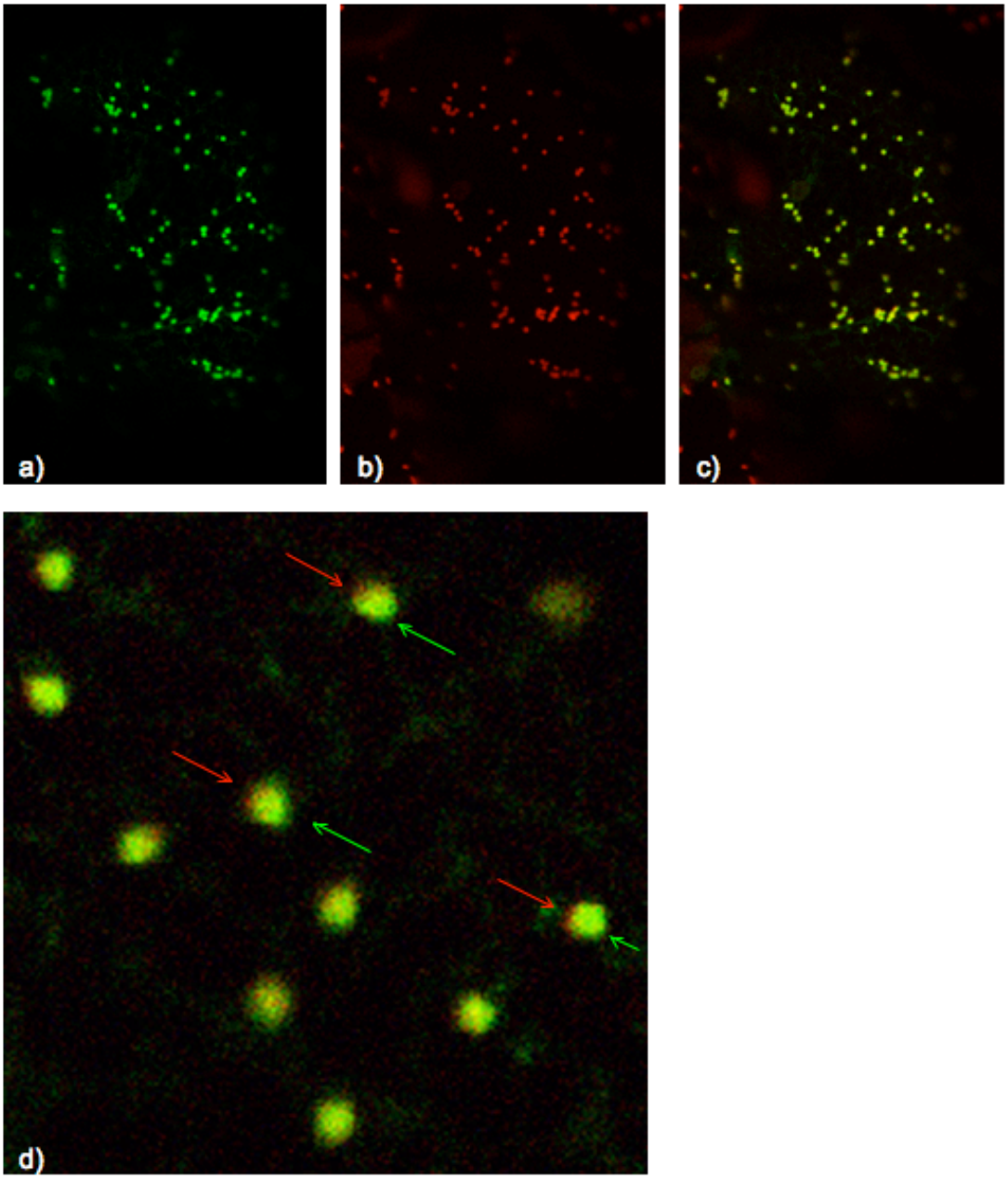

Fig 4.8 AtPEN2:GFP is present in Golgi bodies. Leaves of tobacco plants stably expressing ST-DsRed were infiltrated with *Agrobacteria* carrying pRW350 (*p35S:AtPEN2:GFP*) and imaged by confocal microscopy.
(a) AtPEN2:GFP fluorescence.
(b) ST-DsRed fluorescence in the same cell.
(c) Merge of images showing AtPEN2:GFP and ST-DsRed fluorescence in the Golgi bodies.
(d) Enlarged view of a portion of (c) to show the red (ST-DsRed; red arrows) and green (AtPEN2:GFP; green arrows) poles of the Golgi bodies. Images acquired by B. Kümpers and G. Ingram.

4.6. AtPS1:GFP *and* AtNCT:GFP *are transcribed, but the fusion proteins are not accumulated in vegetative tissue*

Leaves from stably transformed *Arabidopsis* plants expressing the fusion proteins AtPS1:GFPc and AtNCT:GFP were examined under the confocal microscope, however no GFP signal was detected (data not shown). RT-PCR analysis confirmed expression of the full-length transcript for the fusion construct (Fig 4.9). Total protein was extracted from 10-day-old seedlings on 0.5x MS plates, and subjected to Western blots, using an α-GFP antibody for primary detection. AtPEN2:GFP and free mGFP under the control of the 35S promoter are both detectable after less than 5 mins exposure. AtPS1:GFPc and AtNCT:GFP are not detectable until after 1 hr (Fig4.10), even though they are expressed from the same promoter and the same amount of protein was loaded for each sample. The predicted size for AtNCT:GFP is ~100 kDa, however the band appearing on western blots is closer to 116 kDa. The reason for this discrepancy in size may be due to some post-translational modifications, comparable to the glycosylation of mature NICASTRIN (mNCT) in animal systems (Prokop et al., 2004). Mature and immature forms of NICSATRIN can be seen on western blots of proteins from cell lines expressing HsNCT:GST (human NCT fused to GLUTATHIONE-S-TRANSFERASE; Fraering et al., 2004). The lack of a band closer to 100 kDa in western blots with AtNCT:GFP would suggest that the 116 kDa band is the actual size of this fusion protein.

The AtPS1:GFPc fusion protein is predicted as 71 kDa, and a band is detected at ~66 kDa. In the animal systems studied to date, PRESENILIN is present in active γ-secretase complexes as a heterodimer formed from the N- and C-terminal fragments following cleavage of its cytosolic loop. The site of cleavage is at the amino-side of a relatively well-conserved valine (V) residue (Fig 3.3), however mutation of the cleavage site in human PS1 does not abolish cleavage (Brunkan et al., 2005). Therefore, endoproteolysis of PS is a context specific event, not sequence specific. A valine residue is present in AtPS1 within the predicted cytosolic loop region

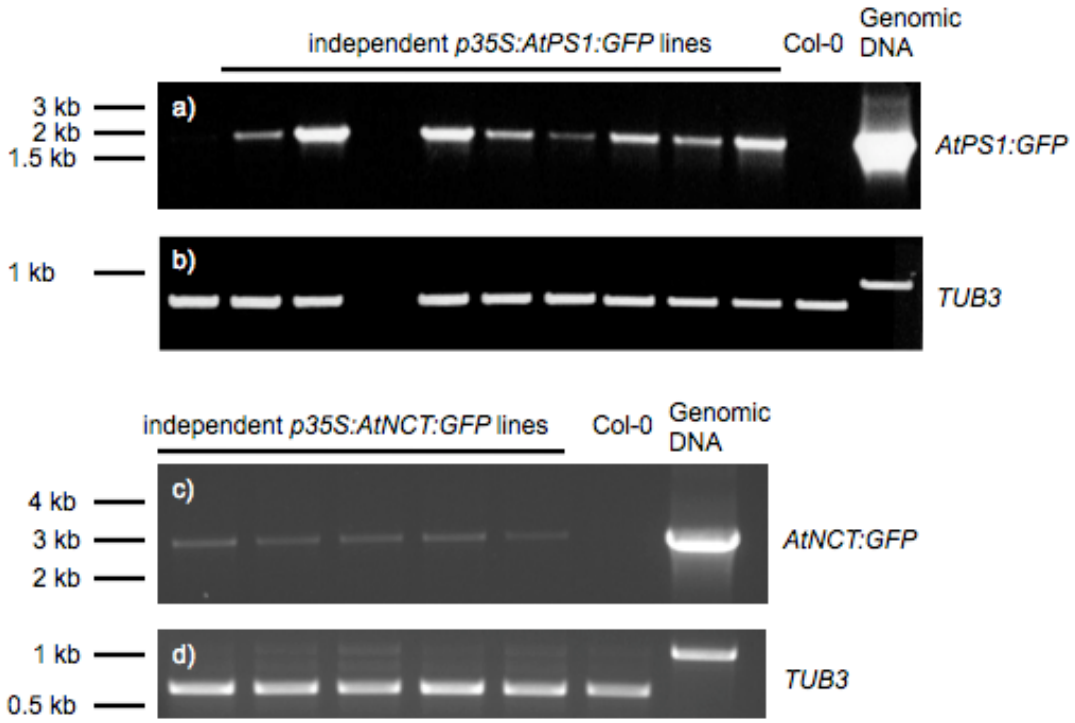

Fig 4.9 *p35S:AtPS1:GFPc* and *p35S:AtNCT:GFP* are expressed in transgenic plants. Total RNA was extracted from leaves of plants grown on soil for ~4 weeks, and cDNA synthesised.
(a) PCR reactions carried out using *AtPS1* specific 5' and *GFP* specific 3' primers (expected size ~2 kb). cDNA synthesised from plants transformed with pRW349 (*p35S:AtPS1:GFPc*) or wild type Col-0 control. Genomic DNA control from an RW349 plant.
(b) PCR reactions carried out on the same samples as in (a) using *TUBULIN3* control primers.
(c) PCR reactions carried out using *AtNCT* specific 5' and *GFP* specific 3' primers (expected size ~2.8 kb). cDNA synthesised from plants transformed with pRW440 (*p35S:AtNCT:GFP*) or wild type Col-0. Genomic DNA control from RW440 plants.
(d) PCR reactions carried out on the same samples as in (c) using *TUBULIN3* control primers. The *TUBULIN3* primers amplify over an excised intron in the cDNA, to show DNA contamination if present. Hence the larger product from genomic DNA.

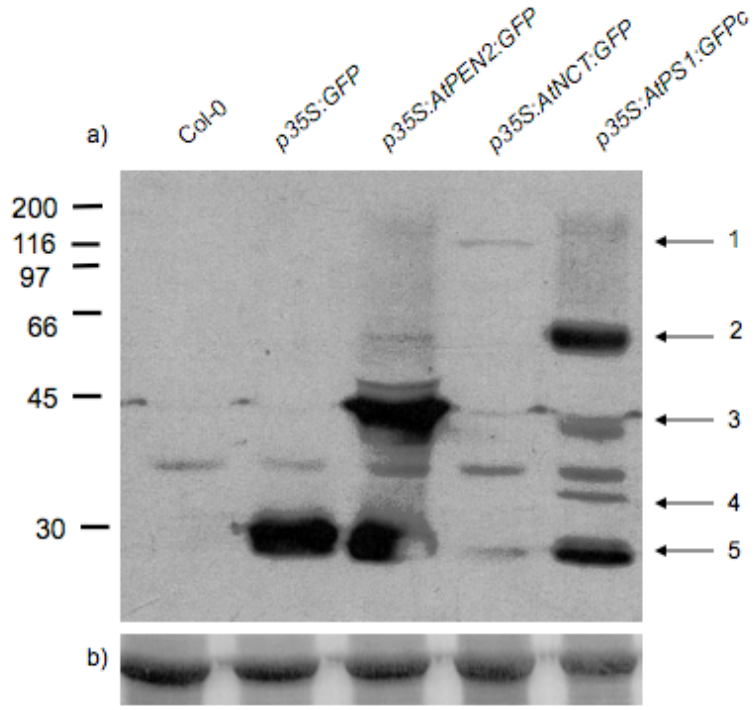

Fig 4.10 AtPEN2:GFP, AtNCT:GFP and AtPS1:GFPc are detectable by immunoblots to varying degrees. Total protein was extracted from 10-day-old seedlings of wild type Col-0 and plants transformed with RW443 (*p35S:GFP*), RW350 (*p35S:AtPEN2:GFP*), RW440 (*p35S:AtNCT:GFP*) and RW349 (*p35S:AtPS1:GFPc*), and subjected to immunoblot analysis using an α-GFP primary antibody.

(a) Signal can be seen for AtNCT:GFP at ~116 kDa (arrow 1), however the predicted size for this fusion protein is 100 kDa. The AtPS1:GFPc holoprotein is detectable at ~66 kDa (arrow 2), close to the predicted size of 71 kDa. PRESENILIN is present in active γ-secretase as a heterodimer, formed from endoproteolysis of PRESENILIN at a valine residue in its cytosolic loop. The predicted size of AtPS1 CTF following cleavage at this conserved valine is ~18 kDa. Therefore, the AtPS1:GFP CFT fusion is ~45 kDa, as seen on the blot (arrow 3). Another band at ~35 kDa (arrow 4) is seen in the AtPS1:GFP extract, that is assumed to be a degradation product of AtPS1:GFP. Free GFP can be seen at ~30 kDa (arrow 5) in all samples except Col-0. Size markers in kDa are indicated on left.

(b) Coomassie stained gel showing large RUBISCO subunit as loading controls for (a).

(V233), in the same position as human PS1. If cleavage occurs at this site, the predicted size for the CTF of AtPS1 is 18.3 kDa (from V233 to C-terminus), and a fusion protein formed of this CTF and GFP would be ~46 kDa. A band of approximately this size is seen in the immunoblot for plants expressing *p35S:AtPS1:GFPc*, indicating that AtPS1 is cleaved within its cytosolic loop, as in animal systems. This is contrary to evidence in animal systems, where a group recently reported that a C-terminal MYC/HIS tag on PS1 inhibited endoproteolysis (Raurell et al., 2008).

A report emerged from animal systems of NICASTRIN being degraded through the 26S proteasome pathway (He et al., 2007), and it was already known that the PS1 holoprotein is degraded by the same pathway (Fraser et al., 1998). Treatment of cells expressing NCT:MYC, when treated with proteasomal inhibitors showed a marked increase in the amount of mNCT, that localised to the ER. Inhibition of the 26S proteasome causes an increase in the amount of PS1 holoprotein, but not NTF/CTF fragments, showing that the rapid turnover of the holoprotein is due to the proteasome. This raised the possibility that the reason for a low accumulation of AtNCT:GFP and AtPS1:GFP in seedlings was degradation. The proteasome inhibitor MG132 was used to test this hypothesis. Seedlings were germinated on 0.5x MS plates for 7 days, transferred to sterile flasks containing 0.5x MS liquid media and grown for a further 5 days with continuous shaking. Flasks were treated with MG132 (or 0.1% DMSO as control) for 24 hrs and total protein extracted and subjected to immunoblot analysis. Figure 4.11 shows there was no difference in accumulation of AtNCT:GFP or AtPS1:GFPc following treatment with MG132, suggesting that the low levels of AtNCT:GFP or AtPS1:GFPc seen in seedlings is not due to degradation by the proteasome. However, as certain batches of MG132 do not apparently produce adequate inhibition of the proteasome, these experimants should be repeated with appropriate controls in place.

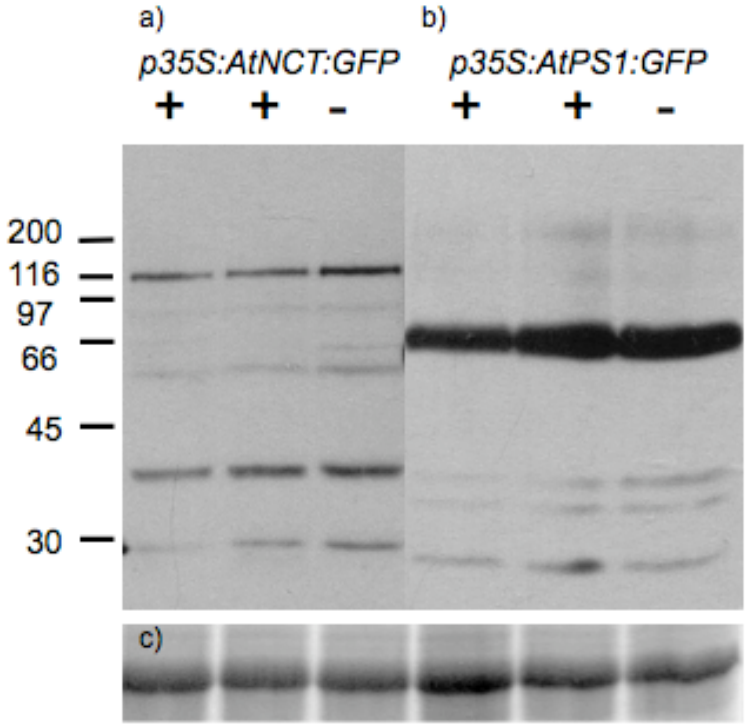

Fig 4.11 AtNCT:GFP and AtPS1:GFPc do not appear to be degraded by the 26S proteasome. Seedlings were grown *in vitro* on plates, and transplanted to liquid culture for a total of 12 days. Flasks were treated with MG132 (+) or DMSO control (-) for 24 hrs prior to protein extraction and immunoblot analysis, using an α-GFP primary antibody (a and b). Size markers in kDa are indicated on left.
(a) *p35S:AtNCT:GFP* plants, with AtNCT:GFP protein at ~116 kDa.
(b) *p35S:AtPS1:GFPc* plants, with the AtPS1:GFP holoprotein at ~66 kDa.
(c) Coomassie stained gel showing large RUBISCO subunit as loading controls.

4.7. AtPS1:GFP is accumulated in developing seeds

As discussed previously, a proteomic study identified peptides from AtPS1, AtAPH1 and AtNCT present in silique samples (Baerenfaller et al., 2008). Siliques and developing seeds from lines stably expressing AtPS1:GFP, AtNCT:GFP and both forms of AtPEN2:GFP were examined under the confocal microscope. AtPEN2:GFP, both under control of the 35S and its native promoter, was highly accumulated, however AtNCT:GFP was not detectable. AtPS1:GFPc is accumulated in developing seeds (Fig4.12), something not seen in any other tissue of the plant examined (e.g. roots, young and rosette leaves). The localisation seen may be in endosperm, a seed storage tissue in plants. Protein was extracted from young, developing siliques from GFP tagged lines, and subjected to immunoblot analysis. Unlike the protein samples extracted from seedlings, where AtPS1:GFPc was only detectable after over 60 mins, the full-length AtPS1:GFPc protein was detectable after just 5 mins in silique samples (Fig4.13). The stability of AtPS1:GFPc in developing seeds is interesting, as there does not seem to be a significantly higher expression from the 35S promoter in siliques compared with seedlings, as seen by the free mGFP control used in the Western blots. The accumulation of AtPS1:GFP in developing seeds adds significance to results obtained in other experiments (see Chapter 6).

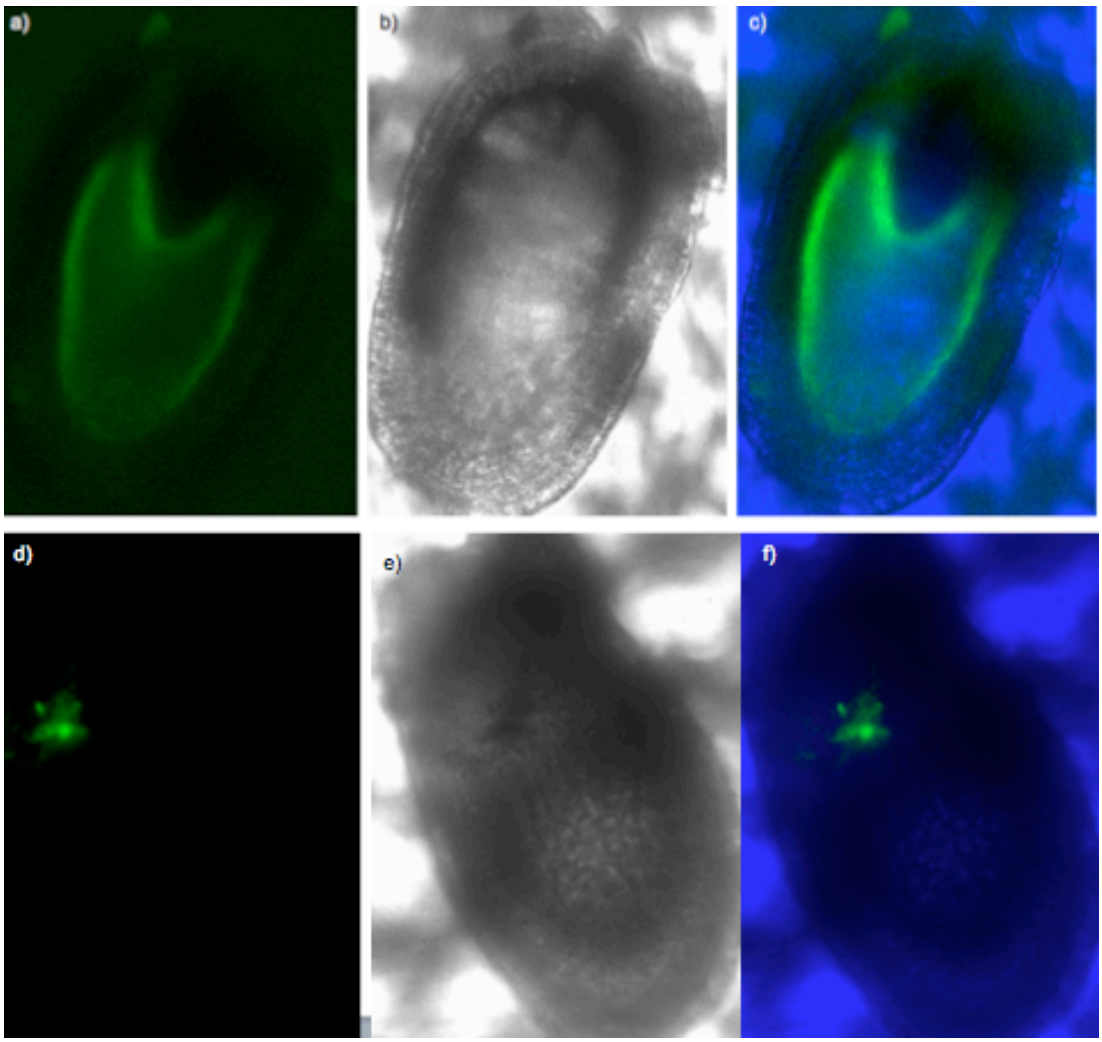

Fig 4.12 AtPS1:GFPc is present in developing seeds.
(a) Confocal image of a developing seed from the 5th silique (approximatley stage 6) of a plant expressing AtPS1:GFPc.
(b) Image of the seed in (a) taken by light microscopy.
(c) Merged image of (a) and (b), showing that AtPS1:GFPc is within the seed, potentially in the endosperm.
(d) Untransformed wild type Col-0 of a similar age as the seed in (a), showing minor auto-fluorescence.
(e) Image of the seed in (d) taken by light microscopy.
(f) Merged image of (d) and (e).
Developing seeds were imaged under the same magnification.

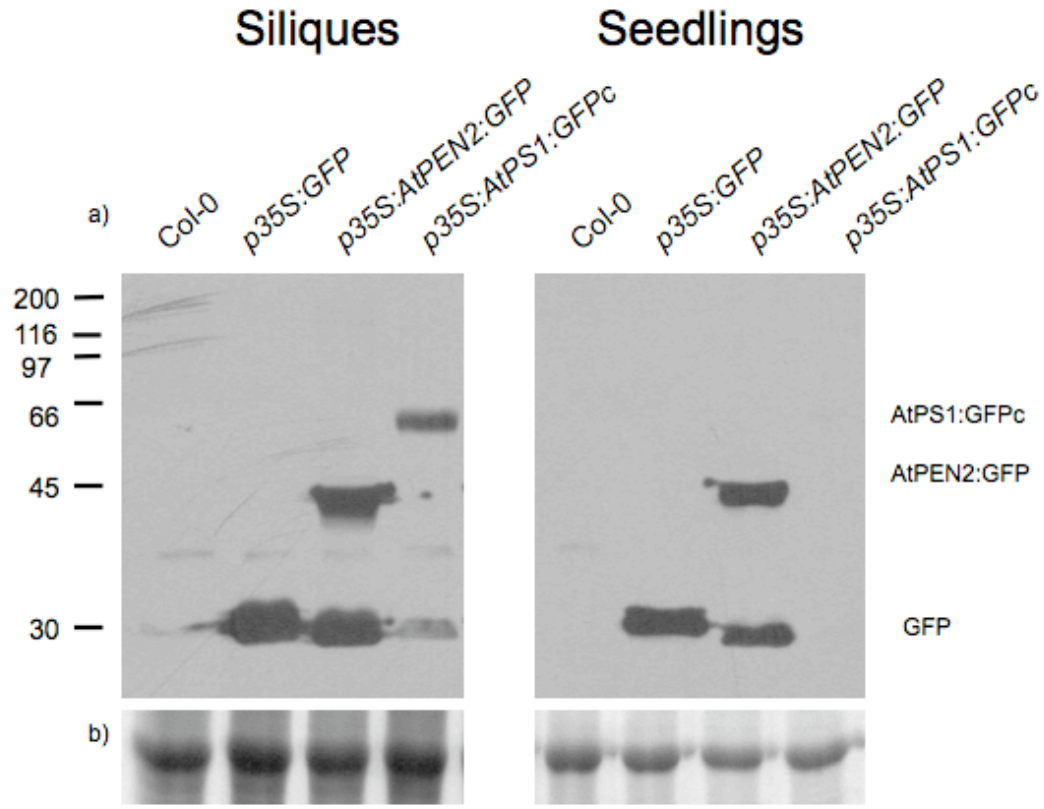

Fig 4.13 AtPS1:GFP is accumulated to a greater degree in siliques compared to seedlings. Total protein was extracted from 10-day-old seedlings grown on plates, or from young developing siliques (stage 3-6), and subjected to immunoblot analysis using an α-GFP primary antibody

(a) GFP and AtPEN2:GFP are seen in both extracts, however AtPS1:GFPc holoprotein (~66 kDa) is seen only in the silique extract, not in the seedling extract.

(b) Coomassie stained gel showing large RUBISCO subunit as loading controls for (a). All protein samples were extracted into 10x (v/w) protein extraction buffer to sample weight, and loaded on to the same gel for transfer. Although there is more total protein loaded in the silique samples, this is not the reason for the difference in the immunoblot for AtPS1:GFP, as AtPEN2:GFP and free GFP are present in comparable amounts in both samples. Size markers in kDa are indicated on left.

4.8. Summary and conclusions

AtPEN2:GFP fusion proteins localise to BFA sensitive Golgi bodies in roots, whether expressed from the 35S promoter, or the genomic *pAtPEN2:AtPEN2g:GFP* fusion, and some co-localisation was found for AtPEN2:GFP with an ER marker in *Arabidopsis* leaves. In human cell lines, GFP:PEN2 is retained in the ER in the absence of PS (Bergman et al., 2004), and functional γ-secretase complexes reside in post-ER compartments, such as the secretory pathway and at the PM. Accumulation of AtPEN2:GFP in Golgi bodies, but not at the PM may be due to different processing/transport routes for the protein between plants and animals, or that AtPEN2:GFP is non-functional, as in the *C. elegans* PEN2:GFP fusion. It is not possible to tell at this point, mainly due to the lack of understanding as to AtPEN2s role. The fact that *pAtPEN2:AtPEN2g:GFP* transgenic plants produce the same sized protein as *p35S:AtPEN2:GFP* plants shows that the mRNA is being spliced in the correct manner.

Accumulation of AtPS1:GFPc in developing seeds is very interesting, due to investigations into substrate identification of the putative *Arabidopsis* γ-secretase complex. As described in Chapter 6, the putative *Arabidopsis* γ-secretase complex may have a role in seed after-ripening requirements. With this potential, the need for further investigation into AtPS1:GFPc, localisation in developing seeds is required. Another version of AtPS1 fused to GFP was constructed, and shows protein accumulation in siliques (Fig 5.9, AtPS1:GFPi accumulation is not as high as AtPS1:GFPc). Localisation of the AtPS1:GFPi fusion protein was not tested here due to time constraints. Given the finding of AtPS1:GFPc accumulates in developing seeds, it would be interesting to see if the N-terminal GFP:AtPEN2 fusion also accumulates here, as GFP:PEN2 fusions are functional in animal systems.

The low accumulation of AtNCT:GFP and AtPS1:GFPc in vegetative tissue does not seem to be due to degradation by the 26S proteasome. An explanation for the low protein levels seen could simply be low translation rate for these constructs. However, accumulation of AtPS1:GFPc is seen in developing seeds, so possibly the

translation rate is differentially regulated in various tissues. Translational control of protein levels is not an uncommon mechanism. One example comes from sucrose signalling, which lowers the amount of protein produced from a *GUS* transcript being expressed from the promoter of the bHLH transcription factor ATB2, without lowering the transcript levels (Rook et al., 1998).

Promoter fusions of *AtPS1, AtPS2, AtNCT, AtAPH1* and *AtPEN2* to a *HISTONE2B:YFP* construct did not produce any signal (Chapter 3). I assumed this to be due to the small sizes of the promoters for *AtPS1, AtPS2, AtAPH1* and *AtPEN2*. Accumulation of AtPEN2:GFP at the correct size from the genomic construct *pAtPEN2:AtPEN2g:GFP* suggests that the intron of *AtPEN2* has a role in control of transcription/translation. Such genomic GFP fusions could be made for *AtPS1, AtPS2* and *AtAPH1* as the resultant constructs, even with the inclusion of promoter, 5' UTR and intron sequences, would be less than 3 kb for each. *AtNCT* has many more introns than the other genes under investigation here, and this would be technically difficult to work with.

This data only applies to one of the *Arabidopsis* PRESENILINs, as *AtPS2* constructs could not be transformed into plants, due to their toxicity in *Agrobacteria*. Therefore, nothing is known about the accumulation of AtPS2 protein in leaves, seedlings and siliques. Current techniques for expression of foreign DNA in *Arabidopsis* include *Agrobacteria* mediated transformation and particle bombardment, both of which were used here. Transient expression in leaves following particle bombardment was somewhat successful, however there was a lot of physical stress placed on the leaves, caused by the low pressure of a partial-vacuum needed for particle bombardment. This could have been utilised to express *p35S:AtPS2:GFP*, but the equipment and resources needed (gold particles) were not freely available to us, as the bombardment with ER:tdT was carried out with the help (and resources) of another group.

5.0. Physical interaction and complex formation

5.1. Introduction

The γ-secretase complex is comprised of four core components, necessary and sufficient to produce γ-secretase activity in yeast, a model organism lacking any native γ-secretase complex members (Edbauer et al., 2003). Components of the γ-secretase complex are found in various internal cellular membrane systems individually, in minor sub-complexes or as the mature active complex. Immature NICASTRIN (iNCT) and APH1 form an early sub-complex in the ER (Niimura et al., 2005), even in the absence of PRESENILIN or PEN2 (Shirotani et al., 2004a). There are two theories regarding the incorporation of the rest of the complex members. Some groups have identified a sub-complex containing iNCT, APH1 and the PS1 holoprotein localised to the ER and Golgi (Capell et al., 2005; Niimura et al., 2005). PEN2 incorporation into the γ-secretase complex is, however, necessary for endoproteolysis of PS and maturation of NCT (Prokop et al., 2004). This evidence suggests that the iNCT/APH1 dimer recruits the PS1 holoprotein in the ER, and the trimeric sub-complex is transported to the Golgi. However, Fraering *et al*. (2004) have shown the PS1 holoprotein associated with PEN2, in the absence of NCT or APH1. This leads to the possibility that two dimeric sub-complexes exist and come together to form the complete complex. Which of these is correct is yet to be determined.

Active γ-secretase complex can be purified from mammalian cell lines, however the measured size of this complex varies considerably between methods used. Capell *et al*. (1998) were able to isolate active γ-secretase from CHAPS solubilised membranes produced from human embryonic kidney (HEK293) cells, and estimated a complex size of 100-150 kDa through glycerol velocity sedimentation. However, the predicted mass of just the four core components of γ-secretase in humans is ~160 kDa. Yu *et al*. (1998) isolated γ-secretase complex members from membranes produced from HEK293 cells solubilised in Digitonin, and found a complex of ~180 kDa containing the PS1 holoprotein, predominately localised to the ER. They also

found an ~250 kDa complex containing the HsPS1-NTF/CTF dimer in both the ER and Golgi. Again, this was carried out through glycerol velocity sedimentation. Li *et al*. (2000a) produced active γ-secretase from HeLa cell membranes solubilised in CHAPS, however their method of gel exclusion chromatography indicated a relative molecular weight of 2000 kDa, suggested by others to be due to aggregation of the protein complexes.

More recently, the method of Blue Native polyacrylamide gel electrophoresis (BN-PAGE) has been used with some success to determine the size of the γ-secretase complex. BN-PAGE allows proteins and protein complexes to be separated according to molecular weight, in their native conformations, due to the exclusion of denaturating detergents such as SDS (Schagger and von Jagow, 1991). Instead, proteins are labelled with the dye Coomassie Blue G-250, which provides a net negative charge to the proteins allowing migration through the gel. Following production of a BN-PAGE gel, the proteins can be electrophoretically transferred to membrane for immunodetection. Edbauer *et al*. (2002) identified a 500-600 kDa complex containing both PS1 and mature NICASTRIN (mNCT), which is eradicated following knockdown of either NCT or PS1, showing that both are required for formation of this high molecular weight complex. Indeed, numerous groups have used BN-PAGE to analyse the γ-secretase complex in animal systems, with differences in complex size depending on detergent used to solubilise the cell membranes.

0.5 % dodecyl-β-D-maltoside (DDM), a non-ionic detergent, is routinely used for membrane solubilisation during work with γ-secretase, and produces estimates of complex size between 440 – 600 kDa on BN-PAGE gels (Edbauer et al., 2002; Steiner et al., 2002; Farmery et al., 2003; Li et al., 2003; Nyabi et al., 2003). However, a higher concentration of DDM (1%) has been shown to cause dissociation of the γ-secretase complex into smaller, inactive sub-complexes (Fraering et al., 2004), where as an alternate detergent Digitonin did not produce this dissociation. 1% Digitonin has been used in the solubilisation of cell membranes in the analysis of γ-secretase, producing estimates of complex size between 250 and 270 kDa

(Kimberly et al., 2003; LaVoie et al., 2003). The discrepancy in sizes produced by varying the detergent is most likely due to the dissociation of non-essential associated proteins that are part of the high molecular weight complex. Very recently, Osenkowski *et al*. (2009) measured purified γ-secretase complex as ~230 kDa with the reliable mothod of scanning transmission electron microscopy. In the same report, they showed that the size of γ-secretase as measured on BN-PAGE westerns varies considerably with the choice of commercial native protein marker.

BN-PAGE has been used in plant proteomics to study various complexes. Examples include the mitochondrial respiratory chain complex, where DDM was used to solubilise the membranes (Sabar et al., 2005), and the super-complexes of *Arabidopsis* photosystems I and II, using Digitonin as the detergent (Heinemeyer et al., 2004).

Here, I have developed a system to study the putative γ-secretase complex in *Arabidopsis*, expressing epitope tagged versions of all four members of the complex in combination in individual plants. BN-PAGE was used to identify potential complexes in which GFP fusions to members of the putative *Arabidopsis* complex members are found.

5.2. Development of a system to study four epitope tagged proteins in individual Arabidopsis *plants*

The insertion of multiple binary vector T-DNAs into the *Arabidopsis* genome has been shown to lead to silencing of the transgenes (reviewed in Vaucheret *et al*., 1998). Due to this phenomenon, it was decided to utilise a system involving a viral peptide capable of producing multiple proteins from single transcripts. The 2A peptide of the foot-and-mouth disease virus (FMDV) causes a novel 'skip' during ribosomal translation, often referred to as cleavage, at the C-terminus of the 2A peptide itself, leading to a continuation of translation without the production of a peptide bond (Donnelly et al., 2001). Use of this molecular technology has been developed in plant systems (Halpin et al., 1999) and used as a research tool in *Arabidopsis* (Samalova et al., 2006).

Small epitope tags with commercially available antibodies (6x HIS, c-MYC and STREPII), along with GFP, were chosen to label the four components of the putative γ-secretase complex in *Arabidopsis*. Oligonucleotides were designed to produce small epitope tags: 6xHIS (HHHHHH, HIS F and HIS R), c-MYC (EQKLISEEDL, MYC F and MYC R) and STREPII (WSHPQFEK, STREP F and STREP R), with *Bam*HI sites on the 5' and 3' ends. *mGFP* was amplified with primers to introduce a *Bam*HI site (GGATCC) at the 5' end and a *Bgl*II site (AGATCT) at the 3' end. The *2A* peptide (QLLNFDLLKLAGDVESNPG) coding sequence from foot-and-mouth disease virus (FMDV) was produced from oligonucleotides with a *Bgl*II site at the 5' end and an *Xho*I site at the 3' end (2A F and 2A R).

The primer pairs for the small epitope tags were annealed at 50^0C and ligated into *Bam*HI cut pBluescript SK (pSK; Fermentas) (HIS pGI507, STREP pGI508 and MYC pGI509), and the 2A peptide primers ligated into *Bgl*II/*Xho*I cut pLitmus 29 (pRW417), and sequenced. To combine the tags with the 2A peptide (Fig 5.1), pRW417 was first cut with *Bgl*II and dephosphorylated, cleaned and cut again with *Xho*I. Each tag was cut out with *Bam*HI. The receiving vector was cut with *Bam*HI/*Xho*I and dephosphorylated. All three DNA fragments were combined in a three-way ligation where the only way for a circularised plasmid to form was through ligation of the tag to the 2A peptide and the plasmid. Resulting positive constructs were sequenced to ensure correct orientation of tag sequences (*HIS:2A* pRW420, *STREP:2A* pRW422, *MYC:2A* pRW424). Ligation of *Bam*HI and *Bgl*II complimentary overhangs destroys the recognition sites for both enzymes.

AtAPH1 and *AtPEN2* were re-amplified with primers to introduce a *Sal*I site at the 5' end and a *Bam*HI site at the 3' end (*AtAPH1*: APH1 5' Sal and APH Bam R (pRW386); *AtPEN2*: PEN2 5' Sal and PEN2 Bam R (pRW387); Fig 5.2), cloned into pGEM-T easy and sequenced. *AtAPH1* (pRW386) and *AtPEN2* (pRW387) were first transferred into pGEM 11Z using the *Not*I/*Bam*HI sites (to produce pRW415 and pRW416 respectively). The *TAG:2A* constructs were added by digesting pRW415

and pRW416 with *Bam*HI/*Sac*I and inserting the *Bam*HI/*Sac*I fragments cut from pRW420, pRW422 and pRW424.

AtNCT was amplified with primers to incorporate a *Sal*I site at the 3' end, upstream on the ATG start codon, and a *Bsm*BI site at the 5' end, followed by a STOP codon (cleavage with the type II restriction endonuclease *Bsm*BI produces a *Bam*HI type overhang in this case). The PCR product was cloned into pGEMT easy and clones were sequenced. *Bam*HI cut small tag sequences, and *Bam*HI/*Bgl*II cut *GFP*, were inserted into *Bsm*BI cut vector, and resultant clones were sequenced to ensure correct orientation of tags. These tagged versions of AtNCT were transferred to pSK as *Sal*I/*Pst*I fragments (Fig 5.3).

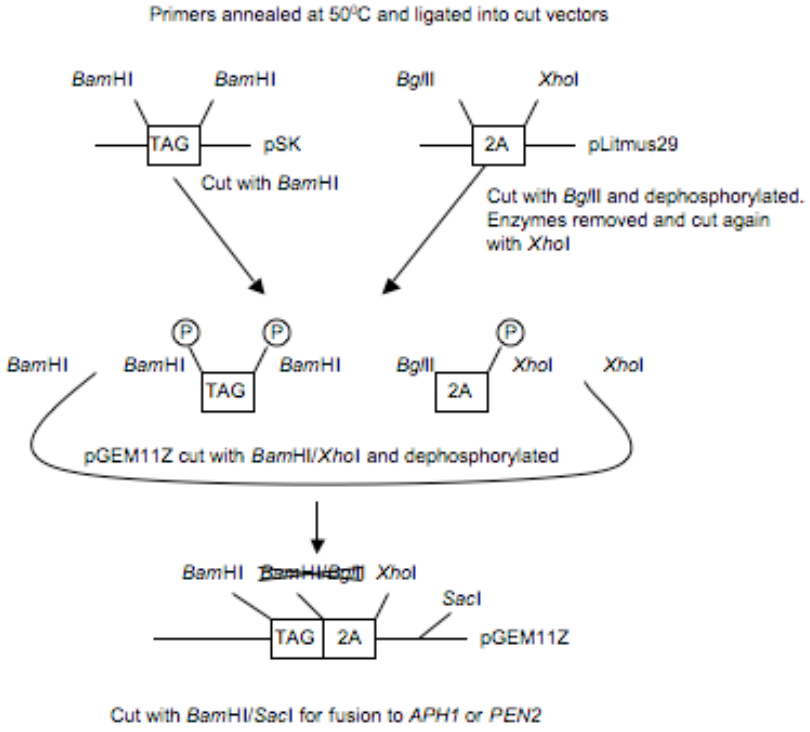

Fig 5.1 Schematic diagram showing construction of *TAG:2A* fusion constructs. Tag and *2A* coding sequences were produced from oligonucleotides and inserted into cut vectors. The vector containing the *2A* sequence was cut with *Bgl*II, dephosphorylated and cleaned. This cut vector was cut again with *Xho*I, and the 64 bp fragment recovered. Small tags were cut from pSK with *Bam*HI, and recovered (*6xHIS* 55 bp, *2xSTREPII* 67 bp, *2xMYC* 79 bp). pGEM11Z was cut with *Bam*HI/*Xho*I, and treated with phosphatase. Ligations were set up with the cut vector, the *2A* sequence and each of the small tags. Ligation of tag sequence to *2A* and vector was essential for re-circularisation of plasmid due to the selective phosphatase treatments. Resulting clones were sequenced to ensure correct orientation of tag sequences.

Research in animal systems with PS1:GFP fusions have inserted GFP into the cytoplasmic loop of PS1 between amino acid residues 351 and 352, in an area previously shown to be non-essential to γ-secretase function (Kaether et al., 2002). Although the sequence similarity within the cytoplasmic loops of human and *Arabidopsis* PSs is less conserved than other regions, it was decided to reproduce this cytoplasmic loop incorporated GFP in the *Arabidopsis* versions. A site was chosen in AtPS1 and AtPS2 to resemble that of Kaether *et al.* (2004), between residues 271-272 for AtPS1 and 303-304 for AtPS2.

AtPS1 and *AtPS2* were amplified with sets of primers to incorporate a *Bam*HI site within their proposed cytosolic loops, for the insertion of *GFP* and other small epitope tags (*AtPS1*: N-terminus with PS1 5' Sal and PS1 Bam R (pRW383); C-terminus with PS1 Bam F and PS1 3' Xho (pRW382); *AtPS2*: N-terminus with PS2 5' Sal and PS2 Bam R (pRW385); C-terminus with PS2 Bam F and PS2 3' Xho (pRW384)). The fragments were cloned into pGEM-T easy and sequenced. For *AtPS1* (Fig 5.4), pRW382 was cut out of pGEM-T easy using *Bam*HI/*Not*I and inserted into pBluescriptII KS (pKS; Fermentas) to make pRW450. pRW450 was digested with *Sal*I/*Bam*HI and the *Sal*I/*Bam*HI fragment from pRW383, containing the N-terminal fragment of *AtPS1*, inserted. This produced a full length coding sequence of *AtPS1* with a *Bam*HI site at 814 nt after the ATG start codon (pRW452).

The N-terminus of *AtPS2* was cut from pRW385 and inserted into pRW384 using the *Bam*HI/*Pst*I sites, to produce pRW404, containing full length *AtPS2* with a *Bam*HI site at 909 nt after the start codon (Fig 5.5). Tags were added to pRW452 (*AtPS1-Bam*HI) and pRW404 (*AtPS2-Bam*HI) by cutting with *Bam*HI (followed by phosphatase treatment) and inserting the small tags cut with *Bam*HI, to produce *PS1/2:TAGi* (internal tag, as opposed to the previously constructed C-terminal fusions). Resulting clones were sequenced to check for single tag insertions. *mGFP* was cut from pGI506 with *Bam*HI/*Bgl*II and inserted into the same *Bam*HI cut vectors.

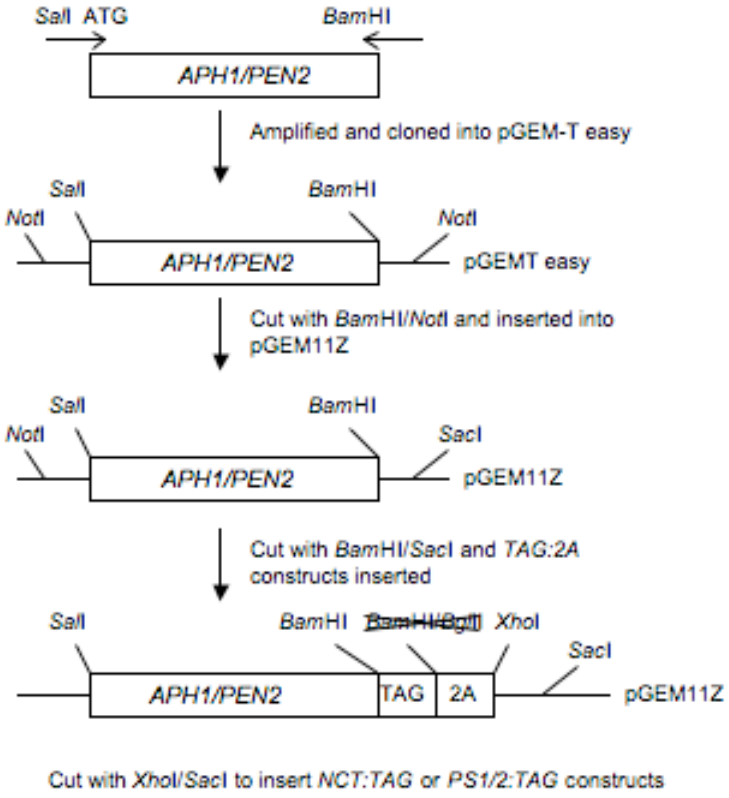

Fig 5.2 Schematic diagram showing production of *APH1:TAG:2A* and *PEN2:TAG:2A* constructs. *AtAPH1* and *AtPEN2* coding sequences were amplified form plasmids (containing the previously cloned ORFs; *AtPEN2* with a mutated internal *SalI* site was used) to incorporate *Sal*I and *Bam*HI sites at the 5' and 3' ends, respectively. No STOP codon was needed. PCR products were cloned into pGEMT easy and resultant clones sequenced to check fidelity of polymerase used. Plasmids were cut with *Bam*HI/*Not*I and inserted into *Bam*HI/*Not*I cut pGEM11Z. *TAG:2A* sequences were introduces through the *Bam*HI/*Sac*I sites.

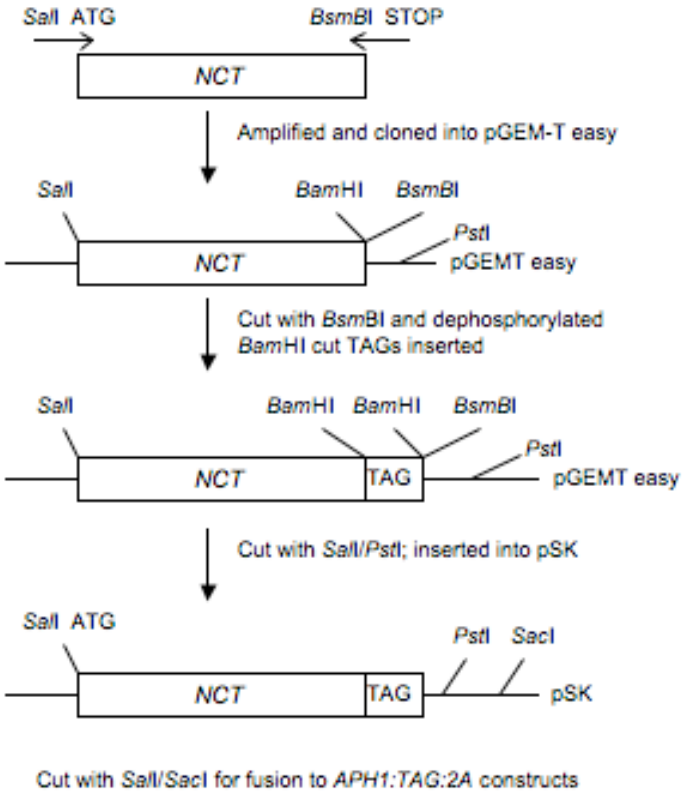

Fig 5.3 Schematic diagram showing construction of *AtNCT:TAG* fusions. The coding sequence of *AtNCT* was amplified with primers to incorporate restriction enzyme sites on the 5' and 3' ends, cloned into pGEMT easy and sequenced. Small tags were introduced at the 3' end as *Bam*HI fragments, into *Bsm*BI cut vector (producing a *Bam*HI complimentary overhang). Tagged versions of *AtNCT* were transferred to pSK as *Sal*I/*Pst*I fragments.

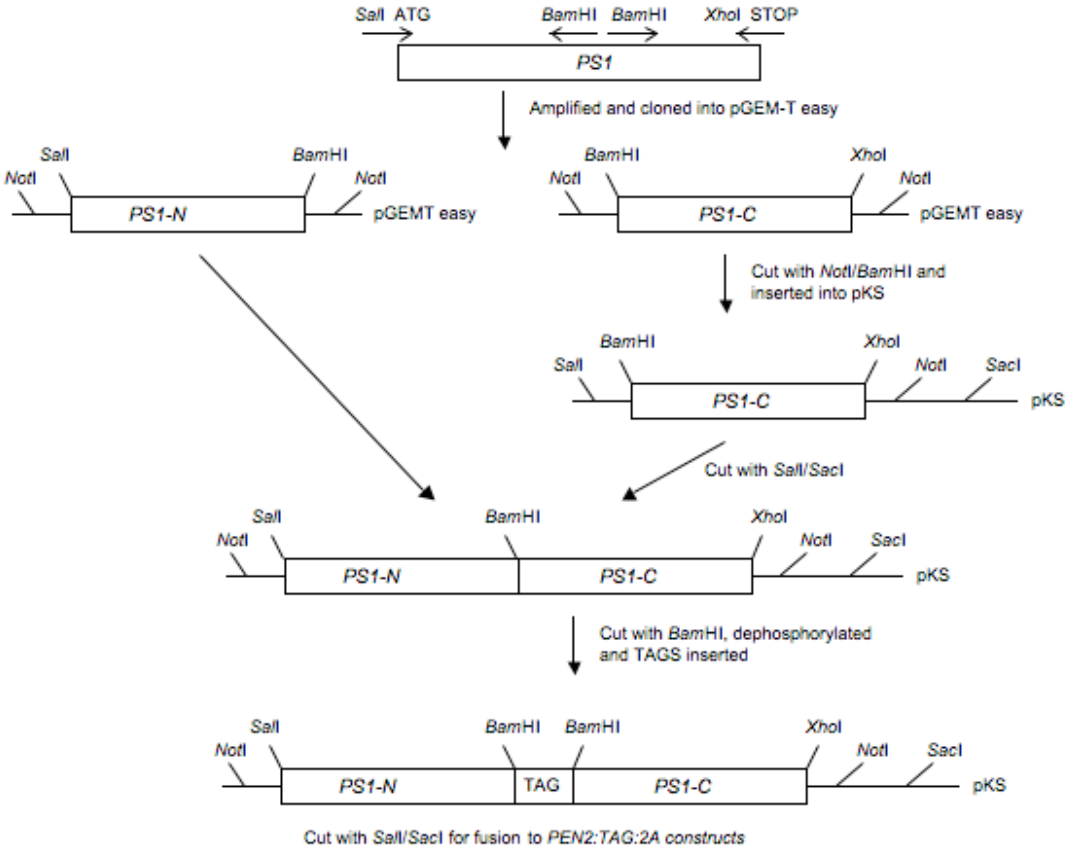

Fig 5.4 Schematic diagram showing construction of *AtPS1* internal tag fusions. N- and C-terminal fragments of *AtPS1* were amplified to incorporate restriction enzyme sites, as shown. Fragment *PS1-C* was transferred to pKS as a *Not*I/*Bam*HI fragment. The *PS1-N* fragment was added as a *Sal*I/*Bam*HI fragment, to produce the complete coding sequence of *AtPS1* with a *Bam*HI site 814 nt from the ATG start codon. Small tags were introduced as *Bam*HI fragments into *Bam*HI cut, and dephosphorylated, vector.

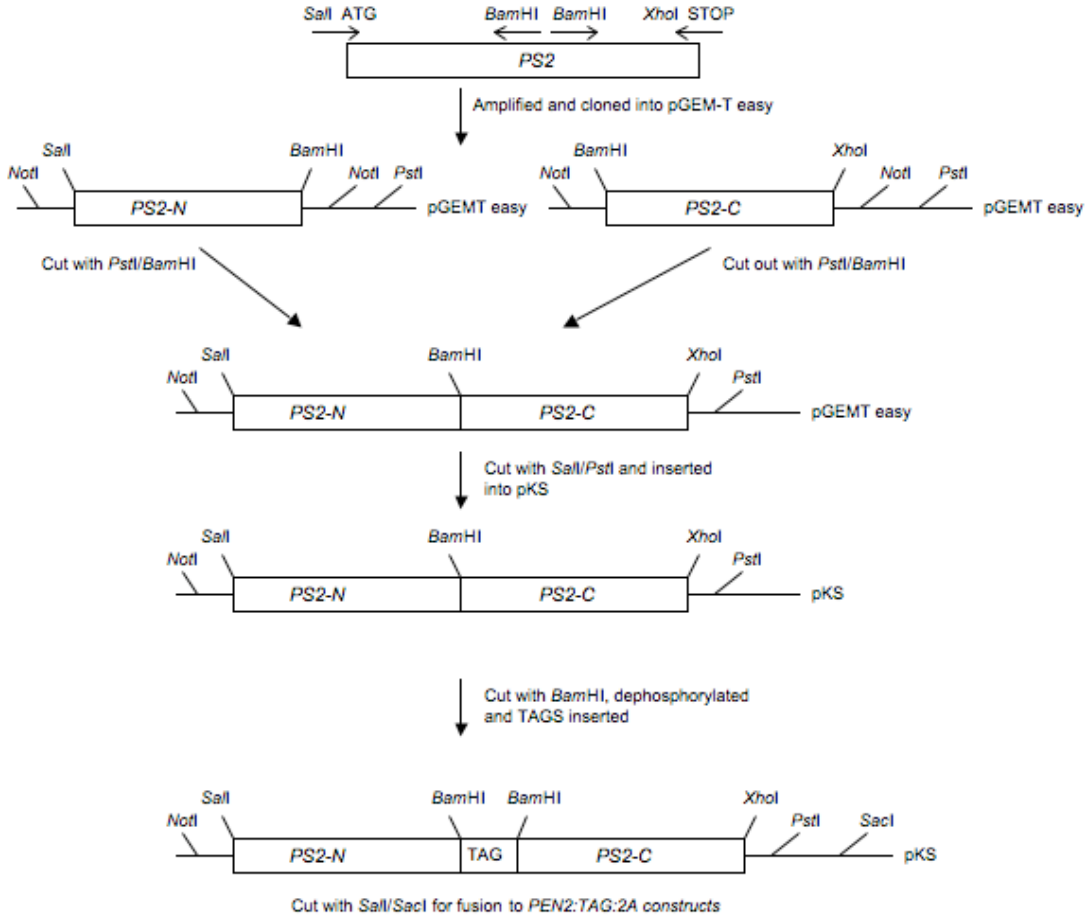

Fig 5.5 Schematic diagram showing construction of *AtPS2* internal tag fusions. N- and C-terminal fragments of *AtPS2* were amplified to incorporate restriction enzyme sites, as shown. Vector containing *PS2-N* was cut with *Bam*HI/*Pst*I and *PS2-C* fragment inserted, to produce the full *AtPS1* coding sequence with a *Bam*HI site 909 nts form the ATG start codon. Tagged versions of *AtPS1* were transferred to pKS as *Sal*I/*Pst*I fragments. Small tags were introduced as *Bam*HI fragments into *Bam*HI cut, and dephosphorylated, vector.

For all constructs containing the 2A peptide, *AtAPH1* was fused upstream of *AtNCT* and *AtPEN2* upstream of *AtPS1* or *AtPS2* (Fig 5.6). Tagged versions of *AtNCT* were cut from pSK using *Sal*I/*Sac*I, and cloned downstream of the 2A peptide, into *Xho*I/*Sac*I cut vector. *AtPS1* and *AtPS2* tagged constructs (in pKS) were cut out with *Sal*I/*Sac*I and inserted into *PEN2:TAG:2A* containing vectors (cut with *Xho*I/*Sac*I) as *Sal*I/*Sac*I inserts.

PEN2:TAG:2A:PS1:TAGi and *PEN2:TAG:2A:PS2:TAGi* constructs were transferred as *Sal*I/*Sac*I fragments into pBIB-Hyg-35S cut with *Sal*I/*Sac*I. Like the *AtPS2:GFPc* constructs, the *PEN2:TAG:2A:PS2:TAGi* constructs were toxic to *Agrobacteria* and hence could not be transformed into *Arabidopsis*. *APH1:TAG:2A:NCT:TAG* constructs were processed in the same way, but cloned into the binary vector pGPTV-Kan-35S (pGPTV-Kan containing the CMV 35S promoter; confers Kanimycin resistance to transformed plants). All possible constructs were transformed into *Arabidopsis* and primary transformants selected on the appropriate antibiotic (see Table 5.1 for construct numbers). Lines segregating 3:1 for resistance were identified in the T_1 generation, and RT-PCR carried out to ensure expression of full-length transcripts in a number of lines for each construct (Fig 5.7).

SDS-PAGE western blots were carried out on protein extracts from seedlings of homozygous insertion transformants, identified in the T_2 generation, to look at protein production. AtNCT:GFP fusion protein is predicted at 100 kDa, but as found in previous experiments, the observed size is closer to 116 kDa, possibly due to post-translational modifications. Western blots with α-GFP antibody on APH1:TAG:2A:NCT:GFP transformants (RW499, RW500 and RW501) produced a band at the same size as AtNCT:GFP, but also a higher band which is most likely a polyprotein produced from the full-length transcript (Fig 5.3; Table 5.2 for predicted protein sizes). This shows that although some of the protein produced with the 2A peptide is forming separate proteins, there is still a significant fraction of the polyprotein. Western blots using antibodies against the small tags on AtAPH1 for each of these constructs did not produce any signal, probably due to the low level of protein present.

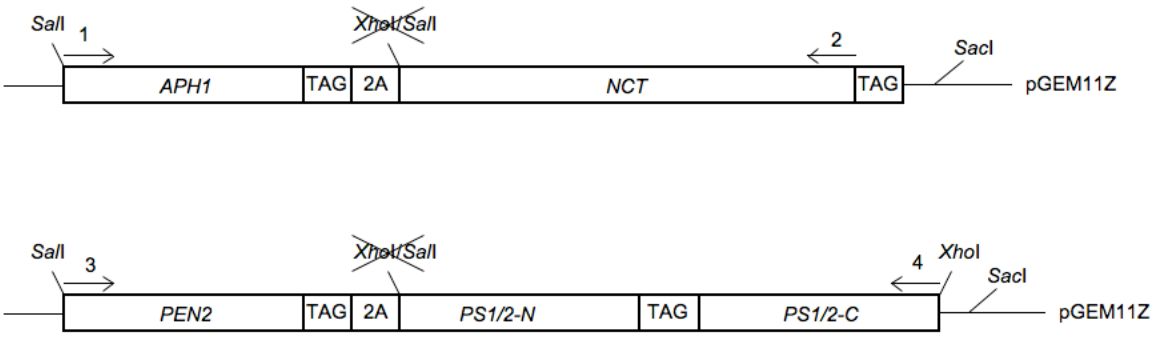

Fig 5.6 Schematic diagrams of *APH1:TAG:2A:NCT:TAG, PEN2:TAG:2A:PS1:TAGi* and *PEN2:TAG:2A:PS2:TAGi*. Constructs were produced by cutting *APH1:TAG* and *PEN2:TAG* containing vectors with *Xho*I/*Sac*I, and inserting the appropriate *Sal*I/*Sac*I fragment. *APH1:TAG:2A:NCT:TAG* constructs were cloned into the binary vector pB?, and *PEN2:TAG:2A:PS1:TAGi* and *PEN2:TAG:2A:PS2:TAGi* constructs into pBIB-Hyg-35S. Arrows 1-4 indicate primers used for RT-PCR (Fig 5.7). 1: APH1 5' Sal. 2: NCT 3' Bam. 3: PEN2 5' Sal. 4: PS1 3' Xho. No primer for AtPS2 was needed, as these constructs could not be transformed into plants.

Construct number	Genes	First tag	Second tag	Predicted polyprotein size (kDa)
493	APH1:NCT	HIS	STREPII	107.5
494	APH1:NCT	STREPII	HIS	107.5
495	APH1:NCT	HIS	MYC	107.9
496	APH1:NCT	MYC	HIS	107.9
497	APH1:NCT	MYC	STREPII	108.2
498	APH1:NCT	STREPII	MYC	108.3
499	APH1:NCT	HIS	GFP	132.5
500	APH1:NCT	MYC	GFP	133.2
501	APH1:NCT	STREPII	GFP	132.9
511	PEN2:PS1	MYC	GFP	93.2
512	PEN2:PS1	STREPII	GFP	92.9
513	PEN2:PS1	HIS	GFP	92.5
514	PEN2:PS1	MYC	STREPII	68.2
515	PEN2:PS1	STREPII	MYC	68.3
516	PEN2:PS1	STREPII	HIS	67.6
517	PEN2:PS1	HIS	STREPII	67.5
518	PEN2:PS1	HIS	MYC	67.9
519	PEN2:PS1	MYC	HIS	67.9

Table 5.1 Clone numbers for 2A peptide constructs transformed into *Arabidopsis*. First tag denotes that fused to APH1 or PEN2, second tag to NCT or PS1. Predicted polyprotein size, in kDa, is included. Following transformation, plants were named as for palsmid number.

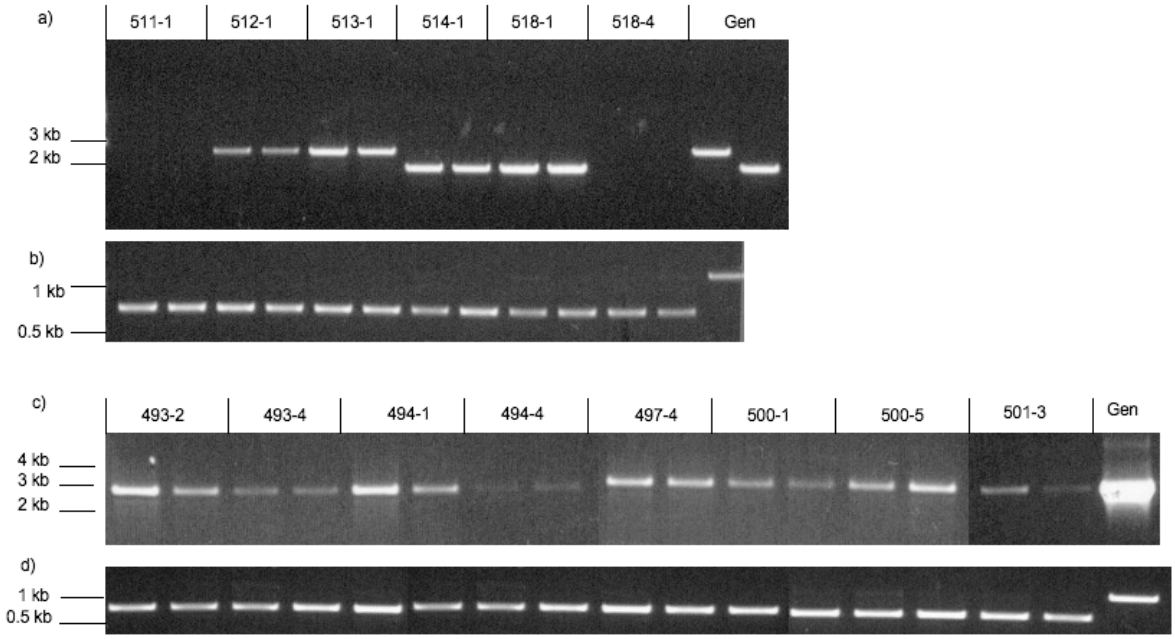

Fig 5.7 Plants transformed with 2A constructs produce full-length transcripts, as seen by RT-PCR. Total RNA was extracted from leaves of plants, cDNA synthesised and RT-PCR amplification carried out. Two plants were tested for a number of independent transformants for each line.
(a) *PEN2:TAG:PS1:TAGi* amplified using PEN2 5' Sal and PS1 3' Xho. Lines 511, 512 and 513 contain GFP as the tag in *AtPS1*, hence the larger product size (~2.5 kb for *GFP* containing lines, ~1.9 kb for small tag containing lines).
(b) *TUBULIN3* control for cDNAs in (a).
(c) *APH1:TAG2A:NCT:TAG* amplified using APH1 5' Sal and NCT 3' Bam (~2.9 kb).
(d) *TUBULIN3* control for cDNAs in (c).

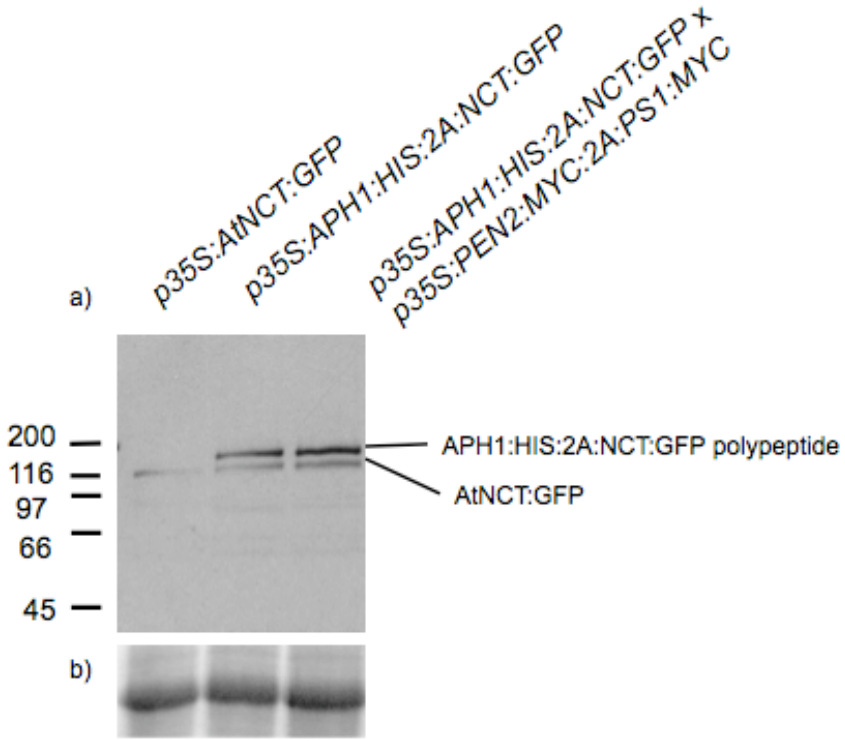

Fig 5.8 AtNCT:GFP is detectable in lines expressing *APH1:TAG:2A:NCT:GFP*.
(a) Western blot of AtNCT:GFP lines using α-GFP antibody. *p35S:AtNCT:GFP* line produces only AtNCT:GFP signal. Predicted size for AtNCT:GFP is 100 kDa, however in all westerns it is closer to 116 kDa. *p35S:APH1:HIS:2A:NCT:GFP* lines show a double band. Lower band is AtNCT:GFP, upper band is the APH1:HIS:2A:NCT:GFP polypeptide. *p35S:APH1:HIS:2A:NCT:GFP* x *p35S:PEN2:STREP:2A:PS1:MYC* (line 8-1) behaves the same as its parental line with respect to AtNCT:GFP accumulation. Size markers in kDa are indicated on left.
(b) Coomassie stained gel showing large RUBISCO subunit as loading controls for (a).

PEN2:TAG:2A:PS1:GFPi (RW511, RW512 and RW513) lines were tested on western blots, but no signal was detected from 10-day-old seedlings. Due to the instability of PS1 in animal systems lacking the other members of the complex, crosses were performed between lines expressing complimentary constructs to obtain plants expressing constructs with the four different tags (Table 5.2). All possible combinations of tags were produced. The resulting F_1 seedlings were grown on 0.5xMS containing both Hygromycin and Kanamycin to select for plants carrying the two binary vectors. Plants resistant to both antibiotics were carried forward for subsequent generations.

Total protein was extracted from 10-day-old seedlings segregating from the F_2 generation of the crosses, selected on antibiotics, and tested on western blots to examine protein levels of the GFP fusion lines. For those lines containing AtNCT:GFP, a similar level of protein was detected, compared with the parental lines, indicating that although the proteins are not accumulated to a greater degree they are not down-regulated either (Fig 5.8).

Lines containing the *PEN2:TAG:2A:PS1:GFPi* constructs did not show any signal on western blots from 10-day-old seedlings, as in the parental lines. Following the discovery of the accumulation of AtPS1:GFPc in siliques (Fig 4.13), similar western blots were carried out with the 2A peptide lines. A band at ~93 kDa was detected in protein extracts from siliques for RW511 (PEN2:MYC:2A:PS1GFPi) with an α-GFP primary antibody (Fig 5.9, lane 5). This is the predicted size for the fused polyprotein, indicating that there is an accumulation of this version. However, there does not appear to be a band for the AtPS1:GFPi holoprotein, suggesting that either the 2A cleavage event does not take place or the cleaved AtPS1:GFPi holoprotein is unstable. However, as AtPS1:GFPi (RW520) holoprotein is somewhat detectable in silique extracts (Fig 5.9, lane 4), the likely explanation is the lack of 2A cleavage. A western blot carried out on RW511 plants (PEN2:MYC:2A:PS1GFPi) using a monoclonal α-c-MYC primary antibody (Clontech) did not produce any signal. Whether this is due to the insertion of the small c-MYC tag within the protein sequence (rather at the extreme N- or C-terminus) is impossible to tell here. If time

had permitted, the fusions of each tag to each *Arabidopsis* protein of interest (both N- and C-terminally) would have made and tested individually, prior to construction of the 2A peptide fusions.

Detection of a band at ~45 kDa in protein extracts from RW349 plants (*p35S:AtPS1:GFPc*; Fig 5.9, lane 3) has been described previously. This band represents a cleavage product of AtPS1:GFPc, closely resembling that formed in animal systems when PRESENILIN is proteolytically cleaved within its cytosolic loop, prior to activation of the γ-secretase complex. A similar sized band is detected for AtPS1:GFPi (Fig 5.9, lane 4), suggesting that this protein is processed in a similar fashion to AtPS1:GFPc. The presence of this band in the extract from RW511 plants (Fig 5.9, lane 5) is difficult to explain, due to the lack of AtPS1:GFPi holoprotein. Potentially, the fusion protein detected at ~93 kDa is treated as cellular "junk" and dealt with accordingly. However, a portion of the translated protein may undergo the 2A cleavage (as seen with APH1:TAG:2A:NCT:GFP, Fig 5.8) to produce separate AtPEN2:TAG:2A and AtPS1:GFPi proteins, and the AtPS1:GFPi protein is cleaved within its cytosolic loop, to produce the ~45 kDa band seen. However, due to the lack of any signal when the α-c-MYC antibody is used, this is impossible to tell without further work.

Lines generated from crosses preformed with RW511, for example 13-2, did not produce any signal from silique extracts (Fig 5.9, lane 8). This may be due to silencing effects caused by the introduction of another transgene following the cross. Although the 2A peptide has been used with success in other studies of plant protein localisation, in this case it seems unsuitable.

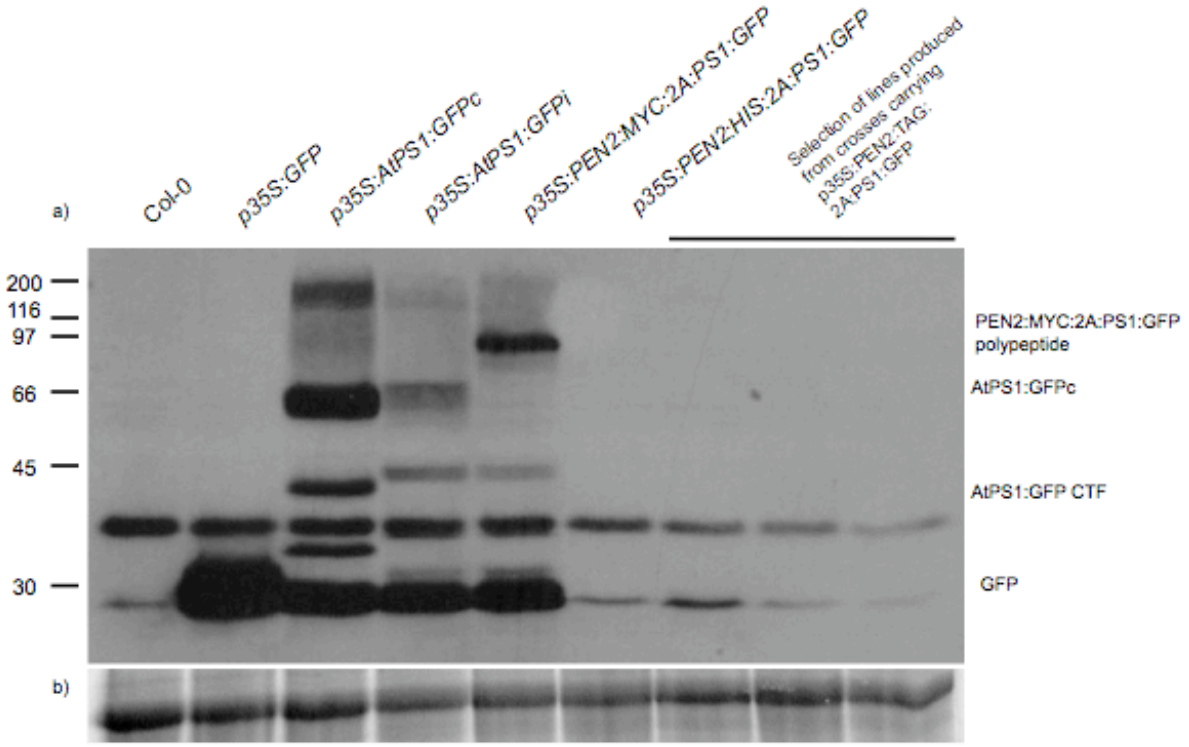

Fig 5.9 PEN2:MYC:2A:PS1:GFP polyprotein is accumulated in siliques.
(a) Total protein was extracted from developing siliques and subjected to immunoblot analysis using an α-GFP antibody. Extract from *p35S:AtPS1:GFPc* line produces signal for AtPS1:GFP holoprotein and cleaved AtPS1:GFP CTF. *p35S:AtPS1:GFPi* line also produces similar sized bands. The *p35S:PEN2:MYC:2A:PS1:GFP* (RW511-9) does not produce AtPS1:GFP holoprotein signal, however it does produce signal at the predicted size for the PEN2:MYC:2A:PS1:GFP polypeptide (93 kDa). Lines produced from crosses carrying *p35S:PEN2:TAG:2A:PS1:GFP* were 6-2 (497-2 x 513-2), 13-3 (511-9 x 494-4) and 17-1 (513-2 x 497-4). Size markers in kDa are indicated on left.
(b) Coomassie stained gel showing large RUBISCO subunit as loading controls for (a).

Cross number	Plant emasculated	Pollen used	Cross number	Plant emasculated	Pollen used
1-1	493-4	511-2	14-1	511-2	494-4
2-1	494-1	511-2	15-1	512-2	495-4
2-2	494-1	511-9	15-2	512-4	495-4
3-1	495-4	512-4	17-1	513-2	497-4
3-2	495-4	512-2	18-1	513-2	498-7
4-1	496-8	512-4	19-1	514-1	499-1
4-2	496-8	512-2	19-2	514-1	499-9
6-1	497-2	513-2	20-1	515-2	499-1
6-2	497-4	513-2	20-2	515-3	499-1
8-1	499-1	515-3	21-1	516-2	500-5
8-2	499-1	515-2	21-2	516-4	500-5
8-3	499-9	515-2	22-1	517-8	500-5
8-4	499-9	515-3	23-1	518-9	501-10
9-1	500-5	516-2	23-2	518-9	501-11
9-2	500-5	516-4	23-3	518-12	501-10
13-1	511-2	493-4	23-4	518-12	501-11
13-2	511-9	493-2	24-1	519-7	501-10
13-3	511-9	494-4	24-2	519-7	501-11

Table 5.2 Crosses carried out using 2A peptide constructs. Lines generated from crosses were designated as for cross number.

5.3. The AtPEN2:GFP and AtPS1:GFPc fusion proteins are part of high molecular weight complexes

Total protein was extracted from 10-day-old seedlings into ice-cold BN-PAGE extraction buffer (see Materials and Methods), and insoluble material removed. 1% Digitonin was chosen as the detergent, as it has been used with success in studies of animal γ-secretase. Loading dye, containing Coomassie Blue G-250, was added to the samples and applied to Novex Native Bis-Tris gradient gels (4-16 %; Invitrogen). Following separation of proteins, gels were either subjected to Coomassie staining or transferred to membrane for immunodetection. Figure 5.10(a) shows lanes from a typical BN-PAGE gel stained with Coomassie Blue R-250.

When transferred to membrane and subjected to immunodetection with an α-GFP primary antibody, a number of bands were detected that do not appear in the Col-0 control (Fig 5.10b). Only the lowest of these bands (below 67 kDa) also appears in extracts from plants expressing free GFP, leading to the conclusion that this band corresponds to GFP that has been cleaved from the AtPEN2:GFP fusion protein, as seen in SDS-PAGE westerns (see Fig 4.1). From this, it can be assumed that the other bands contain the AtPEN2:GFP fusion protein. The predicted molecular weight for AtPEN2:GFP is 44 kDa (AtPEN2 predicted as 16.5 kDa, mGFP6 predicted as 27.5 kDa), which does not correspond to any of the bands observed on the western blots analysed. However, due to the native conformation of proteins running on BN-PAGE gels, the prediction of protein size is not always accurate. I have assumed that the band at ~80 kDa corresponds to "free" AtPEN2:GFP, and the higher molecular weight bands are complexes incorporating AtPEN2:GFP.

Experiments carried out using plants expressing AtPS1:GFPc fusion protein (RW349) produced a similar banding pattern as AtPEN2:GFP (Fig 5.11), but without the band at ~80 kDa, providing further evidence that this band corresponds to "free" AtPEN2:GFP (* in Fig 5.11). Four HMW complexes therefore appear to contain both AtPEN2:GFP and AtPS1:GFPc (those at approximately 140, 170, 230 and 380 kDa), however the other proteins in these complexes are unknown. The predicted weight of the putative *Arabidopsis* γ-secretase complex is ~160 kDa (AtPS1 44 kDa, AtNCT 73 kDa, AtAPH1 27 kDa, AtPEN2 16 kDa), however as one of the proteins in these complexes has GFP (27 kDa) attached, the predicted size is ~190 kDa. This could correspond to the band between the 140 and 232 kDa markers. AtNCT:GFP lines were also tested on BN-PAGE westerns, but no specific signal was detected. The 2A constructs were intended to be used to look at the presence of other γ-secretase components in these HMW complexes, however this was not possible, due to the low production of fusion protein in these plants. Protein extracts from these plants were tested on native westerns, but like AtNCT:GFP samples, no specific signal was detected (data not shown).

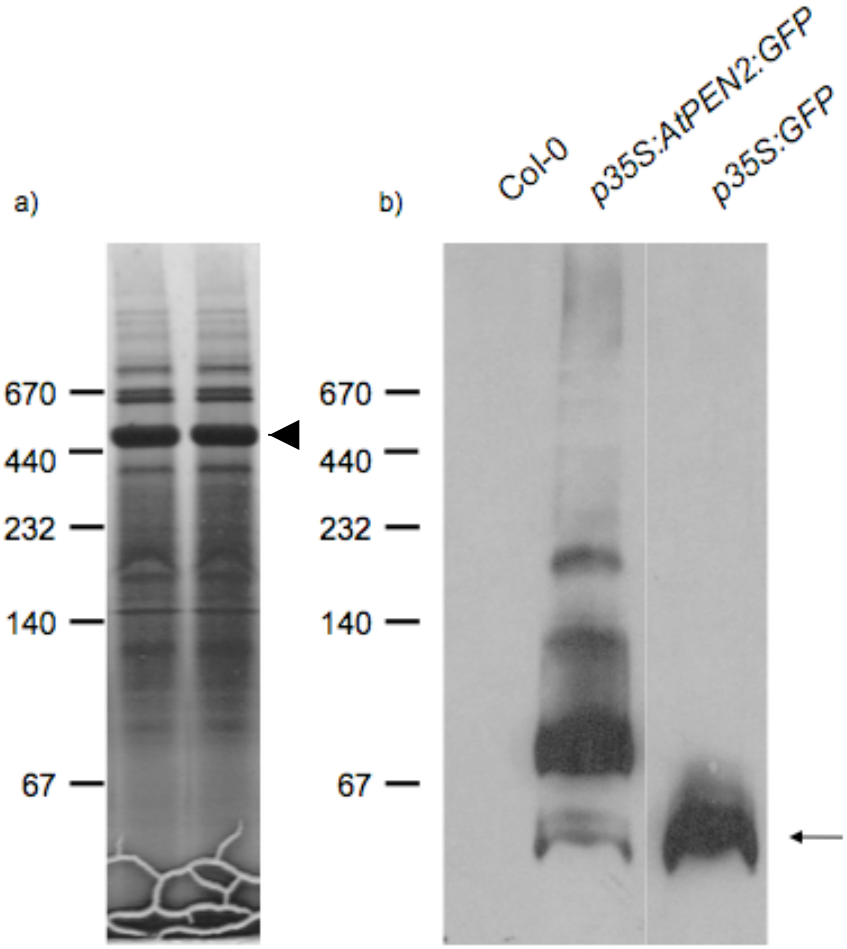

Fig 5.10 AtPEN2:GFP is present in HMW complexes in seedlings. Total protein was extracted from 10-day-old seedlings and applied to a Native PAGE gel. Following separation of proteins and protein complexes, the gel was either stained with Coomassie Blue R250 (a) or transferred to PVDF membrane and subjected to immunoblot analysis with α-GFP antibody (b).
(a) Typical Coomassie Blue stained 4-16% gradient BN-PAGE gel. Cracks at the bottom caused during drying of high percentage gel. Clearly visible in the stained gel is the 55 kDa RuBisCo complex (above the 440 kDa marker, arrow head).
(b) No signal is detected in the Col-0 wild type control. A number of bands are present in the AtPEN2:GFP sample, of which only one is present in the free GFP sample (arrow). Therefore, the presence of the HMW complexes are dependent on AtPEN2:GFP.

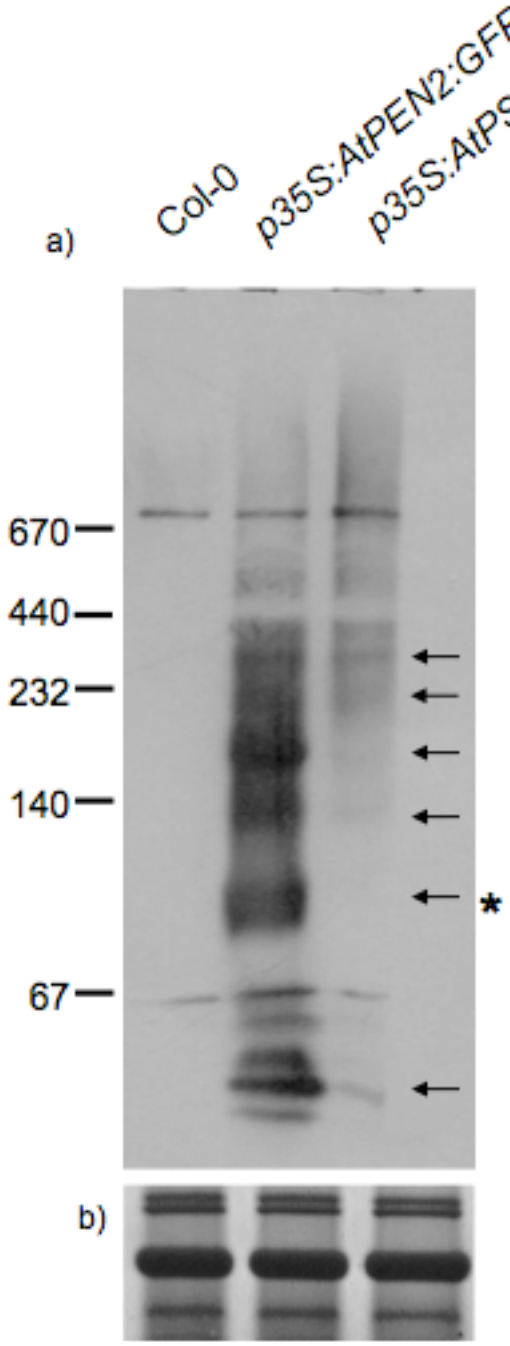

Fig 5.11 AtPEN2:GFP and AtPS1:GFP are present in similarly sized protein complexes in seedlings.
(a) Western blot of BN-PAGE gel, using α-GFP primary antibody. Approximate sizes (in kDa) from HMW native marker kit (GE Healthcare) indicated on left. Arrows indicate bands deemed to be specific to AtPEN2:GFP, with only one not present in AtPS1:GFP (*).
(b) Coomassie stained gel showing RUBISCO complex as loading controls for (a).

5.4. High molecular weight complexes seen in BN-PAGE westerns contain AtPEN2:GFP or AtPS1:GFPc

In order to confirm the identity of the GFP cross-reactive species present in the HMW complexes seen in BN-PAGE western blots, two-dimensional (2D) BN/SDS-PAGE was carried out. This was a new technique for our lab, and most of the details for preparation and running of the second dimension gel came from (Reisinger and Eichacker, 2006). Following electrophoresis in the first dimension of BN-PAGE to separate protein complexes, the components of these complexes were separated by size on a second dimension SDS-PAGE gel. Lanes were cut from a BN-PAGE gel and the proteins solubilised in a denaturating/reducing buffer (containing SDS and 2-mercaptoethanol) and applied to a 12% SDS-PAGE gel. Figure 5.12(a) shows an example of a Coomassie Blue stained gel produced this way, including a stained lane from the native gel for reference. Immediately identifiable are the large and small subunits of RUBISCO, at ~55 kDa and ~20 kDa respectively, released from the large 550 kDa complex visible in the stained BN-PAGE lane.

Western blots were carried out on such gels produced from extracts of Co-0, RW443 (GFP), RW350 (AtPEN2:GFP), and RW349 (AtPS1:GFPc). Results with the 2D approach were difficult to interpret. Using wild type Col-0 as a control for this approach, some background signal is seen (Fig 5.12b). Free GFP (RW443; Fig 5.12c) produces two large spots, mainly below the 67 kDa native marker. RW350 (AtPEN2:GFP; Fig 5.12d) produces a smear of signal at ~45 kDa, in two lines. This smear is not seen in RW443 (free GFP) or Col-0 samples, meaning that the signal is cased by AtPEN2:GFP. It has been assumed that the lines are produced by the proteins entering the stacking gel at different rates as they move out of the gradient gel lane. Another explanation is the fusion of GFP to AtPEN2, as the free GFP sample also has a double band. Aside from this, a large spot of signal is seen just above the 67 kDa native marker, at ~45 kDa on the SDS blot, corresponding to AtPEN2:GFP. Bands can also be seen (within the smear; arrowheads in Fig 5.12d) that align with the bands at 80, 140 and 232 kDa on BN-PAGE westerns on the same sample. This shows that these HMW bands contain AtPEN2:GFP, and that they are not a background artefact.

2D BN/SDS-PAGE westerns with AtPS1:GFPc produced a different pattern from AtPEN2:GFP (Fig 5.5e). There is a higher smear band at the 66 kDa marker (close to the predicted size for AtPS1:GFPc holoprotein seen in SDS-PAGE westerns), and a lower smear band around the 45 kDa marker (the predicted size for AtPS1:GFPc C-terminal fragment). This is interesting, as it suggests that both the AtPS1:GFPc holoprotein and its cleaved C-terminus exist in HMW complexes, although not necessarily in the same complex together.

Although this 2D BN/SDS-PAGE system has not worked perfectly in this case, it has shown good potential for future studies of proteins of interest in the lab. Further work is needed to refine the protocol, such as steps to ensure better reproducibility, and trials with non-GFP fusion proteins (such as those with the small HIS, STREPII and MYC tags) to look into the double banding seen here.

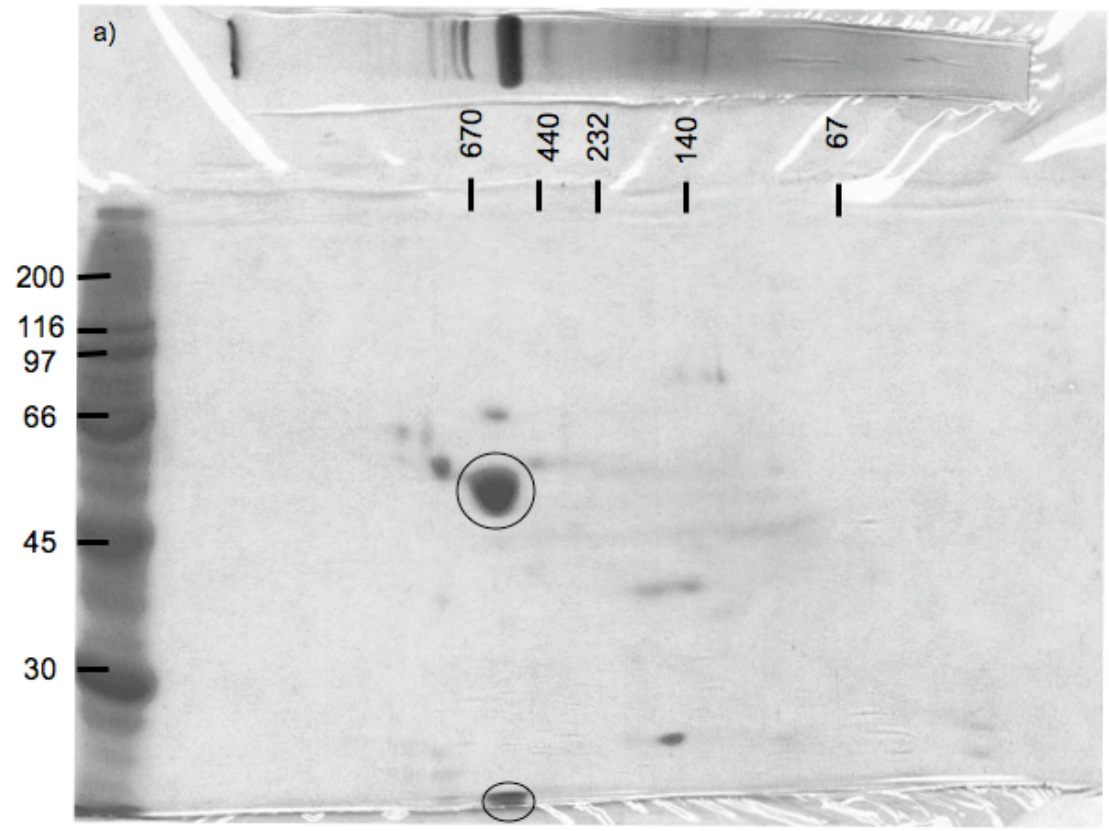

Fig 5.12 2D BN/SDS-PAGE. Following separation of proteins and protein complexes on a 4-16% gradient gel under native conditions, lanes were excised, proteins solubilised and applied to a second dimension SDS-PAGE gel. Presence of SDS in the second dimension gel allows separation of individual proteins by size alone. Proteins can be transferred to membrane for immunodetection. Numbers on the left hand side indicate protein size marker for the second dimension (SDS) gel. Numbers at the top indicate protein size marker for the first dimension (BN) gel.
(a) Example of Coomassie Blue stained gel. The large subunit of RUBISCO is identifiable as the largest spot in the centre of the gel at ~55 kDa (circled), with the small subunit directly below it at the bottom of the gel (also circled). Also depicted is a sample BN-PAGE lane in the approximate position the original was loaded onto the SDS gel. Size markers in kDa are indicated on left of each gel.
(b-e) Western blots using α-GFP primary antibody.
(b) Wild type Col-0 control, showing some background signal.
(c) RW443 (GFP).
(d) RW350 (AtPEN2:GFP), showing signal in a smear at ~45 kDa. Arrowheads indicate the banding within the smear corresponding to some of the bands seen in native westerns.
(e) RW349 (AtPS1:GFP), showing banding at ~44 kDa and ~66 kDa.

b) Col-0

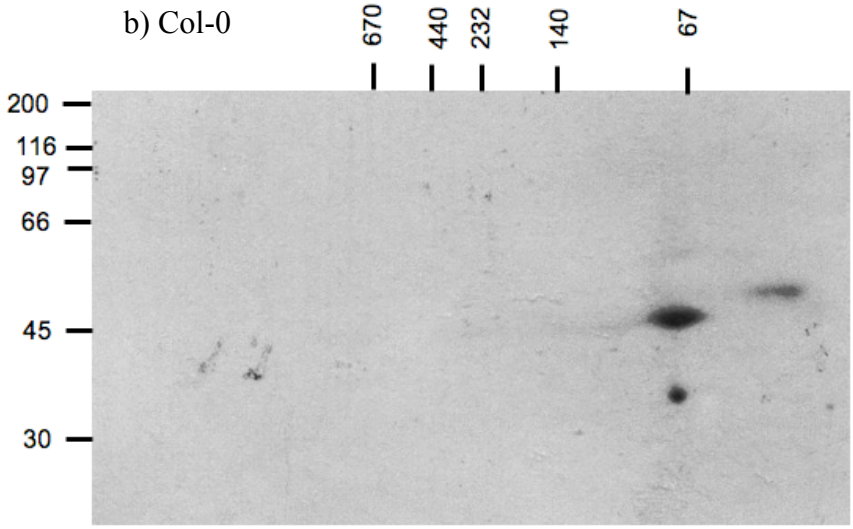

c) *p35S:GFP*

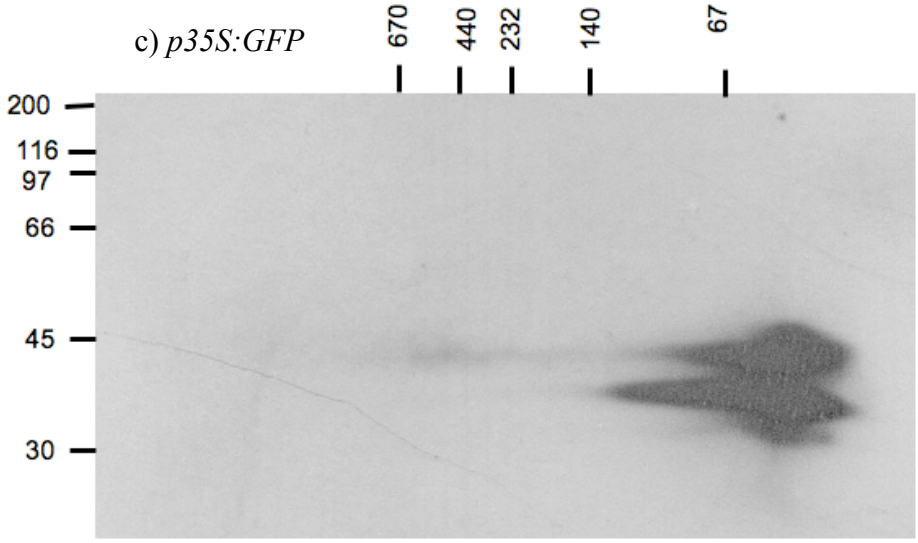

d) *p35S:AtPEN2:GFP*

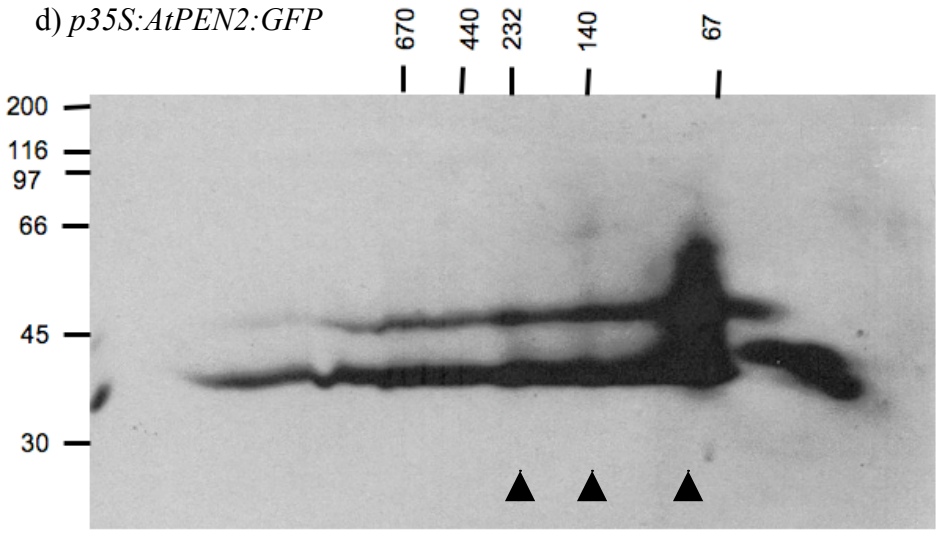

e) *p35S:AtPS1:GFPc*

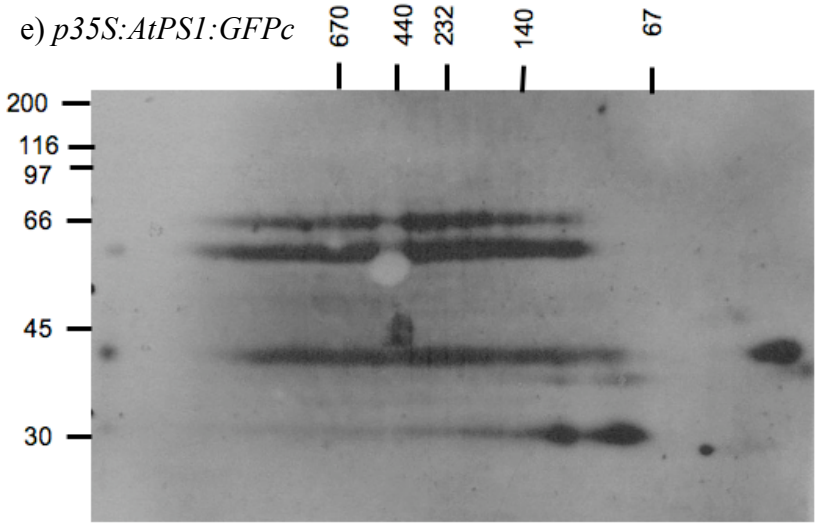

5.5. The AtPEN2:GFP HMW complexes observed in vegetative tissue do not contain AtNCT or AtAPH1

To investigate the potential members of the high molecular weight complexes seen in BN-PAGE western blots with AtPEN2:GFP, crosses were performed between RW350 (*p35S:AtPEN2:GFP*) and the transcriptional null mutants *nct2*, *aph1-1* and the double *ps1-1/ps2-3*. PCR genotyping of antibiotic resistant F2 progeny identified homozygous mutants for *nct2* and *aph1-1*, and a double homozygous *ps1-1/ps2-3*, carrying the RW350 transgene. SDS-PAGE western analysis of these lines shows that AtPEN2:GFP is still produced in comparable amounts in *nct2* and *aph1-1* backgrounds, compared to the parental RW350 line (Fig 5.13a). The double *ps1-1/ps2-3* mutant showed a very little accumulation of AtPEN2:GFP, most likely due to the presence of three different T-DNA insertions in these plants.

BN-PAGE western blots with RW350 plants (*p35S:AtPEN2:GFP*) carrying homozygous *nct2* or *aph1-1* mutations produced the high molecular weight bands seen in the parental RW350 line (Fig 5.13b). This leads to the conclusion that the high molecular weight complexes identified do not contain AtNCT or AtAPH1. Confocal microscopy revealed that the punctate distribution seen in wild-type RW350 plants (Fig 5.14a) was also present in lines carrying mutations in other members of the putative γ-secretase complex (Fig 5.14b).

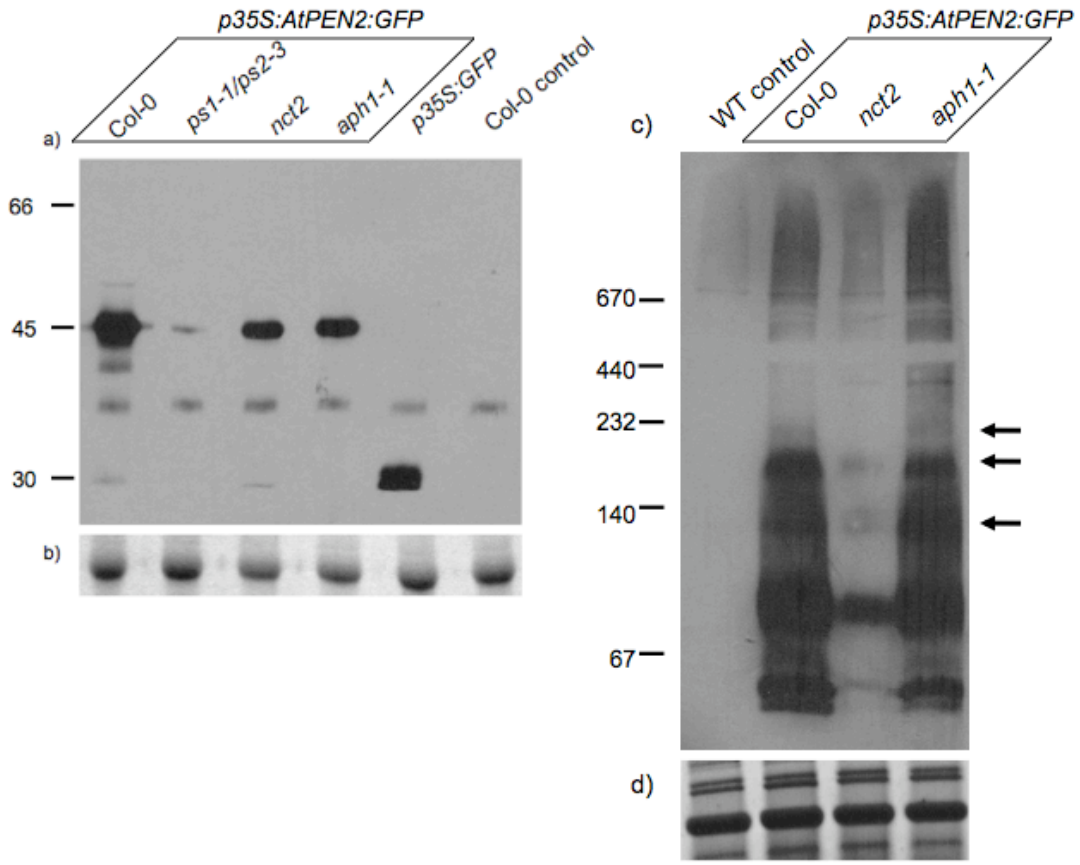

Fig 5.13 AtPEN2:GFP exists in HMW complexes in the absence of AtNCT or AtAPH1.

(a) SDS-PAGE western with α-GFP primary antibody, showing protein accumulation in *p35S:AtPEN2:GFP* lines carrying mutations in other members of the putative *Arabidopsis* γ-secretase complex. *p35S:AtPEN2:GFP* in Col-0 background shown signal for AtPEN2:GFP at 45 kDa. *p35S:AtPEN2:GFP* in *ps1-1/ps2-3*, *nct2* and *aph1-1* backgrounds show a lower accumulation of AtPEN2:GFP protein. Controls of free GFP and untransformed Col-0 were included. Size markers in kDa are indicated on left.

(b) Coomassie stained gel showing large RUBISCO subunit as loading controls for (a).

(c) BN-PAGE western with α-GFP primary antibody, showing the HMW complexes (indicated by arrows) in the *p35S:AtPEN2:GFP* in Col-0 background, are also present in lines downregulated for *AtNCT* (*nct2* background) and *AtAPH1* (*aph1-1* background). Untransformed Col-0 wild type does not show any α-GFP cross-reactive species.

(d) Coomassie stained gel showing RUBISCO complex as loading controls for (c).

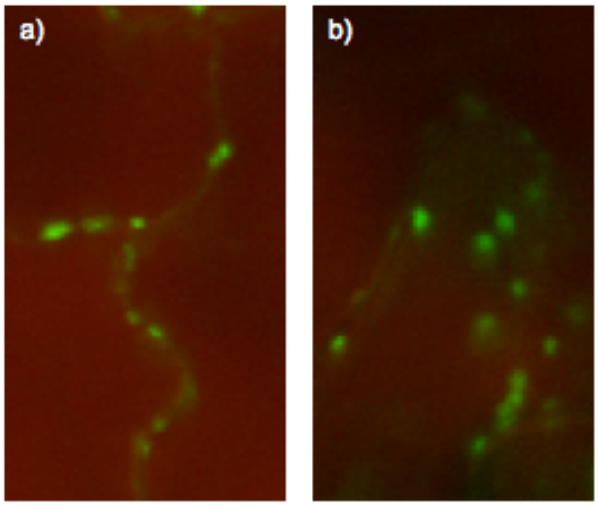

Fig 5.14 Punctate distribution of AtPEN2:GFP is present in a line downregulated for *AtAPH1*. Confocal microscopy revealed the characteristic punctate distribution of AtPEN2:GFP in Col-0 background (a) is still present in a line carrying an *aph1-1* homozygous insertion (b). Images were acquired at the same magnification.

5.6. AtPS1:GFPc stability may depend on the presence of AtNCT and AtAPH1

AtPS1:GFPc holoprotein, and the potential cleaved C-terminus, is visible on western blots in extractions from young siliques (Fig 5.15, lane 2). Crosses were performed between RW349 (*p35S:PS1:GFPc*) and *nct2* and *aph1-1*, to look at the stability of AtPS1:GFPc in the absence of other members of the putative γ-secretase complex in *Arabidopsis*. Homozygous mutants for *nct2* and *aph1-1* were identified from lines carrying the *p35S:AtPS1:GFPc* transgene, along with wild type segregating lines. Seed generated from these lines weregerminated and grown for 5 weeks on soil, and protein extracted from young siliques and analysed by western blot (Fig 5.15).

Less AtPS1:GFPc protein is present in the lines carrying homozygous mutations in both *nct2* (Fig 5.15 lane 5) and *aph1-1* (Fig 5.15 lane 3), suggesting that either the transcription is downregulated or the protein is destabilised under these conditions. cDNA synthesis with RNA extracted from siliques has not been possible by methods I have tried in the lab, possibly due to contamination with polysaccharides (Vicient and Delseny, 1999), although steps were take to limit the amount of carbohydrates in all RNA extractions. Due to this, testing the transcription level of *AtPS1:GFPc* in silique tissue was not possible.

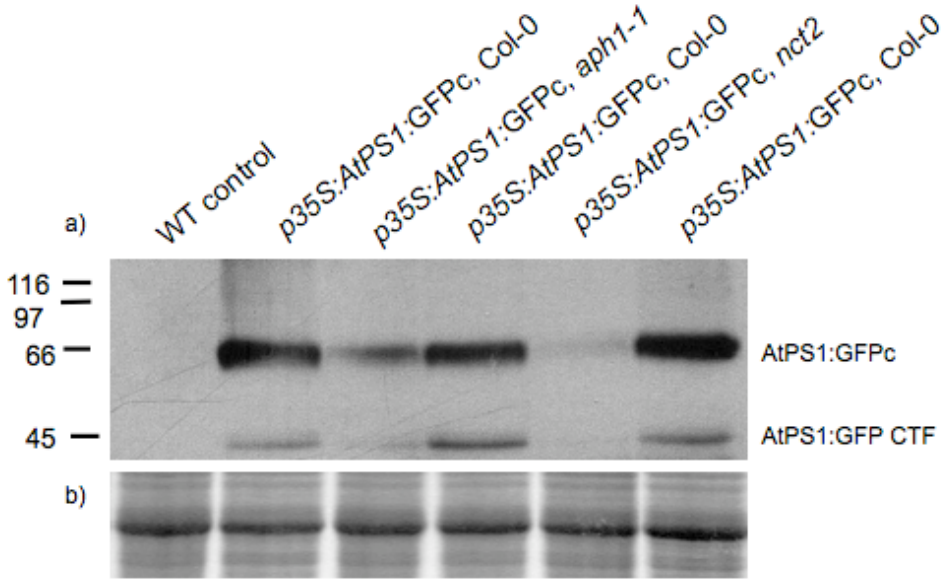

Fig 5.15 Lack of AtNCT or AtAPH1 potentially destabilises AtPS1:GFP in siliques. RW349 (*p35S:AtPS1:GFPc*) was crossed to mutant lines *nct2* and *aph1-1*, and homozygous insertional lines identified in the subsequent generations. Plants carrying the *p35S:AtPS1:GFPc* transgene were grown on soil for 5 weeks and protein extracted from young developing siliques.
(a) Western blot probed with α-GFP primary antibody. Untransformed Col-0 wild type control does not show any signal. Parental *p35S:AtPS1:GFPc* (RW349) line shows signal at ~66 kDa (AtPS1:GFPc) and ~45 kDa (CTF AtPS1:GFPc). RW349 in *aph1-1* homozygous background shows a lower protein accumulation compared to that of the wild type background. RW349 in *nct2* homozygous background shows an even lower protein accumulation compared to the *aph1-1* background. Size markers in kDa are indicated on left.
(b) Coomassie stained gel showing large RUBISCO subunit as loading controls for (a).

5.7. Summary and Conclusions

A great amount of work went into producing the 2A peptide constructs, in the hope that they could be used to provide evidence for, or against, a γ-secretase complex in *Arabidopsis*. Although 2A peptide constructs have been used in other studies in *Arabidopsis*, efficient cleavage of the 2A peptide did not occur here. I was not able to make all of the individually tagged versions for each protein, due to the length of time it would have taken to produce and test so many transgenic plant lines, so whether or not the low protein abundance seen here is due to my construction of the

2A peptide constructs themselves, or intrinsic problems with the proteins is not clear. If these tagged protein lines were to be produced, pair-wise combinations could be crossed to determine the presence or absence in the HMW complexes seen for AtPEN2:GFP and AtPS1:GFPc. Although, due to the presence of AtPEN2:GFP HMW complexes in *AtNCT* and *AtAPH1* downregulated lines, this may be redundant.

This is the first time our lab has employed the BN-PAGE and 2D BN/SDS-PAGE techniques described here. For this reason, there is still a problem with inconsistent results, possibly due to the protein samples being loaded. A high level of background signal is detected on western blots produced from BN-PAGE gels. This may be due to the polyclonal α-GFP antibody or α-sheep secondary, however switching to a commercially available (Invitrogen) monoclonal α-GFP primary (and α-mouse secondary) did not produce any signal whatsoever. Again, for this reason, it would be useful to have produced lines with individual proteins tagged with the small epitope tags.

The BN-PAGE western blots described here were all carried out with extracts form 10-day-old seedlings. Siliques, or more accurately developing seeds, definitely contain more AtPS1:GFPc protein than seedlings, so protein extracts from siliques should produce more signal on BN-PAGE westerns. Trials with protein extracted from siliques, like that used in Figure 5.15 for AtPS1:GFPc, were unsuccessful on native gels. This is possibly due to overloading of protein onto the gel, something that could be remedied with time to run further gels.

6.0. Substrate identification

6.1. Introduction

Numerous substrates of the γ-secretase complex have been identified in animal systems, most notable being NOTCH and APP (Table 6.1). NOTCH is involved in nearly every stage of animal development; the two main functions being restriction of cell fates in multipotent cell lines, and specification of cell fates and creating boundaries (reviewed in Lai, 2004). The Aβ peptide is released from the AMYLOID-β-PRECURSOR PROTEIN (APP), following β- and γ-secretase cleavages. APP has a number of cellular functions, including neuronal differentiation, transcriptional regulation and cell adhesion (reviewed in (Thinakaran and Koo, 2008). Depending on the cleavage site of γ-secretase, Aβ40 or Aβ42 is produced, with Aβ42 being the major constituent of the plaques formed in the brains of Alzheimer's disease patients (Miller et al., 1993; Iwatsubo et al., 1994), caused by the C-terminus of Aβ42 acting as a 'seed' for aggregation (Yan and Wang, 2006).

Other γ-secretase substrates of note include cell adhesion proteins CD44 (Okamoto et al., 2001), N- and E-cadnerins (Marambaud et al., 2003; Park et al., 2008), the NOTCH ligand DELTA (Six et al., 2003), and the receptor tyrosine kinase ErbB4 (Sardi et al., 2006), and many others (Table 6.1). The substrate specificity for γ-secretase is not clearly (if at all) defined, with most of the substrates identified through systematic searches for the protease activity responsible for the cleavage of a protein of interest. Although many of the intracellular domains (ICDs) released following γ-secretase cleavage have assigned signalling properties, there are a number that seem to do nothing, earning γ-secretase the nickname 'proteasome of the membrane' (Kopan and Ilagan, 2004).

Substrate	Functions	ICD in nucleus
APP	Cell adhesion and migration	Yes
APPL1, 2	Cell adhesion and migration	Yes
NOTCH 1-4	Cell specification during development	Yes
DELTA	Notch ligand	Yes
JAGGED	Notch ligand	Yes
ErbB-4	Growth factor receptor tyrosine kinase	Yes
NRG-1	ErbB ligand	Yes
EphB2	Neurogenesis, angiogenesis receptor tyrosine kinase	ND
EphrinB1, B2	Ligand for Eph receptors	Yes
CSF-1R	Cell proliferation receptor tyrosine kinase	Yes
LAR	Neyronal receptor protein tyrosine phosphatase	Yes
RPTP	Cell adhesion receptor protein tyrosine phosphatase	Yes
E-cadherin	Epidermal cell adhesion	No
N-cadherin	Neuronal cell adhesion	No
Pcdh	Cadherin-related adhesion protein	Yes
CD44	Cell adhesion and tumour growth	Yes
NRADD	Apoptosis in neuronal cells	Yes
GHR	Growth hormone receptor	Yes
SorLA	Intracellular sorting and trafficking of cargo proteins	Yes

Table 6.1 A selection of γ-secretase substrates in animals. Many intracellular domains (ICDs) are found in the nucleus following cleavage by γ-secretase (for EphB2, it has not been determined (ND) as no experimental evidence is available). Information adapted from Wakabayashi and De Strooper (2008) and references therein.

A recent study was carried out to clarify the issue of substrate specificity that, while identifying new substrates and shedding some light on substrate specificity, also raised new questions (Hemming et al., 2008). Chimeric proteins formed of known γ-secretase substrates and other (non-substrate) type-I transmembrane proteins were employed to test the need for ectodomain shedding (Fig 6.1). Fusion of non-substrate ectodomain to substrate TMD and ICD did not lead to cleavage by γ-secretase, most likely due to the lack of ectodomain shedding. The reciprocal experiment (substrate ectodomain fused to non-substrate TMD and ICD) allowed ectodomain shedding, cleavage of the TMD by γ-secretase and subsequent release of the ICD, suggesting that ectodomain shedding is a sufficient signal for γ-secretase recognition. Further experiments using truncated proteins resembling the native protein following ectodomain shedding (a lumenal stump, TMD and ICD) produced different results. The truncated substrate protein was cleaved by γ-secretase, however the truncated non-substrate was not, showing that an extracellular stump is not sufficient signal for γ-secretase cleavage, and other physical properties of the substrate must be recognised by γ-secretase. Although the truncated non-substrate was not processed by γ-secretase, it was physically associated with the complex, as shown by immunoprecipitation with γ-secretase complex members, using antibodies directed towards the ICD of the truncated non-substrate. This did not occur when full-length non-substrate was used, showing that the extracellular non-substrate stump is recognised, but not processed by γ-secretase.

Fusion of the substrate lumenal stump to non-substrate TMD and ICD was not a substrate, but the reciprocal fusion protein was. Therefore, the amino acid sequence of the lumenal stump is not recognised specifically by γ-secretase. An interesting role of the TMD was revealed by the fusion of non-substrate stump and TMD to the ICD of a substrate protein, as this fusion was not a substrate for γ-secretase. The reciprocal fusion of substrate stump and TMD to the ICD of non-substrate protein was not a substrate for γ-secretase either. This provides further evidence that γ-secretase has more specificity than simply recognising lumenal stumps, but ectodomain shedding can by-pass this specificity.

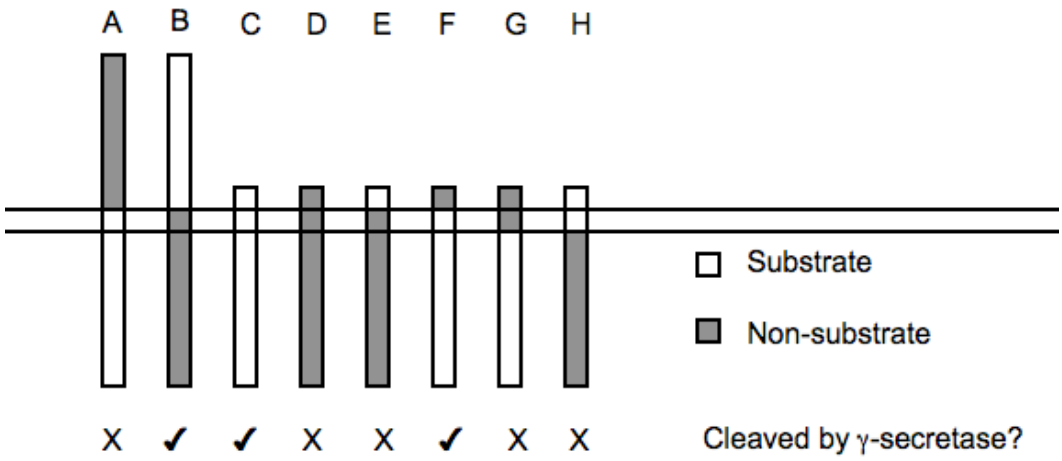

Fig 6.1 Substrate specificity of γ-secretase. Protein constructs were expressed in HEK293 cells to test the substrate specificity of γ-secretase using VASORTIN (VAS, a known substrate; white) and INTEGRIN (INT, non-substrate; grey). Fusion of INT ectodomain to the TMD and ICD of VAS was shown not to be a substrate (A), however the reciprocal fusion protein was a substrate (B), likely due to ectodomain shedding of B but not of A. A truncated version of VAS, resembling the native protein following ectodomain shedding, was sufficient to become a γ-secretase substrate (C). A similar version of INT was not a substrate (D), showing that ectodomain shedding is not sufficient for cleavage by γ-secretase. Fusion of the lumenal stump of VAS to the TMD and ICD of INT was not a substrate (E). The reciprocal protein fusion was a substrate (F), revealing that if the TMD and ICD of a substrate are present, the lumenal stump sequence is irrelevant. This does not extend to just the ICD (G) or stump and TMD of VAS (H). Adapted from Hemming *et al*. (2008).

Of all the γ-secretase substrates identified in animal systems to date, none are conserved in *Arabidopsis*. During my research into the putative *Arabidopsis* γ-secretase complex, it was assumed that any phenotypes associated with the homozygous transcriptional null mutants identified would provide a starting point in the search for *Arabidopsis* substrates. As this was not the case (due to lack of gross morphological phenotypes), other methods of substrate identification were explored. Here, I describe immunoprecipitation, yeast-two-hybrid and 2D differential in gel electrophoresis experiments used to identify potential substrates.

6.2. ACR4 is not cleaved in a PRESENILIN dependent fashion in Arabidopsis

The receptor-like kinase (RLK) *Arabidopsis* CRINKLY4 (ACR4) is expressed during embryo development and continues to be expressed throughout plant growth, where it is restricted to the epidermal L1 layer of apical meristems and young developing organs (Gifford et al., 2003). ACR4 is a type I membrane protein, with an essential extracellular domain and a functional cytosolic kinase domain, which localises to the plasma membrane (Gifford et al., 2005). Previous research in our lab with a functional ACR4:GFP fusion protein revealed that ACR4 undergoes cleavage at or near the TMD, leading to the suspicion of an I-Clip being involved in signalling by ACR4. When total protein was extracted from inflorescence meristems of plants expressing ACR4:GFP under its native promoter (*pACR4:ACR4:GFP*) and subjected to western blot with an α-GFP primary antibody, a number of bands are seen (Fig 6.2 lane2). Full length ACR4:GFP is estimated at 125 kDa, however this is not seen on the western blot. The intracellular domain of ACR4 (from amino acid 455 to the C-terminus) is estimated at 50 kDa, when combined with GFP gives ~87 kDa, which is the approximate size of the highest band on the western blot. This was hypothesised to be a product of cleavage of the TMD of ACR4.

A line expressing *pACR4:ACR4:GFP* was crossed into the double *ps1-1*/*ps2-3* mutant, to study the effect of the putative *Arabidopsis* γ-secretase complex on ACR4 cleavage. Plants segregating in the F_2 generation were genotyped for the *ps1-1* and *ps2-3* insertions, and a double homozygous mutant plant was identified, carrying *pACR4:ACR4:GFP*. Total protein was extracted from inflorescence meristems from plants in the subsequent generation, and tested on a western blot with α-GFP primary antibody (Fig 6.1, lane3). The bands in the mutant are essentially identical to that of the parental line, showing that the PRESENILINs of *Arabidopsis* (and therefore the putative γ-secretase complex) are not responsible for the cleavage of ACR4.

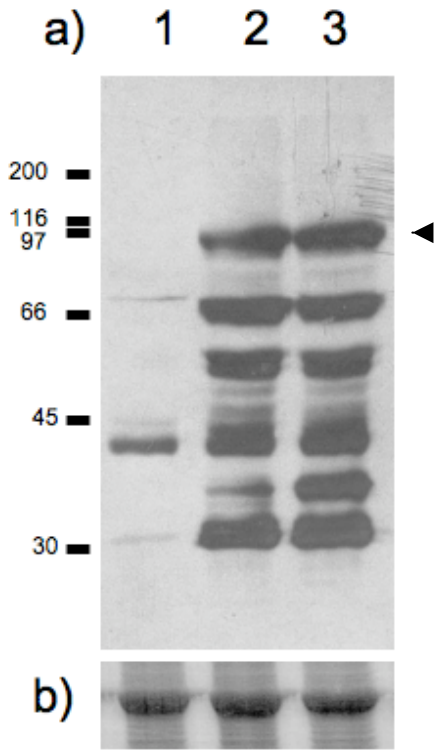

Fig 6.2 The putative γ-secretase complex in *Arabidopsis* is not involved in ACR4 processing. Protein was extracted from inflorescences of plants to look at the processing of ACR4:GFP in a *ps1-1/ps2-3* background. (a) Western blot using an α-GFP primary antibody. Lane 1: Col-0 control. Lane 2: Plants expressing ACR4:GFP (*pACR4:ACR4:GFP*). Lane 3: Double homozygous mutant plant produced following a *pACR4:ACR4:GFP* x *ps1-1/ps2-3* cross. Arrowhead indicates the ~87 kDa band mentioned in text as being a cleavage product of ACR4:GFP. Size markers in kDa are indicated on left.
(b) Coomassie stained gel showing large RUBISCO subunit as loading controls for (a).

6.3. Immunoprecipitation of GFP fusion proteins

Animal substrates of the γ-secretase complex can be immunoprecipitated with the intact complex. GFP binding protein covalently linked to Sepharose beads was available in the lab (a gift from Dr. H. Leonhardt; Rothbauer et al., 2008). This was used for immunoprecipitations with plants stably expressing AtPEN2:GFP and AtPS1:GFP. Total protein was extracted from 10-day-old seedlings into ice-cold Tris-buffered saline (TBS; 50 mM Tris pH7.5, 150 mM NaCl) supplemented with 0.1 % TritonX-100 and protease inhibitor cocktail. Following sedimentation of insoluble material, the supernatant was incubated with GBP-Sepharose for 1 hour. Beads were recovered and washed three times in TBS, and proteins eluted in 1x protein loading dye (see Materials and Methods). A portion of the IP was tested on a western blot to check if the GFP fusion proteins were present in the sample. As seen in Figure 6.3(a), AtPEN2:GFP is present, but no signal for AtPS1:GFP is detectable. Samples were separated on SDS-PAGE gels that were subsequently silver stained using a commercial kit compatible with mass spectrometry (SilverSnapII, Pierce).

Four bands, detected in the AtPEN2:GFP, sample were deemed specific to this sample (Fig 6.3b). From western blots carried out on the same samples, the bands at 45 kDa and 30 kDa cross-react with an α-GFP antibody, and are AtPEN2:GFP and GFP respectively. The three bands indicated in Figure 6.3(b) were excised from the gel and analysed by mass spectrometry (the 30 kDa GFP band was not included). AtPEN2 was identified from each band, along with a number of common cellular proteins, for example RUBISCO subunits, ACTIN and HSP70 (Table 6.2). None of the other members of the putative *Arabidopsis* γ-secretase complex were identified, likely due to the fact that TritonX-100 has been shown to destabilise the γ-secretase complex during extractions from animal cells (Li et al., 2000a), a fact that was not known to me at the time of the experiments. The IP was carried out with the inclusion of CHAPS as the detergent (shown not to disrupt the γ-secretase complex), however the pull-down was unsuccessful under these conditions, possibly due to an adverse effect of this detergent on the GBP affinity. Other detergents, such as DDM and Digitonin, have been used to solubilise membranes and maintain the γ-secretase complex in its native form. The use of these detergents in immunoprecipitations, along with protein extracts form siliques, could provide a greater understanding of the interactions between the members of the putative *Arabidopsis* γ-secretase complex.

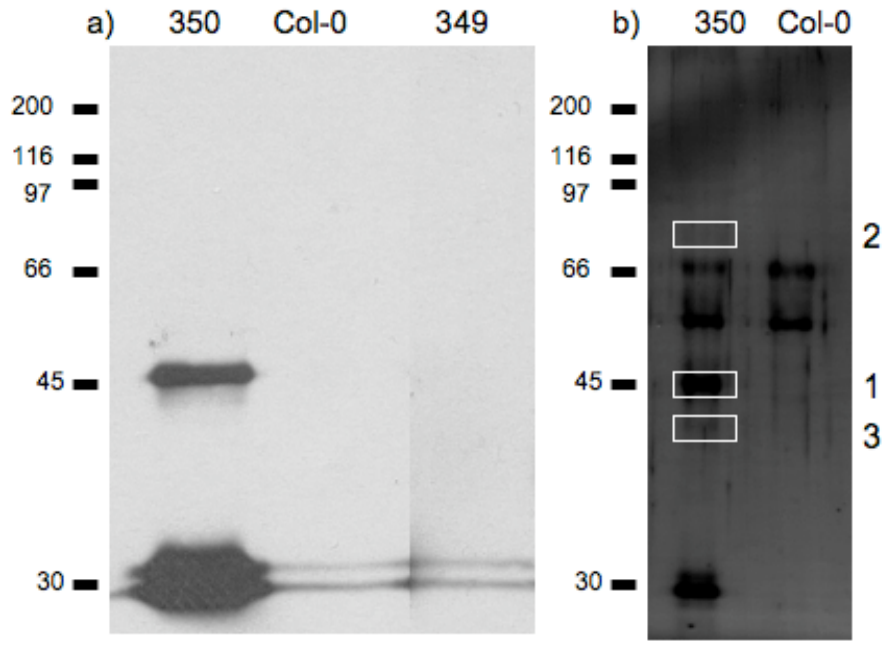

Fig 6.3 Immunoprecipitation of AtPEN2:GFP.
(a) Western blot using an α-GFP antibody. AtPEN2:GFP expressing plants (*p35S:AtPEN2:GFP*) produce signal at 45 kDa and 30 kDa, corresponding to AtPEN2:GFP and GFP respectively. The IP with AtPS1:GFP expressing plants (*p35S:AtPS1:GFPc*) did not produce any signal here.
(b) Silver stained gel of IP from AtPEN2:GFP (*p35S:AtPEN2:GFP*) and wild type Col-0 plants. Immunoprecipitations were eluted from GBP-Sepharose beads in 50 µL 1x protein loading dye at 80 ^{0}C for 5 mins. 5 µL of this was run on a 12 % gel. After silver staining, bands indicated (1-3) were excised and frozen prior to processing for MS.
Size markers in kDa are indicated on left.

Band 1 - Protein Description	Mass	Peptides
Ribulose bisphosphate (RUBISCO)	**52347**	**10**
Actin-7 (Actin-2)	**41937**	**7**
Glutamine synthetase	**47780**	**7**
Gamma-secretase subunit PEN2-like protein	**16535**	**3**
Photosystem II 44 kDa reaction center protein	**52063**	**2**
Actin-2	42078	1

Band 2 - Protein Description	Mass	Peptides
Heat shock cognate 70 kDa protein 1	**71712**	**14**
Luminal-binding protein 1 precursor (BiP1)	**73869**	**3**
Ribulose bisphosphate carboxylase (RUBISCO)	**52347**	**3**
Gamma-secretase subunit PEN2-like protein	**16535**	**2**
Probable rhamnose biosynthetic enzyme 1	**75837**	**2**
Heat shock cognate 70 kDa protein 3 (Hsc70.3)	71559	1

Band 3 - Protein Description	Mass	Peptides
Probable arginase	**38071**	**6**
ATP synthase gamma chain 1	**41171**	**2**
Protochlorophyllide reductase B	**43560**	**2**
Nitrilase 1	38553	1
Gamma-secretase subunit PEN2-like protein	16535	1
Glyceraldehyde-3-phosphate dehydrogenase A	42748	1

Control - Protein Description	Mass	Peptides
5-methyltetrahydropteroyltriglutamate--homocysteine methyltransferase	**84646**	**7**
Ribulose bisphosphate carboxylase (RUBISCO)	**53435**	**2**
Delta 1-pyrroline-5-carboxylate synthetase A	**78110**	**2**
Ribulose bisphosphate carboxylase (RUBISCO)	52347	1
Myrosinase precursor	61664	1

Table 6.2 MS results from AtPEN2:GFP immunoprecipitation. Bands 1-3 correspond to those excised from a silver stained gel (indicated in Fig 6.3b). Many "housekeeping" proteins were identified, such as ACTIN and RUBISCO subunits. AtPEN2 was identified in every sample, excluding the control (cut from a portion of gel not showing staining).

6.4. Split-Ubiquitin yeast-two-hybrid assay for potential substrates and binding partners

Commonly used yeast-two-hybrid (Y2H) assays fuse the protein of interest (bait) to the DNA-binding domain of GAL4, and prey proteins to the GAL4 activation domain (reviewed in (Ratushny and Golemis, 2008). Interactions between bait and

prey promote transcription of reporter genes, allowing growth on media lacking certain amino acids (histidine (SD-His), and for greater stringency both histidine and alanine (SD-His-Ade)). This system works for soluble cytosolic proteins, or fragments of such, however it is less useful for intrinsic membranous proteins. A newer version of the Y2H assay involves the use of split-Ubiquitin (Stagljar et al., 1998). The C-terminal half of Ubiquitin, along with an artificial transcription factor (Cub-LexA-VP16) is fused to the bait, with the N-terminal half (Nub) fused to the prey. A modified Nub (NubG, so-called due to a isoleucine to glycine substitution) is used in the screening vector, which does not naturally interact with Cub, instead requiring the two halves to be brought into close proximity by protein-protein interactions between bait and prey. Following interaction between bait and prey, Ub is reconstituted and recognised by a Ub-specific protease, causing release of the transcription factor, which translocates to the nucleus and regulates expression of reporter genes, as in the original Y2H system. Using this system, interactions between membrane proteins can effectively be detected. See Figure 6.4 for a work flow diagram of the Y2H process from selection of prey constructs to interactor confirmation.

Primers were designed to amplify *AtPS1* and *AtPS2* to incorporate *Sfi*I restriction sites in-frame for cloning into the Y2H vectors pBTB-STE and pBR3-N (Dualsystems Biotech). pBTB-STE contains the STE2 leader sequence, to improve translation of the bait, and incorporates Cub-LexA-VP16 at the C-terminus of the bait. Both *AtPS1* and *AtPS2* were inserted into pBTB-STE (pRW321 and pRW370 respectively) and transformed into the yeast reporter strain NMY51. Experiments were carried out to look for auto-activation of reporter genes, by transformation of lines harbouring pRW321 or pRW370 with the control vectors pAI-Alg5 and pDL2-Alg5. pAI-Alg5 contains a protein (full-length Alg5) fused to the unmodified NubI, and due to NubI's native affinity for Cub acts as a positive interaction for any Cub fusion that is properly integrated into the membrane. Both pRW321 and pRW370 produced the correct response (growth on media lacking His and Ade). pDL2-Alg5 is essentially the same protein fusion as that in pAI-Alg5, however it contains NubG, and so acts as a negative interaction marker. pRW370 produced the correct response

when transformed with pDL2-Alg5 (on growth on media lacking His and Ade), but pRW321 showed growth on this media, meaning that this construct produces auto-activation of the reporter genes and is therefore of no use in a Y2H screen.

Reports emerged about the topology of the PRESENILINs, with a change from the C-terminus being cytosolic to it being embedded in the membrane (Spasic et al., 2006). Following this it was decided to change the bait Y2H from pBTB-STE, to pBT3-N, which causes LexA-VP16-Cub to be fused to the N-terminus of the bait protein. *AtPS1* and *AtPS2* were cloned into pBT3-N, using the *Sfi*I restriction site, to produce pRW389 and pRW390 respectively. Following transformation into NMY51, both vectors showed the correct growth responses with pAI-Alg5 (positive) and pDL2-Alg5 (negative) on selective media. Growth of yeast containing pRW389 or pRW390 was comparable to the control vector, pCCW-Alg5 (a bait vector containing full-length Alg5 fused to Cub-LexA-VP16), showing that the AtPS1/2 fusion proteins were not damaging to yeast health. Large-scale transformations were carried out to test the transformation efficiency, prior to transformation with the plasmid library. Transformation efficiency ranged from $5x10^4$ to $2x10^5$ colony forming units per gram of DNA (cfu/g), up to a factor of ten out from the recommended efficiency of $1.5x10^6$ to $2.5x10^6$. Following advice given in the DUALmembrane handbook, the library transformation was carried out twice for each bait (AtPS1 and AtPS2) using the commercially produced *Arabidopsis* library (Dualsystems). A number of colonies were found growing on selective media following transformation of pRW389 and pRW390 with the plasmid library, however all of these were false positives as they could also produce colonies when transformed along with empty pBT3-N vector. Although no interacting proteins were identified through this Y2H screen, this may be due to the lack of other members of the putative γ-secretase complex in yeast.

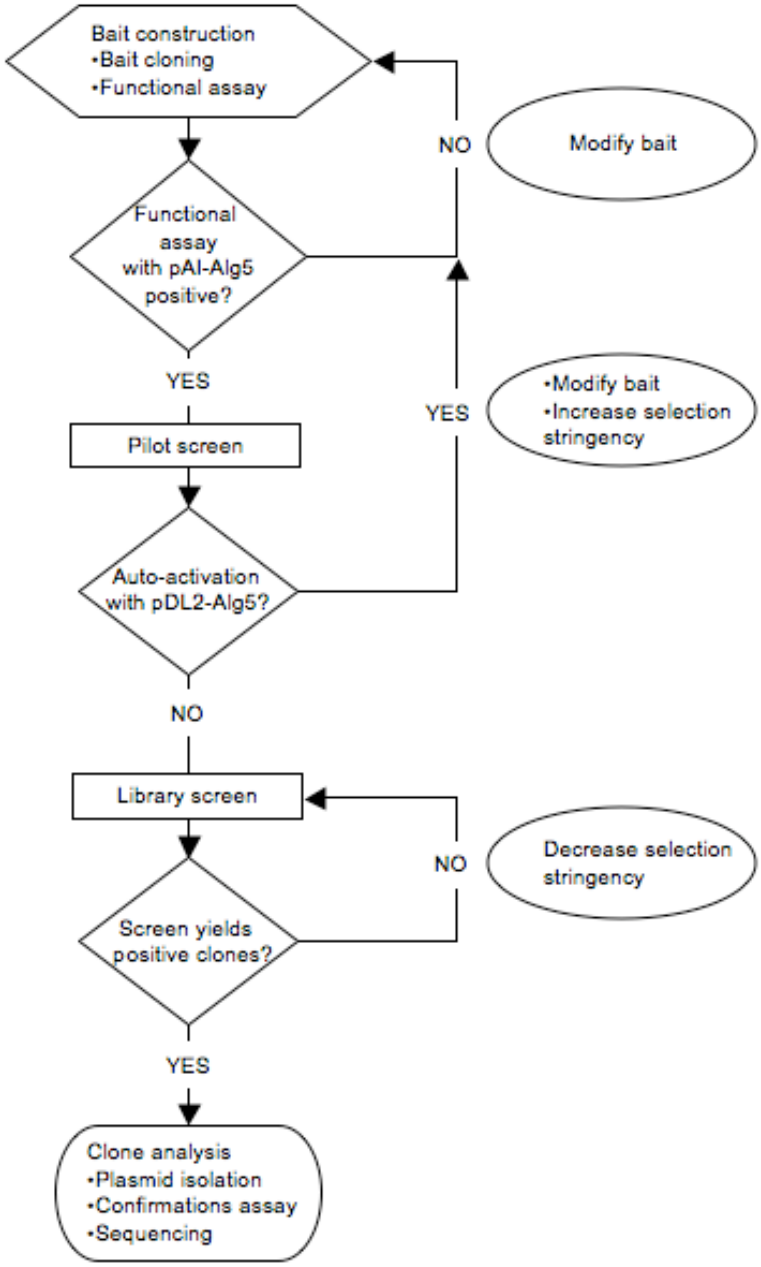

Fig 6.4 Workflow diagram for Y2H screen. pAI-Alg5 contains full length Alg5 fused to unmodified NubI, causing a positive response even in the absence of interaction between bait and prey, and allows confirmation of expression and correct localisation of the bait. If growth is not seen with pAI-Alg5 on selective media, the bait may not be expressed, or inserted into the membrane in the incorrect orientation, and either modification of the bait plasmid or increase of selection stringency is required. Selection can be carried out on SD-His, SD-His supplemented with 3-AT, or for the highest stringency SD-His-Ade. pDL2-Alg5 contains the mutated NubG, fused to full length Alg5, and acts as a negative control as the bait should not specifically interact with Alg5. Growth on selective media of yeast containing pDL2-Alg5 and bait plasmid means that the bait is auto-activating, possibly due to overexpression or cleavage of the bait protein, and modification of the bait plasmid is required. Following selection of positive interactors from a screen, the prey plasmid is recovered from the yeast and tested for auto-activation, through growth on selective media with an empty bait vector.

6.5. Two-dimensional differential in gel electrophoresis as a tool to identify potential γ-secretase substrates in Arabidopsis

Two-dimensional differential in gel electrophoresis (2D DIGE) is a relatively new tool that can be used to study differences in protein amounts at the proteome level (Unlu et al., 1997; Marouga et al., 2005). The basic principal of 2D electrophoresis involves separation of protein samples, first according to charge using an isoelectric focusing strip (IEF), followed by weight on a SDS-PAGE gel. In order to determine a difference between individual samples using 2D electrophoresis, multiple gels must be run for each sample and the task of identifying spots that have changed between these gels is very labour intensive. The biggest advantage of 2D DIGE is that up to three samples can be applied to the same gel, making differences in protein amount readable directly from the gel. To allow this, the protein samples must be pre-labelled with fluorescent dyes. Three dyes are commercially available, Cy2, Cy3 and Cy5 (Amersham), allowing an internal standard to be run with the two samples, depending on the type of labelling taking place. Minimal labelling of a single lysine residue in a protein is possible with all three CyDyes, however only a small proportion of the total protein sample is labelled, resulting in the need for a greater amount of protein to be loaded to the gel. Saturation labelling is only possible with Cy3 and Cy5, which are covalently attached to every cysteine residue present in each protein in the sample. The greater ratio of dye to protein in saturation labelling allows detection of spots even when small amounts of protein have been loaded. In this experiment, saturation labelling was used as it was suspected that any changes in protein amounts would be small, due to the lack of obvious phenotype in the double mutant line.

Protein samples are pre-labelled with the relevant CyDye, mixed and applied to the first dimension IEF strip. Following the second dimension SDS gel, the protein spots are detected by excitation of the fluorescent dye at the particular frequency for that dye, and a digital image recorded. The digital images can be accurately compared through specific software to identify protein spots that have changed in size, mass or charge. Once these spots have been identified, they can be correlated to

spots on a preparatory scale stained 2D gel, allowing excision and analysis by mass spectrometry (MS).

2D DIGE was carried out in an attempt to identify substrates for the putative *Arabidopsis* γ-secretase complex. The double *ps1-1/ps2-3* homozygous mutant was compared to wild-type Col-0. All above ground tissue of plants (Fig 6.5) grown on soil for 5 weeks, after germination on plates, was chosen as the sample material, as this gave a broad range of tissues where *AtPS1* and *AtPS2* are expressed. At the time this experiment was carried out, it was not known about the presence of AtPS1, AtAPH1 and AtNCT protein in siliques (Fig 3.8; Baerenfaller et al., 2008), or the accumulation of AtPS1:GFP in developing seeds (Fig 4.12). Had this been known, the selection of plant tissue would undoubtedly have changed, and been restricted to siliques.

Plants were grown under long day conditions (16 hrs light/8 hrs dark) on soil in a mixed assortment to minimise differences caused by light intensity and humidity. The material was flash frozen in liquid nitrogen, ground to a fine powder and resuspended in precipitation solution (10% trichloroacetic acid (TCA) in acetone, supplemented with 0.07% 2-mercaptoethanol). Proteins were precipitated and pelleted, washed three times with 10 % TCA in acetone (to remove 2-mercaptoethanol) and air-dried. The pellets were resuspended in solubilisation buffer (8 M urea, 2% CHAPS, 30 mM Tris-HCl pH 8.5), and insoluble material removed. The 2D DIGE was performed at the University of York, and included spot analysis and MS identification. Wild type or mutant samples were labelled with Cy3, and the internal standard (a mix of all six samples) with Cy5. First dimension separation was carried out on pH 4-7 IEF strips, as test gels had shown a higher concentration of protein spots within this range. Six gels were prepared, to allow for analysis of three plants of each genotype for statistical analysis, and images were acquired using a Molecular Imager FX Pro (Bio-Rad). SameSpots software (Nonlinear Dynamics) was used to analyse the images and perform statistical tests (one way ANOVA test; Fig 6.6).

Fig 6.5 Choice of plant material for 2D DIGE. Plants were germinated and grown on 0.5x MS plates for 10 days, and transferred to soil to grow for 5 weeks. Total protein was extracted from all above ground tissues of plants, such as that in picture (Col-0 as control and double *ps1-1/ps2-3* mutants). This stage of development was chosen as it provided a good cross-section of tissues that show *AtPS1* and *AtPS2* expression, including rosette and cauline leaves, floral inflorescences, open and closed flowers, developing siliques and maturing seeds.

As suspected, the difference between wild type and mutant samples was small. Nine spots with a statistically significant (p-value less than 0.05) change between wild type and mutant were identified. In addition, spots with the highest fold difference (although not statistically significant) were included. All but one of the spots were lower in the mutant compared to wild type, and for this reason, the wild type sample was chosen to run on the preparatory gels. Staining with Coomassie Brilliant Blue is less sensitive than the fluorescent dyes used in 2D DIGE, and not all spots were visible in the prepatory gels. Loading more protein does not compensate for the shortcomings of Coomassie Blue, as the higher concentration of protein in the IEF strip leads to smearing. In total, 14 protein spots were picked and identified by MS, including eight with a statistically significant change and six with the greatest fold difference (Fig 6.7, Table 6.3, Table 6.4).

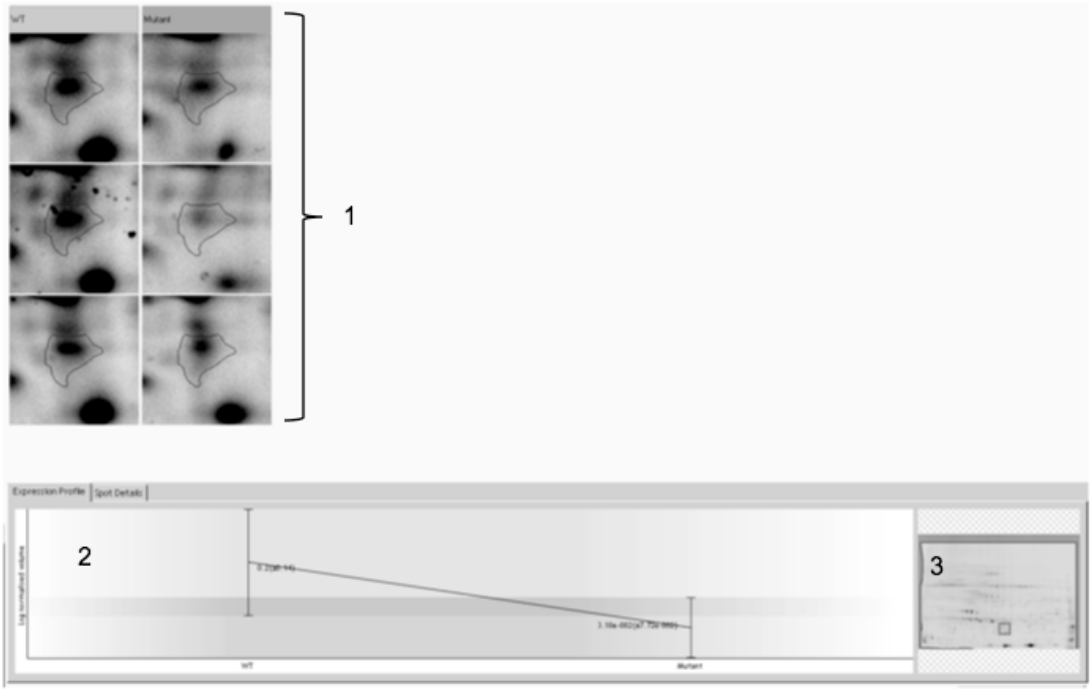

Fig 6.6 Example of screen shot from SameSpots analysis program for spot 62. Shown are (1) enlarged pictures of the spot from each wild type and mutant plant, (2) graphical change in spot volume and (3) position on 2D gel.

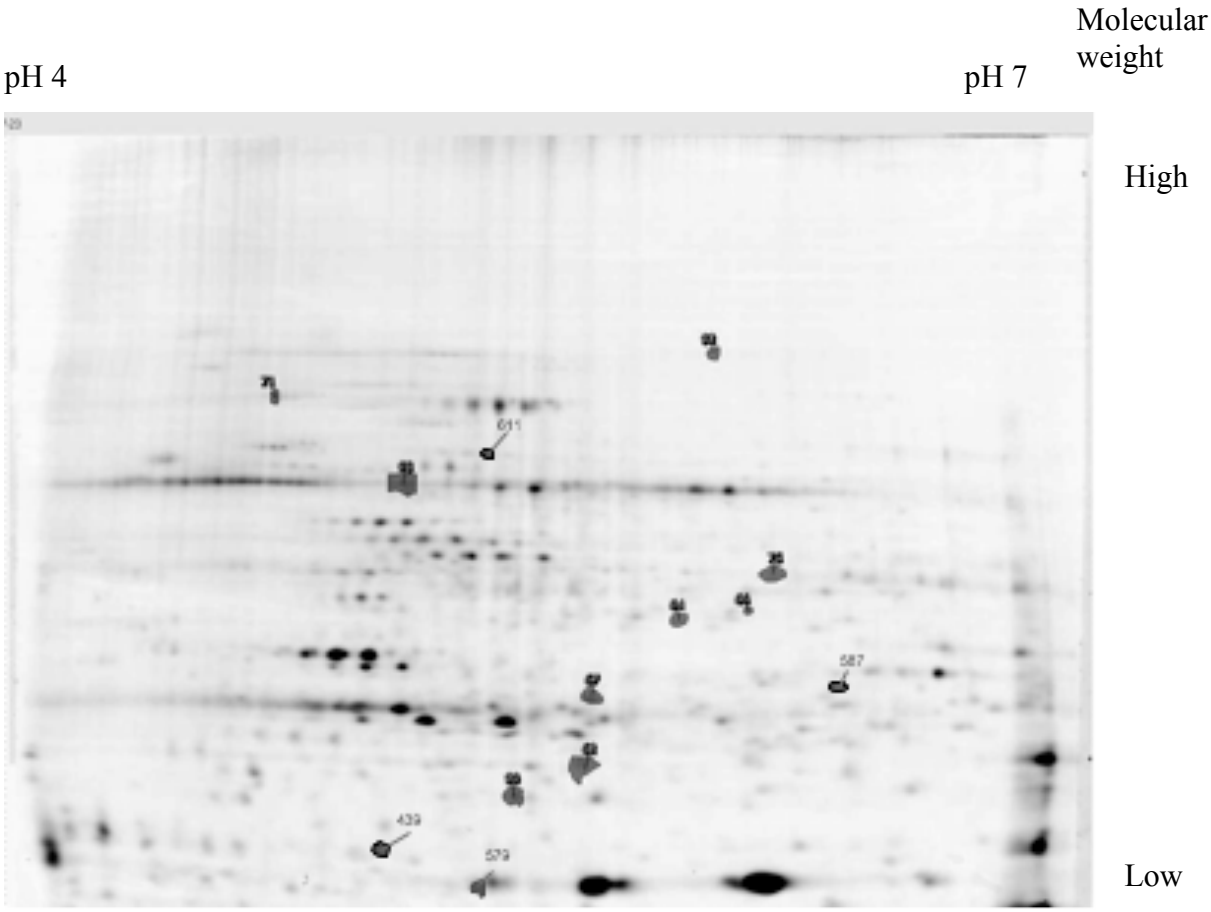

Fig 6.7 2D DIGE gel, stained with Coomassie Blue. Spots indicated were picked and identified by MS. pH gradient of first dimension IEF strip runs from left to right (4-7).

Spot	Protein	Gene number	Mw (Da)	pI	ANOVA (p)	Fold
62	AtGLP3	At5g20630	21,836	6.77	0.0329	1.5
64	MDC1	At1g04410	35,570	6.51	0.0349	1.5
66	MDC1	At1g04410	35,570	6.51	0.0198	1.5
67	GILT	At4g12960	26,081	7.53	0.034	1.4
71	CPHSPC70-1	At4g24280	76,507	4.81	0.042	1.4
75	Aldolase	At3g52930	38,540	6.41	0.0266	1.4
90	CSD2	At2g28190	22,244	7.02	0.0472	1.3
93	RBCL	AtCg00490	52,955	6.24	0.00756	1.3
439	CSD1	At1g08830	15,078	5.38	0.468	1.7
456	GAPC1	At3g04120	36,914	7.15	0.0557	1.7
579	RBCS1A	At1g67090	20,216	7.83	0.0907	1.5
587	CRA1	At5g44120	52,595	7.88	0.128	1.5
611	Chaperonin	At3g13470	63,341	5.4	0.0633	-1.5
676	CSP41A	At3g63140	43,929	8.74	0.202	1.4

Table 6.3 Proteins identified by MS following 2D DIGE. Theoretical molecular weight (in Daltons) and isoelectric point (pI) are included. ANOVA p-value represents the statistical significance of difference in spot. A value of 0.05 or lower was used as the threshold in this case. Fold refers to the difference between wild type and mutant, with a positive number meaning that the protein is more abundant in wild type.

Spot	Protein	Function	Expression profile
64/66	MDC1	Production of malate from pyruvate	Ubiquitous expression and protein accumulation
71	CPHSPC70-1	Response to cold and protein folding (chloroplast)	Ubiquitous expression and protein accumulation
75	FBA	Putative fructose-bisphosphate aldolase	Ubiquitous expression and protein accumulation
90	CSD2	Formation of H_2O_2 form peroxide radicals (chloroplast)	Ubiquitous expression and protein accumulation
93	RUBISCO large	Carbon dioxide fixation (chloroplast)	Ubiquitous expression and protein accumulation
439	CSD1	Formation of H_2O_2 form peroxide radiacals	High expression in leaves. Protein found in cotyledons, leaves and roots
456	GAPC1	Involved in glycolysis, and potentially ROS signalling	Ubiquitous expression and protein accumulation
579	RUBISCO small	Carbon dioxide fixation (chloroplast)	Ubiquitous expression and protein accumulation
611	Chaperonin	Involved in protein folding	Expression highest in rosette leaves. Ubiquitous protein accumulation
676	CSP41A	Involved in rRNA maturation (chloroplast)	Ubiquitous expression and protein accumulation
62	AtGLP3	Germin-like protein. Unknown function	Highest expression in young leaf organs, pedicels and petioles. Protein accumulation universal
67	GILT	Putative thio-reductase	High expression in developing siliques. Protein restricted to siliques
587	CRA1	Seed nutrient reserve protein	Expression in late seed development. Protein only found in seeds

Table 6.4 Proteins identified by MS following 2D DIGE. Functions taken from TAIR entries for each locus, expression from e-FP browser and protein accumulation from AtProteome.

Most of the proteins identified had a ubiquitous expression profile and encode "housekeeping" proteins with known functions, such as enzymes, chaperones and RUBISCO. However, three of them either showed a limited expression profile or had no known function: AtGLP3, GILT and CRA1.

Spot 62 AtGLP3 (At5g20630)

GERMIN-LIKE PROTEIN 3, a member of a group of proteins with similarity to the GERMIN subfamily of cupins. The cupin super-family contains a range of proteins with a β-barrel and His-containing motifs (Dunwell et al., 2001). It is one of the most diverse protein families and includes, among others, seed storage proteins. GERMIN is an oxalate oxidase, which releases H_2O_2, used in cell wall restructuring and potentially in plant defence (Carter et al., 1998). However, a study of AtGLP1 to 3 showed that these proteins lacked any oxalate oxidase activity (Membre et al., 2000). *AtGLP3* is expressed in various areas throughout *Arabidopsis*, with high expression seen in cotyledons, juvenile leaves, leaf primordia, pedicels and petioles. The protein is, however, present in siliques, and has been shown to undergo S-nitrosylation following infection by *Pst* avrB in leaves (Romero-Puertas et al., 2008). Expression of *AtGLP3* follows a circadian rhythm, with the peak occurring at the start of the night (Staiger et al., 1999).

Little is known about the function of AtGLP3 apart from its circadian rhythm of expression and S-nitrosylation after infection by *Pst* avrB. During previous experiments looking for phenotypes of insertional mutants of the members of the putative *Arabidopsis* γ-secretase complex, plants (including the double *ps1-1/ps2-3* mutant) were challenged with *Pst* avrB, however no difference was seen between wild type and any of the mutants.

Spot 67 GILT (At4g12960)

GAMMA-INTERFERON INDUCIBLE LYSOSOMAL THIOL REDUCTASE family protein, an enzyme capable of catalysing the reduction of disulphide bonds. The founding member of this family was identified following its upregulation by treatment of a monocyte cell line with gamma-interferon (γ-INF; Luster et al., 1988),

and GILTs have been found in a wide range of species (Phan et al., 2001). In humans, GILT is located in the lysosome, as it works best at an acidic pH, unlike cytosolic thiol reductases such as THIOREDOXIN (Arunachalam et al., 2000). The *Arabidopsis* genome contains five GILT family proteins. Expression of *At4g12960* is highest during embryogenesis, during seed stage 3-6, in particular in the seed coat, and is barely expressed in leaves. Protein accumulation is almost exclusive to siliques.

Spot 587 CRA1 (At5g44120)

CRUCIFERIN A1, an 11S globulin seed storage protein. Specific proteins are stored in seeds as a nitrogen source for germinating seedlings (Muntz, 1998). CRA1 is synthesised as a ~50 kDa precursor, but stored processed into a ~30 kDa acidic α-peptide linked to a ~20 kDa basic β-peptide by a single disulphide bond (Dickinson et al., 1989). Receptors in the ER recognise a signal sequence in storage proteins and facilitate transport to protein storage vacuoles (PSVs), where VACUOLAR PRECESSING ENZYME (VPE) cleaves CRA1 into its mature form (Shimada et al., 2003a; Gruis et al., 2004). 11S globulins are stored in stacked hexameric complexes, which is thought to protect from proteases in the vacuole (Jung et al., 1998). Expression of *CRA1* is restricted to late seed development (stage 8-10), in particular to the embryos, and the protein is only found in seeds.

6.6. Examination of a role for the putative Arabidopsis *γ-secretase complex in seed development*

Although the change in CRA1 was out side the statistically significant range (0.128), the result, along with that for At4g12960 (GILT), was quite intriguing due to the discovery of AtPS1, AtAPH1 and AtNCT protein in siliques. Seed weight of double *ps1-1/ps2-3* and *nct2/aph1-1* mutants and Col-0 wild type was measured to look at potential storage protein accumulation deficiency in the mutants. Seed was aliquoted in batches of 100 and accurately weighed. Average weight of seed collected from each mutant did not vary significantly compared to wild type (Fig 6.8).

Experiments were designed to look at germination of mutant seed, compared to wild type, under a variety of conditions. First, germination rate on 0.5xMS with and without sucrose was assessed. Seed from a mutant of each member of the putative *Arabidopsis* γ-secretase complex (*ps1-1, ps2-3, nct2, aph1-1, pen2-2, ps1-1/ps2-3* and *nct2/aph1-1*), GFP fusion lines (RW520, RW350 and RW440) and wild type were surface sterilised and stratified in water at 4 ^{0}C for 48 hrs. Plates were prepared with solid 0.5xMS containing (+) 0.6% sucrose, or lacking (-) additional sugars. Stratified seed (40 per line) were applied to the plates, each with a Col-0 control, and placed in growth chambers at 24 ^{0}C for 64 hrs. Germination rate was scored, however there was no significant difference between any of the lines, with near 100% germination in all cases (Fig 6.9).

Next, germination on media lacking a nitrogen source was investigated. A modified version of 0.5xMS was made without ammonium or potassium nitrates (the nitrogen sources present in MS salts; see Materials and Methods). Forty seeds were germinated on plates lacking nitrogen, sucrose, nitrogen and sucrose, and complete media as a control. Although differences were seen between plants on the different medias, each line behaved the same on individual plates, i.e. no difference was seen between wild type and mutant plants. It would appear that the putative members of the *Arabidopsis* γ-secretase complex have no role in germination of stratified seed.

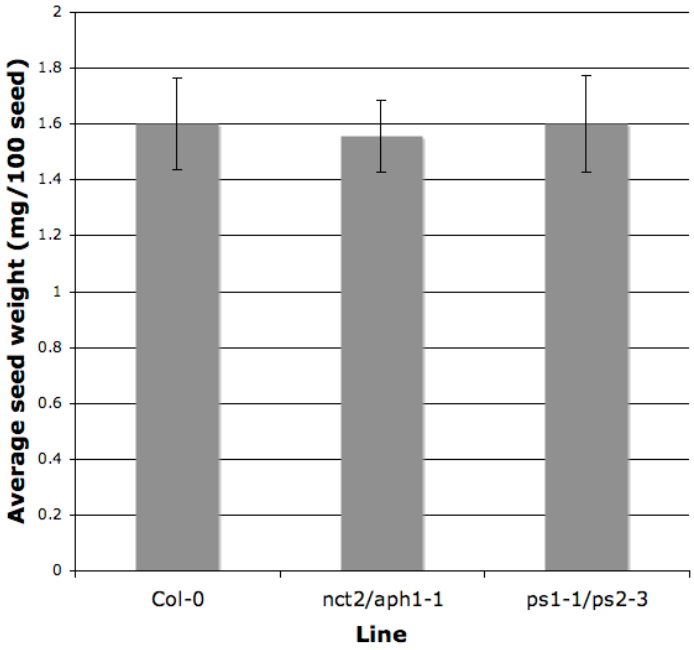

Fig 6.8 Seed of *nct2/aph1-1* and *ps1-1/ps2-3* do not show a significant difference to wild type seed. Average seed weights were measured for 100 seeds per sample (seven repetitions) of each line indicated. Data collected by B. Kümpers.

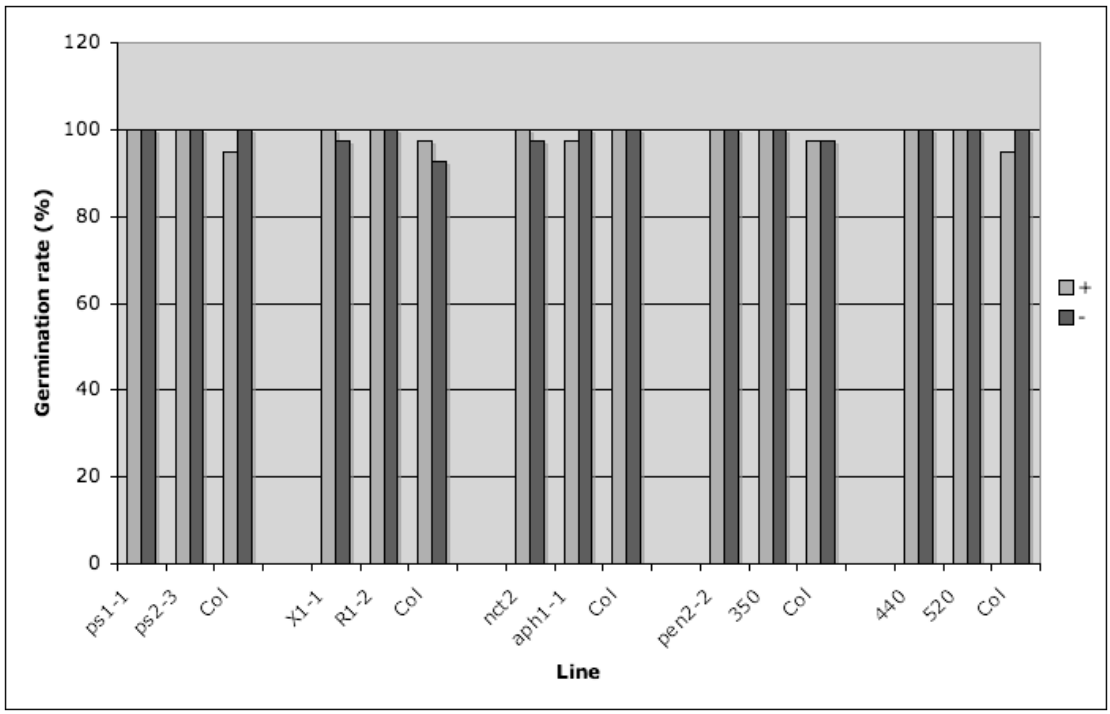

Fig 6.9 Germination rate without sucrose. Forty seeds were stratified and germinated on 0.5xMS with (+) or without (-) sucrose. Germination rate is expressed as a percentage of germinated seedlings to total seed sowed. Each grouping of three represents individual plates, with a Col-0 control. RW350 (*p35S:AtPEN2:GFP*), RW440 (*p35S:AtNCT:GFP*) and RW349 (*p35S:AtPS1:GFP*).

The above germination experiments were carried out on fully matured, ripe seeds. Alonso-Blanco *et al*. (2003) identified seven QTLs (quantative trait loci) that affect after-ripening requirement of seeds (defined as the number of days of dry storage required for 50% of seeds to germinate), from crosses between *Arabidopsis* accessions with low (Landsbreg *erecta*; L*er*) and high dormancy (Cape Verde Islands; Cvi). Two of these QTLs, *DOG2* and *DOG4* (for *DELAY OF GERMINATION*) map to similar regions as *AtPS2* and *AtPEN2* respectively. Initial experiments (carried out by B. Kümpers and G. Ingram) into germination of *ps1-1/ps2-3, nact2/aph1-1* and *pen2-2* seed, have revealed a potential role in the need for after-ripening requirements. Ripe seed was harvested from non-senescing plants, and stored in air permeable bags for a number of days after harvest (DAH) prior to testing for germination efficiency. There has been an inconsistent germination rate for the double mutants compared to wild type (Fig 6.10). Col-0 shows a gradual increase in germination efficiency 0% at 4 DAH, to ~50% at 9 DAH and finally >90% at 15 DAH. Although *ps1-1/ps2-3* and *nact2/aph1-1* show the low germination efficiency at 4 DAH, their germination efficiency at 9 and 15 DAH is widely variable. At 9 DAH *ps1-1/ps2-3* seed had between 10 and 70% germination efficiency and *nct2/aph1-1* seed had between 0 and 100%, while at the same time point Col-0 seed had lower variability (40 to 60%). The problem with such experiments is the low dormancy of the Col-0 background of the mutant lines. Further investigation into this is needed, possibly by introgression of the mutations in the putative γ-secretase complex members into a high dormancy background, such as Cvi.

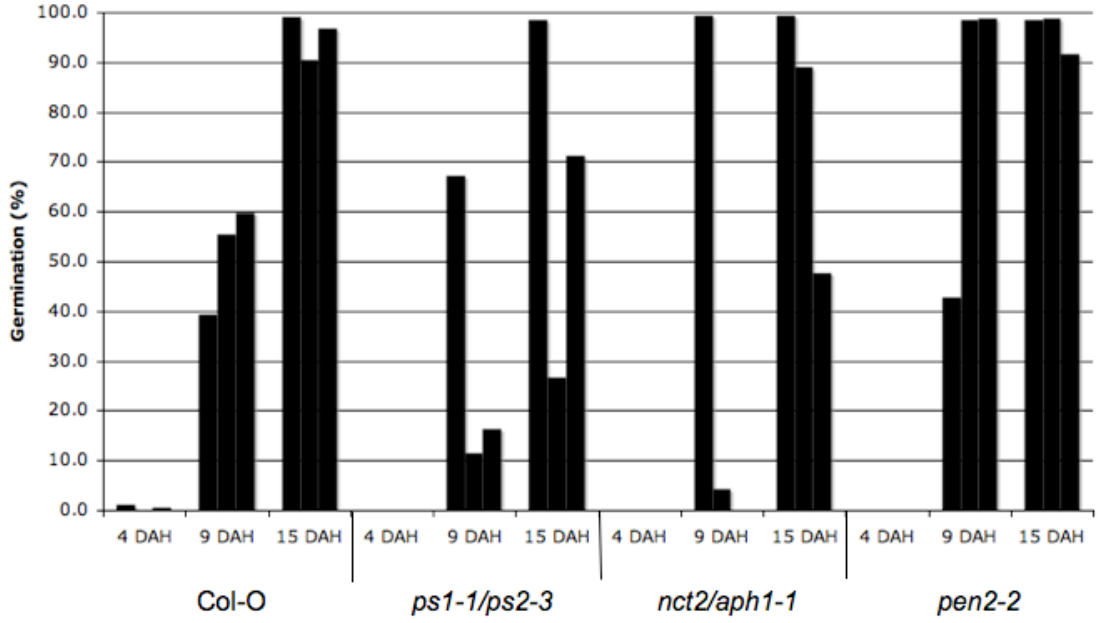

Fig 6.10 Initial results indicate that *ps1-1/ps2-3* and *nct2/aph1-1* double mutants show greater heterogeneity in after-ripening than wild type. Fresh seed was collected from non-senescing plants and stored in air permeable bags. Germination efficiency was tested at various time points days after harvest (4, 9 and 15 DAH). At each time point, three replicates were carried out. Individual samples were taken from pools of seed collected from independent trays of plants, grown under the same conditions. Data collected by G. Ingram.

6.7. Summary and Conclusions

Although this search for *Arabidopsis* γ-secretase substrates has not produced any specific proteins, it has produced some intriguing lines of investigation. Further work is needed with GFP fusion protein pull-downs, to not only find substrates, but also to identify other proteins in complexes with AtPEN2 and AtPS1. Use of other detergents, such as Digitonin, would enable solubilisation of membranes while maintaining the HMW complexes seen in BN-PAGE gels (Fig 5.11). DDM is another choice of detergent that could be employed, but altering the concentration of DDM has been shown to disrupt the γ-secretase complex. AtPS1:GFP accumulates to far greater levels in silique tissues, compared to seedlings. It follows that using

silique extracts for AtPS1:GFP pull-downs would have a greater chance of producing results. Given enough time and resources, IPs from silique extracts could be prepared and eluted in a native state, applied to 2D BN/SDS-PAGE gels and silver stained, allowing MS analysis of proteins within the HMW complexes seen for AtPEN2:GFP and AtPS1:GFP.

Potentially, the 2D DIGE experiment could be repeated with proteins extracted exclusively form siliques, however due to the cost associated with this approach it was not possible to pursue this line of investigation. Further investigation into the variability in germination efficiencies of *ps1-1/ps2-3* and *nact2/aph1-1* double mutants is required. These preliminary results for seed after-ripening requiremens suggest that the double mutants tested are sensitive to some environmental factor they were exposed to during seed development. The two *DELAY OF GERMINATION* QTLs (Alonso-Blanco et al., 2003) that map to similar regions as *AtPS2* and *AtPEN2* could be quite interesting. Whether these QTLs are caused by variations in members of the putative *Arabidopsis* γ-secretase complex was impossible to tell here, due to time constraints. The Col-0 ecotype has a low dormancy requirement, making it a useful tool in the lab as numerous generations can be grown in a relatively short time span. This does not help with experiments into seed dormancy. T-DNA insertion libraries are not made in many ecotype backgrounds, such as Cvi, making production of specific knockout mutants in these backgrounds difficult. Introgression of the *ps1-1, ps2-3, nct2, aph1-1* and *pen2-2* mutations into a Cvi background would require a lot of work, due to the numerous generations required to achieve this. Potentially, sequencing of the genomic area surrounding *AtPS2* and *AtPEN2* in the Cvi background could be carried out, to look for variations between this high dormancy and low dormancy (Col-0 and L*er*) ecotypes.

7.0. Discussion

Like the other classes of I-Clips, homologues of PRESENILIN are predicted in the *Arabidopsis* genome, however, until now, no research has been carried out on the potential for *Arabidopsis* to form a γ-secretase complex. The aim of this project was to answer whether presenilin complexes exist in *Arabidopsis*, and what roles they may have.

7.1. A potential role for the Arabidopsis *γ-secretase complex members in seed after-ripening*

Various pieces of evidence, collected throughout my project, have accumulated to indicate a potential role for the *Arabidopsis* components of the γ-secretase complex. Individually, the results are not entirely compelling, but when combined indicate a potential role in seed after-ripening.

The first evidence came from the 2D DIGE experiment, comparing wild type plants to *ps1-1/ps2-3* double mutants. Nine protein spots in total were identified with a statistically significant change between wild type and mutant (Table 6.3). Eight of these could be picked from a stained preparative gel and analysed by MS. Also included were six spots with the greatest fold difference, although they were not statistically significant. Most of the proteins identified had a ubiquitous expression profile, and were "housekeeping" proteins, such as cellular enzymes, chaperones and RUBISCO subunits. A GILT protein is statistically significantly lowered in the mutant. This gene is only expressed in young siliques, and protein accumulation is only seen in the same tissue. The GILT protein (At4g12960) has no known function, but it is predicted to have thiol reductase activity. Another protein whose accumulation was altered, although not reduced by a statistically significant amount, was the nutrient reservoir CRA1 (At5g44120). *CRA1* expression is restricted to siliques, during late seed development. CRA1 is an 11S seed storage protein, and in *Arabidopsis* is the single most abundant protein in dry seeds.

The *Arabidopsis* proteome map (AtProteome) was released towards the end of my project. This contains entries for AtPS1, AtAPH1 and AtNCT (Fig 3.8; AtPS2 and AtPEN2 were not detected). AtNCT peptides were detected in most tissues, with the greatest accumulation in siliques. Peptides from AtPS1 and AtAPH1 were only found in siliques. At this time, plants transformed with *p35S:AtPS1:GFP* had been tested for expression and protein accumulation. The construct was expressed, however very little protein could be detected by western blots and none was visible by confocal microscopy in rosette leaves or seedlings. Developing siliques were tested, and GFP signal could easily be detected by confocal microscopy, potentially in the endosperm (Fig 4.13). AtPS1:GFP was much more abundant on western blots in samples extracted from young siliques, compared to seedling extracts (Fig 4.14). How this tissue specific protein accumulation is achieved is unknown, but could be due to some form of tissue specific translational control. It is known that some signalling events can alter translation rates from specific transcripts, without altering the mRNA level, an example is sucrose mediating ATB2 translation (Rook et al., 1998). In this example, specific leader sequences in the mRNA are required to achieve the sucrose regulation. As the *p35S:AtPS1:GFP* construct contains only the *AtPS1* ORF and not the 5' or 3' UTRs, translational control of this type may not be occurring for *p35S:AtPS1:GFP*. AtPS1:GFP is not degraded by the 26S proteasome in seedlings, as treatment with MG132 does not lead to an increase in AtPS1:GFP levels. However, other agents of protein degradation are available in plant cells, such as the proteases in the vacuole (Muntz, 2007). The genomic *pAtPEN2:AtPEN2g:GFP* construct produced AtPEN2:GFP fusion protein in all tissues of plants. Expression and protein accumulation from a similar construct produced with *AtPS1* could help to study this tissue specific accumulation further.

AtPS1:GFP is specifically accumulated in developing seeds, and *ps1-1/ps2-3* knockout plants accumulate less of the storage protein CRA1 (although this decrease is not statistically significant). To investigate the potential of the putative *Arabidopsis* γ-secretase complex's involvement in seed development and fitness, germination rates were tested. No difference was seen between wild type and the double *ps1-1/ps2-3* or *nct2/aph1-1* mutants on media lacking nitrogen, sucrose and

both nitrogen and sucrose. Therefore, the members of the putative *Arabidopsis* γ-secretase complex do not have a role in germination of stratified seeds. However, initial experiments into the need for seed after-ripening have shown a highly variable germination rate for unstratified seed from *ps1-1/ps2-3* and *nct2/aph1-1* mutants, compared to wild type, when sowed at 9 days after harvest (Fig 6.10). Interestingly, the QTLs *DOG2* and *DOG4*, involved in seed after-ripening requirements (Alonso-Blanco et al., 2003), map to similar regions as *AtPS2* and *AtPEN2* respectively. Gene loci have not been identified for these QTLs. The $DOG2^{Cvi}$ allele confers a decreased requirement for after-ripening, whereas $DOG4^{Cvi}$ has the opposite effect. Perhaps coincidentally, *ps1-1/ps2-3* shows a lower germination efficiency than Col-0 at 9 DAH (hence higher after-ripening requirements) and *pen2-2* shows a higher germination efficiency.

To clarify this, further investigation into seed after-ripening requirements for the *ps1-1, ps2-3, nct2, aph1-1* and *pen2-2* mutant lines is needed, with enough replicates to allow statistical analysis. Unfortunately for these types of experiment, the Col-0 background has a low dormancy requirement, with nearly 100% germination efficiency after only two weeks of after-ripening. Therefore, introduction of the *ps2-3* and *pen2-2* mutations into a background with high dormancy requirement, such as Cvi, could provide a way to study their involvement in seed after-ripening. Also, testing different environmental conditions during seed development (such as light intensity, day length, temperature, and water availability) could be used to identify potential signalling pathways in which the putative *Arabidopsis* γ-secretase complex could be involved.

Seed dormancy and after-ripening requirements are poorly understood due to complex genetic and environmental effects. For this reason, a detailed model for the action of the putative *Arabidopsis* γ-secretase complex is difficult to put forward with the amount of data collected through the course of my project. However, given the potential specific localisation of AtPS1:GFPc in the endosperm of developing seeds, this member of the putative *Arabidopsis* γ-secretase complex could have a role in the GA/abscisic acid (ABA) signalling network during embryogenesis. GA and

ABA are both plant hormones essential for embryogenesis, although they have antagonistic effects on seed dormancy. ABA is a known positive regulator of seed dormancy while GA releases seeds from dormancy and promotes completion of germination, a process that is dependent on and regulated by the endosperm/aleurone layer (Holdsworth et al., 2008). Therefore, a potential role for the putative *Arabidopsis* γ-secretase complex involves modifying a component of a GA or ABA signalling pathway during seed development, and hence altering after-ripening requirements. Two possible outcomes of γ-secretase cleavage could have roles in plant signalling. The first, cleavage of a membrane bound transcription factor to release the TF moiety from the membrane, as in many of the animal γ-secretase dependent pathways. *Arabidopsis* has been shown to contain a number of such membrane bound transcription factors, such as those involved in ER stress signalling (Liu et al., 2008; Iwata et al., 2008) and others that have unassigned functions (Zupicich et al., 2001; Chen Et al., 2008). Secondly, the release of a small "Aβ-like" peptide could be capable of acting as a ligand to a receptor, with similarities to the CLAVATA signalling pathway.

The *Arabidopsis* genome contains genes predicted to encode the components of the γ-secretase complex and at least three of these proteins are produced in siliques. Fusion protein constructs show that AtPEN2:GFP and AtPS1:GFP exist in HMW complexes, which do not necessarily contain other members of the γ-secretase complex AtNCT or AtAPH1. AtPS1:GFP is accumulated to a greater degree in developing seeds than elsewhere in the plant. Although no specific substrates were identified, the *Arabidopsis* γ-secretase complex members may have a role in seed after-ripening requirements. How this is achieved, and if the *Arabidopsis* PRESENILINs/γ-secretase complex is capable of RIP, remains unknown.

Appendix

Tissue samples for development and chemical treatments used in AtGenExpress microarray experiments. Figures 3.5 and 3.6 show graphical representations of the results obtained from such microarray experiments.

Developmental map (Fig 3.5)					
Tissue cluster	tissue	genotype	age	time	treatment
root	roots	Wt	7 days	N/A	N/A
root	roots	Wt	17 days	N/A	N/A
root	root	Wt	15 days	N/A	N/A
root	root	Wt	8 days	N/A	N/A
root	root	Wt	8 days	N/A	N/A
root	root	Wt	21 days	N/A	N/A
root	root	Wt	21 days	N/A	N/A
stem	hypocotyl	Wt	7 days	N/A	N/A
stem	1st node	Wt	21+ days	N/A	N/A
stem	stem, 2nd internode	Wt	21+ days	N/A	N/A
leaf	cotyledons	Wt	7 days	N/A	N/A
leaf	leaves 1 + 2	Wt	7 days	N/A	N/A
leaf	rosette leaf #4, 1 cm long	Wt	10 days	N/A	N/A
leaf	rosette leaf #4, 1 cm long	gl1-T	10 days	N/A	N/A
leaf	rosette leaf # 2	Wt	17 days	N/A	N/A
leaf	rosette leaf # 4	Wt	17 days	N/A	N/A
leaf	rosette leaf # 6	Wt	17 days	N/A	N/A
leaf	rosette leaf # 8	Wt	17 days	N/A	N/A
leaf	rosette leaf # 10	Wt	17 days	N/A	N/A
leaf	rosette leaf # 12	Wt	17 days	N/A	N/A
leaf	rosette leaf # 12	gl1-T	17 days	N/A	N/A
leaf	leaf 7, petiole	Wt	17 days	N/A	N/A
leaf	leaf 7, proximal half	Wt	17 days	N/A	N/A
leaf	leaf 7, distal half	Wt	17 days	N/A	N/A
leaf	leaf	Wt	15	N/A	N/A

			days		
leaf	senescing leaves	Wt	35 days	N/A	N/A
leaf	cauline leaves	Wt	21+ days	N/A	N/A
whole plant	seedling, green parts	Wt	7 days	N/A	N/A
whole plant	seedling, green parts	Wt	8 days	N/A	N/A
whole plant	seedling, green parts	Wt	8 days	N/A	N/A
whole plant	seedling, green parts	Wt	21 days	N/A	N/A
whole plant	seedling, green parts	Wt	21 days	N/A	N/A
whole plant	developmental drift	Wt	21 days	N/A	N/A
whole plant	as above	Wt	22 days	N/A	N/A
whole plant	as above	Wt	23 days	N/A	N/A
whole plant	vegetative rosette	Wt	7 days	N/A	N/A
whole plant	vegetative rosette	Wt	14 days	N/A	N/A
whole plant	vegetative rosette	Wt	21 days	N/A	N/A
apex	shoot apex, vegetative + young leaves	Wt	7 days	N/A	N/A
apex	shoot apex, vegetative	Wt	7 days	N/A	N/A
apex	shoot apex, transition (before bolting)	Wt	14 days	N/A	N/A
apex	shoot apex, inflorescence (after bolting)	Wt	21 days	N/A	N/A
apex	shoot apex, inflorescence (after bolting)	clv3-7	21+ days	N/A	N/A
apex	shoot apex, inflorescence (after bolting)	lfy-12	21+ days	N/A	N/A
apex	shoot apex, inflorescence (after bolting)	ap1-15	21+ days	N/A	N/A
apex	shoot apex, inflorescence (after bolting)	ap2-6	21+ days	N/A	N/A
apex	shoot apex, inflorescence (after bolting)	ufo-1	21+ days	N/A	N/A
apex	shoot apex, inflorescence (after bolting)	ap3-6	21+ days	N/A	N/A
apex	shoot apex, inflorescence (after bolting)	ag-12	21+ days	N/A	N/A

flowers	flowers stage 9	Wt	21+ days	N/A	N/A
flowers	flowers stage 10/11	Wt	21+ days	N/A	N/A
flowers	flowers stage 12	Wt	21+ days	N/A	N/A
flowers	flower stage 12	clv3-7	21+ days	N/A	N/A
flowers	flower stage 12	lfy-12	21+ days	N/A	N/A
flowers	flower stage 12	ap1-15	21+ days	N/A	N/A
flowers	flower stage 12	ap2-6	21+ days	N/A	N/A
flowers	flower stage 12	ufo-1	21+ days	N/A	N/A
flowers	flower stage 12	ap3-6	21+ days	N/A	N/A
flowers	flower stage 12	ag-12	21+ days	N/A	N/A
flowers	flowers stage 15	Wt	21+ days	N/A	N/A
flowers	flower	Wt	28 days	N/A	N/A
floral organs	flowers stage 15, pedicels	Wt	21+ days	N/A	N/A
floral organs	flowers stage 12, sepals	Wt	21+ days	N/A	N/A
floral organs	flowers stage 15, sepals	Wt	21+ days	N/A	N/A
floral organs	flowers stage 12, petals	Wt	21+ days	N/A	N/A
floral organs	flowers stage 15, petals	Wt	21+ days	N/A	N/A
floral organs	flowers stage 12, stamens	Wt	21+ days	N/A	N/A
floral organs	flowers stage 15, stamen	Wt	21+ days	N/A	N/A
floral organs	mature pollen	Wt	6 wk	N/A	N/A
floral organs	flowers stage 12, carpels	Wt	21+ days	N/A	N/A
floral organs	flowers stage 15, carpels	Wt	21+ days	N/A	N/A
seeds	siliques, w/ seeds stage 3	Wt	8 wk	N/A	N/A
seeds	siliques, w/ seeds stage 4	Wt	8 wk	N/A	N/A
seeds	siliques, w/ seeds stage 5	Wt	8 wk	N/A	N/A
seeds	seeds, stage 6	Wt	8 wk	N/A	N/A
seeds	seeds, stage 7	Wt	8 wk	N/A	N/A
seeds	seeds, stage 8	Wt	8 wk	N/A	N/A
seeds	seeds, stage 9	Wt	8 wk	N/A	N/A

seeds	seeds, stage 10	Wt	8 wk	N/A	N/A
Chemical stresses (Fig 3.6)					
tissue cluster	tissue	genotype	age	time	treatment
baseline wt	seedling	Col	N/A	0.5 h	H2O
baseline wt	seedling	Col	N/A	1 h	H2O
baseline wt	seedling	Col	N/A	3 h	H2O
baseline wt	seedling	Col	N/A	0.5 h	10uM ABA
baseline wt	seedling	Col	N/A	1 h	10uM ABA
baseline wt	seedling	Col	N/A	3 h	10uM ABA
baseline wt	seedling	Col	N/A	0.5 h	10uM ACC
baseline wt	seedling	Col	N/A	1 h	10uM ACC
baseline wt	seedling	Col	N/A	3 h	10uM ACC
baseline wt	seedling	Col	N/A	0.5 h	10nM BL
baseline wt	seedling	Col	N/A	1 h	10nM BL
baseline wt	seedling	Col	N/A	3 h	10nM BL
baseline wt	seedling	Col	N/A	0.5 h	1uM GA
baseline wt	seedling	Col	N/A	1 h	1uM GA
baseline wt	seedling	Col	N/A	3 h	1uM GA
baseline wt	seedling	Col	N/A	0.5 h	1uM IAA
baseline wt	seedling	Col	N/A	1 h	1uM IAA
baseline wt	seedling	Col	N/A	3 h	1uM IAA
baseline wt	seedling	Col	N/A	0.5 h	1uM MJ
baseline wt	seedling	Col	N/A	1 h	1uM MJ
baseline wt	seedling	Col	N/A	3 h	1uM MJ
baseline wt	seedling	Col	N/A	0.5 h	1uM zeatin
baseline wt	seedling	Col	N/A	1 h	1uM zeatin
baseline wt	seedling	Col	N/A	3 h	1uM zeatin
substances_I	seedling	Col	N/A	3 h	H2O
substances_I	seedling	Col	N/A	12 h	H2O
substances_I	seedling	Col	N/A	3 h	10uM Brz91
substances_I	seedling	Col	N/A	12 h	10uM Brz91
substances_I	seedling	Col	N/A	3 h	10uM Brz220
substances_I	seedling	Col	N/A	12 h	10uM Brz220
substances_I	seedling	Col	N/A	3 h	10uM paclobutrazol
substances_I	seedling	Col	N/A	12 h	10uM paclobutrazol
substances_I	seedling	Col	N/A	3 h	1uM PNO8
substances_I	seedling	Col	N/A	12 h	1uM PNO8
substances_I	seedling	Col	N/A	3 h	10uM propiconazole
substances_I	seedling	Col	N/A	12 h	10uM propiconazole

substances_I	seedling	Col	N/A	3 h	10uM prohexadione
substances_I	seedling	Col	N/A	12 h	10uM prohexadione
substances_I	seedling	Col	N/A	3 h	10uM uniconazole
substances_I	seedling	Col	N/A	12 h	10uM uniconazole
substances_II	seedling	Col	N/A	3 h	H2O
substances_II	seedling	Col	N/A	3 h	10uM 2,4,6T
substances_II	seedling	Col	N/A	3 h	10uM AVG (aminoethoxyvinylglycine)
substances_II	seedling	Col	N/A	3 h	10uM AGNO3
substances_II	seedling	Col	N/A	3 h	10uM B9 (daminozide)
substances_II	seedling	Col	N/A	3 h	3uM Brz220
substances_II	seedling	Col	N/A	3 h	10uM cycloheximide
substances_II	seedling	Col	N/A	3 h	1uM ibuprofen
substances_II	seedling	Col	N/A	3 h	10uM MG132
substances_II	seedling	Col	N/A	3 h	10uM NPA
substances_II	seedling	Col	N/A	3 h	10uM PCIB
substances_II	seedling	Col	N/A	3 h	10uM PNO8
substances_II	seedling	Col	N/A	3 h	10uM salicylic acid
substances_II	seedling	Col	N/A	3 h	10uM TIBA
det2_substances	seedling	det2-1	N/A	3 h	H2O
det2_substances	seedling	det2-1	N/A	3 h	1uM 3-dehydroteasterone
det2_substances	seedling	det2-1	N/A	3 h	1uM 3-dehydro-6-deoxoteasterone
det2_substances	seedling	det2-1	N/A	3 h	1uM 6-deoxocastasterone
det2_substances	seedling	det2-1	N/A	3 h	1uM 6-deoxocathasterone
det2_substances	seedling	det2-1	N/A	3 h	1uM 6-deoxoteasterone
det2_substances	seedling	det2-1	N/A	3 h	1uM 6-deoxotyphasterol
det2_substances	seedling	det2-1	N/A	3 h	10nM brassinolide
det2_substances	seedling	det2-1	N/A	3 h	10uM campestanol
det2_substances	seedling	det2-1	N/A	3 h	100nM castasterone
det2_substances	seedling	det2-1	N/A	3 h	1uM cathasterone
det2_substances	seedling	det2-1	N/A	3 h	1uM teasterone
det2_substances	seedling	det2-1	N/A	3 h	1uM typhasterol
det2-1 / BL	seedling	det2-1	N/A	0.5 h	H2O
det2-1 / BL	seedling	det2-1	N/A	1 h	H20
det2-1 / BL	seedling	det2-1	N/A	3 h	H2O
det2-1 / BL	seedling	det2-1	N/A	0.5 h	10nM BL
det2-1 / BL	seedling	det2-1	N/A	1 h	10nM BL
det2-1 / BL	seedling	det2-1	N/A	3 h	10nM BL
ga1-5 / GA	seedling	ga1-5	N/A	0.5 h	H2O
ga1-5 / GA	seedling	ga1-5	N/A	1 h	H2O
ga1-5 / GA	seedling	ga1-5	N/A	3 h	H2O
ga1-5 / GA	seedling	ga1-5	N/A	0.5 h	1uM GA
ga1-5 / GA	seedling	ga1-5	N/A	1 h	1uM GA
ga1-5 / GA	seedling	ga1-5	N/A	3 h	1uM GA
ga1-3 / GA	seeds	ga1-3	N/A	3 h	control

ga1-3 / GA	seeds	ga1-3	N/A	6 h	control
ga1-3 / GA	seeds	ga1-3	N/A	9 h	control
ga1-3 / GA	seeds	ga1-3	N/A	3 h	5um GA
ga1-3 / GA	seeds	ga1-3	N/A	6 h	5um GA
ga1-3 / GA	seeds	ga1-3	N/A	9 h	5um GA
hormone mutants	seedling	Ler	N/A	No h	No
hormone mutants	seedling	ga1-5 (Ler)	N/A	No h	No
hormone mutants	seedling	Ws	N/A	No h	No
hormone mutants	seedling	bri1	N/A	No h	No
zeatin	seedling	Col	N/A	3 h	control
zeatin	seedling	ARR21Cox	N/A	3 h	control
zeatin	seedling	Col	N/A	3 h	control
zeatin	seedling	Col	N/A	3 h	20um zeatin
zeatin	seedling	ARR22ox	N/A	3 h	control
zeatin	seedling	ARR22ox	N/A	3 h	20um zeatin
sulfate starvation	seedling	Col	N/A	2 h	0um sulfate
sulfate starvation	seedling	Col	N/A	4 h	0um sulfate
sulfate starvation	seedling	Col	N/A	8 h	0um sulfate
sulfate starvation	seedling	Col	N/A	12 h	0um sulfate
sulfate starvation	seedling	Col	N/A	24 h	0um sulfate
sulfate starvation	seedling	Col	N/A	0 h	1500um sulfate
sulfate starvation	seedling	Col	N/A	2 h	1500um sulfate
sulfate starvation	seedling	Col	N/A	4 h	1500um sulfate
sulfate starvation	seedling	Col	N/A	8 h	1500um sulfate
sulfate starvation	seedling	Col	N/A	12 h	1500um sulfate
sulfate starvation	seedling	Col	N/A	24 h	1500um sulfate
ABA	seeds	Col	N/A	0 h	No
ABA	seeds	Col	N/A	24 h	No
ABA	seeds	Col	N/A	24 h	3um ABA
ABA	seeds	Col	N/A	24 h	30um ABA
seed imbibition	seeds	Col	N/A	0 h	imbibition
seed imbibition	seeds	Col	N/A	1 h	imbibition
seed imbibition	seeds	Col	N/A	3 h	imbibition
temperature	seeds	Col	N/A	96 h	4^{o}C
temperature	seeds	Col	N/A	96 h	22^{o}C

References

Ades, S.E. (2008). Regulation by destruction: design of the sigmaE envelope stress response. Curr Opin Microbiol **11,** 535-540.

Akiyama, Y., Kanehara, K., and Ito, K. (2004). RseP (YaeL), an Escherichia coli RIP protease, cleaves transmembrane sequences. Embo J **23,** 4434-4442.

Alonso-Blanco, C., Bentsink, L., Hanhart, C.J., Blankestijn-de Vries, H., and Koornneef, M. (2003). Analysis of natural allelic variation at seed dormancy loci of Arabidopsis thaliana. Genetics **164,** 711-729.

Annaert, W., and De Strooper, B. (1999). Presenilins: molecular switches between proteolysis and signal transduction. Trends Neurosci **22,** 439-443.

Aravind, L., and Koonin, E.V. (2000). The U box is a modified RING finger - a common domain in ubiquitination. Curr Biol **10,** R132-134.

Arawaka, S., Hasegawa, H., Tandon, A., Janus, C., Chen, F., Yu, G., Kikuchi, K., Koyama, S., Kato, T., Fraser, P.E., and St George-Hyslop, P. (2002). The levels of mature glycosylated nicastrin are regulated and correlate with gamma-secretase processing of amyloid beta-precursor protein. J Neurochem **83,** 1065-1071.

Arunachalam, B., Phan, U.T., Geuze, H.J., and Cresswell, P. (2000). Enzymatic reduction of disulfide bonds in lysosomes: characterization of a gamma-interferon-inducible lysosomal thiol reductase (GILT). Proc Natl Acad Sci U S A **97,** 745-750.

Azevedo, C., Santos-Rosa, M.J., and Shirasu, K. (2001). The U-box protein family in plants. Trends Plant Sci **6,** 354-358.

Baerenfaller, K., Grossmann, J., Grobei, M.A., Hull, R., Hirsch-Hoffmann, M., Yalovsky, S., Zimmermann, P., Grossniklaus, U., Gruissem, W., and Baginsky, S. (2008). Genome-scale proteomics reveals Arabidopsis thaliana gene models and proteome dynamics. Science **320,** 938-941.

Becker, D. (1990). Binary vectors which allow the exchange of plant selectable markers and reporter genes. Nucleic Acids Res **18,** 203.

Beers, E.P., Jones, A.M., and Dickerman, A.W. (2004). The S8 serine, C1A cysteine and A1 aspartic protease families in Arabidopsis. Phytochemistry **65,** 43-58.

Bengoechea-Alonso, M.T., and Ericsson, J. (2007). SREBP in signal transduction: cholesterol metabolism and beyond. Curr Opin Cell Biol **19,** 215-222.

Bergeron, F., Leduc, R., and Day, R. (2000). Subtilase-like pro-protein convertases: from molecular specificity to therapeutic applications. J Mol Endocrinol **24,** 1-22.

Bergman, A., Hansson, E.M., Pursglove, S.E., Farmery, M.R., Lannfelt, L., Lendahl, U., Lundkvist, J., and Naslund, J. (2004). Pen-2 is sequestered in the endoplasmic reticulum and subjected to ubiquitylation and proteasome-mediated degradation in the absence of presenilin. J Biol Chem **279,** 16744-16753.

Blennow, K., de Leon, M.J., and Zetterberg, H. (2006). Alzheimer's disease. Lancet **368,** 387-403.

Blilou, I., Frugier, F., Folmer, S., Serralbo, O., Willemsen, V., Wolkenfelt, H., Eloy, N.B., Ferreira, P.C., Weisbeek, P., and Scheres, B. (2002). The Arabidopsis HOBBIT gene encodes a CDC27 homolog that links the plant cell cycle to progression of cell differentiation. Genes Dev **16,** 2566-2575.

Blobel, G., and Dobberstein, B. (1975). Transfer of proteins across membranes. I. Presence of proteolytically processed and unprocessed nascent immunoglobulin light chains on membrane-bound ribosomes of murine myeloma. J Cell Biol **67,** 835-851.

Boevink, P., Oparka, K., Santa Cruz, S., Martin, B., Betteridge, A., and Hawes, C. (1998). Stacks on tracks: the plant Golgi apparatus traffics on an actin/ER network. Plant J **15,** 441-447.

Bolte, S., Talbot, C., Boutte, Y., Catrice, O., Read, N.D., and Satiat-Jeunemaitre, B. (2004). FM-dyes as experimental probes for dissecting vesicle trafficking in living plant cells. J Microsc **214,** 159-173.

Bolter, B., Nada, A., Fulgosi, H., and Soll, J. (2006). A chloroplastic inner envelope membrane protease is essential for plant development. FEBS Lett **580,** 789-794.

Brodersen, P., Petersen, M., Pike, H.M., Olszak, B., Skov, S., Odum, N., Jorgensen, L.B., Brown, R.E., and Mundy, J. (2002). Knockout of Arabidopsis accelerated-cell-death11 encoding a sphingosine transfer protein causes activation of programmed cell death and defense. Genes Dev **16,** 490-502.

Brou, C., Logeat, F., Gupta, N., Bessia, C., LeBail, O., Doedens, J.R., Cumano, A., Roux, P., Black, R.A., and Israel, A. (2000). A novel proteolytic cleavage involved in Notch signaling: the role of the disintegrin-metalloprotease TACE. Mol Cell **5,** 207-216.

Brukhin, V., Gheyselinck, J., Gagliardini, V., Genschik, P., and Grossniklaus, U. (2005). The RPN1 subunit of the 26S proteasome in Arabidopsis is essential for embryogenesis. Plant Cell **17,** 2723-2737.

Brunkan, A.L., and Goate, A.M. (2005). Presenilin function and gamma-secretase activity. J Neurochem **93,** 769-792.

Brunkan, A.L., Martinez, M., Walker, E.S., and Goate, A.M. (2005). Presenilin endoproteolysis is an intramolecular cleavage. Mol Cell Neurosci **29,** 65-73.

Callahan, R., and Egan, S.E. (2004). Notch signaling in mammary development and oncogenesis. J Mammary Gland Biol Neoplasia **9,** 145-163.

Callis, J., and Vierstra, R.D. (2000). Protein degradation in signaling. Curr Opin Plant Biol **3,** 381-386.

Campbell, E.A., Tupy, J.L., Gruber, T.M., Wang, S., Sharp, M.M., Gross, C.A., and Darst, S.A. (2003). Crystal structure of Escherichia coli sigmaE with the cytoplasmic domain of its anti-sigma RseA. Mol Cell **11,** 1067-1078.

Campbell, W.A., Iskandar, M.K., Reed, M.L., and Xia, W. (2002). Endoproteolysis of presenilin in vitro: inhibition by gamma-secretase inhibitors. Biochemistry **41,** 3372-3379.

Campos-Ortega, J.A. (1993). Mechanisms of early neurogenesis in Drosophila melanogaster. J Neurobiol **24,** 1305-1327.

Capell, A., Beher, D., Prokop, S., Steiner, H., Kaether, C., Shearman, M.S., and Haass, C. (2005). Gamma-secretase complex assembly within the early secretory pathway. J Biol Chem **280,** 6471-6478.

Capell, A., Grunberg, J., Pesold, B., Diehlmann, A., Citron, M., Nixon, R., Beyreuther, K., Selkoe, D.J., and Haass, C. (1998). The proteolytic fragments of the Alzheimer's disease-associated presenilin-1 form heterodimers and occur as a 100-150-kDa molecular mass complex. J Biol Chem **273,** 3205-3211.

Capron, A., Okresz, L., and Genschik, P. (2003). First glance at the plant APC/C, a highly conserved ubiquitin-protein ligase. Trends Plant Sci **8,** 83-89.

Carter, C., Graham, R.A., and Thornburg, R.W. (1998). Arabidopsis thaliana contains a large family of germin-like proteins: characterization of cDNA and genomic sequences encoding 12 unique family members. Plant Mol Biol **38,** 929-943.

Cervantes, S., Gonzalez-Duarte, R., and Marfany, G. (2001). Homodimerization of presenilin N-terminal fragments is affected by mutations linked to Alzheimer's disease. FEBS Lett **505,** 81-86.

Chen, F., Yu, G., Arawaka, S., Nishimura, M., Kawarai, T., Yu, H., Tandon, A., Supala, A., Song, Y.Q., Rogaeva, E., Milman, P., Sato, C., Yu, C., Janus, C., Lee, J., Song, L., Zhang, L., Fraser, P.E., and St George-Hyslop, P.H. (2001). Nicastrin binds to membrane-tethered Notch. Nat Cell Biol **3,** 751-754.

Chen, G., Bi, Y.R., and Li, N. (2005). EGY1 encodes a membrane-associated and ATP-independent metalloprotease that is required for chloroplast development. Plant J **41,** 364-375.

Chen, Y.N., Salbaugh, E., and Brandizzi, F. (2008). Membrane-tethered transcription factors in Arabidopsis thaliana: novel regulators in stress response and development. Curr Opin Plant Biol **11**, 695-701.

Chinchilla, D., Bauer, Z., Regenass, M., Boller, T., and Felix, G. (2006). The Arabidopsis receptor kinase FLS2 binds flg22 and determines the specificity of flagellin perception. Plant Cell **18,** 465-476.

Cho, S.K., Ryu, M.Y., Song, C., Kwak, J.M., and Kim, W.T. (2008). Arabidopsis PUB22 and PUB23 are homologous U-Box E3 ubiquitin ligases that play combinatory roles in response to drought stress. Plant Cell **20,** 1899-1914.

Chung, H.M., and Struhl, G. (2001). Nicastrin is required for Presenilin-mediated transmembrane cleavage in Drosophila. Nat Cell Biol **3,** 1129-1132.

Chyung, J.H., Raper, D.M., and Selkoe, D.J. (2005). Gamma-secretase exists on the plasma membrane as an intact complex that accepts substrates and effects intramembrane cleavage. J Biol Chem **280,** 4383-4392.

Clough, S.J., and Bent, A.F. (1998). Floral dip: a simplified method for Agrobacterium-mediated transformation of Arabidopsis thaliana. Plant J **16,** 735-743.

Conlon, R.A., Reaume, A.G., and Rossant, J. (1995). Notch1 is required for the coordinate segmentation of somites. Development **121,** 1533-1545.

Cserzo, M., Wallin, E., Simon, I., von Heijne, G., and Elofsson, A. (1997). Prediction of transmembrane alpha-helices in prokaryotic membrane proteins: the dense alignment surface method. Protein Eng **10,** 673-676.

Csorba, T.R. (1991). Proinsulin: biosynthesis, conversion, assay methods and clinical studies. Clin Biochem **24,** 447-454.

Cui, W., Liu, W., and Wu, G. (1995). A simple method for the transformation of Agrobacterium tumefaciens by foreign DNA. Chin J Biotechnol **11,** 267-274.

Daxinger, L., Hunter, B., Sheikh, M., Jauvion, V., Gasciolli, V., Vaucheret, H., Matzke, M., and Furner, I. (2008). Unexpected silencing effects from T-DNA tags in Arabidopsis. Trends Plant Sci **13,** 4-6.

De Strooper, B., Annaert, W., Cupers, P., Saftig, P., Craessaerts, K., Mumm, J.S., Schroeter, E.H., Schrijvers, V., Wolfe, M.S., Ray, W.J., Goate, A., and Kopan, R. (1999). A presenilin-1-dependent gamma-secretase-like protease mediates release of Notch intracellular domain. Nature **398,** 518-522.

DeBose-Boyd, R.A., Brown, M.S., Li, W.P., Nohturfft, A., Goldstein, J.L., and Espenshade, P.J. (1999). Transport-dependent proteolysis of SREBP: relocation of site-1 protease from Golgi to ER obviates the need for SREBP transport to Golgi. Cell **99,** 703-712.

Dharmasiri, N., Dharmasiri, S., and Estelle, M. (2005). The F-box protein TIR1 is an auxin receptor. Nature **435,** 441-445.

Dickinson, C.D., Hussein, E.H., and Nielsen, N.C. (1989). Role of posttranslational cleavage in glycinin assembly. Plant Cell **1,** 459-469.

Doelling, J.H., Yan, N., Kurepa, J., Walker, J., and Vierstra, R.D. (2001). The ubiquitin-specific protease UBP14 is essential for early embryo development in Arabidopsis thaliana. Plant J **27,** 393-405.

Donnelly, M.L., Luke, G., Mehrotra, A., Li, X., Hughes, L.E., Gani, D., and Ryan, M.D. (2001). Analysis of the aphthovirus 2A/2B polyprotein 'cleavage' mechanism indicates not a proteolytic reaction, but a novel translational effect: a putative ribosomal 'skip'. J Gen Virol **82,** 1013-1025.

Downes, B.P., Stupar, R.M., Gingerich, D.J., and Vierstra, R.D. (2003). The HECT ubiquitin-protein ligase (UPL) family in Arabidopsis: UPL3 has a specific role in trichome development. Plant J **35,** 729-742.

Downes, B.P., Saracco, S.A., Lee, S.S., Crowell, D.N., and Vierstra, R.D. (2006). MUBs, a family of ubiquitin-fold proteins that are plasma membrane-anchored by prenylation. J Biol Chem **281,** 27145-27157.

Dunwell, J.M., Culham, A., Carter, C.E., Sosa-Aguirre, C.R., and Goodenough, P.W. (2001). Evolution of functional diversity in the cupin superfamily. Trends Biochem Sci **26,** 740-746.

Edbauer, D., Winkler, E., Haass, C., and Steiner, H. (2002). Presenilin and nicastrin regulate each other and determine amyloid beta-peptide production via complex formation. Proc Natl Acad Sci U S A **99,** 8666-8671.

Edbauer, D., Winkler, E., Regula, J.T., Pesold, B., Steiner, H., and Haass, C. (2003). Reconstitution of gamma-secretase activity. Nat Cell Biol **5,** 486-488.

Edwards, P.A., Tabor, D., Kast, H.R., and Venkateswaran, A. (2000). Regulation of gene expression by SREBP and SCAP. Biochim Biophys Acta **1529,** 103-113.

Escobar, N.M., Haupt, S., Thow, G., Boevink, P., Chapman, S., and Oparka, K. (2003). High-throughput viral expression of cDNA-green fluorescent protein fusions reveals novel subcellular addresses and identifies unique proteins that interact with plasmodesmata. Plant Cell **15,** 1507-1523.

Farmer, E.E., and Ryan, C.A. (1992). Octadecanoid Precursors of Jasmonic Acid Activate the Synthesis of Wound-Inducible Proteinase Inhibitors. Plant Cell **4,** 129-134.

Farmery, M.R., Tjernberg, L.O., Pursglove, S.E., Bergman, A., Winblad, B., and Naslund, J. (2003). Partial purification and characterization of gamma-secretase from post-mortem human brain. J Biol Chem **278,** 24277-24284.

Feng, L., Yan, H., Wu, Z., Yan, N., Wang, Z., Jeffrey, P.D., and Shi, Y. (2007). Structure of a site-2 protease family intramembrane metalloprotease. Science **318,** 1608-1612.

Fluhrer, R., and Haass, C. (2007). Signal peptide peptidases and gamma-secretase: cousins of the same protease family? Neurodegener Dis **4,** 112-116.

Flynn, J.M., Neher, S.B., Kim, Y.I., Sauer, R.T., and Baker, T.A. (2003). Proteomic discovery of cellular substrates of the ClpXP protease reveals five classes of ClpX-recognition signals. Mol Cell **11,** 671-683.

Fraering, P.C., LaVoie, M.J., Ye, W., Ostaszewski, B.L., Kimberly, W.T., Selkoe, D.J., and Wolfe, M.S. (2004). Detergent-dependent dissociation of active gamma-secretase reveals an interaction between Pen-2 and PS1-NTF and offers a model for subunit organization within the complex. Biochemistry **43,** 323-333.

Francis, R., McGrath, G., Zhang, J., Ruddy, D.A., Sym, M., Apfeld, J., Nicoll, M., Maxwell, M., Hai, B., Ellis, M.C., Parks, A.L., Xu, W., Li, J., Gurney, M., Myers, R.L., Himes, C.S., Hiebsch, R., Ruble, C., Nye, J.S., and Curtis, D. (2002). aph-1 and pen-2 are required for Notch pathway signaling, gamma-secretase cleavage of betaAPP, and presenilin protein accumulation. Dev Cell **3,** 85-97.

Fraser, P.E., Levesque, G., Yu, G., Mills, L.R., Thirlwell, J., Frantseva, M., Gandy, S.E., Seeger, M., Carlen, P.L., and St George-Hyslop, P. (1998). Presenilin 1 is actively degraded by the 26S proteasome. Neurobiol Aging **19,** S19-21.

Freeman, M. (2008). Rhomboid proteases and their biological functions. Annu Rev Genet **42,** 191-210.

Friedmann, E., Lemberg, M.K., Weihofen, A., Dev, K.K., Dengler, U., Rovelli, G., and Martoglio, B. (2004). Consensus analysis of signal peptide peptidase and homologous human aspartic proteases reveals opposite topology of catalytic domains compared with presenilins. J Biol Chem **279,** 50790-50798.

Fulop, K., Tarayre, S., Kelemen, Z., Horvath, G., Kevei, Z., Nikovics, K., Bako, L., Brown, S., Kondorosi, A., and Kondorosi, E. (2005). Arabidopsis anaphase-promoting complexes: multiple activators and wide range of substrates might keep APC perpetually busy. Cell Cycle **4,** 1084-1092.

Gagne, J.M., Downes, B.P., Shiu, S.H., Durski, A.M., and Vierstra, R.D. (2002). The F-box subunit of the SCF E3 complex is encoded by a diverse superfamily of genes in Arabidopsis. Proc Natl Acad Sci U S A **99,** 11519-11524.

Garcia-Lorenzo, M., Sjodin, A., Jansson, S., and Funk, C. (2006). Protease gene families in Populus and Arabidopsis. BMC Plant Biol **6,** 30.

Ge, X., Dietrich, C., Matsuno, M., Li, G., Berg, H., and Xia, Y. (2005). An Arabidopsis aspartic protease functions as an anti-cell-death component in reproduction and embryogenesis. EMBO Rep **6,** 282-288.

Gifford, M.L., Dean, S., and Ingram, G.C. (2003). The Arabidopsis ACR4 gene plays a role in cell layer organisation during ovule integument and sepal margin development. Development **130,** 4249-4258.

Gifford, M.L., Robertson, F.C., Soares, D.C., and Ingram, G.C. (2005). ARABIDOPSIS CRINKLY4 function, internalization, and turnover are dependent on the extracellular crinkly repeat domain. Plant Cell **17,** 1154-1166.

Glotzer, M., Murray, A.W., and Kirschner, M.W. (1991). Cyclin is degraded by the ubiquitin pathway. Nature **349,** 132-138.

Gordon, W.R., Vardar-Ulu, D., Histen, G., Sanchez-Irizarry, C., Aster, J.C., and Blacklow, S.C. (2007). Structural basis for autoinhibition of Notch. Nat Struct Mol Biol **14,** 295-300.

Goutte, C., Tsunozaki, M., Hale, V.A., and Priess, J.R. (2002). APH-1 is a multipass membrane protein essential for the Notch signaling pathway in Caenorhabditis elegans embryos. Proc Natl Acad Sci U S A **99,** 775-779.

Gray, W.M., Kepinski, S., Rouse, D., Leyser, O., and Estelle, M. (2001). Auxin regulates SCF(TIR1)-dependent degradation of AUX/IAA proteins. Nature **414,** 271-276.

Grebe, M., Xu, J., Mobius, W., Ueda, T., Nakano, A., Geuze, H.J., Rook, M.B., and Scheres, B. (2003). Arabidopsis sterol endocytosis involves actin-mediated trafficking via ARA6-positive early endosomes. Curr Biol **13,** 1378-1387.

Gridley, T. (2003). Notch signaling and inherited disease syndromes. Hum Mol Genet **12 Spec No 1,** R9-13.

Gruis, D., Schulze, J., and Jung, R. (2004). Storage protein accumulation in the absence of the vacuolar processing enzyme family of cysteine proteases. Plant Cell **16,** 270-290.

Gruis, D.F., Selinger, D.A., Curran, J.M., and Jung, R. (2002). Redundant proteolytic mechanisms process seed storage proteins in the absence of seed-type members of the vacuolar processing enzyme family of cysteine proteases. Plant Cell **14,** 2863-2882.

Guilfoyle, T.J., Ulmasov, T., and Hagen, G. (1998). The ARF family of transcription factors and their role in plant hormone-responsive transcription. Cell Mol Life Sci **54,** 619-627.

Haass, C., and Selkoe, D.J. (1993). Cellular processing of beta-amyloid precursor protein and the genesis of amyloid beta-peptide. Cell **75,** 1039-1042.

Halpin, C., Cooke, S.E., Barakate, A., El Amrani, A., and Ryan, M.D. (1999). Self-processing 2A-polyproteins--a system for co-ordinate expression of multiple proteins in transgenic plants. Plant J **17,** 453-459.

Han, S., Green, L., and Schnell, D.J. (2009). The Signal Peptide Peptidase is required for pollen function in Arabidopsis. Plant Physiol.

Hasegawa, H., Sanjo, N., Chen, F., Gu, Y.J., Shier, C., Petit, A., Kawarai, T., Katayama, T., Schmidt, S.D., Mathews, P.M., Schmitt-Ulms, G., Fraser, P.E., and St George-Hyslop, P. (2004). Both the sequence and length of the C terminus of PEN-2 are critical for intermolecular interactions and function of presenilin complexes. J Biol Chem **279,** 46455-46463.

Hatakeyama, S., Yada, M., Matsumoto, M., Ishida, N., and Nakayama, K.I. (2001). U box proteins as a new family of ubiquitin-protein ligases. J Biol Chem **276,** 33111-33120.

Hayashi, Y., Yamada, K., Shimada, T., Matsushima, R., Nishizawa, N.K., Nishimura, M., and Hara-Nishimura, I. (2001). A proteinase-storing body

that prepares for cell death or stresses in the epidermal cells of Arabidopsis. Plant Cell Physiol **42,** 894-899.

Haze, K., Yoshida, H., Yanagi, H., Yura, T., and Mori, K. (1999). Mammalian transcription factor ATF6 is synthesized as a transmembrane protein and activated by proteolysis in response to endoplasmic reticulum stress. Mol Biol Cell **10,** 3787-3799.

He, G., Qing, H., Tong, Y., Cai, F., Ishiura, S., and Song, W. (2007). Degradation of nicastrin involves both proteasome and lysosome. J Neurochem **101,** 982-992.

Hebert, S.S., Serneels, L., Dejaegere, T., Horre, K., Dabrowski, M., Baert, V., Annaert, W., Hartmann, D., and De Strooper, B. (2004). Coordinated and widespread expression of gamma-secretase in vivo: evidence for size and molecular heterogeneity. Neurobiol Dis **17,** 260-272.

Heinemeyer, J., Eubel, H., Wehmhoner, D., Jansch, L., and Braun, H.P. (2004). Proteomic approach to characterize the supramolecular organization of photosystems in higher plants. Phytochemistry **65,** 1683-1692.

Hemming, M.L., Elias, J.E., Gygi, S.P., and Selkoe, D.J. (2008). Proteomic profiling of gamma-secretase substrates and mapping of substrate requirements. PLoS Biol **6,** e257.

Herreman, A., Van Gassen, G., Bentahir, M., Nyabi, O., Craessaerts, K., Mueller, U., Annaert, W., and De Strooper, B. (2003). gamma-Secretase activity requires the presenilin-dependent trafficking of nicastrin through the Golgi apparatus but not its complex glycosylation. J Cell Sci **116,** 1127-1136.

Herreman, A., Hartmann, D., Annaert, W., Saftig, P., Craessaerts, K., Serneels, L., Umans, L., Schrijvers, V., Checler, F., Vanderstichele, H., Baekelandt, V., Dressel, R., Cupers, P., Huylebroeck, D., Zwijsen, A., Van Leuven, F., and De Strooper, B. (1999). Presenilin 2 deficiency causes a mild pulmonary phenotype and no changes in amyloid precursor protein processing but enhances the embryonic lethal phenotype of presenilin 1 deficiency. Proc Natl Acad Sci U S A **96,** 11872-11877.

Hicke, L. (2001). Protein regulation by monoubiquitin. Nat Rev Mol Cell Biol **2,** 195-201.

Hiraiwa, N., Nishimura, M., and Hara-Nishimura, I. (1999). Vacuolar processing enzyme is self-catalytically activated by sequential removal of the C-terminal and N-terminal propeptides. FEBS Lett **447,** 213-216.

Hirokawa, T., Boon-Chieng, S., and Mitaku, S. (1998). SOSUI: classification and secondary structure prediction system for membrane proteins. Bioinformatics **14,** 378-379.

Holdsworth, M.J., Bentsink, L., and Soppe, J.J. (2008). Molecular networks regulating Arabidopsis seed maturation, after-ripening, dormancy and germination. New Phytologist **179**, 33-54.

Hu, Y., and Fortini, M.E. (2003). Different cofactor activities in gamma-secretase assembly: evidence for a nicastrin-Aph-1 subcomplex. J Cell Biol **161,** 685-690.

Huibregtse, J.M., Scheffner, M., and Howley, P.M. (1991). A cellular protein mediates association of p53 with the E6 oncoprotein of human papillomavirus types 16 or 18. Embo J **10,** 4129-4135.

Hunt, M.D., Neuenschwander, U.H., Delaney, T.P., Weymann, K.B., Friedrich, L.B., Lawton, K.A., Steiner, H.Y., and Ryals, J.A. (1996). Recent advances in systemic acquired resistance research--a review. Gene **179,** 89-95.

Ikeuchi, T., and Sisodia, S.S. (2003). The Notch ligands, Delta1 and Jagged2, are substrates for presenilin-dependent "gamma-secretase" cleavage. J Biol Chem **278,** 7751-7754.

Inoue, H., Nojima, H., and Okayama, H. (1990). High efficiency transformation of Escherichia coli with plasmids. Gene **96,** 23-28.

Inoue, K., Baldwin, A.J., Shipman, R.L., Matsui, K., Theg, S.M., and Ohme-Takagi, M. (2005). Complete maturation of the plastid protein translocation channel requires a type I signal peptidase. J Cell Biol **171,** 425-430.

Ishikawa, A., Kimura, Y., Yasuda, M., Nakashita, H., and Yoshida, S. (2006). Salicylic acid-mediated cell death in the Arabidopsis len3 mutant. Biosci Biotechnol Biochem **70,** 1447-1453.

Iso, T., Hamamori, Y., and Kedes, L. (2003). Notch signaling in vascular development. Arterioscler Thromb Vasc Biol **23,** 543-553.

Iwata, Y., Fedoroff, N.V., and Koizumi, N. (2008). Arabidopsis bZIP60 Is a Proteolysis-Activated Transcription Factor Involved in the Endoplasmic Reticulum Stress Response. Plant Cell **20,** 3107-3121.

Iwatsubo, T., Odaka, A., Suzuki, N., Mizusawa, H., Nukina, N., and Ihara, Y. (1994). Visualization of A beta 42(43) and A beta 40 in senile plaques with end-specific A beta monoclonals: evidence that an initially deposited species is A beta 42(43). Neuron **13,** 45-53.

Jackson, C.L., and Casanova, J.E. (2000). Turning on ARF: the Sec7 family of guanine-nucleotide-exchange factors. Trends Cell Biol **10,** 60-67.

Johnson, K.L., Degnan, K.A., Ross Walker, J., and Ingram, G.C. (2005). AtDEK1 is essential for specification of embryonic epidermal cell fate. Plant J **44,** 114-127.

Jung, R., Scott, M.P., Nam, Y.W., Beaman, T.W., Bassuner, R., Saalbach, I., Muntz, K., and Nielsen, N.C. (1998). The role of proteolysis in the processing and assembly of 11S seed globulins. Plant Cell **10,** 343-357.

Kaether, C., Haass, C., and Steiner, H. (2006). Assembly, trafficking and function of gamma-secretase. Neurodegener Dis **3,** 275-283.

Kaether, C., Lammich, S., Edbauer, D., Ertl, M., Rietdorf, J., Capell, A., Steiner, H., and Haass, C. (2002). Presenilin-1 affects trafficking and processing of betaAPP and is targeted in a complex with nicastrin to the plasma membrane. J Cell Biol **158,** 551-561.

Kaether, C., Scheuermann, J., Fassler, M., Zilow, S., Shirotani, K., Valkova, C., Novak, B., Kacmar, S., Steiner, H., and Haass, C. (2007). Endoplasmic reticulum retention of the gamma-secretase complex component Pen2 by Rer1. EMBO Rep **8,** 743-748.

Kanaoka, M.M., Urban, S., Freeman, M., and Okada, K. (2005). An Arabidopsis Rhomboid homolog is an intramembrane protease in plants. FEBS Lett **579,** 5723-5728.

Kang, J.G., Pyo, Y.J., Cho, J.W., and Cho, M.H. (2004). Comparative proteome analysis of differentially expressed proteins induced by K+ deficiency in Arabidopsis thaliana. Proteomics **4,** 3549-3559.

Katsube, K., and Sakamoto, K. (2005). Notch in vertebrates--molecular aspects of the signal. Int J Dev Biol **49,** 369-374.
Kepinski, S., and Leyser, O. (2005). The Arabidopsis F-box protein TIR1 is an auxin receptor. Nature **435,** 446-451.
Kidd, S., and Lieber, T. (2002). Furin cleavage is not a requirement for Drosophila Notch function. Mech Dev **115,** 41-51.
Kim, A.C., Oliver, D.C., and Paetzel, M. (2008). Crystal structure of a bacterial signal Peptide peptidase. J Mol Biol **376,** 352-366.
Kim, H., Ki, H., Park, H.S., and Kim, K. (2005). Presenilin-1 D257A and D385A mutants fail to cleave Notch in their endoproteolyzed forms, but only presenilin-1 D385A mutant can restore its gamma-secretase activity with the compensatory overexpression of normal C-terminal fragment. J Biol Chem **280,** 22462-22472.
Kim, J., Kleizen, B., Choy, R., Thinakaran, G., Sisodia, S.S., and Schekman, R.W. (2007). Biogenesis of gamma-secretase early in the secretory pathway. J Cell Biol **179,** 951-963.
Kim, S.H., and Sisodia, S.S. (2005a). A sequence within the first transmembrane domain of PEN-2 is critical for PEN-2-mediated endoproteolysis of presenilin 1. J Biol Chem **280,** 1992-2001.
Kim, S.H., and Sisodia, S.S. (2005b). Evidence that the "NF" motif in transmembrane domain 4 of presenilin 1 is critical for binding with PEN-2. J Biol Chem **280,** 41953-41966.
Kimberly, W.T., LaVoie, M.J., Ostaszewski, B.L., Ye, W., Wolfe, M.S., and Selkoe, D.J. (2003). Gamma-secretase is a membrane protein complex comprised of presenilin, nicastrin, Aph-1, and Pen-2. Proc Natl Acad Sci U S A **100,** 6382-6387.
Kinch, L.N., Ginalski, K., and Grishin, N.V. (2006). Site-2 protease regulated intramembrane proteolysis: Sequence homologs suggest an ancient signaling cascade. Protein Sci **15,** 84-93.
Kinoshita, T., Yamada, K., Hiraiwa, N., Kondo, M., Nishimura, M., and Hara-Nishimura, I. (1999). Vacuolar processing enzyme is up-regulated in the lytic vacuoles of vegetative tissues during senescence and under various stressed conditions. Plant J **19,** 43-53.
Kirkitadze, M.D., and Kowalska, A. (2005). Molecular mechanisms initiating amyloid beta-fibril formation in Alzheimer's disease. Acta Biochim Pol **52,** 417-423.
Kmiec-Wisniewska, B., Krumpe, K., Urantowka, A., Sakamoto, W., Pratje, E., and Janska, H. (2008). Plant mitochondrial rhomboid, AtRBL12, has different substrate specificity from its yeast counterpart. Plant Mol Biol **68,** 159-171.
Kopan, R., and Ilagan, M.X. (2004). Gamma-secretase: proteasome of the membrane? Nat Rev Mol Cell Biol **5,** 499-504.
Kotchoni, S.O., and Gachomo, E.W. (2006). The reactive oxygen species network pathways:an essential prerequisite for perception of pathogen attack and the acquired disease resistance in plants. J Biosci **31,** 389-404.
Kovacs, D.M., Fausett, H.J., Page, K.J., Kim, T.W., Moir, R.D., Merriam, D.E., Hollister, R.D., Hallmark, O.G., Mancini, R., Felsenstein, K.M., Hyman, B.T., Tanzi, R.E., and Wasco, W. (1996). Alzheimer-associated presenilins

1 and 2: neuronal expression in brain and localization to intracellular membranes in mammalian cells. Nat Med **2,** 224-229.

Kozutsumi, Y., Segal, M., Normington, K., Gething, M.J., and Sambrook, J. (1988). The presence of malfolded proteins in the endoplasmic reticulum signals the induction of glucose-regulated proteins. Nature **332,** 462-464.

Krawitz, P., Haffner, C., Fluhrer, R., Steiner, H., Schmid, B., and Haass, C. (2005). Differential localization and identification of a critical aspartate suggest non-redundant proteolytic functions of the presenilin homologues SPPL2b and SPPL3. J Biol Chem **280,** 39515-39523.

Kurepa, J., Toh, E.A., and Smalle, J.A. (2008). 26S proteasome regulatory particle mutants have increased oxidative stress tolerance. Plant J **53,** 102-114.

Kuroyanagi, M., Nishimura, M., and Hara-Nishimura, I. (2002). Activation of Arabidopsis vacuolar processing enzyme by self-catalytic removal of an auto-inhibitory domain of the C-terminal propeptide. Plant Cell Physiol **43,** 143-151.

Kuroyanagi, M., Yamada, K., Hatsugai, N., Kondo, M., Nishimura, M., and Hara-Nishimura, I. (2005). Vacuolar processing enzyme is essential for mycotoxin-induced cell death in Arabidopsis thaliana. J Biol Chem **280,** 32914-32920.

Lai, E.C. (2004). Notch signaling: control of cell communication and cell fate. Development **131,** 965-973.

Lampard, G.R., Macalister, C.A., and Bergmann, D.C. (2008). Arabidopsis stomatal initiation is controlled by MAPK-mediated regulation of the bHLH SPEECHLESS. Science **322,** 1113-1116.

LaPointe, C.F., and Taylor, R.K. (2000). The type 4 prepilin peptidases comprise a novel family of aspartic acid proteases. J Biol Chem **275,** 1502-1510.

Laudon, H., Hansson, E.M., Melen, K., Bergman, A., Farmery, M.R., Winblad, B., Lendahl, U., von Heijne, G., and Naslund, J. (2005). A nine-transmembrane domain topology for presenilin 1. J Biol Chem **280,** 35352-35360.

LaVoie, M.J., and Selkoe, D.J. (2003). The Notch ligands, Jagged and Delta, are sequentially processed by alpha-secretase and presenilin/gamma-secretase and release signaling fragments. J Biol Chem **278,** 34427-34437.

LaVoie, M.J., Fraering, P.C., Ostaszewski, B.L., Ye, W., Kimberly, W.T., Wolfe, M.S., and Selkoe, D.J. (2003). Assembly of the gamma-secretase complex involves early formation of an intermediate subcomplex of Aph-1 and nicastrin. J Biol Chem **278,** 37213-37222.

Lazarov, V.K., Fraering, P.C., Ye, W., Wolfe, M.S., Selkoe, D.J., and Li, H. (2006). Electron microscopic structure of purified, active gamma-secretase reveals an aqueous intramembrane chamber and two pores. Proc Natl Acad Sci U S A **103,** 6889-6894.

Lee, J.R., Urban, S., Garvey, C.F., and Freeman, M. (2001). Regulated intracellular ligand transport and proteolysis control EGF signal activation in Drosophila. Cell **107,** 161-171.

Lee, K., Tirasophon, W., Shen, X., Michalak, M., Prywes, R., Okada, T., Yoshida, H., Mori, K., and Kaufman, R.J. (2002). IRE1-mediated unconventional mRNA splicing and S2P-mediated ATF6 cleavage merge to

regulate XBP1 in signaling the unfolded protein response. Genes Dev **16,** 452-466.

Lee, M.K., Borchelt, D.R., Kim, G., Thinakaran, G., Slunt, H.H., Ratovitski, T., Martin, L.J., Kittur, A., Gandy, S., Levey, A.I., Jenkins, N., Copeland, N., Price, D.L., and Sisodia, S.S. (1997). Hyperaccumulation of FAD-linked presenilin 1 variants in vivo. Nat Med **3,** 756-760.

Lemberg, M.K., and Freeman, M. (2007a). Functional and evolutionary implications of enhanced genomic analysis of rhomboid intramembrane proteases. Genome Res **17,** 1634-1646.

Lemberg, M.K., and Freeman, M. (2007b). Cutting proteins within lipid bilayers: rhomboid structure and mechanism. Mol Cell **28,** 930-940.

Lemberg, M.K., Bland, F.A., Weihofen, A., Braud, V.M., and Martoglio, B. (2001). Intramembrane proteolysis of signal peptides: an essential step in the generation of HLA-E epitopes. J Immunol **167,** 6441-6446.

Lensch, M., Herrmann, R.G., and Sokolenko, A. (2001). Identification and characterization of SppA, a novel light-inducible chloroplast protease complex associated with thylakoid membranes. J Biol Chem **276,** 33645-33651.

Levy-Lahad, E., Wijsman, E.M., Nemens, E., Anderson, L., Goddard, K.A., Weber, J.L., Bird, T.D., and Schellenberg, G.D. (1995). A familial Alzheimer's disease locus on chromosome 1. Science **269,** 970-973.

Li, T., Ma, G., Cai, H., Price, D.L., and Wong, P.C. (2003). Nicastrin is required for assembly of presenilin/gamma-secretase complexes to mediate Notch signaling and for processing and trafficking of beta-amyloid precursor protein in mammals. J Neurosci **23,** 3272-3277.

Li, Y.M., Lai, M.T., Xu, M., Huang, Q., DiMuzio-Mower, J., Sardana, M.K., Shi, X.P., Yin, K.C., Shafer, J.A., and Gardell, S.J. (2000a). Presenilin 1 is linked with gamma-secretase activity in the detergent solubilized state. Proc Natl Acad Sci U S A **97,** 6138-6143.

Li, Y.M., Xu, M., Lai, M.T., Huang, Q., Castro, J.L., DiMuzio-Mower, J., Harrison, T., Lellis, C., Nadin, A., Neduvelil, J.G., Register, R.B., Sardana, M.K., Shearman, M.S., Smith, A.L., Shi, X.P., Yin, K.C., Shafer, J.A., and Gardell, S.J. (2000b). Photoactivated gamma-secretase inhibitors directed to the active site covalently label presenilin 1. Nature **405,** 689-694.

Liu, J.X., Srivastava, R., and Howell, S.H. (2008). Stress-induced expression of an activated form of AtbZIP17 provides protection from salt stress in Arabidopsis. Plant Cell Environ **31,** 1735-1743.

Liu, J.X., Srivastava, R., Che, P., and Howell, S.H. (2007). Salt stress responses in Arabidopsis utilize a signal transduction pathway related to endoplasmic reticulum stress signaling. Plant J **51,** 897-909.

Logeat, F., Bessia, C., Brou, C., LeBail, O., Jarriault, S., Seidah, N.G., and Israel, A. (1998). The Notch1 receptor is cleaved constitutively by a furin-like convertase. Proc Natl Acad Sci U S A **95,** 8108-8112.

Luster, A.D., Weinshank, R.L., Feinman, R., and Ravetch, J.V. (1988). Molecular and biochemical characterization of a novel gamma-interferon-inducible protein. J Biol Chem **263,** 12036-12043.

Marambaud, P., Wen, P.H., Dutt, A., Shioi, J., Takashima, A., Siman, R., and Robakis, N.K. (2003). A CBP binding transcriptional repressor produced by the PS1/epsilon-cleavage of N-cadherin is inhibited by PS1 FAD mutations. Cell **114,** 635-645.

Marouga, R., David, S., and Hawkins, E. (2005). The development of the DIGE system: 2D fluorescence difference gel analysis technology. Anal Bioanal Chem **382,** 669-678.

Martinez, I.M., and Chrispeels, M.J. (2003). Genomic analysis of the unfolded protein response in Arabidopsis shows its connection to important cellular processes. Plant Cell **15,** 561-576.

Martoglio, B., and Dobberstein, B. (1998). Signal sequences: more than just greasy peptides. Trends Cell Biol **8,** 410-415.

Maule, A.J. (2008). Plasmodesmata: structure, function and biogenesis. Curr Opin Plant Biol **11,** 680-686.

Maupin-Furlow, J.A., Wilson, H.L., Kaczowka, S.J., and Ou, M.S. (2000). Proteasomes in the archaea: from structure to function. Front Biosci **5,** D837-865.

Mayer, U., and Nusslein-Volhard, C. (1988). A group of genes required for pattern formation in the ventral ectoderm of the Drosophila embryo. Genes Dev **2,** 1496-1511.

McGurl, B., Pearce, G., Orozco-Cardenas, M., and Ryan, C.A. (1992). Structure, expression, and antisense inhibition of the systemin precursor gene. Science **255,** 1570-1573.

Membre, N., Bernier, F., Staiger, D., and Berna, A. (2000). Arabidopsis thaliana germin-like proteins: common and specific features point to a variety of functions. Planta **211,** 345-354.

Miller, D.L., Papayannopoulos, I.A., Styles, J., Bobin, S.A., Lin, Y.Y., Biemann, K., and Iqbal, K. (1993). Peptide compositions of the cerebrovascular and senile plaque core amyloid deposits of Alzheimer's disease. Arch Biochem Biophys **301,** 41-52.

Morais, V.A., Crystal, A.S., Pijak, D.S., Carlin, D., Costa, J., Lee, V.M., and Doms, R.W. (2003). The transmembrane domain region of nicastrin mediates direct interactions with APH-1 and the gamma-secretase complex. J Biol Chem **278,** 43284-43291.

Morais, V.A., Brito, C., Pijak, D.S., Crystal, A.S., Fortna, R.R., Li, T., Wong, P.C., Doms, R.W., and Costa, J. (2006). N-glycosylation of human nicastrin is required for interaction with the lectins from the secretory pathway calnexin and ERGIC-53. Biochim Biophys Acta **1762,** 802-810.

Muller, T., Meyer, H.E., Egensperger, R., and Marcus, K. (2008). The amyloid precursor protein intracellular domain (AICD) as modulator of gene expression, apoptosis, and cytoskeletal dynamics-relevance for Alzheimer's disease. Prog Neurobiol **85,** 393-406.

Munro, S. (1995). An investigation of the role of transmembrane domains in Golgi protein retention. Embo J **14,** 4695-4704.

Muntz, K. (1998). Deposition of storage proteins. Plant Mol Biol **38,** 77-99.

Muntz, K. (2007). Protein dynamics and proteolysis in plant vacuoles. J Exp Bot **58,** 2391-2407.

Muntz, K., Belozersky, M.A., Dunaevsky, Y.E., Schlereth, A., and Tiedemann, J. (2001). Stored proteinases and the initiation of storage protein mobilization in seeds during germination and seedling growth. J Exp Bot **52,** 1741-1752.

Murase, K., Hirano, Y., Sun, T.P., and Hakoshima, T. (2008). Gibberellin-induced DELLA recognition by the gibberellin receptor GID1. Nature **456,** 459-463.

Murphy, M.P., Das, P., Nyborg, A.C., Rochette, M.J., Dodson, M.W., Loosbrock, N.M., Souder, T.M., McLendon, C., Merit, S.L., Piper, S.C., Jansen, K.R., and Golde, T.E. (2003). Overexpression of nicastrin increases Abeta production. Faseb J **17,** 1138-1140.

Nakaune, S., Yamada, K., Kondo, M., Kato, T., Tabata, S., Nishimura, M., and Hara-Nishimura, I. (2005). A vacuolar processing enzyme, deltaVPE, is involved in seed coat formation at the early stage of seed development. Plant Cell **17,** 876-887.

Ni, J., and Clark, S.E. (2006). Evidence for functional conservation, sufficiency, and proteolytic processing of the CLAVATA3 CLE domain. Plant Physiol **140,** 726-733.

Niimura, M., Isoo, N., Takasugi, N., Tsuruoka, M., Ui-Tei, K., Saigo, K., Morohashi, Y., Tomita, T., and Iwatsubo, T. (2005). Aph-1 contributes to the stabilization and trafficking of the gamma-secretase complex through mechanisms involving intermolecular and intramolecular interactions. J Biol Chem **280,** 12967-12975.

Nyabi, O., Bentahir, M., Horre, K., Herreman, A., Gottardi-Littell, N., Van Broeckhoven, C., Merchiers, P., Spittaels, K., Annaert, W., and De Strooper, B. (2003). Presenilins mutated at Asp-257 or Asp-385 restore Pen-2 expression and Nicastrin glycosylation but remain catalytically inactive in the absence of wild type Presenilin. J Biol Chem **278,** 43430-43436.

Nyborg, A.C., Herl, L., Berezovska, O., Thomas, A.V., Ladd, T.B., Jansen, K., Hyman, B.T., and Golde, T.E. (2006). Signal peptide peptidase (SPP) dimer formation as assessed by fluorescence lifetime imaging microscopy (FLIM) in intact cells. Mol Neurodegener **1,** 16.

Ohashi-Ito, K., and Bergmann, D.C. (2006). Arabidopsis FAMA controls the final proliferation/differentiation switch during stomatal development. Plant Cell **18,** 2493-2505.

Okamoto, I., Kawano, Y., Murakami, D., Sasayama, T., Araki, N., Miki, T., Wong, A.J., and Saya, H. (2001). Proteolytic release of CD44 intracellular domain and its role in the CD44 signaling pathway. J Cell Biol **155,** 755-762.

Okochi, M., Steiner, H., Fukumori, A., Tanii, H., Tomita, T., Tanaka, T., Iwatsubo, T., Kudo, T., Takeda, M., and Haass, C. (2002). Presenilins mediate a dual intramembranous gamma-secretase cleavage of Notch-1. Embo J **21,** 5408-5416.

Orengo, C.A., Jones, D.T., and Thornton, J.M. (1994). Protein superfamilies and domain superfolds. Nature **372,** 631-634.

Osenkowski, P., Li, H., Ye, W., Li, D., Aeschbach, L., Fraering, P.C., Wolfe, M.S., and Selkoe, D.J. (2009). Cryoelectron microscopy structure of purified gamma-secretase at 12 A resolution. J Mol Biol **385,** 642-652.

Pardossi-Piquard, R., Yang, S.P., Kanemoto, S., Gu, Y., Chen, F., Bohm, C., Sevalle, J., Li, T., Wong, P.C., Checler, F., Schmitt-Ulms, G., St George-

Hyslop, P., and Fraser, P.E. (2009). APH1 polar transmembrane residues regulate the assembly and activity of presenilin complexes. J Biol Chem.

Park, C.S., Kim, O.S., Yun, S.M., Jo, S.A., Jo, I., and Koh, Y.H. (2008). Presenilin 1/gamma-secretase is associated with cadmium-induced E-cadherin cleavage and COX-2 gene expression in T47D breast cancer cells. Toxicol Sci **106,** 413-422.

Phan, U.T., Maric, M., Dick, T.P., and Cresswell, P. (2001). Multiple species express thiol oxidoreductases related to GILT. Immunogenetics **53,** 342-346.

Pillitteri, L.J., Bogenschutz, N.L., and Torii, K.U. (2008). The bHLH protein, MUTE, controls differentiation of stomata and the hydathode pore in Arabidopsis. Plant Cell Physiol **49,** 934-943.

Portin, P. (2002). General outlines of the molecular genetics of the Notch signalling pathway in Drosophila melanogaster: a review. Hereditas **136,** 89-96.

Prokop, S., Shirotani, K., Edbauer, D., Haass, C., and Steiner, H. (2004). Requirement of PEN-2 for stabilization of the presenilin N-/C-terminal fragment heterodimer within the gamma-secretase complex. J Biol Chem **279,** 23255-23261.

Rather, P.N., Ding, X., Baca-DeLancey, R.R., and Siddiqui, S. (1999). Providencia stuartii genes activated by cell-to-cell signaling and identification of a gene required for production or activity of an extracellular factor. J Bacteriol **181,** 7185-7191.

Ratovitski, T., Slunt, H.H., Thinakaran, G., Price, D.L., Sisodia, S.S., and Borchelt, D.R. (1997). Endoproteolytic processing and stabilization of wild-type and mutant presenilin. J Biol Chem **272,** 24536-24541.

Ratushny, V., and Golemis, E. (2008). Resolving the network of cell signaling pathways using the evolving yeast two-hybrid system. Biotechniques **44,** 655-662.

Raurell, I., Codina, M., Casagolda, D., Del Valle, B., Baulida, J., de Herreros, A.G., and Dunach, M. (2008). Gamma-secretase-dependent and -independent effects of presenilin1 on beta-catenin.Tcf-4 transcriptional activity. PLoS One **3,** e4080.

Rawson, R.B., Zelenski, N.G., Nijhawan, D., Ye, J., Sakai, J., Hasan, M.T., Chang, T.Y., Brown, M.S., and Goldstein, J.L. (1997). Complementation cloning of S2P, a gene encoding a putative metalloprotease required for intramembrane cleavage of SREBPs. Mol Cell **1,** 47-57.

Reisinger, V., and Eichacker, L.A. (2006). Analysis of membrane protein complexes by blue native PAGE. Proteomics **6 Suppl 2,** 6-15.

Rhee, S.Y., Beavis, W., Berardini, T.Z., Chen, G., Dixon, D., Doyle, A., Garcia-Hernandez, M., Huala, E., Lander, G., Montoya, M., Miller, N., Mueller, L.A., Mundodi, S., Reiser, L., Tacklind, J., Weems, D.C., Wu, Y., Xu, I., Yoo, D., Yoon, J., and Zhang, P. (2003). The Arabidopsis Information Resource (TAIR): a model organism database providing a centralized, curated gateway to Arabidopsis biology, research materials and community. Nucleic Acids Res **31,** 224-228.

Richards, D.E., King, K.E., Ait-Ali, T., and Harberd, N.P. (2001). HOW GIBBERELLIN REGULATES PLANT GROWTH AND DEVELOPMENT: A Molecular Genetic Analysis of Gibberellin Signaling. Annu Rev Plant Physiol Plant Mol Biol **52,** 67-88.

Risseeuw, E.P., Daskalchuk, T.E., Banks, T.W., Liu, E., Cotelesage, J., Hellmann, H., Estelle, M., Somers, D.E., and Crosby, W.L. (2003). Protein interaction analysis of SCF ubiquitin E3 ligase subunits from Arabidopsis. Plant J **34,** 753-767.

Robinson, D.G., Jiang, L., and Schumacher, K. (2008). The endosomal system of plants: charting new and familiar territories. Plant Physiol **147,** 1482-1492.

Rojo, E., Zouhar, J., Carter, C., Kovaleva, V., and Raikhel, N.V. (2003). A unique mechanism for protein processing and degradation in Arabidopsis thaliana. Proc Natl Acad Sci U S A **100,** 7389-7394.

Romero-Puertas, M.C., Campostrini, N., Matte, A., Righetti, P.G., Perazzolli, M., Zolla, L., Roepstorff, P., and Delledonne, M. (2008). Proteomic analysis of S-nitrosylated proteins in Arabidopsis thaliana undergoing hypersensitive response. Proteomics **8,** 1459-1469.

Rook, F., Gerrits, N., Kortstee, A., van Kampen, M., Borrias, M., Weisbeek, P., and Smeekens, S. (1998). Sucrose-specific signalling represses translation of the Arabidopsis ATB2 bZIP transcription factor gene. Plant J **15,** 253-263.

Rothbauer, U., Zolghadr, K., Muyldermans, S., Schepers, A., Cardoso, M.C., and Leonhardt, H. (2008). A versatile nanotrap for biochemical and functional studies with fluorescent fusion proteins. Mol Cell Proteomics **7,** 282-289.

Russ, W.P., and Engelman, D.M. (2000). The GxxxG motif: a framework for transmembrane helix-helix association. J Mol Biol **296,** 911-919.

Rutledge, B.J., Zhang, K., Bier, E., Jan, Y.N., and Perrimon, N. (1992). The Drosophila spitz gene encodes a putative EGF-like growth factor involved in dorsal-ventral axis formation and neurogenesis. Genes Dev **6,** 1503-1517.

Sabar, M., Balk, J., and Leaver, C.J. (2005). Histochemical staining and quantification of plant mitochondrial respiratory chain complexes using blue-native polyacrylamide gel electrophoresis. Plant J **44,** 893-901.

Sagi, G., Katz, A., Guenoune-Gelbart, D., and Epel, B.L. (2005). Class 1 reversibly glycosylated polypeptides are plasmodesmal-associated proteins delivered to plasmodesmata via the golgi apparatus. Plant Cell **17,** 1788-1800.

Samalova, M., Fricker, M., and Moore, I. (2006). Ratiometric fluorescence-imaging assays of plant membrane traffic using polyproteins. Traffic **7,** 1701-1723.

Sardi, S.P., Murtie, J., Koirala, S., Patten, B.A., and Corfas, G. (2006). Presenilin-dependent ErbB4 nuclear signaling regulates the timing of astrogenesis in the developing brain. Cell **127,** 185-197.

Satiat-Jeunemaitre, B., and Hawes, C. (1994). G.A.T.T. (A General Agreement on Traffic and Transport) and Brefeldin A in Plant Cells. Plant Cell **6,** 463-467.

Sato, C., Takagi, S., Tomita, T., and Iwatsubo, T. (2008). The C-terminal PAL motif and transmembrane domain 9 of presenilin 1 are involved in the formation of the catalytic pore of the gamma-secretase. J Neurosci **28,** 6264-6271.

Schagger, H., and von Jagow, G. (1991). Blue native electrophoresis for isolation of membrane protein complexes in enzymatically active form. Anal Biochem **199,** 223-231.

Schmid, M., Davison, T.S., Henz, S.R., Pape, U.J., Demar, M., Vingron, M., Scholkopf, B., Weigel, D., and Lohmann, J.U. (2005). A gene expression map of Arabidopsis thaliana development. Nat Genet **37,** 501-506.

Schoof, H., Lenhard, M., Haecker, A., Mayer, K.F., Jurgens, G., and Laux, T. (2000). The stem cell population of Arabidopsis shoot meristems in maintained by a regulatory loop between the CLAVATA and WUSCHEL genes. Cell **100,** 635-644.

Schroeter, E.H., Ilagan, M.X., Brunkan, A.L., Hecimovic, S., Li, Y.M., Xu, M., Lewis, H.D., Saxena, M.T., De Strooper, B., Coonrod, A., Tomita, T., Iwatsubo, T., Moore, C.L., Goate, A., Wolfe, M.S., Shearman, M., and Kopan, R. (2003). A presenilin dimer at the core of the gamma-secretase enzyme: insights from parallel analysis of Notch 1 and APP proteolysis. Proc Natl Acad Sci U S A **100,** 13075-13080.

Serneels, L., Dejaegere, T., Craessaerts, K., Horre, K., Jorissen, E., Tousseyn, T., Hebert, S., Coolen, M., Martens, G., Zwijsen, A., Annaert, W., Hartmann, D., and De Strooper, B. (2005). Differential contribution of the three Aph1 genes to gamma-secretase activity in vivo. Proc Natl Acad Sci U S A **102,** 1719-1724.

Shah, S., Lee, S.F., Tabuchi, K., Hao, Y.H., Yu, C., LaPlant, Q., Ball, H., Dann, C.E., 3rd, Sudhof, T., and Yu, G. (2005). Nicastrin functions as a gamma-secretase-substrate receptor. Cell **122,** 435-447.

Shen, G., Adam, Z., and Zhang, H. (2007). The E3 ligase AtCHIP ubiquitylates FtsH1, a component of the chloroplast FtsH protease, and affects protein degradation in chloroplasts. Plant J **52,** 309-321.

Shen, J., Bronson, R.T., Chen, D.F., Xia, W., Selkoe, D.J., and Tonegawa, S. (1997). Skeletal and CNS defects in Presenilin-1-deficient mice. Cell **89,** 629-639.

Sherrington, R., Rogaev, E.I., Liang, Y., Rogaeva, E.A., Levesque, G., Ikeda, M., Chi, H., Lin, C., Li, G., Holman, K., and et al. (1995). Cloning of a gene bearing missense mutations in early-onset familial Alzheimer's disease. Nature **375,** 754-760.

Shewry, P.R., Napier, J.A., and Tatham, A.S. (1995). Seed storage proteins: structures and biosynthesis. Plant Cell **7,** 945-956.

Shimada, T., Fuji, K., Tamura, K., Kondo, M., Nishimura, M., and Hara-Nishimura, I. (2003a). Vacuolar sorting receptor for seed storage proteins in Arabidopsis thaliana. Proc Natl Acad Sci U S A **100,** 16095-16100.

Shimada, T., Yamada, K., Kataoka, M., Nakaune, S., Koumoto, Y., Kuroyanagi, M., Tabata, S., Kato, T., Shinozaki, K., Seki, M., Kobayashi, M., Kondo, M., Nishimura, M., and Hara-Nishimura, I. (2003b). Vacuolar processing enzymes are essential for proper processing of seed storage proteins in Arabidopsis thaliana. J Biol Chem **278,** 32292-32299.

Shirotani, K., Edbauer, D., Kostka, M., Steiner, H., and Haass, C. (2004a). Immature nicastrin stabilizes APH-1 independent of PEN-2 and presenilin: identification of nicastrin mutants that selectively interact with APH-1. J Neurochem **89,** 1520-1527.

Shirotani, K., Edbauer, D., Prokop, S., Haass, C., and Steiner, H. (2004b). Identification of distinct gamma-secretase complexes with different APH-1 variants. J Biol Chem **279,** 41340-41345.

Shiu, S.H., and Bleecker, A.B. (2003). Expansion of the receptor-like kinase/Pelle gene family and receptor-like proteins in Arabidopsis. Plant Physiol **132,** 530-543.

Shpak, E.D., McAbee, J.M., Pillitteri, L.J., and Torii, K.U. (2005). Stomatal patterning and differentiation by synergistic interactions of receptor kinases. Science **309,** 290-293.

Silverstone, A.L., Mak, P.Y., Martinez, E.C., and Sun, T.P. (1997). The new RGA locus encodes a negative regulator of gibberellin response in Arabidopsis thaliana. Genetics **146,** 1087-1099.

Six, E., Ndiaye, D., Laabi, Y., Brou, C., Gupta-Rossi, N., Israel, A., and Logeat, F. (2003). The Notch ligand Delta1 is sequentially cleaved by an ADAM protease and gamma-secretase. Proc Natl Acad Sci U S A **100,** 7638-7643.

Slomnicki, L.P., and Lesniak, W. (2008). A putative role of the Amyloid Precursor Protein Intracellular Domain (AICD) in transcription. Acta Neurobiol Exp (Wars) **68,** 219-228.

Smalle, J., and Vierstra, R.D. (2004). The ubiquitin 26S proteasome proteolytic pathway. Annu Rev Plant Biol **55,** 555-590.

Spasic, D., Tolia, A., Dillen, K., Baert, V., De Strooper, B., Vrijens, S., and Annaert, W. (2006). Presenilin-1 maintains a nine-transmembrane topology throughout the secretory pathway. J Biol Chem **281,** 26569-26577.

Stagljar, I., Korostensky, C., Johnsson, N., and te Heesen, S. (1998). A genetic system based on split-ubiquitin for the analysis of interactions between membrane proteins in vivo. Proc Natl Acad Sci U S A **95,** 5187-5192.

Staiger, D., Apel, K., and Trepp, G. (1999). The Atger3 promoter confers circadian clock-regulated transcription with peak expression at the beginning of the night. Plant Mol Biol **40,** 873-882.

Steiner, H., Winkler, E., and Haass, C. (2008). Chemical cross-linking provides a model of the gamma-secretase complex subunit architecture and evidence for close proximity of the C-terminal fragment of presenilin with APH-1. J Biol Chem **283,** 34677-34686.

Steiner, H., Winkler, E., Edbauer, D., Prokop, S., Basset, G., Yamasaki, A., Kostka, M., and Haass, C. (2002). PEN-2 is an integral component of the gamma-secretase complex required for coordinated expression of presenilin and nicastrin. J Biol Chem **277,** 39062-39065.

Steiner, H., Duff, K., Capell, A., Romig, H., Grim, M.G., Lincoln, S., Hardy, J., Yu, X., Picciano, M., Fechteler, K., Citron, M., Kopan, R., Pesold, B., Keck, S., Baader, M., Tomita, T., Iwatsubo, T., Baumeister, R., and Haass, C. (1999). A loss of function mutation of presenilin-2 interferes with amyloid beta-peptide production and notch signaling. J Biol Chem **274,** 28669-28673.

Struhl, G., and Adachi, A. (1998). Nuclear access and action of notch in vivo. Cell **93,** 649-660.

Sun, T., Goodman, H.M., and Ausubel, F.M. (1992). Cloning the Arabidopsis GA1 Locus by Genomic Subtraction. Plant Cell **4,** 119-128.

Sutter, J.U., Campanoni, P., Tyrrell, M., and Blatt, M.R. (2006). Selective mobility and sensitivity to SNAREs is exhibited by the Arabidopsis KAT1 K+ channel at the plasma membrane. Plant Cell **18,** 935-954.

Swarbreck, D., Wilks, C., Lamesch, P., Berardini, T.Z., Garcia-Hernandez, M., Foerster, H., Li, D., Meyer, T., Muller, R., Ploetz, L., Radenbaugh, A., Singh, S., Swing, V., Tissier, C., Zhang, P., and Huala, E. (2008). The Arabidopsis Information Resource (TAIR): gene structure and function annotation. Nucleic Acids Res **36,** D1009-1014.

Szekeres, M. (2003). Brassinosteroid and systemin: two hormones perceived by the same receptor. Trends Plant Sci **8,** 102-104.

Tamura, T., Asakura, T., Uemura, T., Ueda, T., Terauchi, K., Misaka, T., and Abe, K. (2008). Signal peptide peptidase and its homologs in Arabidopsis thaliana--plant tissue-specific expression and distinct subcellular localization. Febs J **275,** 34-43.

Tanaka, H., Onouchi, H., Kondo, M., Hara-Nishimura, I., Nishimura, M., Machida, C., and Machida, Y. (2001). A subtilisin-like serine protease is required for epidermal surface formation in Arabidopsis embryos and juvenile plants. Development **128,** 4681-4689.

Thinakaran, G., and Koo, E.H. (2008). Amyloid precursor protein trafficking, processing, and function. J Biol Chem **283,** 29615-29619.

Thines, B., Katsir, L., Melotto, M., Niu, Y., Mandaokar, A., Liu, G., Nomura, K., He, S.Y., Howe, G.A., and Browse, J. (2007). JAZ repressor proteins are targets of the SCF(COI1) complex during jasmonate signalling. Nature **448,** 661-665.

Thomas, C.L., Bayer, E.M., Ritzenthaler, C., Fernandez-Calvino, L., and Maule, A.J. (2008). Specific targeting of a plasmodesmal protein affecting cell-to-cell communication. PLoS Biol **6,** e7.

Tomita, T., Watabiki, T., Takikawa, R., Morohashi, Y., Takasugi, N., Kopan, R., De Strooper, B., and Iwatsubo, T. (2001). The first proline of PALP motif at the C terminus of presenilins is obligatory for stabilization, complex formation, and gamma-secretase activities of presenilins. J Biol Chem **276,** 33273-33281.

Trujillo, M., Ichimura, K., Casais, C., and Shirasu, K. (2008). Negative regulation of PAMP-triggered immunity by an E3 ubiquitin ligase triplet in Arabidopsis. Curr Biol **18,** 1396-1401.

Tusnady, G.E., and Simon, I. (2001). The HMMTOP transmembrane topology prediction server. Bioinformatics **17,** 849-850.

Unlu, M., Morgan, M.E., and Minden, J.S. (1997). Difference gel electrophoresis: a single gel method for detecting changes in protein extracts. Electrophoresis **18,** 2071-2077.

Urban, S., and Wolfe, M.S. (2005). Reconstitution of intramembrane proteolysis in vitro reveals that pure rhomboid is sufficient for catalysis and specificity. Proc Natl Acad Sci U S A **102,** 1883-1888.

Urban, S., Lee, J.R., and Freeman, M. (2001). Drosophila rhomboid-1 defines a family of putative intramembrane serine proteases. Cell **107,** 173-182.

van der Hoorn, R.A., and Jones, J.D. (2004). The plant proteolytic machinery and its role in defence. Curr Opin Plant Biol **7,** 400-407.

Vaucheret, H., Beclin, C., Elmayan, T., Feuerbach, F., Godon, C., Morel, J.B., Mourrain, P., Palauqui, J.C., and Vernhettes, S. (1998). Transgene-induced gene silencing in plants. Plant J **16,** 651-659.

Verdecia, M.A., Joazeiro, C.A., Wells, N.J., Ferrer, J.L., Bowman, M.E., Hunter, T., and Noel, J.P. (2003). Conformational flexibility underlies ubiquitin ligation mediated by the WWP1 HECT domain E3 ligase. Mol Cell **11,** 249-259.

Vetrivel, K.S., Cheng, H., Lin, W., Sakurai, T., Li, T., Nukina, N., Wong, P.C., Xu, H., and Thinakaran, G. (2004). Association of gamma-secretase with lipid rafts in post-Golgi and endosome membranes. J Biol Chem **279,** 44945-44954.

Vicient, C.M., and Delseny, M. (1999). Isolation of total RNA from Arabidopsis thaliana seeds. Anal Biochem **268,** 412-413.

Vierstra, R.D. (2003). The ubiquitin/26S proteasome pathway, the complex last chapter in the life of many plant proteins. Trends Plant Sci **8,** 135-142.

Von Groll, U., Berger, D., and Altmann, T. (2002). The subtilisin-like serine protease SDD1 mediates cell-to-cell signaling during Arabidopsis stomatal development. Plant Cell **14,** 1527-1539.

Wakabayashi, T., and De Strooper, B. (2008). Presenilins: members of the gamma-secretase quartets, but part-time soloists too. Physiology (Bethesda) **23,** 194-204.

Wang, J., Brunkan, A.L., Hecimovic, S., Walker, E., and Goate, A. (2004). Conserved "PAL" sequence in presenilins is essential for gamma-secretase activity, but not required for formation or stabilization of gamma-secretase complexes. Neurobiol Dis **15,** 654-666.

Wang, J., Beher, D., Nyborg, A.C., Shearman, M.S., Golde, T.E., and Goate, A. (2006a). C-terminal PAL motif of presenilin and presenilin homologues required for normal active site conformation. J Neurochem **96,** 218-227.

Wang, Y., Zhang, Y., and Ha, Y. (2006b). Crystal structure of a rhomboid family intramembrane protease. Nature **444,** 179-180.

Weidemann, A., Eggert, S., Reinhard, F.B., Vogel, M., Paliga, K., Baier, G., Masters, C.L., Beyreuther, K., and Evin, G. (2002). A novel epsilon-cleavage within the transmembrane domain of the Alzheimer amyloid precursor protein demonstrates homology with Notch processing. Biochemistry **41,** 2825-2835.

Weihofen, A., Binns, K., Lemberg, M.K., Ashman, K., and Martoglio, B. (2002). Identification of signal peptide peptidase, a presenilin-type aspartic protease. Science **296,** 2215-2218.

Wolfe, M.S., Xia, W., Ostaszewski, B.L., Diehl, T.S., Kimberly, W.T., and Selkoe, D.J. (1999). Two transmembrane aspartates in presenilin-1 required for presenilin endoproteolysis and gamma-secretase activity. Nature **398,** 513-517.

Yamada, K., Nishimura, M., and Hara-Nishimura, I. (2004). The slow wound-response of gammaVPE is regulated by endogenous salicylic acid in Arabidopsis. Planta **218,** 599-605.

Yamasaki, A., Eimer, S., Okochi, M., Smialowska, A., Kaether, C., Baumeister, R., Haass, C., and Steiner, H. (2006). The GxGD motif of presenilin contributes to catalytic function and substrate identification of gamma-secretase. J Neurosci **26,** 3821-3828.

Yan, Y., and Wang, C. (2006). Abeta42 is more rigid than Abeta40 at the C terminus: implications for Abeta aggregation and toxicity. J Mol Biol **364,** 853-862.

Ye, J., Rawson, R.B., Komuro, R., Chen, X., Dave, U.P., Prywes, R., Brown, M.S., and Goldstein, J.L. (2000). ER stress induces cleavage of membrane-bound ATF6 by the same proteases that process SREBPs. Mol Cell **6,** 1355-1364.

Yee, D., and Goring, D.R. (2009). The diversity of plant U-box E3 ubiquitin ligases: from upstream activators to downstream target substrates. J Exp Bot **60,** 1109-1121.

Young, J.C., and Hartl, F.U. (2003). A stress sensor for the bacterial periplasm. Cell **113,** 1-2.

Yu, G., Chen, F., Levesque, G., Nishimura, M., Zhang, D.M., Levesque, L., Rogaeva, E., Xu, D., Liang, Y., Duthie, M., St George-Hyslop, P.H., and Fraser, P.E. (1998). The presenilin 1 protein is a component of a high molecular weight intracellular complex that contains beta-catenin. J Biol Chem **273,** 16470-16475.

Yu, G., Nishimura, M., Arawaka, S., Levitan, D., Zhang, L., Tandon, A., Song, Y.Q., Rogaeva, E., Chen, F., Kawarai, T., Supala, A., Levesque, L., Yu, H., Yang, D.S., Holmes, E., Milman, P., Liang, Y., Zhang, D.M., Xu, D.H., Sato, C., Rogaev, E., Smith, M., Janus, C., Zhang, Y., Aebersold, R., Farrer, L.S., Sorbi, S., Bruni, A., Fraser, P., and St George-Hyslop, P. (2000). Nicastrin modulates presenilin-mediated notch/glp-1 signal transduction and betaAPP processing. Nature **407,** 48-54.

Zhao, G., Cui, M.Z., Mao, G., Dong, Y., Tan, J., Sun, L., and Xu, X. (2005). gamma-Cleavage is dependent on zeta-cleavage during the proteolytic processing of amyloid precursor protein within its transmembrane domain. J Biol Chem **280,** 37689-37697.

Zheng, J., Yang, X., Harrell, J.M., Ryzhikov, S., Shim, E.H., Lykke-Andersen, K., Wei, N., Sun, H., Kobayashi, R., and Zhang, H. (2002). CAND1 binds to unneddylated CUL1 and regulates the formation of SCF ubiquitin E3 ligase complex. Mol Cell **10,** 1519-1526.

Zipfel, C., Kunze, G., Chinchilla, D., Caniard, A., Jones, J.D., Boller, T., and Felix, G. (2006). Perception of the bacterial PAMP EF-Tu by the receptor EFR restricts Agrobacterium-mediated transformation. Cell **125,** 749-760.

Zupicich, J., Brenner, S., Skarnes, W. (2001). Computational prediction of membrane-tethered transcription factors. Genome Biol **2**, 50-56.